

Alma Mater Studiorum - Università di Bologna

DOTTORATO DI RICERCA IN  
INGEGNERIA CIVILE, CHIMICA, AMBIENTALE E DEI MATERIALI

Ciclo 34

**Settore Concorsuale:** 08/A3 - INFRASTRUTTURE E SISTEMI DI TRASPORTO, ESTIMO E VALUTAZIONE

**Settore Scientifico Disciplinare:** ICAR/04 - STRADE, FERROVIE ED AEROPORTI

VULNERABLE USERS' PROTECTION  
WITH ADVANCED RECYCLING PAVING MATERIALS  
Design and Characterisation of Rubber-Based Impact-Absorbing Pavement  
Materials for Bike Lanes and Sidewalks

**Presentata da:** Ngongo Christina Jessie Makoundou

**Coordinatore Dottorato**

Alessandro Tugnoli

**Supervisore**

Cesare Sangiorgi

**Co-supervisor**

Viveca Wallqvist  
Kent Johansson  
Fredrik Ardefors



## Declaration

The content of the thesis is the result of work carried out as part of the Horizon 2020-Marie Skłodowska-Curie Actions-Innovative Training Networks project “SAFERUP!: Sustainable, Accessible, Safe, Resilient and Smart Urban Pavements”.



# SAFERUP!

Thinking Beyond the Pavement



This project has received funding from the European Union’s Horizon 2020 research and innovation programme under the Marie Skłodowska-Curie grant agreement N° 765057

*End-of-Life tyres*

*Crumb Rubber*

*Paving Materials*

*Impact-Absorbing Pavement*

*Urban Pavement*

*Vulnerable Road Users*

## Abstract

Our cities are constantly evolving and the necessity to keep them up to date with the best technologies is vital. The focus of various research is the improvement of the condition of the urban infrastructures and their safety. On the roads, the specific needs of cyclists and pedestrians are often neglected.

The Vulnerable Road Users (VRUs), among whom cyclists and pedestrians are, rarely benefit from the most innovative safety measures. Inspired by playgrounds and aiming to reduce pavement-impact related VRUs injuries, the development of Impact-Absorbing Pavements (IAP) used as novel sidewalks and bike lanes surface layers may help decrease injuries, fatalities, and the related societal costs. Safety on the road constitutes a major challenge in cities. The possibility of generalizing the design of shock-absorbing pavements in urban areas and addressing this challenge may contribute to reduce road fatalities and injuries to almost zero.

To achieve this goal, the End-of-Life Tyres (ELTs) crumb rubber (CR) is used as a primary resource, bringing its elastic properties into the surface layer. The thesis is divided into five main chapters. The first concerns the formulation and the definition of a feasible mix. The second chapter studies in detail the mechanical properties. The environmental outcomes and the ageing effect are also assessed. The third chapter explains the steps adopted while moving from the laboratory experiments to the material modelling. The chapter describes the modelling of the material to be able to simulate accidents and measure the impact of more accurate values on the injury reduction, especially on the head. The fourth chapter is reserved for the field trial. The fifth chapter gives some perspectives on the research and proposes a way to optimize and improve the data and results collected during the doctoral research.

The main findings of this thesis come from the different studies described. The formulations and mix design allowed a mixture classification thanks to several parameters evaluation. It was observed that the specimens made following the cold protocol have noticeable performances and reduce the overall carbon footprint impact of this innovative material. The mechanical, leaching, and weather resistance results allowed for shortlisting of the best mixtures. The material modelling and the accident simulation proved the performance of the IAP against skull fracture, and the field trial confirmed the good results obtained in the laboratory for the cold made material.

Finally, the outcomes of this thesis open many prospective to the IAP development, such as the use of a plant-based binder or recycled aggregates but also gave a positive vision of the possibility of developing a material that can be an ally to the cities of the future both regarding the safety of the users and the circular economy.

## Acknowledgements

I would like to thank my supervisors Prof. Cesare Sangiorgi, Dr. Viveca Wallqvist and Eng. Kenth Johansson for their continuous support and guidance related to all my research activities. Working with them through the SAFERUP! framework was a great learning experience, and I am grateful to them for providing me with this opportunity to do my PhD in a collaborative way between the University of Bologna and the Research Institutes of Sweden.

I will cherish all the fruitful discussions we had on the road pavement, vulnerable road users' safety and surface chemistry. I am also grateful for our exchange on many other topics that were never confined only to my research interests. The help I received from them in the research group(s) integration, preparing and reviewing articles for journal publications and presenting my work during technical events was significant. They were very supportive in trying out new ideas at the laboratory and helpful in the completion of my experimental activities. I will always admire them as great people.

I would like to gratefully acknowledge the outstanding support of Svensk Däckåtervinning (SDAB). Special thanks to Fredrik Ardefors for his precious help and support during the full PhD period.

I would like to thank everyone in the Road laboratory at the University of Bologna for their consideration and support during the past years. I would like to specially mention Piergiorgio, Giulia and my PhD colleagues Abbas and Sergio for their support in and out of the laboratory. I also want to thank all the other Early-stage Researchers of the SAFERUP! project for their collaboration and great company for the past years.

Also, the Material division of the Research Institutes of Sweden and Prof. Kleiven and the KTH Neuronic group, especially Pooya, for the warm welcome, the collaboration, the trust, and wonderful support during my visiting periods in Sweden.

I would also like to acknowledge the help I received from Amela, Jens and Filippo in conducting different research and experiments. I would also like to thank Ettore and Sandro for their help in the laboratory with the different testing apparatus.

I would like to thank my friends worldwide, with whom I had several exchanges about my PhD life, for their support in times. My parents and sisters for the full trust and incommensurable support no matter when and even from kilometres distance.

And finally, Camilla. I cannot thank Camilla enough for her outstanding support, gentleness, warmth, admiration, and understanding during this strange, complex, yet memorable cycle of my life

# List of Contents

<i>Declaration</i> .....	<i>ii</i>
<i>Abstract</i> .....	<i>iv</i>
<i>Acknowledgements</i> .....	<i>v</i>
<i>List of Contents</i> .....	<i>vi</i>
<i>List of Figures</i> .....	<i>xii</i>
<i>List of Tables</i> .....	<i>xvi</i>
<i>List of Abbreviations</i> .....	<i>xvii</i>
<i>List of Papers</i> .....	<i>xviii</i>
<b>Introduction</b> .....	<b>1</b>
<b>Research questions</b> .....	<b>7</b>
<b>Layout of the thesis</b> .....	<b>9</b>
<b>Chapter 1. Laboratory Development and Design</b> .....	<b>11</b>
1. Overview.....	12
2. Development of Functional Rubber-Based Impact-Absorbing Pavements for Cyclist and Pedestrian Injury Reduction.....	13
2.1. Vulnerable Road Users' Safety and Public Health.....	13
2.2. Recycling and Responsible Consumption for Sustainable Urban Communities.....	13
2.3. Inspirations and previous studies.....	14
2.4. Implementation of the current study.....	15
2.5. Materials and Methods.....	16
2.5.1. End-of-Life Tyre rubber.....	16
2.5.2. Bituminous binder.....	18
2.5.3. Virgin aggregates.....	18
2.5.4. Mix design and production of specimens.....	19
2.5.5. Characterisation.....	21
2.5.5.1. Geometrical and volumetric analysis.....	21
2.5.5.2. Cantabro loss test.....	21
2.5.5.3. Indirect Tensile Stiffness Modulus (ITSM) and Indirect Tensile Strength (ITS).....	22
2.5.5.4. Head Injury Criterion (HIC).....	22

2.6.	Results and Discussion.....	24
2.6.1.	Geometrical and Volumetric assessment .....	24
2.6.2.	Cantabro loss and abrasion results .....	25
2.6.3.	Pavement mechanical performances .....	26
2.6.4.	Attenuation of impacts and injury prevention .....	27
2.6.4.1.	Influence of the rubber amount .....	27
2.6.4.2.	Influence of the testing temperature .....	28
2.6.4.3.	Influence of the testing layer thickness .....	29
2.7.	Conclusions .....	30
3.	Impact-Absorbing Pavements made with cold and warm asphalt binders and recycled rubber: a preliminary laboratory study. ....	32
3.1.	Pedestrians and Cyclist safety and protection: the Impact-absorbing pavements concept for urban road infrastructures. ....	32
3.2.	End-of-life tyres, waste management and recycled rubber. ....	32
3.3.	Previous studies.....	33
3.4.	Paper Focus .....	33
3.5.	Materials and Methods.....	36
3.5.1.	Crumb rubber .....	36
3.5.2.	Aggregates.....	36
3.5.3.	Binders .....	36
3.5.4.	Reference mix and size distribution .....	38
3.5.5.	Mixture's design.....	38
3.5.6.	Production of samples .....	39
3.5.7.	Characterisations .....	39
3.5.7.1.	Organoleptic mixture descriptions. ....	39
3.5.7.2.	Expansions and swelling phenomenon.....	40
3.5.7.3.	Volumetric analysis.....	40
3.5.7.4.	Stiffness measurements .....	40
3.5.7.5.	Head Injury Criterion (HIC) and Abbreviated Injury Scale (AIS).....	40
3.5.8.	Natural ageing procedure (NAP) conditions .....	41
3.6.	Results and Discussion.....	41
3.6.1.	Visual and Organoleptic properties of the mixtures and samples. ....	41
3.6.2.	Volumetric properties of the different asphalt mixtures .....	44
3.6.3.	Mechanical tests .....	46

3.6.3.1. Stiffness and mechanical properties assessment pre- and post-natural ageing procedure.....	46
3.6.3.2. Impact attenuation and injury prevention.....	47
3.7. Conclusions.....	48
4. Outcomes.....	49
<b>Chapter 2. Mechanical, Chemical and Freeze-thaw cycles analysis</b>	<b>50</b>
1. Overview.....	51
2. Mechanical and leaching characterization of impact-absorbing rubberised asphalts for urban pavements.....	52
2.1. Introduction.....	52
2.2. Methodology.....	54
2.2.1. Experimental Plan.....	54
2.2.2. Rubberised impact-absorbing asphalt mixture.....	54
2.2.3. Production of samples.....	55
2.2.4. Testing criteria.....	56
2.2.5. Mechanical tests.....	57
2.2.5.1. Uniaxial Unconfined Stress-Relaxation test and calculations.....	58
2.2.5.2. Axial Unconfined Destructive Compression Procedure.....	59
2.2.6. Dynamic Surface Leaching Test.....	59
2.3. Results and Discussions.....	61
2.3.1. Relaxation of the samples.....	61
2.3.1.1. Elastic recovery of the materials.....	61
2.3.1.2. Stress-Strain analysis and calculation of the relaxation modulus.....	62
2.3.2. Failure behaviour during the compressive test.....	63
2.3.2.1. Failure analysis.....	63
2.3.2.2. Stress-strain curve analysis and calculation of the elastic modulus.....	64
2.4. Conclusions.....	70
3. Influence of Freeze-Thaw Cycles on Mechanical Properties of Highly Rubberised Asphalt Mixtures Made with Warm and Cold Asphalt Binders.....	72
3.1. Introduction.....	72
3.2. Materials and Methods.....	73
3.2.1. Raw Materials.....	73
3.2.2. Highly-rubberised asphalt concrete samples' production.....	75
3.2.3. Freeze and thaw procedure.....	76

3.2.4. Characterisation.....	78
3.2.4.1. Densities and Air voids .....	78
3.2.4.2. Indirect Tensile Stiffness Modulus .....	78
3.2.4.3. Indirect Tensile Strength .....	78
3.2.4.4. Cantabro loss .....	79
3.2.4.5. Measures of Particle loss, pH, and Electric Conductivity-Total Dissolved Solid .....	79
3.3. Results and Discussion.....	80
3.3.1. Volumetric, geometrical properties of the mixtures and observations.....	80
3.3.2. Mechanical performances .....	81
3.3.2.1. ITSM at 5°C .....	81
3.3.2.2. ITS at 5°C.....	82
3.3.3. Particle loss .....	85
3.3.3.1. Cantabro loss .....	85
3.3.3.2. Particle loss in the thaw waters .....	87
3.3.4. Leaching analysis .....	88
3.4. Conclusions .....	89
4. Outcomes .....	90
<b>Chapter 3. Material modelling and accident cases simulations .....</b>	<b>92</b>
1. Overview .....	93
2. A rubberized impact-absorbing pavement can reduce the head injury risk in vulnerable road users: a bicycle and a pedestrian accident case study.....	94
2.1. Background .....	94
2.2. Methods.....	95
2.2.1. Samples Production Method .....	95
2.2.2. Mechanical Testing and Material Modeling .....	97
2.2.3. Validation Of Material Model Using Standard HIC Drop Test .....	99
2.2.4. Bicycle Accident Case .....	99
2.2.5. Pedestrian Accident Case .....	100
2.3 Results .....	100
2.4. Discussion .....	103
2.5. Conclusions .....	106
3. Outcomes .....	106
<b>Chapter 4. Field trial .....</b>	<b>107</b>

1. Overview .....	108
2. Laboratory and in-situ characterisation of a recycled-based Impact-absorbing pavement made with a dry and cold production and construction procedure .....	109
2.1. Introduction .....	109
2.2. Methods.....	110
2.2.1. Preparation and production of the samples in the laboratory .....	111
2.2.2. Production of the IAP and construction in-situ .....	112
2.3. Characterisation methods .....	113
2.3.1. Mechanical characterisation of the IAP .....	113
2.3.2. Shock-attenuation performance of the IAP.....	113
2.3.3. Surface analysis and friction behaviour of the material .....	114
2.3.3.1. Skidding analysis in the laboratory using a Slip Tester .....	114
2.3.3.2. Skidding in-situ analysis using a British pendulum .....	115
2.3.3.3. Sand test .....	115
2.3.4. Tracking of the Natural Ageing of the trial field.....	116
2.4. Results and Discussion.....	116
2.4.1. Mechanical properties .....	116
2.4.2. Impact-attenuation properties.....	117
2.4.3. Friction values.....	118
2.4.3.1. Macrotexture and roughness .....	118
2.4.3.2. Slip risk and coefficient of friction.....	119
2.4.3.3. BPN value and skidding risk in-situ.....	120
2.4.4. Observations on the trial site.....	121
2.5. Conclusions .....	123
3. Outcomes .....	124

**Chapter 5. Optimization to extend the industrial perspective of the IAP.....125**

1. Overview .....	126
2. Functionalization of Crumb Rubber Surface for the Incorporation into Asphalt Layers of Reduced Stiffness: An Overview of Existing Treatment Approaches .....	127
2.1. Introduction .....	127
2.2. Rubber tyres and their use in asphalt pavements .....	128
2.2.1. 2.1 History and waste management of tyres.....	128
2.2.2. Properties of the recycled rubbers .....	130

2.2.3. The use of recycled rubber in the road construction sector.....	130
2.2.3.1. Wet and dry processes in asphalt pavements applications .....	130
2.2.3.2. Rubber-Binder interaction.....	131
2.3. Surface treatments and their effect on rubber-bitumen interactions .....	132
2.3.1. Surface modification of polymers .....	132
2.3.1.1. Gamma radiation .....	133
2.3.1.2. UV-Ozone treatment .....	138
2.3.1.3. Microwaves irradiation .....	142
2.3.1.4. Plasma treatment .....	145
2.3.2. Advantages and disadvantages of the main solution for an application to highly rubberized road pavements. ....	149
2.4. Conclusions .....	151
3. Outcomes .....	153
<b>Conclusions.....</b>	<b>154</b>
<i>References.....</i>	<i>159</i>

## List of Figures

Figure 1.1: CR particles used in the experimental mixtures: Coarse, Medium and Fine.....	17
Figure 1.2: Scheme of the experimental investigations' approach. ....	19
Figure 1.3: Production steps for the rubberised impact-absorbing pavement (IAP) samples. .....	20
Figure 1.4: Developed testing procedure for the assessment of the basic performance of IAP. .....	21
Figure 1.5: Scheme of the impact-attenuating properties testing method. ....	23
Figure 1.6: pictures of the hic test device installation ready for in-situ (left) and laboratory (right) testing.....	24
Figure 1.7: Overall aspect of compacted IAP 2a (left) and reference AC (right). ....	24
Figure 1.8: Vertical expansion after one month and six months for the mixes REF AC, IAP 1, IAP 2a and IAP 3. ....	25
Figure 1.9: Cantabro loss showing the abrasion properties of the tested specimens. ....	26
Figure 1.10: Laboratory HIC values when increasing the dropping height at room temperature ( $22^{\circ}\text{C}\pm 1^{\circ}\text{C}$ ). ....	28
Figure 1.11: Tape-delimited impacted zone after several drops of the HIC-meter head: REF AC (left); IAP 3 (right). ....	28
Figure 1.12: Scheme of the samples assembly to assess the influence of the layer thickness. .....	29
Figure 1.13: CFH at HIC=1000 including IAP 2abc and IAP 2ab @ four temperatures: - $10^{\circ}\text{C}$ , $-2^{\circ}\text{C}$ , $23^{\circ}\text{C}$ and $40^{\circ}\text{C}$ . ....	30
Figure 1.14: Article approach for impact-absorbing pavement design. ....	35
Figure 1.15 Experimental programme .....	38
Figure 1.16: Graphical representation of the mixtures' proportions .....	39
Figure 1.17: Visual and organoleptic assessment mixtures made with cold process. ....	42
Figure 1.18: Visual aspect of the samples before and after the Natural Ageing Procedure (NAP). ....	43
Figure 1.19: Volumetric properties and expansion values of the different asphalt mixtures	45
Figure 1.20: Stiffness and mechanical properties assessment pre and post NAP. ITSM [MPa] $5^{\circ}\text{C}$ .....	47
Figure 1.21: HIC meter installation and Impact attenuation and injury prevention performances Critical Fall Height (CFH) @ HIC 1000 [m] .....	48
Figure 2.1: Experimental plan of the study. The scheme describes the raw materials used, including the rubber, the aggregates, and the different binders. The dry process was used to produce different specimens compacted by means of gyratory and static compaction. These were tested with the DSLT and UCT tests. ....	54
Figure 2.2: Neat rubber SEM and granulometry curves from [80]. The figure contains a SEM picture of the rubber mix and the granulometric data of the two adopted rubbers, allowing a rubber size distribution of 0-4 mm [80] .....	55
Figure 2.3: Scheme illustrating the 40 mm cores obtained from 150 mm samples for the uniaxial tests.....	56
Figure 2.4: a. Compressive tests setup; b. Stress-strain graph of a stress-relaxation test illustrating the hysteresis during the relaxation phase.....	58

Figure 2.5: Glass vessel containing the rubberised asphalt in direct contact with the water.	60
Figure 2.6: Average Elastic recovery values for the maximum applied strain .....	62
Figure 2.7: Relaxation Stress- $\sigma$ and Vertical Strain- $\epsilon$ curve.....	63
Figure 2.8: Typical failures after destructive testing. a. sample fails with no loss of cohesion (A1, A4 and B1); b. sample fails with loss of cohesion (A2, A3 and B2). .....	64
Figure 2.9: Quasi-static (a) and Dynamic (b) Compressive Stress- $\sigma$ and Vertical Strain- $\epsilon$ curves. ....	65
Figure 2.10: Changes in a) Electric conductivity and b) pH of leachants at different stages of DSLT for rubberised asphalt specimens. ....	67
Figure 2.11: Cumulative release of elements from unit surface of rubberized asphalt specimens. a) Elements with release concentration <6 mg/m <sup>2</sup> , b) Elements with release concentration between 6 and 60 mg/m <sup>2</sup> , c) Elements with release concentration > 60 mg/m <sup>2</sup> . ....	70
Figure 2.12: Rubberised asphalt production procedure. ....	75
Figure 2.13: Vertical and horizontal expansion of the samples. ....	76
Figure 2.14: Summary of the experimental programme for each F-T cycle.....	77
Figure 2.15: EC-TDS, pH and Particle loss measurement procedure .....	80
Figure 2.16: R2-C aspect after the 5 <sup>th</sup> freezing cycle of the F-T cycles.....	81
Figure 2.17: ITSM (@5°C) values for each mixture vs. cycles.....	82
Figure 2.18: Comparison of the samples after 10 F-T cycles. In the left column, the samples before ITS test; in the right column, samples after testing. The red circle represents the deformation of the sample. The arrow highlights the crack initiated by the ITS on the samples.....	84
Figure 2.19: ITS values for tests carried out at 5°C and different cycles.....	85
Figure 2.20: Cantabro loss percentage of the rubberised asphalt specimens at different stages of the F-T procedure.....	86
Figure 2.21: Aspect of the samples after the Cantabro test at the control time (no F-T). ....	87
Figure 2.22: Loss of asphalt concrete samples material in the thaw waters after 1, 5 and 10 F-T cycles.....	87
Figure 2.23: Changes in a. Electric conductivity and b. pH of thaw waters at different stages of F-T procedure for rubberised asphalt specimens. ....	89
Figure 3.1: Study scheme of the experiments and simulations. (1,2) production of rubberized asphalt, (3) Compression test and HIC drop test on the samples, (4. a) HIC drop test simulations for different impact speeds, (4. b) An isometric view of the bicycle accident reconstruction case study on different asphalt mixtures, (4. c) The sagittal view of the pedestrian accident case on different asphalt mixture and the velocity vectors defined according to the local coordinate system on the center of gravity of the head. The blue arrow refers to the direction of the linear velocity. ....	97
Figure 3.2: Linear regression analysis of the 33% sample material modeling with and without viscoelastic material parameters. ....	98
Figure 3.3: Linear regression analysis of maximum acceleration from the HIC drop test results and the simulation results for each asphalt sample.....	100
Figure 3.4: a) Comparison of peak von Mises stresses (MPa) on the cortical bone between the 0% and 33% rubber contents. The level of plasticity for cortical bone was set to 80.0 MPa. The highest stresses on the skull bone occurred at the impact position for the	

individual case; (b) Comparison of the peak 1st principal Green-Lagrange strain on the brain tissue between 0% and 33% rubber contents. The black circles correspond to the reported medical records of head injury in the bicycle and pedestrian case. Medical image for the bicycle case is from *The Accident Analysis & Prevention*, Vol. 91, Madelen Fahlstedt, Peter Halldin, Svein Kleiven, The protective effect of a helmet in three bicycle accidents—A finite element study, 135-143, Copyright (2021, Licence number: 5218740986803), with permission from Elsevier; the injury region is marked with a red circle. Medical image for the pedestrian case is from “An in-depth analysis of real world fall accidents involving brain trauma.” (2009), Michael D. Gilchrist and Mary C. Doorly, Copyright (CC BY-NC-ND 3.0 IE), the injury region is marked with arrows. .... 101

Figure 3.5: Comparison of the peak linear acceleration (g) between different rubber contents in the bicycle and pedestrian case. The risk of skull fracture was calculated for each of the simulations using the acceleration-time nodal history of a node on the center of gravity of the head. .... 103

Figure 4.1: Scheme of the research plan conducted in this study. .... 110

Figure 4.2: Image of the rubber mix used in the IAP formulation: Coarse, Medium, and fine. .... 111

Figure 4.3: Gradation curve of the HRA used as a reference for the design of the IAP .... 112

Figure 4.4: Sample with different surface characteristics: Non-treated (NT); Simple treatment (ST); Aggregate treatment (AT)..... 112

Figure 4.5: Delimitation of the impact zone with a laser. .... 114

Figure 4.6: Illustration of the Brungraber Mark IIIB slip tester and feet tests used..... 115

Figure 4.7: British Pendulum test in-situ ..... 115

Figure 4.8: Determination of the macrotexture depth according to the volume sand patch method..... 115

Figure 4.9: Weather measured from June 2021 to December 2021 in Imola, Italy [142]... 116

Figure 4.10: Mechanical properties of the IAP material. a. Relaxation stress - time; b. Compression Stress - vertical strain;..... 117

Figure 4.11: IAP Impact-attenuating performances of the IAP material. .... 118

Figure 4.12: Visual macrotexture of the pavement and results of the sand test after six months of exploitation..... 119

Figure 4.13: COF of the different samples (non-treated (NT), simple treatment (ST) and aggregate treatment (AT)), tested with different footwear pads (FR, TR, GN and GR), at 3 different surface configurations (dry, water-wetted and iced). .... 120

Figure 4.14: Walking and biking trails on the IAP after its construction. .... 121

Figure 4.15: Visual assessment of the degradation of the surface after and before six months of exploitation. .... 122

Figure 4.16: Profile picture of a core and picture of the top and base layer of the field trial ..... 122

Figure 5.1: Different rubber recycling processes and potential applications (adapted from European Tyre Recycling Association, Rubber Manufactures’ association, Swedish Tyre Recycling Association). .... 129

Figure 5.2: Scheme of the different possible treatment methods and the main solutions described in this review (adapted from [160,171–181]) ..... 133

Figure 5.3: (a) Simplified scheme of the gamma ray initiation; (b) Picture of a GammaCell 220 instrument designed for lab work *Nordion*<sup>TM</sup>; (c) Scheme of a commercial irradiator designed for industrial scale work *Nordion*<sup>TM</sup>. ..... 134

Figure 5.4: Simplified scheme of the gamma ray reaction initiation and effect on rubber surface. .... 135

Figure 5.5: (a) Simplified scheme of the UV-Ozone initiation; (b) Picture of a UV-Ozone instrument designed for lab work *Samco*<sup>TM</sup>; (c) Picture of a brewing industry using UV-Ozone treatment *Mellifiq*<sup>TM</sup>. ..... 139

Figure 5.6: Simplified scheme of the Ozone reaction initiation and effect on rubber surface. .... 140

Figure 5.7: Simplified scheme of the Ozone action under different humidity conditions [192]. ..... 141

Figure 5.8: (a) Simplified scheme of the microwaves formation by magnetron; (b) Picture of a microwave instrument designed for lab work *Labpulse*<sup>®</sup>; (c) Picture of Large-scale microwave chain *Xujia*<sup>TM</sup>. ..... 142

Figure 5.9: Simplified scheme of the microwaves effect on rubber surface. .... 143

Figure 5.10: Proposed mechanism while incorporating microwaves-treated or untreated rubber [198]. ..... 144

Figure 5.11: (a) Simplified scheme of the Plasma formation; (b) Picture of a plasma generator designed for lab work *Rotalab*<sup>TM</sup>; (c) Picture of a Large-scale plasma treatment chain *Henniker*<sup>TM</sup>. ..... 146

Figure 5.12: Simplified scheme of plasma effect on rubber surface. .... 147

## List of Tables

Table 1.1: Typical properties of the experimental crumb rubber.....	17
Table 1.2: Results from the PAH analysis. ....	18
Table 1.3: Characteristics of 25/55 Polymer-Modified Bitumen.....	18
Table 1.4: Properties of the virgin aggregates.....	19
Table 1.5: Content of each mix by weight and by volume based on the aggregate and the total mix. ....	20
Table 1.6: Abbreviated Injury Scale AIS classification of the injury type by HIC [20]. ....	23
Table 1.7: Densities and air voids content values for each tested mixture. ....	25
Table 1.8: Average tensile strength and stiffness modulus of the different mixes.....	26
Table 1.9: HIC and related AIS code corresponding to the fall for each specimen from an equal drop height (0.2 m) at $T_{amb}$ . ....	27
Table 1.10: Preliminary results and values from [57] and [29,52] studies.....	33
Table 1.11: CR typical values .....	36
Table 1.12: Aggregates typical values .....	36
Table 1.13: bitumen's typical values.....	37
Table 1.14: Emulsions typical values.....	37
Table 1.15: Organoleptic assessment characterization.....	39
Table 1.16: Natural Ageing Procedure (NAP) weather conditions.....	41
Table 1.17: Classification of the injuries type by HIC of the designed mixtures at 0.2 m of drop. ....	46
Table 2.1: Impact-Absorbing Pavements made with cold and hot/warm asphalt binders and recycled rubber: summary of the preliminary characteristics of the mixtures (Chapter 1, part 2). ....	57
Table 2.2: Crumb rubber typical values .....	74
Table 2.3: Crumb rubber sieve analysis .....	74
Table 2.4: Mixture composition in the percentage of the volume of the total mixture .....	76
Table 2.5: Densities and voids values of the specimens produced .....	81
Table 3.1: Summary of rubberized asphalt samples material properties and dimensions.....	96
Table 3.2: simulation results of the pedestrian accident on different rubberized asphalt samples.....	102
Table 5.1: Summary of studies on the procedures and results using Gamma ray treatment. ....	137
Table 5.2: Summary of the studies on the procedures and results using UV-Ozone treatment. ....	141
Table 5.3: Summary of studies on the procedures and results using microwaves treatment. ....	144
Table 5.4: Summary of studies on the procedures and results using plasma treatment. ....	148
Table 5.5: Comparison between main physical surface treatment solutions. ....	151

## List of Abbreviations

AFM	Atomic force microscopy
AIS	Abbreviated Injury Score
ASTM	American Society for Testing and Materials
ATR-IR	Attenuated total reflection Infrared
CFH	Critical Fall Height
CR	Crumb rubber
DSC	Differential Scanning Calorimetry
ELT	End-of-Life Tyre
EN	European Norm
EU	European Union
FEM	Finite Element Method
F-T	Freeze and Thaw
FTIR	Fourier transform infrared
GHG	Greenhouse gas
GPC	Gas-phase chromatography
HIC	Head Injury Criterion
HRA	Hot-Rolled Asphalt
IAP	Impact-Absorbing Pavement
IR	Infrared
ISO	International Organization for Standardization
ITS	Indirect Tensile Strength
ITSM	Indirect Tensile Stiffness Modulus
LCA	Life-cycle analysis
LVE	Linear Visco-Elasticity
MA	Mineral Aggregates
PAH	Polycyclic aromatic hydrocarbons
RAP	Reclaimed Asphalt Pavement
RTFOT	Rolling Thin Film Ovens
SAP	Shock-Absorbing Pavement
SEM	Scanning Electron Microscopy
TGA	Thermogravimetric analysis
UCS	Uniaxial Compression Strength
UV	Ultraviolet
WHO	World Health Organization
XPS	X-ray photoelectron spectroscopy
XRD	X-ray diffraction

## List of Papers

This doctoral dissertation consists of a summary of the following papers. The enumeration of the papers follows the order of apparition in the thesis layout.

1. **Makoundou, C.**; Sangiorgi, C.; Johansson, K.; Wallqvist, V.; Development of Functional Rubber-Based Impact-Absorbing Pavements for Cyclist and Pedestrian Injury Reduction. *Sustainability* 2021, 13, 11283.  
DOI: <https://doi.org/10.3390/su132011283>
2. **Makoundou, C.**; Sangiorgi, C.; Johansson, K.; Wallqvist, V.; Impact-Absorbing Pavements made with cold and warm asphalt binders and recycled rubber: a preliminary laboratory study.  
*Under review in Materials and Structures, Springer, Switzerland.*
3. **Makoundou, C.**; Fathollahi, A.; Kleiven, S.; Sangiorgi, C; Coupe, S.; Mechanical and leaching characterisation of impact-absorbing rubberised asphalts for urban pavements.  
*Under review in Materials and Structures, Springer, Switzerland.*
4. **Makoundou, C.**; Sangiorgi, C. Influence of Freeze–Thaw Cycles on the Mechanical Properties of Highly Rubberised Asphalt Mixtures Made with Warm and Cold Asphalt Binders. *Materials* 2022, 15, 2701.  
DOI: <https://doi.org/10.3390/ma15072701>
5. Sahandifar, P.; **Makoundou, C.**; Fahlstedt, M.; Sangiorgi, C.; Johansson, K.; Wallqvist, V.; Kleiven, S.; A rubberised impact-absorbing pavement reduces the head injury risk for vulnerable road users: a bicycle and a pedestrian accident case study.  
*Accepted in Traffic Injury Prevention, Taylor & Francis, United Kingdom.*
6. **Makoundou, C.**; Sangiorgi, C.; Johansson, K.; Wallqvist, V.; Laboratory and in-situ characterisation of a dry recycled-based Impact-absorbing pavement cold produced and laid.  
*In preparation for submission to Scientific report, Nature, United Kingdom.*
7. **Makoundou, C.**; Johansson, K.; Wallqvist, V.; Sangiorgi, C. Functionalization of Crumb Rubber Surface for the Incorporation into Asphalt Layers of Reduced Stiffness: An Overview of Existing Treatment Approaches. *Recycling* 2021, 6, 19.  
DOI: <https://doi.org/10.3390/recycling6010019>

# Introduction

Scientists have been discussing the consequences of urbanization and the issues related to the development of cities and the increase of the urban population for a long time [1]. As a result, potential solutions were studied and developed to make the cities more livable. Today such issues are still under the lens but in a new framework: the city of the future. This concept implies that the problems mentioned above are solved thanks to technology and new, green, and smart strategies and approaches [2–9].

Among urban infrastructures, transport networks are fundamental. They permit the transportation of goods and people, inside and outside the city. Still, today roads represent the major transport infrastructure inside the cities as they connect with capillarity every place. However, their safety is sub-optimal, especially for a specific category of road users defined as Vulnerable Road Users (VRU) [4,10].

This research is part of the Horizon 2020-Marie Skłodowska-Curie Actions-Innovative Training Networks SAFERUP! Project, which focuses on innovative solutions for urban roads. One of the pillars of this project is the users' safety and the willingness to decrease the number of injuries, fatalities and related health costs on roads to almost zero.

When looking at the ecosystem of a normal urban road, it is easy to identify different types of users, such as trucks, busses, cars, motorbikes, scooters, cyclists, and pedestrians, a hint of this is given in *Figure 1*. The VRUs are the least protected and the most at risk among these. Indeed, according to the World Health Organization or European Conference of Ministers of Transport 2000 [10,11], VRUs are road users who lack any shield, unlike car or bus users. Thus, users of motorcycles, scooters, bicycles, or pedestrians fall into this category. For this reason, the focus is, in particular, on these users.



Figure 1: Road sharing illustration, London, 2018

In terms of safety, for some of these VRUs, various tools of individual protection have already been developed and are used successfully, such as safety helmets or protective clothing. This equipment protects in case of an accident, such as collisions [12,13] and falls [14–16]. However, when laws do not make it mandatory, the use of this equipment is left to the individual choice of the person. Moreover, it is difficult for pedestrians to imagine the use of individual protection equipment to increase their safety. This causes many injuries and fatalities. Indeed, 22 % of road deaths are pedestrians, especially the elderly, representing 5% among cyclists [17,18].

As shown in *Table 1* [19], many aspects have been considered to make roads safer for VRUs, in particular pedestrians, the most at risk in this category.

Among the presented measures, the main importance is to ensure reserved spaces on the road for cyclists and pedestrians. It is vital to provide more sidewalks and bike lanes, especially after the breakdown of the Covid-19 pandemic in the last years that convinced many to use bikes or commute walking and increased the number of VRUs [20–23]. Moreover, different sources [10,24–26] have advised the construction of more bike lanes to help to stop the overuse of cars during the pandemic time in which people were avoiding public transportation to prevent infection. Although all of these are valuable measures, one aspect is missing: the role of the road pavement.

Table 1: Key measures and specific interventions for improving pedestrian safety. [19]

<b>Key measures</b>	<b>Examples of interventions</b>
Reduce pedestrian exposure to vehicular traffic	Provide sidewalks
	Install and/or upgrade traffic and pedestrian signals
	Construct pedestrian refuge islands and raised medians
	Construct enhanced marked crossings
	Provide vehicle restriction/diversion measures
	Install overpasses/underpasses
	Improve mass transit route design
	Reduce traffic volumes by switching journeys from the car to public transport, walk and cycle for distances and purposes where these options work well
	Reduce speed limit
	Implement area-wide lower speed limit programmes, for example, 30 km/h
Reduce vehicle speeds	Implement road-narrowing measures
	Install speed management measures at road sections
	Install speed management measures at intersections
	Provide school route improvements
	Provide crossing enhancements
Improve sight distance and/or visibility between motor vehicles and pedestrians	Implement lighting/crossing illumination measures
	Reduce or eliminate obstruction by physical objects including parked vehicles
	Install signals to alert motorists that pedestrians are crossing
Improve pedestrian and motorist safety awareness and behaviour	Improve visibility of pedestrians
	Provide education, outreach, and training
	Develop and/or enforce traffic laws on speed, drinking and driving, pedestrian right-of-way, red light disobedience, commercial roadside activity and traffic control
Improve vehicle design for pedestrian protection	Implement ‘walking school bus’ programmes
	Develop vehicle safety standards and laws for pedestrian protection
Improve vehicle design for pedestrian protection	Enforce vehicle safety standards and laws for pedestrian protection
	Publicize consumer information on pedestrian safety by make and model of car, for example, results of New Car Assessment Programmes
Improve care for the injured pedestrians	Organize pre-hospital trauma care systems
	Establish inclusive trauma care systems
	Offer early rehabilitation services

Some studies [27–29] show that the stiff pavement has a role in the injuries of the VRUs. Therefore, proposing and working on developing softer versions is a promising way to reduce them. Indeed, thanks to impact attenuation tests and user-feeling surveys conducted during the studies mentioned above, such an approach's potential was confirmed, and the results obtained were encouraging. Additionally, the outcomes proved that this could convince people to cycle or walk instead of massively using the car. By employing softer and less stiff materials, the main objective is to make sidewalks and bike lanes less dangerous and reduce possible human injuries resulting from falls caused by collisions or not.

Furthermore, softer pavement can act as collective protection, available to all the VRUs, against injuries and beneficial for all the users. Employing this material while restructuring the urban infrastructures can decrease injuries and fatalities to the lowest in the near future.

As inspiration, rubber-based playground materials have been successfully used as pavements to minimize injuries. Nevertheless, the possibility of generalizing the use on roads has been poorly investigated. To extend the utilization, two aspects need to be considered together. First, the material must abate the risk of injuries thanks to a considerable amount of rubber, similar to the quantity used in playgrounds (around 100%). At the same time, it must be produced, laid, and maintained using already known road paving methods. Ultimately, a largescale development of the material will allow using rubber coming from ELT, a waste product of the evolution of urban cities. This action will also foster the use of this material in alternative applications and not anymore in the burning, which is responsible for large greenhouse gas (GHG) emissions.

Indeed, every year, millions of tonnes of tyres are produced. Recycling the rubber coming from ELTs is a good way to reduce the use of raw resources and positively impact the circular economy model while exploiting rubber properties to prevent injuries (*Figure 2*).

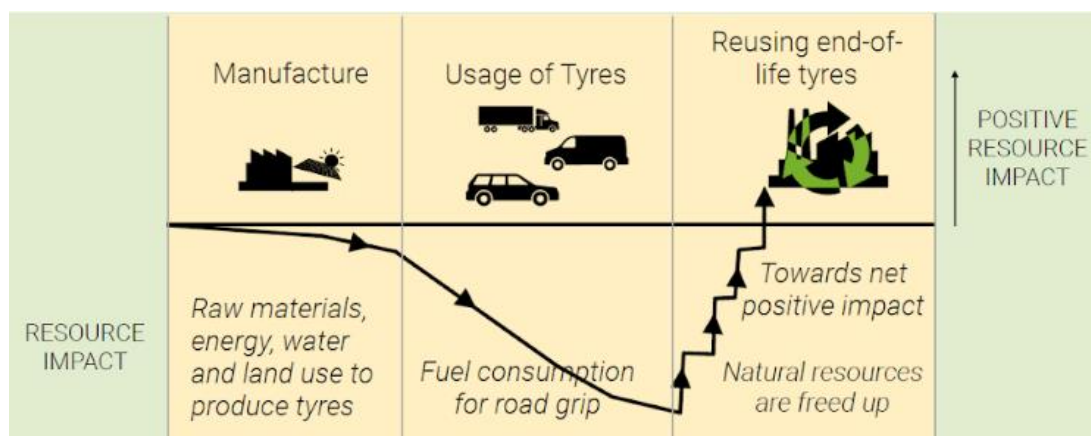


Figure 2: Resources impact of the reuse of ELTs [30].

**Figure 3** compares different applications for ELTs from two perspectives, GHG savings and circular economy. The goal is to reuse the rubber in as many ways as possible, prioritizing the ones with the highest environmental benefit. For every new reuse step, the negative impact on the planet’s resources and greenhouse gas emissions are reduced. The use of rubber in asphalt materials is considered a very impactful solution because, as shown in **Figure 3**, it saves on greenhouse emissions and can reuse rubber already recycled previously in other applications. Incorporating ELT rubber into roads will have a double effect, increasing the users’ safety and fostering responsible consumption and a circular economy.

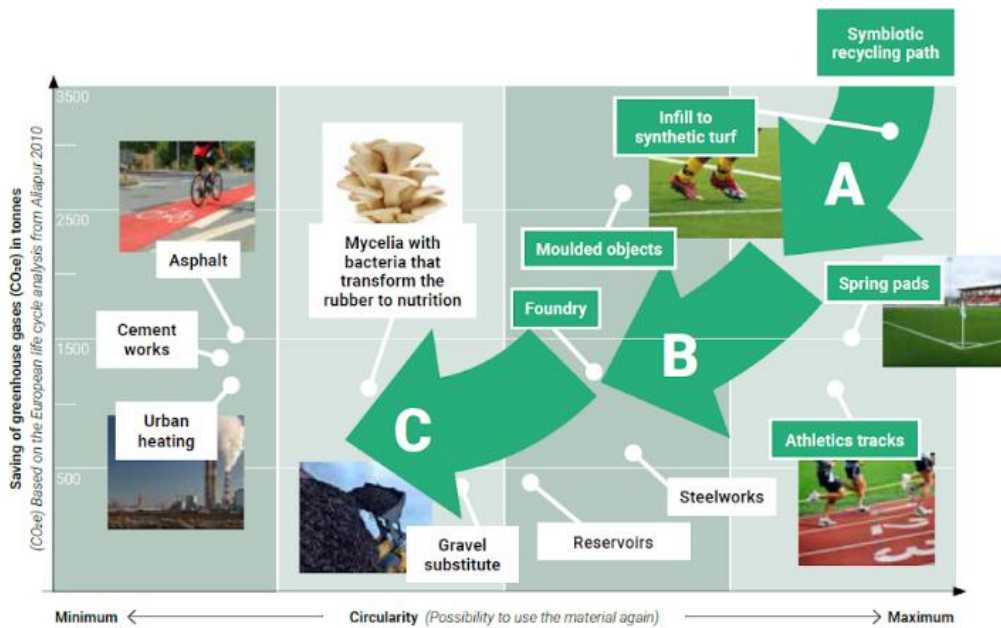


Figure 3: Circularity and GHG saving of several application recycling end-of-life tyres at a different stage of the rubber recycling life [30].

Finally, these are the context and the inputs of the research described in this thesis. This study provides a unique solution to different the need for cities to be safer, especially for the VRUs and to adopt sustainable and circular production and construction: the design of a highly rubberized material to create an impact-absorbing pavement (IAP) which improves the safety of the VRUs, minimizing their injuries. **Figure 4** represents the intersection of different fields involved in this research.

The focus is made all along with this thesis on the development of bituminous mixtures incorporating rubber, which has been studied for decades. The innovative aspects are the increase in the quantities of rubber used, the possibility of using traditional production and construction methods and machines, and the willingness to reduce externalities (smell, fumes...) [31–35].

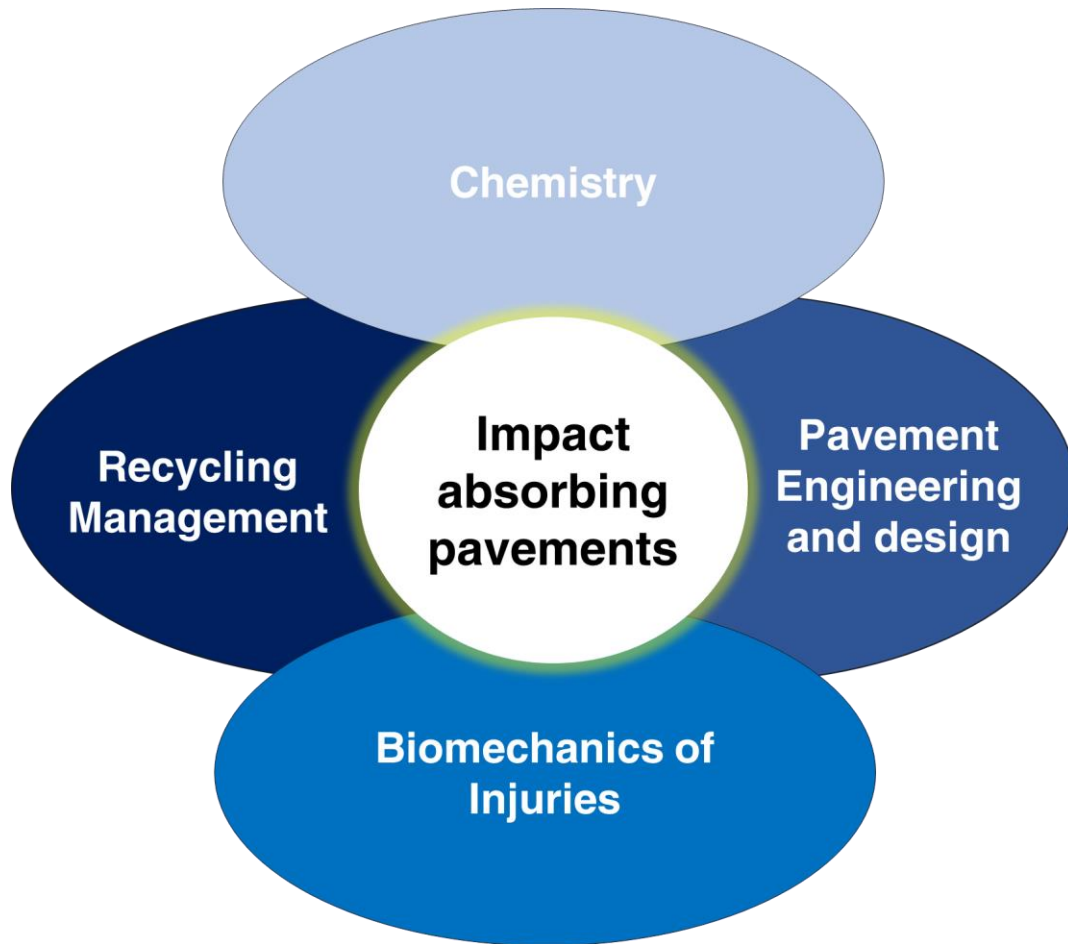


Figure 4: Intersection of the field of the research project.

## Research questions

The objective of this research project was to propose the design of innovative, functional, and durable impact-absorbing materials for bicycle lanes and sidewalks pavements. Several research questions arose from the investigation of the background and previous studies.

The first experiments were focused on the formulation and the proof of the feasibility of the material. These aspects led to the following questions:

- How to design pavement materials with a high quantity of recycled rubber from ELT and suitable for building bicycle and pedestrian lanes?
- How much rubber is possible to incorporate into the mix for it to be viable and effective regarding the impact-attenuation?
- How does the rubber need to be incorporated to positively affect the technical but also environmental and economic aspects?
- How to avoid or reduce the smell and fumes released during the production process?
- How to solve problems linked to the use of large quantities of rubber, such as high binder consumption?

Thus, after collecting data on the mix design, the need to understand the newly developed materials' overall properties arose. Indeed, new materials need to be assessed in several aspects. In this case, the focus was on the mechanical and chemical parameters. Also, the influence of the outdoor conditions was considered, and the following questions needed to be explored:

- How to test this novel material accurately?
- What is the overall mechanical structure of this material?
- Can this pavement be hazardous to the environment?
- How will this pavement react in real outdoor weather conditions?
- Can this newly developed pavement be recycled?

In parallel, other questions concerned the collection of data on the biomechanical side of injuries:

- What is the effect of this material if a pedestrian or a cyclist occurs to fall on it?
- Does this pavement have a real effect on the injury reduction?
- How can it be improved to maximize the injury reduction?

The pavement is meant to be laid on large portions of urban infrastructures. Naturally, the reproducibility of the laboratory development must be assessed in situ, and thus

the upscaling possibility verified to confirm laboratory criteria and optimize other parameters:

- Can the process developed in the laboratory be upscaled and reproduced in-situ, maintaining the same quality and performances?
- Is it possible to maintain this pavement over time, and which methods are the best?
- What is missing in the pavement design for it to be durable?

Finally, thanks to some outcomes of the research, the perspective to ameliorate the material technically, environmentally, and financially were drawn:

- Which optimization can be done to ensure the environmentally friendly effect of this material, increase the recycling impact and make possible its recyclability after the exploitation?

## Layout of the thesis

The thesis consists of a compilation of scientific articles organized into five Chapters, as shown in *Figure 5*. Each chapter addresses a specific subject that aimed to be solved through the doctoral research. The main problematics of the design of a new IAP are stated through the sections and the main research questions are answered through the different articles selected for this thesis. Each chapter starts with a contextualization of the study in the full project and ends by listing the main outcomes that the study gave.

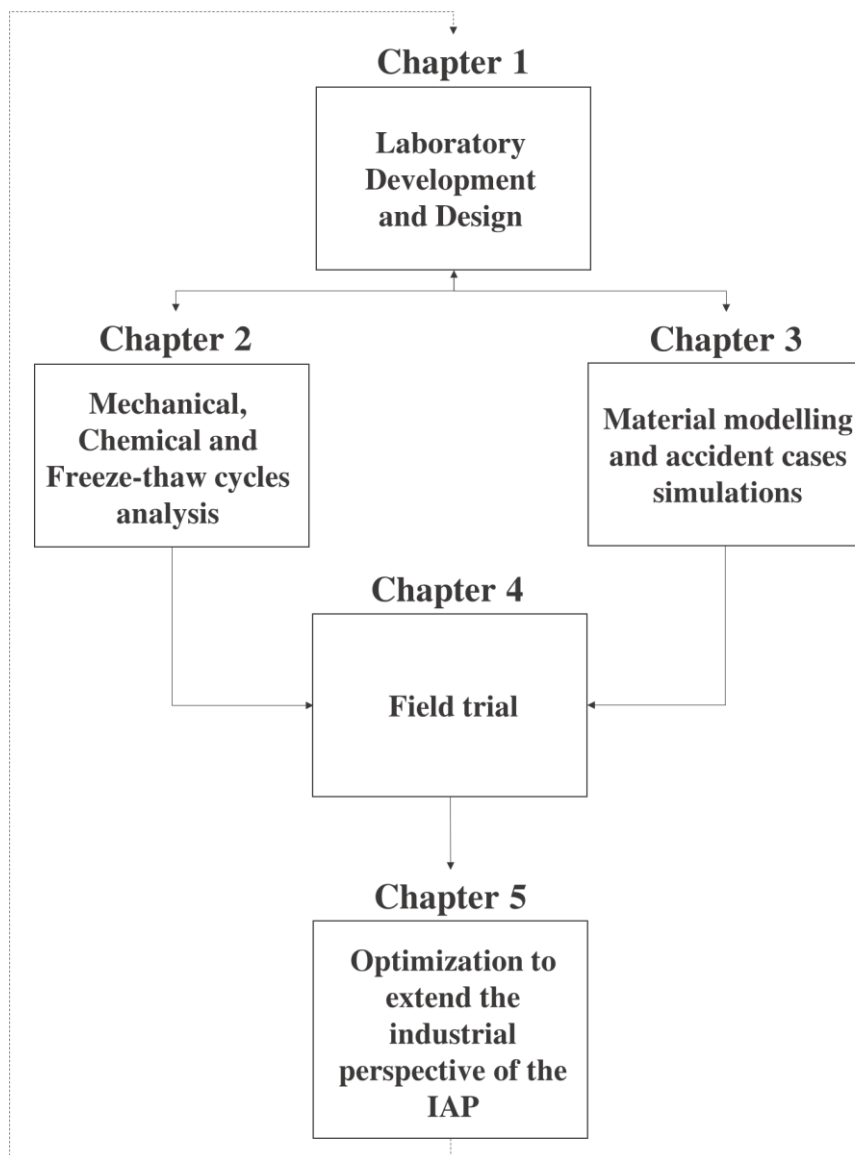


Figure 5: Research layout scheme

**Chapter 1: Laboratory Development and Design** contains two articles describing the formulation and design steps to obtain feasible formulations. These papers mainly explain several experimental stages from the material analysis, the formulation, and the production.

**Chapter 2: Mechanical, Chemical and Freeze-thaw cycles analysis** contains two papers explaining the different methods of characterization used to analyse mechanically, environmentally, and against weather change the selected material and define common criteria and properties for the future steps.

**Chapter 3: Material modelling and accident cases simulations** contains a unique paper on the material modelling that led to the simulation of two accident cases: one involving a pedestrian and one with a cyclist. Focused on the biomechanics of injuries, it gave preliminary results of the actual injury reduction allowed by the developed material.

**Chapter 4: Field trial** contains one paper on the field trial construction and analysis. This chapter mentions the upscaling of the laboratory work and testing of the selected formulation under real urban conditions.

Finally, **Chapter 5: Optimization to extend the industrial perspective of the IAP** contains a paper about the possible rubber functionalization that can be useful for improving the mixture and optimising the overall performance of the developed material. This chapter also mentions other perspectives for possible future research, thanks to the results of the doctoral project.

# Chapter 1. Laboratory Development and Design

The work proposed in this chapter is extracted from the following manuscripts:

- **Makoundou, C.;** Sangiorgi, C.; Johansson, K.; Wallqvist, V.; Development of Functional Rubber-Based Impact-Absorbing Pavements for Cyclist and Pedestrian Injury Reduction. *Sustainability* 2021, 13, 11283.  
DOI: <https://doi.org/10.3390/su132011283>

*Conceptualization, C.M., C.S., K.J. and V.W.; methodology, C.M.; software, C.M.; validation, C.M., C.S., K.J. and V.W.; formal analysis, C.M.; investigation, C.M.; resources, C.M., C.S., K.J. and V.W.; data curation, C.M.; writing—original draft preparation, C.M.; writing—review and editing, C.M., C.S., K.J. and V.W.; visualization, C.M.; supervision, C.S., K.J. and V.W.; project administration, C.S.; funding acquisition, C.S. All authors have read and agreed to the published version of the manuscript.*

- **Makoundou, C.;** Sangiorgi, C.; Johansson, K.; Wallqvist, V.; Impact-Absorbing Pavements made with cold and warm asphalt binders and recycled rubber: a preliminary laboratory study. *Under review in Materials and Structures, Springer, Switzerland.*

*CS, VW, KJ, CM: Conceptualisation; CM: Data curation; CM: Formal analysis; CS, VW, KJ: Funding acquisition; CS, CM: Investigation; CM: Methodology; CS, VW, KJ: Supervision; CM: Writing - original draft; CM, CS, VW, KJ: Writing - review & editing. All authors have read and agreed to the submitted version of the manuscript.*

## **1. Overview**

The first section focuses on the laboratory formulation and the preliminary tests to develop an impact-absorbing paving material for bicycle lanes and sidewalks. The section aims to describe the approach used in the laboratory, prove the feasibility of the material, propose a production procedure, and choose the best mixtures to be selected for more complete analysis. Also, the environmental impact of the mixture is investigated. Indeed, the final aim for the newly developed material is to be functional and as green as possible.

This section contains two papers. The first one is a study on the variation of the rubber and binder amounts during the mix design. Therefore, only one type of rubber and one type of binder were used. The main objective was to propose a method with partial substitution of the aggregates. Moreover, the goal was also to define the right rubber amount to permit the mixture's production and compaction and possibly obtain impact-attenuation properties on the pavement specimens. Subsequently, after defining the best amount of rubber, the type of rubber and binder were changed and became the variable parameters. The study of the influence of these changes is the focus of the second paper. The aim was to study five types of binders with different characteristics, taking into consideration their possible modifications and their temperatures of production and laying.

In this section, each paper starts by introducing the concept and the background. Then, the materials and methods part is described, followed by the results and discussion one. Finally, the articles are concluded with the valuable results of the studies.

## **2. Development of Functional Rubber-Based Impact-Absorbing Pavements for Cyclist and Pedestrian Injury Reduction**

### **2.1. Vulnerable Road Users' Safety and Public Health**

Road traffic injuries result in an alarming and non-negligible amount of death in the world. More than half of deaths occur among people classified as Vulnerable Road Users (VRUs), including pedestrians and cyclists [10,36]. Several previous studies have shown that stiff surfaces are one of the main reasons for vulnerable users' traffic injuries. To protect these users, research on innovative and sustainable Impact-Absorbing Pavements (IAP) surface layers has now become crucial [28,29].

Moreover, because roads are an essential part of the human living environment and the urban population is increasing, VRUs are increasingly subject to fall accidents impacting mostly heads, shoulders and hips [1,2]. In 2021, the World Health Organization specified that a critical number of people (between 20 and 50 million) are forced to live with disabilities resulting from non-fatal injuries caused by the design of roads, which is often unsafe and inadequate for pedestrians, cyclists or motorcyclists. [10].

In addition to the injuries and disabilities resulting from road traffic accidents, the safety of roads also influences other public health issues. Indeed, urban roads that do not include safe walking and cycling infrastructures can result in more reliance on car transportation. In these cases, people are less likely to walk or cycle, leading to other health problems that are related to a sedentary lifestyle, for instance, ischaemic heart disease and even obesity [10]. The fear of falling, especially for the elderly, can also be observed and cause social isolation or even anxiety. All these points are assembled in the European Sustainable Development Goal (SDG) 3, which aims to ensure healthy lives and promote well-being for all ages. In particular, target 3.6 aims to considerably decrease the death rates caused by road traffic accidents and related injuries [37].

### **2.2. Recycling and Responsible Consumption for Sustainable Urban Communities**

While designing new solutions, the environmental and sustainable perspective must be included in the technical performance requirements. Undeniably, using recycled materials instead of non-renewable resources is an effective method. The pavement industry represents one of the open improvement sectors where the use of recycled tyre rubber, in different shapes, offers a means to increase the life cycle of the overly engineered tyres, reduce CO<sub>2</sub> emissions, reduce the use of raw virgin mineral materials, and improve citizens' quality of life [38]. Numerous SDGs are associated with this approach to encourage cities to become more resilient and sustainable. The

responsible consumption of already existing materials also impacts the protection of lands and reduces ecosystem degradation. The climate can also be indirectly preserved. Therefore, along with SDG 3, SDGs 11, 12, 13 and 15 are also linked directly or indirectly to the research on the development of IAPs [37].

For pavement materials, the stiffness modulus is a crucial value in the analysis of the stress-strain response behaviour under a traffic load [39]. The traditional flexible pavements need high stiffness that allows heavy vehicles to apply a load without large deformation. Contrary to the currently used road materials, a low-stiffness elastic pavement can withstand larger deformations and spring back to its original dimensions. The deformation of the material makes possible the absorption of the impact forces. This is the reason why cars' external materials can deform to absorb the energy created by the impact of an accident. Therefore, a low stiffness pavement is considered a valid development to reduce the risk of injuries in case of a fall onto the pavement, thanks to the elastic properties of the recycled crumb rubber, which have been exploited for many years to enhance the flexibility and elasticity of road pavements. This material can be used as a carrier of the required stiffness. In fact, the incorporation of crumb rubber (CR), itself a low-stiffness material, in substantial quantities can decrease the stiffness of traditional pavement surfaces while contributing to their durability (fewer cracks) and the waste management of End-of-Life Tyres (ELTs) [32,40]. Therefore, the main objective of this research is to design an innovative surface layer by using CR from ELTs, allowing the reuse of waste materials in parallel with reducing the risk of injuries for fallen VRUs in the urban environment [28,29].

### **2.3. Inspirations and previous studies**

The present research is inspired by playground paving materials that are used to reduce children's injuries in parks and are often partly made of recycled rubber. To rethink them for applications in urban pavements is the main challenge in terms of developing Impact-Absorbing Pavements [28,29]. The proposed innovative paving material should be able to abate the risks of injuries for VRUs in all weather conditions and, at the same time, be durable and friendly to the environment, including the absence of emissions, fumes, or odours, without chemical leaching and particle release. Furthermore, the developed material should be produced and laid using existing technologies, and it should withstand occasional slow and heavy traffic during maintenance. Two major studies have recently been conducted on cement concrete, and asphalt concrete mixes containing high rubber contents to develop shock-absorbing properties for pavements [27–29]. The main application for those low stiffness pavement layers is limited to sidewalks and bicycle lanes. According to these studies, while mentioning IAPs, the comfort and appearance (survey-based), the stiffness (compressive strength and elastic compressive modulus), the friction or ice-affinity properties (friction tester), and impact-attenuation capabilities (according to

falling speed, height, area of impact, and severity, as measured via the Head Injury Criterion (HIC)) [41] are the main criteria to be adopted for the materials' characterisation [2].

Another study on rubberised shock-absorbing concrete [27] showed that it is possible to produce rubber-modified (from 59 to 77% rubber volume) concretes with sufficient load-bearing capacity for cyclists and pedestrians. The results were based on the compressive strength and elastic modulus inputs of the succession of produced samples (up to 7 MPa). These values were compared to the pressure applied by an 80 kg human walking on the material with flat-heeled shoes. The tested materials resisted the deformation applied by this pressure. However, constraints were raised about the unknown behaviour of those materials over time, as well as adverse weather conditions.

Previous studies on concrete and asphalt concretes [28,29] have demonstrated the effectiveness of high-rubber-content material on the significant decrease in HIC values. The feasibility of laying a 63% (volume) rubber content material was also proven. In Sweden, laboratory results were confirmed by field trials at the AstaZero testing facility [29]. This in situ experiment was conducted to collect information on the behaviour of the material in outdoor conditions and to evaluate the users' comfort and riding impressions regarding the experimental materials.

At present, the preliminary studies on high-content rubber materials to reach valuable shock-absorbing properties are considered the starting point of the ongoing research. Considerable assessment efforts are necessary for the durability of the proposed materials. Furthermore, the impact-absorbing properties must be consistent over time and in different weather conditions [28].

#### **2.4. Implementation of the current study**

As previously mentioned, this research focuses on bituminous mixes for flexible pavements with shock-absorbing properties. It should be used as an alternative pavement for footpaths and bicycle lanes, improving the life cycle of tyres while reducing VRUs' injuries through durable, softer, safer and recycled material.

Tyre rubber is being used successfully as the primary component in terms of volume on playground materials. However, the mixing, production and construction methods are significantly different from those of bituminous asphalt paving (for example, handwork and non-bituminous binders). The challenge with this material is to ensure that it is produced and laid following the same methods as those already used in the asphalt industry. In this industry, when it comes to rubberized asphalt, the amount of rubber in the mix is limited and never reaches values comparable to those of playgrounds.

With this study, the objective is to introduce a new manner of producing impact-absorbing pavements. The aim is to implement and deploy this solution on urban roads and lay several meters with better conditions for the workers. By using known methods and existing machinery and facilities, the development of such material can have a better future, for instance, in terms of costs. Different formulations with distinct quantities of recycled rubber and binders have been produced and tested. The selected starting mixture is based on a typical Hot Rolled Asphalt (HRA), also known for containing a relatively large quantity of fine aggregates compared to other standard dense mixes. The mix design goal is to substitute a volume of natural fines with a graded quantity of CR (0–4 mm). The supplied CR was preliminarily analysed, focusing on the possible release of chemicals, using the most suitable types of PAH (Polycyclic Aromatic Hydrocarbon) analysis [42].

Traditional bituminous mixture characterisation has been performed at different temperatures, including the Indirect Tensile Stiffness Modulus test [43], the Indirect Tensile Strength test [44] and the Cantabro loss test [45]. The tests aimed to quantify the stiffness and the abrasion resistance properties of the different asphalt materials. Furthermore, due to the significant amount of rubber inside the mixtures, the specimens were also tested to comply with the playgrounds' or artificial tracks' testing methods, i.e. the HICs and the CFHs were also measured.

Those preliminary tests were meant to optimise the material in terms of the use of recycled materials, their stiffness and strength, their layer durability and the impact-attenuation performance of the IAP.

## **2.5. Materials and Methods**

### ***2.5.1. End-of-Life Tyre rubber***

The waste management of the ELTs and the CR production were undertaken in Sweden. These CR were used for the experimental production of IAP samples. They were produced using the ambient shredding process and were classified into three different size distributions ranging from 0 mm to 4 mm, as illustrated in *Figure 1.1*.



Figure 1.1: CR particles used in the experimental mixtures: Coarse, Medium and Fine.

Several tests were performed to measure the main characteristics of the rubber samples (**Table 1.1**). The parameter linked to the chemical characteristics and exposure risks for the workers and daily users of products containing rubber granules (e.g., playgrounds, road pavements, artificial turfs and suchlike) was also measured. One of the most significant values was that representing the presence of eight Polycyclic Aromatic Hydrocarbons (PAHs 8), which were limited to a total concentration of 20 mg/kg (0.002 % by weight) by the European Chemicals Agency [42,46,47].

Table 1.1: Typical properties of the experimental crumb rubber.

Crumb Rubber (CR) granulates	Particle size (mm)	Bulk Density <sup>1</sup> (kg.m <sup>3</sup> ) EN 1097-3	Specific gravity <sup>2</sup> EN 1097-6	PAHs 8 REACH <sup>1</sup> (mg/kg) (specification ≤20)
Fine (F)	0–1.2	0.440	1.028	6.5
Medium (M)	1–2.8	0.440	1.028	6.5
Coarse (C)	2.5–4	0.440	1.028	6.5

<sup>1</sup> Value given by the supplier. <sup>2</sup> Measured values.

In addition to the values of PAHs 8 given by the supplier, a complete analysis of 16 PAHs was performed. PAHs represent a class of organic compounds that can cause severe health issues if not under control. Eight of them are usually subject to limitations (PAHs 8). At the same time, it is strongly recommended by the European legislations to analyse the group of sixteen (PAHs 16) for their potential health and ecological influence by skin contact, inhalation or ingestion through food, for instance [42,46,48]. The lower the amounts of detected PAHs, the better the tested materials are in terms of risks for the health and the environment. The objective of the limitation is to ensure that the cancer risk from PAH exposure remains at a low level for the users who are in contact with the rubber granules. That includes workers installing and maintaining the rubberised surfaces, players using the pitches or playgrounds [42,47], or the potential VRU of the developed IAP.

Determination of the PAH content was made following the AfPS GS 2014:01 PAK standards [46]. The results and limits are presented in **Table 1.2**.

Table 1.2: Results from the PAH analysis.

PAH 16	Concentration detected (mg/kg)	Sum of PAH detected (mg/kg)
TOTAL PAH 16		Sum 16 PAH Approx.2.3
Naphthalene	< 0.5	Sum PAH-L < 1.5
Acenaphthylene	< 0.5	
Acenaphthene	< 0.5	
Fluorene	< 0.5	Sum PAH-M Approx. 1.0
Phenanthrene	< 0.5	
Anthracene	< 0.5	
Fluoranthene	< 0.5	
Pyrene	1.0	
Benzo a anthracene	< 0.5	Sum PAH-H Approx.1.3
Chrysene	< 0.5	
Benzo b,j fluoranthene	1.3	
Benzo k fluoranthene	< 0.5	
Benzo a pyrene	< 5	
Indeno123cdpyrene	< 5	
Dibenzo ah anthracene	< 5	
Benzo ghi perylene	< 5	

### 2.5.2. Bituminous binder

The binder used in this study was a 25/55 Styrene-Butadiene-Styrene (SBS) modified bitumen (PmB 1) specifically designed for the incorporation of rubber into the bituminous binder at lower production temperatures (i.e., 160°C). The density of the binder was 1.050 g/cm<sup>3</sup>. The typical binder parameters values are shown in **Table 1.3**.

Table 1.3: Characteristics of 25/55 Polymer-Modified Bitumen.

Measured Properties <sup>1</sup>	Unit	Value	Standard
Penetration @25 °C	0.1 mm	25/55	EN 1426
Softening point	°C	≥ 70	EN 1427
Flashpoint	°C	≥ 250	EN 2592
Dynamic viscosity @160°C	Pa·s	≥ 0.4	EN 13702-1
Fraass breaking point	°C	≤ -15	EN 12593

<sup>1</sup> Values from the binder supplier.

### 2.5.3. Virgin aggregates

Limestones, basalt, mixed sand and a commercial limestone filler were used as natural lithic skeletons and additives for the asphalt mixture. The aggregates came from different Italian suppliers, and their characteristic values are shown in **Table 1.4**.

Table 1.4: Properties of the virgin aggregates.

Virgin aggregates <sup>1</sup>	Particle size (mm) EN 933-1	Specific Gravity EN 1097-6
Limestone 1	8–14	2.661
Limestone 2	4–8	2.669
Sand	0–4	2.608
Basalt	0–2	2.685
Limestone filler	≤ 0.063	2.667

<sup>1</sup> Measured values.

The entire experimental plan is represented in **Figure 1.2**. The work was divided into three main sections: the mix design, the production of specimens and the compacted materials' characterisation.

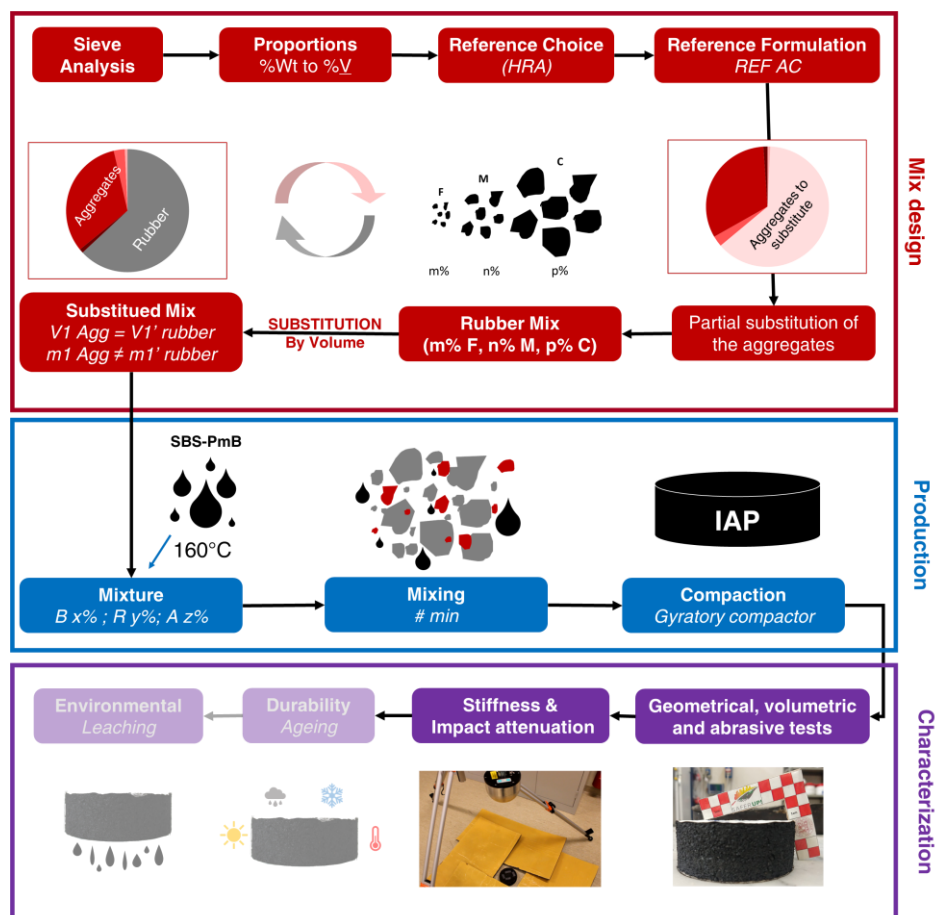


Figure 1.2: Scheme of the experimental investigations' approach.

### 2.5.4. Mix design and production of specimens

The chosen reference mix is a Hot Rolled Asphalt (HRA). It is a dense material containing a considerable amount of sand and other fine materials. The mix design process and its proposed formulations were designed using the weight and the volume units to calibrate the substitution of sands with large amounts of rubber in the mixtures. Firstly, the rubber bulk density (given by the supplier) was used for the

initial mix proportions to obtain an estimated volume fraction [29]. All experimental values are reported in *Table 1.5*.

The production of samples required mixing the aggregates with bitumen (160°C) before adding the rubber. All constituents were mixed into a homogeneous binder coating before being compacted using a standard gyratory compactor. The compaction was performed using an angle of 1.250°, an applied pressure of 600.000 KPa, and a speed of 30.000 Rpm, and by applying 80 cycles (*Figure 1.3*)



Figure 1.3: Production steps for the rubberised impact-absorbing pavement (IAP) samples.

Firstly, IAP samples with fixed amounts of rubber (IAP 2a, IAP 2b and IAP 2c) were produced to identify the quantity of binder needed to prevent the loss of particles. Afterwards, samples with a fixed amount of bitumen were produced with four different amounts of rubber (REF, IAP 1, IAP 2a, IAP 3). All mixtures' proportions are detailed in *Table 1.5*.

Table 1.5: Content of each mix by weight and by volume based on the aggregate and the total mix.

Mixtures	% Weight			% Volume				
	Name	Rubber size	% Rubber (aggregates)	% Rubber (total mix)	% Binder (total mix)	% Rubber (aggregates)	% Rubber (total mix)	% Binder (total mix)
REF AC /			0	0	8	0	0	8
IAP 1	FM		17	14	18	35	30	14
IAP 2a	FM		34	28	18	63	52	16
IAP 2b	FM		34	27	21	63	51	19

IAP 2c	FM	34	27	23	63	50	21
IAP 3	FMC	41	33	18	66	56	15

### 2.5.5. Characterisation

A procedure was developed using standard asphalt mixture characterisation methods to analyse the samples and evaluate the different rubberised bituminous mixtures' mechanical and impact-attenuating performances. The laboratory test and their order are schematised in **Figure 1.4**. The developed protocol includes geometrical and volumetric analysis and mechanical, abrasive and impact-attenuation tests.

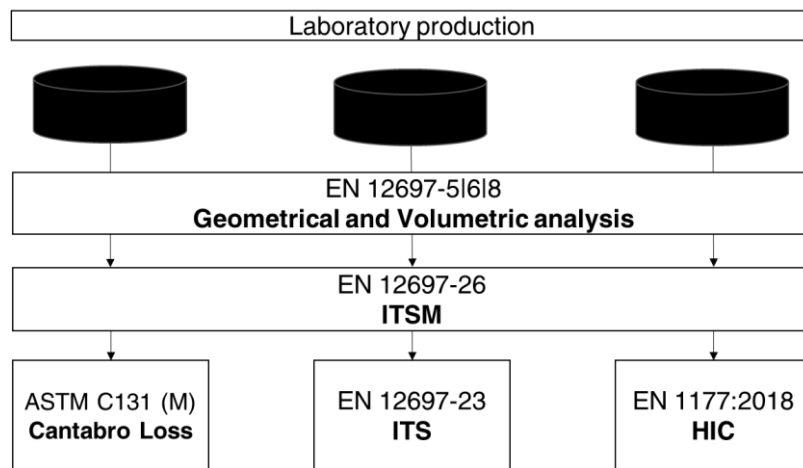


Figure 1.4: Developed testing procedure for the assessment of the basic performance of IAP.

#### 2.5.5.1. Geometrical and volumetric analysis

After producing the cylindrical samples, the first characteristics to be measured were the weights and dimensions. After compaction, the vertical and horizontal expansion, which mainly occurred due to rubber swelling, were also measured. Indeed, after compaction, an internally measured height value was given by the compactor. This height was verified manually a few minutes after compaction, and an expansion was recorded. This manual measurement was also repeated 15 days and 1 month, and 6 months after the time of the samples' production.

#### 2.5.5.2. Cantabro loss test

The Cantabro loss (CL) method [45] is generally used to determine the abrasion loss of compacted asphalt samples using the Los Angeles abrasion machine. This machine can induce the loss of abraded material via rotation for several cycles at a fixed speed (30–33 rpm for 300 revolutions).

The CL can function as an indication of the durability and the resistance to abrasion of the sample by means of the following equation:

$$CL [\%] = \frac{m_i - m_f}{m_{fi}} \times 100 \quad (1.1)$$

*CL: Cantabro loss (%)*

*m<sub>i</sub>: the initial mass of the specimen (g)*

*m<sub>f</sub>: the final mass of the specimen (g)*

Only the IAP 2 and REF AC (as the first produced samples) were tested using the Cantabro loss testing procedure. This was because of doubts that arose regarding the method's effectiveness for the designed samples. This doubt was clarified later, thus confirming the Cantabro test method as effective for testing highly rubberised IAP samples.

#### 2.5.5.3. Indirect Tensile Stiffness Modulus (ITSM) and Indirect Tensile Strength (ITS)

The preliminary mechanical characterisation was mainly performed by employing the Indirect Tensile Stiffness Modulus (ITSM) [43] and the Indirect Tensile Strength (ITS) [44] tests on cylindrical samples. These are very common and referenced testing methods for compacted samples of asphalt concrete. The ITSM, determined by the IT-CY method, is a non-destructive test that provides data on the stiffness of the sample at a specific temperature (it was conducted at 5°C and 10 °C), while the ITS measures the maximum tensile stress, calculated from the peak load applied at failure of the sample. The ITS test was conducted at 10°C and 25°C.

#### 2.5.5.4. Head Injury Criterion (HIC)

Several injury criteria exist to determine the effects of a collision, a fall or an impact as the origin of injuries. The neck injury criteria (NIC), the tibia index (TI) and the HIC are related to head injuries [49]. Determined after a series of tests on cadaveric heads in the 1960s, this value is nowadays derived from the measurement of acceleration and fall time thanks to accelerometers and sensors inside of an artificial concentric head (approx. 5 kg in mass). The falling device simulates a simplified version of adult human head behaviour during an impact. Frequently used in impact sports or collision studies, the HIC is an excellent indicator of the damage that could be caused to the skull and brain, and it is defined as:

$$HIC = \left\{ \left[ \frac{1}{t_2 - t_1} \int_{t_1}^{t_2} a(t) dt \right]^{2.5} (t_2 - t_1) \right\}_{max}, \quad (1.2)$$

*t<sub>1</sub>: start time*

*t<sub>2</sub>: end time*

*a: acceleration*

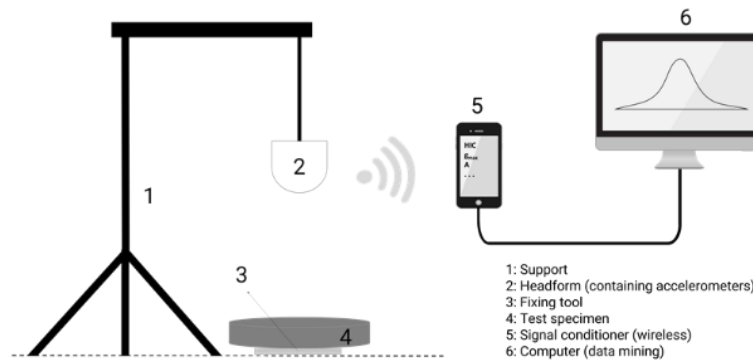


Figure 1.5: Scheme of the impact-attenuating properties testing method.

To test the IAPs, the present study used testing methods that were established for the assessment of the impact-attenuation properties [10] and which are usually employed to measure the impact attenuation of surfacing materials. A scheme and pictures of the test device and the testing set-up are shown in **Figure 1.5** and **Figure 1.6**, respectively. Through the measurement of the severity of a head injury that is likely to arise from an impact, i.e., HIC, the method allows the calculation of the Critical Fall Height (CFH) of the pavement and the maximum Free Height of Fall for which a paved surface provides an adequate level of impact attenuation. A HIC lower or equal to 1000 is considered an acceptable limit for playgrounds [41]. The HIC can also be related to the Abbreviated Injury Scale (AIS) used to classify injuries from abrasion (1) to a fatal injury (6) [50]. **Table 1.6** shows the classification of the injuries according to the HIC values.

Table 1.6: Abbreviated Injury Scale AIS classification of the injury type by HIC [20].

HIC	AIS code	Severity	Description
> 1860	6	Maximum	Fatal, not survivable.
[1859–1575]	5	Critical	Unconscious for >24 hours; large hematoma
[1574–1255]	4	Severe	Unconscious for 6–24 hours; open skull fracture
[1254–900] 1000	3	Serious	Unconscious for 1–6 hours; depressed skull fracture
[899–520]	2	Moderate	Unconscious for <1 hour; linear skull fracture
[519–135]	1	Minor	Headache or dizziness
< 135	0	Null	No injury

The instrumented artificial head strikes the tested surface from different drop heights. The signals emitted by the accelerometers in the device during each impact are processed to yield a severity from the measured impact energy, defined as the HIC, and to determine the peak acceleration ( $g_{max}$ ). The method determines the drop heights at which HIC is at a maximum of 1000, and the  $g_{max}$  is 200. This procedure is used to calculate the CFH of the impacted pavement [3].

The IAPs' samples were tested at different temperatures ranging from  $-10^{\circ}\text{C}$  to  $+40^{\circ}\text{C}$  to obtain an extensive range of values corresponding to the various climate conditions.

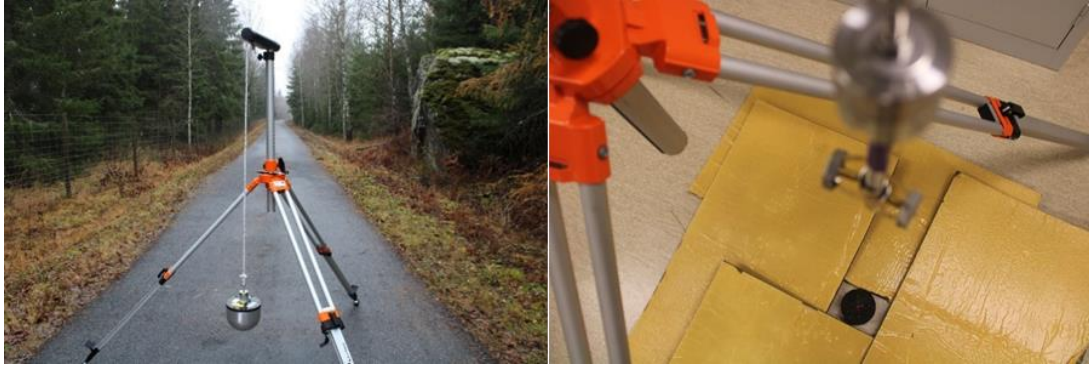


Figure 1.6: pictures of the hic test device installation ready for in-situ (left) and laboratory (right) testing

## 2.6. Results and Discussion

### 2.6.1. Geometrical and Volumetric assessment

For each mix, a minimum of three replicates were produced to perform the planned tests. The preliminary visual assessment and test measurements provided valid initial information on the overall performance of the rubberised samples. Specific geometrical and mass measurements allowed the calculation of the specimens' densities and air void content. The results are listed in **Table 1.7**.

All compacted samples were in satisfactory initial conditions, and their inner cohesion and adhesion appeared to be sufficient to keep the lithic and rubber particles together after the extraction from the compaction mould. The specific weight of IAP specimens containing high amounts of rubber was approximately 1/3 less than the reference asphalt concrete specimens' value. **Figure 1.7** directly compares the two pictures of the reference standard asphalt and the IAP 2a specimens.

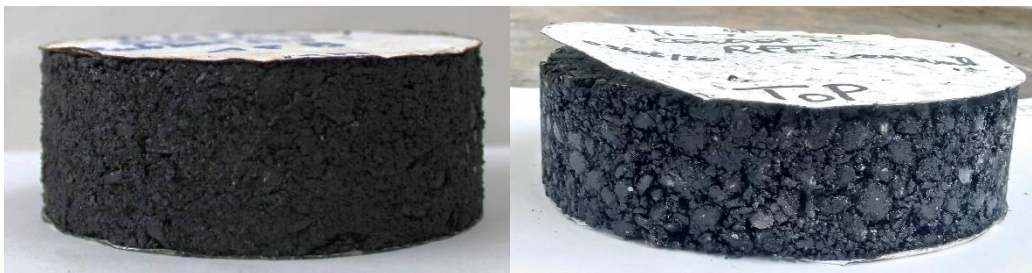


Figure 1.7: Overall aspect of compacted IAP 2a (left) and reference AC (right).

The geometrical measurements of the specimens showed an anisotropic volumetric expansion that occurred independently of the origin or type of rubber and bitumen. This phenomenon was due to the content of the rubber, its elastic recovery after compaction, and the swelling reactions that occurred due to the bitumen/rubber interactions. This expansion also caused the loss of some rubber particles from the

external specimen surface after compaction. The expansion developed with a high-volume rate variation directly after the compaction and slowly faded with time. **Figure 1.8** describes the development of the vertical expansion one month and six months after the time of production for most of the mixes.

This phenomenon was hardly visible with the AC reference samples, while it was more evident in the rubberised samples. The average expansion value of IAP 3 was lower than those of IAP1 and IAP 2a, despite containing more rubber in terms of percentage. However, IAP 3 contained coarse aggregates while IAP 1 and IAP 2a did not. By reducing the available surface and porosity for the diffusion causing the swelling, this phenomenon, initiated between the bitumen and the rubber, was reduced, and expansion of the sample was consequently limited.

Table 1.7: Densities and air voids content values for each tested mixture.

Mixes	EN12697-6 D Density (g/cm <sup>3</sup> )	EN12697-5 Maximum Density (g/cm <sup>3</sup> )	EN12697-8 VA (%)	EN12697-8 VMA (%)	EN12697-8 VFB (%)
REF AC	2.273	2.207	2.9	33.7	91.4
IAP 1	1.740	1.605	7.8	38.0	79.6
IAP 2a	1.460	1.383	5.2	38.9	82.8
IAP 2b	1.541	1.423	7.7	42.4	80.3
IAP 2c	1.654	1.586	4.1	30.1	90.4
IAP 3	1.443	1.371	5.0	33.7	83.4

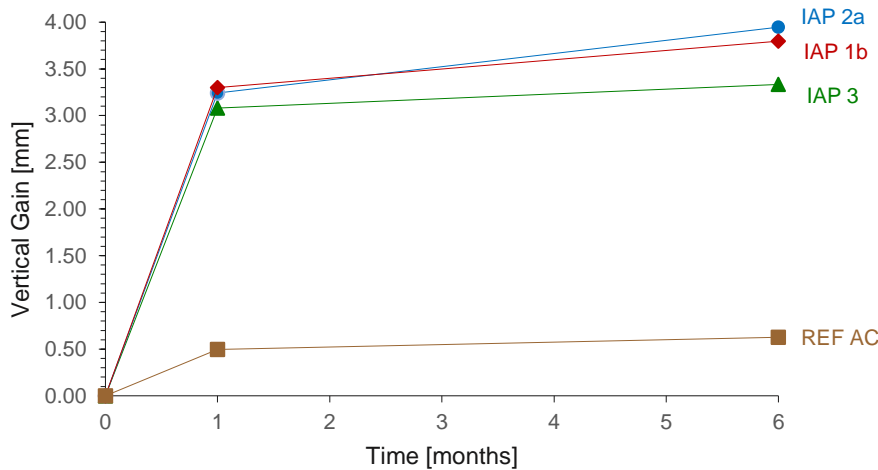


Figure 1.8: Vertical expansion after one month and six months for the mixes REF AC, IAP 1, IAP 2a and IAP 3.

### 2.6.2. Cantabro loss and abrasion results

**Figure 1.9** shows that the material abrasion was reduced (by approximately 4–5 times) for the reference sample as compared to the rubberised samples. This seemed to be caused by the addition of high quantities of rubber in the mix, which provided elastic properties to the samples that could partially bounce inside the Los Angeles apparatus. Even if the binder significantly influenced the particle’s loss, the difference

between IAP 2a (18% wt. binder) and IAP 2b (21% wt. binder) was negligible. Although the severity of the tests seemed to be reduced with bouncy samples, the results of the rubber specimen were still noteworthy.

Even if the test was conducted only for the REF AC and IAP 2 samples, the results with IAP 3 would most likely be comparable to those of IAP 2a. and with IAP 1 having higher loss values than the IAP 2 samples.

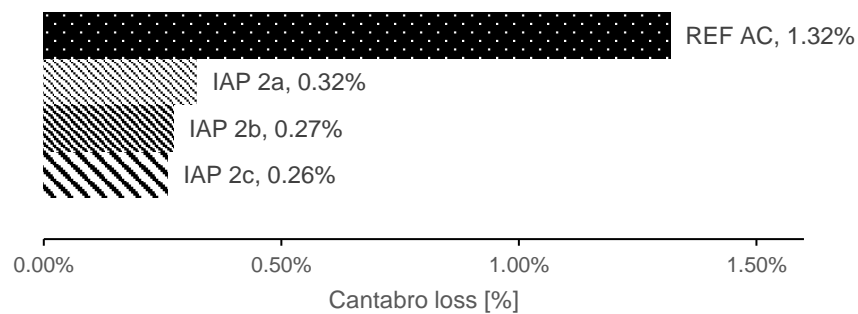


Figure 1.9: Cantabro loss showing the abrasion properties of the tested specimens.

### 2.6.3. Pavement mechanical performances

ITSM and ITS tests could give valid insights into the stiffness modulus and the required stress for the initiation of tensile cracking of the sample. However, even if the tests were conducted at cold temperatures, it was challenging to measure consistent values. The prominent elastic behaviour of the material influenced the actual observation of the cracks and, thus, the effective value of the indirect tensile strength. **Table 1.8** shows that at 5°C, the mechanical properties of the rubberised asphalt differed from the reference material, and the stiffness was considerably reduced by the addition of rubber even at low test temperatures (5°C and 10°C). The obtained modulus was reduced by more than six times when comparing the reference material with IAP 3, the mix that had a higher quantity of rubber (**Table 1.8**).

The tested samples gave promising results in terms of the final objective of reducing the impact severity by decreasing the material's stiffness. Alternative methods such as direct tensile, stress relaxation and compression tests are foreseen to improve and optimise the mechanical measure of the rubberised materials.

Table 1.8: Average tensile strength and stiffness modulus of the different mixes.

Mixes	ITS (MPa) 10°C	ITS (MPa) 25°C	Stiffness modulus (MPa) 5°C	Stiffness modulus (MPa) 10°C
REF AC	2.69	1.78	12,496	11,654
IAP 1	0.91	/	1236	/
IAP 2a	0.36	0.35	301	229
IAP 2b	0.51	0.31	273	194

IAP 2c	0.48	0.26	202	124
IAP 3	0.44	0.29	248	/

### 2.6.4. Attenuation of impacts and injury prevention

#### 2.6.4.1. Influence of the rubber amount

The use of CR in large quantities had a beneficial effect on the circular use of tyres, the recycling of the rubber and the elastic properties of the newly formulated impact-absorbing bituminous material. The IAP 3 samples attenuated more the impacts than the IAP 2, IAP 1 or REF AC samples. Indeed, from the same dropping height, the AIS code was reduced to 0 (null) with IAP 3, while it was 3 (severe) for the REF AC samples (**Table 1.9**). Moreover, as shown in **Figure 1.10**, by increasing the amount of rubber, the drop height could be increased, albeit still recording lower HIC values than those obtained from the REF AC. A rough direct relationship can be seen between the increase in impact-absorbing properties and the quantity of rubber.

Table 1.9: HIC and related AIS code corresponding to the fall for each specimen from an equal drop height (0.2 m) at  $T_{amb}$ .

Mixes	%Rubber (wt.)	Drop Height (m)	HIC	Standard deviation HIC	Related AIS code
REF AC	0	0.2	1111	6	3
IAP 1	14	0.2	470	46	1
IAP 2a	28	0.2	160	17	1
IAP 2b	27	0.2	170	19	1
IAP 2c	27	0.2	109	9	0
IAP 3	33	0.2	114	5	0
*PLAYGROUNDS	> 50	0.2	22	/	0
*RUBBER CONCRETE	20–30	0.2	195	/	1

Values obtained in preliminary studies [29].

Furthermore, the head impact altered the REF AC sample surface after several drops, while the IAP 3 sample was almost intact. This can also be considered a positive outcome in terms of the surface durability of the highly rubberised samples. The pictures in **Figure 1.11** clearly support these observations. White tape was used as a tool to delimitate the impacted zone during the HIC test. The impacted zone for IAP3 was higher. This variation was due to the need to modify the test head height more often than for the reference (higher drop height). Thus, the impact zone precision was lower, while the REF AC needed a few set modifications during the test. However, at a lower drop height, the surface of the REF AC was more degraded. Therefore, the achievement of the required impact-absorbing properties did not negatively affect the surface durability of the material.

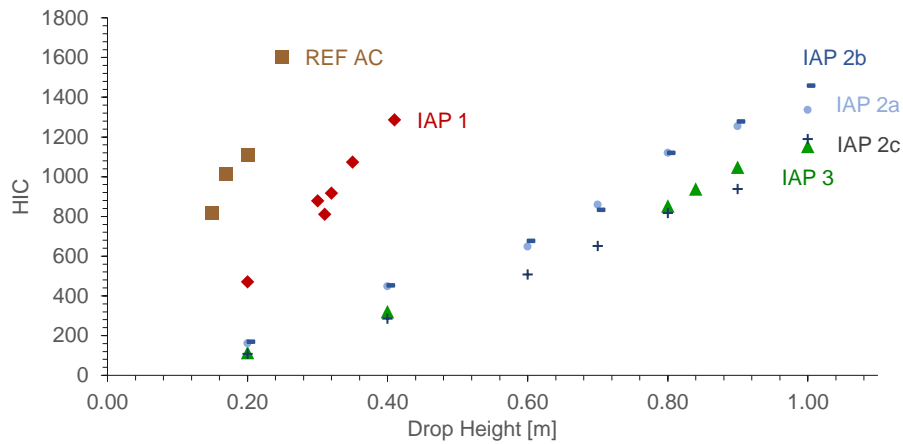


Figure 1.10: Laboratory HIC values when increasing the dropping height at room temperature ( $22^{\circ}\text{C}\pm 1^{\circ}\text{C}$ ).



Figure 1.11: Tape-delimited impacted zone after several drops of the HIC-meter head: REF AC (left); IAP 3 (right).

#### 2.6.4.2. Influence of the testing temperature

In addition to the rubber quantity, the temperature had a considerable influence on the measured HIC values. Consequently, the CFH was also affected by temperature. Intuitively, for these kinds of visco-elastic materials, the impact-attenuating properties at  $40^{\circ}\text{C}$  are higher than those at  $-10^{\circ}\text{C}$ . All the test results are shown in **Figure 1.13**.

Even if **Figure 1.13** clearly shows that IAP 2c had better attenuation properties than IAP 3 at  $40^{\circ}\text{C}$ , the influence of the rubber variable was predominant over the binder dosage one. When the amount of bitumen increased, the sample with the largest quantity of bitumen for a given volume of rubber exhibited a slight increase in the CFH values at high temperatures. In general, the targeted amount of bitumen should be as low as possible to limit costs. Moreover, the CFH at  $-10^{\circ}\text{C}$  or  $-2^{\circ}\text{C}$  for IAP 3 was still higher than the CFH of IAP 2c at the same temperature and the CFH at  $+40^{\circ}\text{C}$

for IAP 1. As the IAP 2 and IAP 3 mix had similar behaviour, IAP 3 was found to be preferable as an impact-absorbing material for the above-mentioned reasons.

#### 2.6.4.3. Influence of the testing layer thickness

To evaluate the thickness influence on the HIC values, samples were assembled by simple superposition in the laboratory, as shown in **Figure 1.12**. Hence, the IAP 2ab (approx. 90 mm) and IAP 2abc (approx. 130 mm) compositions made it possible to compare the behaviour of HIC and CFH with different layer thicknesses. A double-sided adhesive was used between the samples.

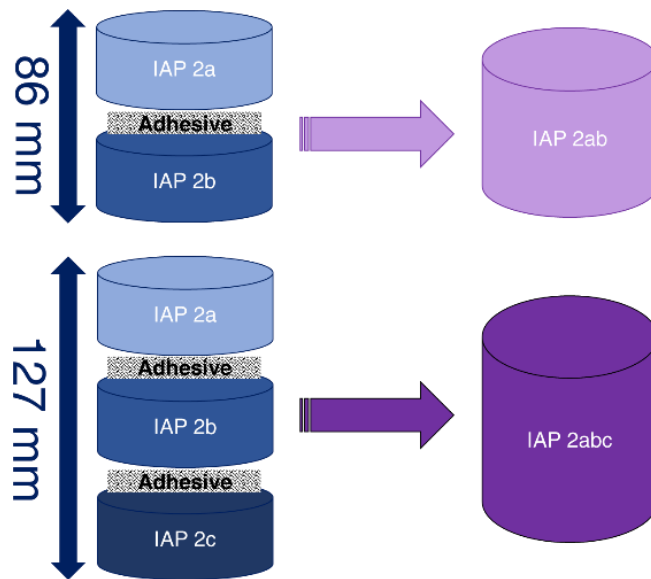


Figure 1.12: Scheme of the samples assembly to assess the influence of the layer thickness.

Augmenting the layer thickness from 4 cm to 9 cm increased the CFH values by approximately 0.5 m. Besides, when the layer height was increased to 13 cm, the CFH values were approximately doubled, as shown in **Figure 1.13**.

Even if the 4 cm thick IAP 3 sample had a positive effect in terms of lowering the AIS code to 0 and, therefore, approached the recommendations for playgrounds (i.e. **Table 1.9**), the goal for the present application was to have a CFH above 1 m (even at low temperatures). In fact, a CFH higher than 1 meter is considered the minimum requirement for validating the formulation as adequate in terms of reducing injuries from VRUs' falls. The objective is to be far below the reference value of the concussion HIC 1000 [51].

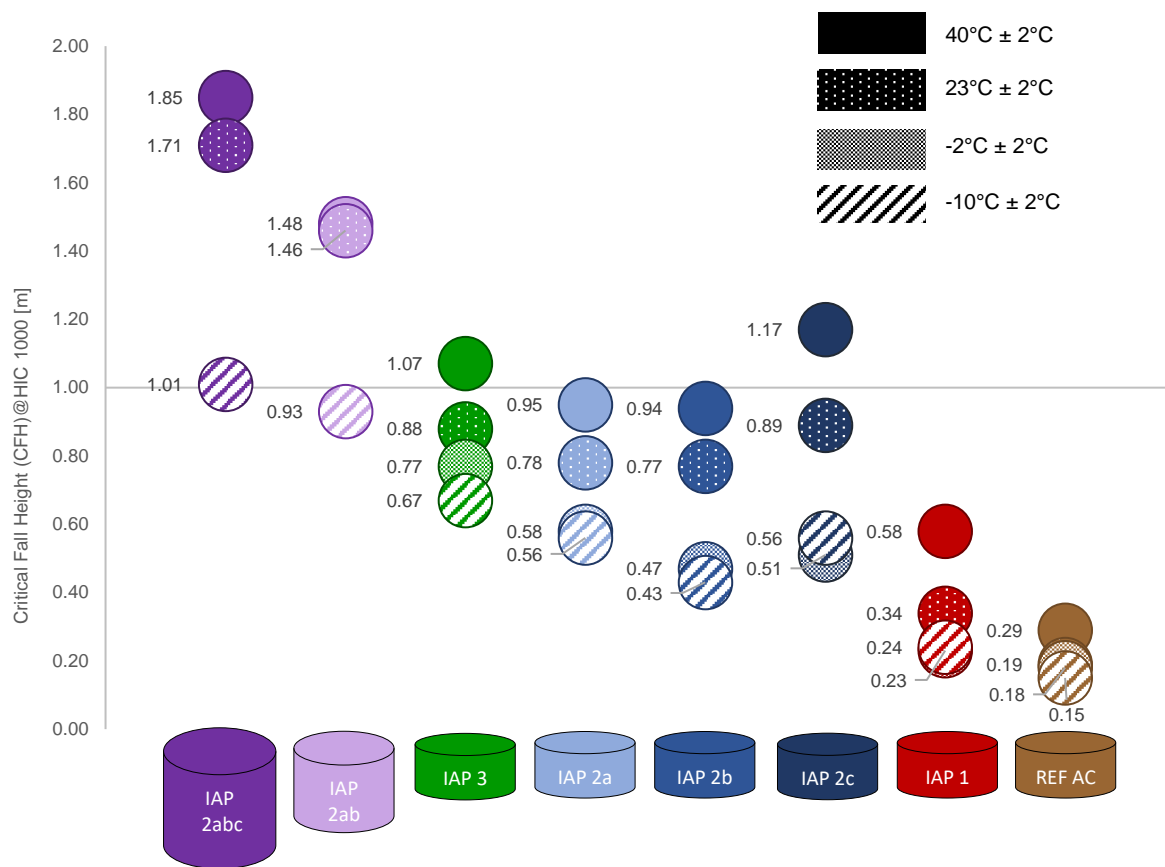


Figure 1.13: CFH at HIC=1000 including IAP 2abc and IAP 2ab @ four temperatures: -10°C, -2°C, 23°C and 40°C.

## 2.7. Conclusions

The laboratory work performed on the different formulations provided noteworthy results. The main relevant and preliminary conclusions that can be drawn are as follows:

- Adopting the dry process method made it possible to produce samples with a rubber content larger than 30% total weight (larger than 50% total volume). Those bituminous samples also contained coarse crumb rubber particles (0 mm to 4 mm size).
- The bitumen quantity should be kept as low as possible for a given rubber amount as the CFH variation observed between the IAP 2a 2b 2c and IAP 3 was not significant.
- The swelling reaction played a role in the geometrical expansion of the material. However, the addition of a high amount of rubber did not cause critical abrasion behaviour when tested with the Cantabro loss method. The

percentage of loss was four times less than the reference asphalt, but future work will have to specifically assess the reliability of the applied test method.

- As a result of ITSM measurements, it was observed that for the IAP 3 samples containing 33% wt. rubber, the stiffness modulus was 40 times smaller than the reference asphalt. Additional stiffness or mechanical tests are needed to investigate different testing methods or conditions (i.e. simulating different climates).
- The greater the amount of rubber that was added, the higher the impact-attenuation effect that was measured through HIC, and the higher the calculated CFH. The addition of rubber consistently enhanced this property even at low testing temperatures.
- The obtained HIC and CFH were approaching the recommendations for playgrounds. IAP 3 samples lowered the AIS parameter from 3 (REF AC) to 0, thus reducing the risk of severe injuries.
- The optimal thickness of the pavement rubber layer appeared to be between 4 and 9 cm. The thickest samples recorded auspicious results even at cold temperatures. Thicker layers can require multiple layers using the traditional paving techniques.

The obtained results align with the targeted material characteristics; however, additional work is required to investigate other temperature conditions, as well as durability and surface properties. Furthermore, the mechanical analysis must be improved, and stress–relaxation or compression tests need to be incorporated within the mechanical characterisation procedure. The tests also raised interesting questions, especially regarding bitumen’s actual role in optimising the required impact-absorbing properties in terms of its quantity, costs and actual sustainability. The use of alternative binders, possibly bio-based ones, will be considered a means of increasing the sustainability of the materials.

### **3. Impact-Absorbing Pavements made with cold and warm asphalt binders and recycled rubber: a preliminary laboratory study.**

#### **3.1. Pedestrians and Cyclist safety and protection: the Impact-absorbing pavements concept for urban road infrastructures.**

Pedestrians and cyclists are among the Vulnerable Road Users (VRUs), who are the most at risk in traffic and are not protected by an external shield [11]. However, while considering their safety, especially in an urban area, pavement which can be responsible for incidents and is often the first contact surface for the VRU after a fall, is rarely the first element to be considered. In fact, road safety devices are mainly designed for wheeled vehicles even if already in 1998, up to 40% percent of the journeys in Europe were travelled by foot or bicycle [11]. Nowadays, the number of VRUs has increased, especially in the past months, due to the Covid-19 crisis. The immediate necessity to avoid shared transport means increased the need for urban areas to be correctly equipped to be able to welcome the amount of news VRUs encouraged by the governments to reduce car overuse [24].

However, several aspects, including the negative perception of bicycles and pedestrians' safety in cities, are making the habit change and the willingness to use the roads as a VRU difficult. Therefore, to foster safer shared urban space, the effort made on the VRUs' protection, through the development of more adapted and safe surfaces, is crucial to obtain a positive change [24]. Creating Impact-Absorbing Pavements (IAP) can be a starting point to the design of more adapted roads and policy changes to encourage the people to cycle or walk instead of massively using the car, another path to terrible environmental results and climate degradation. The role of such materials is to make the sidewalks or bicycle lanes' surface layer less dangerous and reduce possible humans' traumas and injuries resulting from falls (mainly). Playground materials are successfully used as paving materials to minimise injuries. However, the possibility of extending it to a more general use has been poorly investigated since then [27,29,52]. Indeed, adapting it to everyday use would mean that the IAP material should be able to abate the risks of injuries for VRUs in an urban area and be possibly produced, laid, and maintained using already known road paving methods.

#### **3.2. End-of-life tyres, waste management and recycled rubber.**

Alongside the technical properties required, the design of new solutions must consider and include an environmental perspective in the overall performance assessments. The responsible consumption of the resources through recycling has an essential role in the material's effect on the climate and the conservation of raw resources. To achieve this, recycled rubber is successfully used in the road industry as a waste transformed into a primary raw resource [31–33,53,54].

The circular use of tyres by exploiting the End-of-Life Tyres (ELTs) has a central place in the development of the flexible and impact-attenuating surfacing such as playgrounds or artificial turf. Bringing into the layers their elastic mechanical properties, the rubber crumb obtained after the shredding of ELTs can be introduced both in the binder (wet process) or as an aggregate (dry process) [32,55,56]. As the main component in a mix, the rubber can noticeably increase the impact attenuation properties of the material [57,52]. However, the use of a relatively high quantity of ELTs has shown several production-related issues such as reduced workability, smells, or release of fumes at high temperatures. The type and shape of crumb rubber, the adopted binder and the mixing temperatures are generally responsible for these possible issues that limit the exploitation of highly rubberised materials.

### 3.3. Previous studies

Some studies have been made to assess the possibility of producing and laying a material containing a consequent amount of rubber. Several mixtures with different rubber and binder content have been prepared and characterised to design testing procedure adapted from the bituminous mix one and be able to set reference values to a preliminary stage material.

The previous studies gave reference values on the targeted stiffness needed to confirm the good results of this material concerning the impact-attenuation properties. The mentioned values are reported in *Table 1.10*. From these previous studies, the production-related issues due to the high amount of rubber were the main constraints raised. In addition, the unknown behaviour of those materials in time or natural weather conditions has a significant role in the design method. The paper focuses on the assessment of these two main characteristics.

Table 1.10: Preliminary results and values from [57] and [29,52] studies

Mixtures	%Rubber (volume)	Stiffness [MPa]	Drop Height [m]	HIC	Standard deviation HIC	Related AIS code
*Reference	0	10095	0.2	1111	6	3 Severe
*IAP 3 Test 1 (PmB)	~50%	248	0.2	114	5	0 Null
**PLAYGROUNDS	>> 50	/	0.2	22	/	0 Null
**RUBBER CONCRETE	~50%	/	0.2	195	/	1 Minor

\* Preliminary study from [57]\*\* Preliminary studies [29,52]

### 3.4. Paper Focus

The innovative material intended to be designed originates from ELT management and recycling. It could not have existed without bringing this waste into new raw materials. The current article focuses on the feasibility of Impact-Absorbing Pavements (IAP) made with warm and especially cold asphalt binders, and a

significant amount of recycled rubber. The preliminary results obtained are discussed in this article.

The described research focuses on the temperature-related variables, studying warm (160°) and cold (20-25°C) temperature mix production using the dry process. The tested samples contained more than 30% weight (i.e., more than 50% volume) of rubber and were produced with five different binders: a Polymer Modified Binder (1), a 50-70 pen neat binder (2), a Latex modified bitumen emulsion (3), an SBS modified bitumen emulsion (4) and a synthetic non-bituminous emulsion (5).

The selection of mixes followed previous studies to optimise the rubber amount to get impact absorbing properties verified utilising the head injury criterion or with accident simulations [57]. The first mix contained more rubber particles (A), while the second had less rubber but more large aggregates to enhance the internal structure and possibly reduce the binder quantity (B).

Standardised and purposely adapted methods have been used for the production and the volumetric and mechanical characterisation of the materials, as well as for the conditioning and ageing of the various samples. The adaptation of known methods was needed to assess an unusual mix containing more rubber than generally.

Furthermore, to evaluate the durability and the effects of natural weather, the analysis was performed before and after a Natural Ageing Procedure (NAP) of 3 months under light-exposed, cold, and humid weather conditions. Temperatures ranged between 15 and -7 °C, with around 82% of humidity on average, including several rain and snow events and an estimated Ultra-Violet (UV) index of 2-3 corresponding to a low to moderate exposure level were reported.

After possibly identifying the best mixture according to the defined criteria like the workability, cohesion of the mixture, fume and smell release, impact attenuation, and durability, this research may enable the trials in the field to scale up the process. The favourable scaling of such a process may open the prospect of developing new production methods, implementing IAP, and observing good injury reduction numbers. Finally, after its end-of-life, the future of this material must be investigated to allow, if possible, its reinsertion in the process. **Figure 1.14** summarises the approach of the paper.

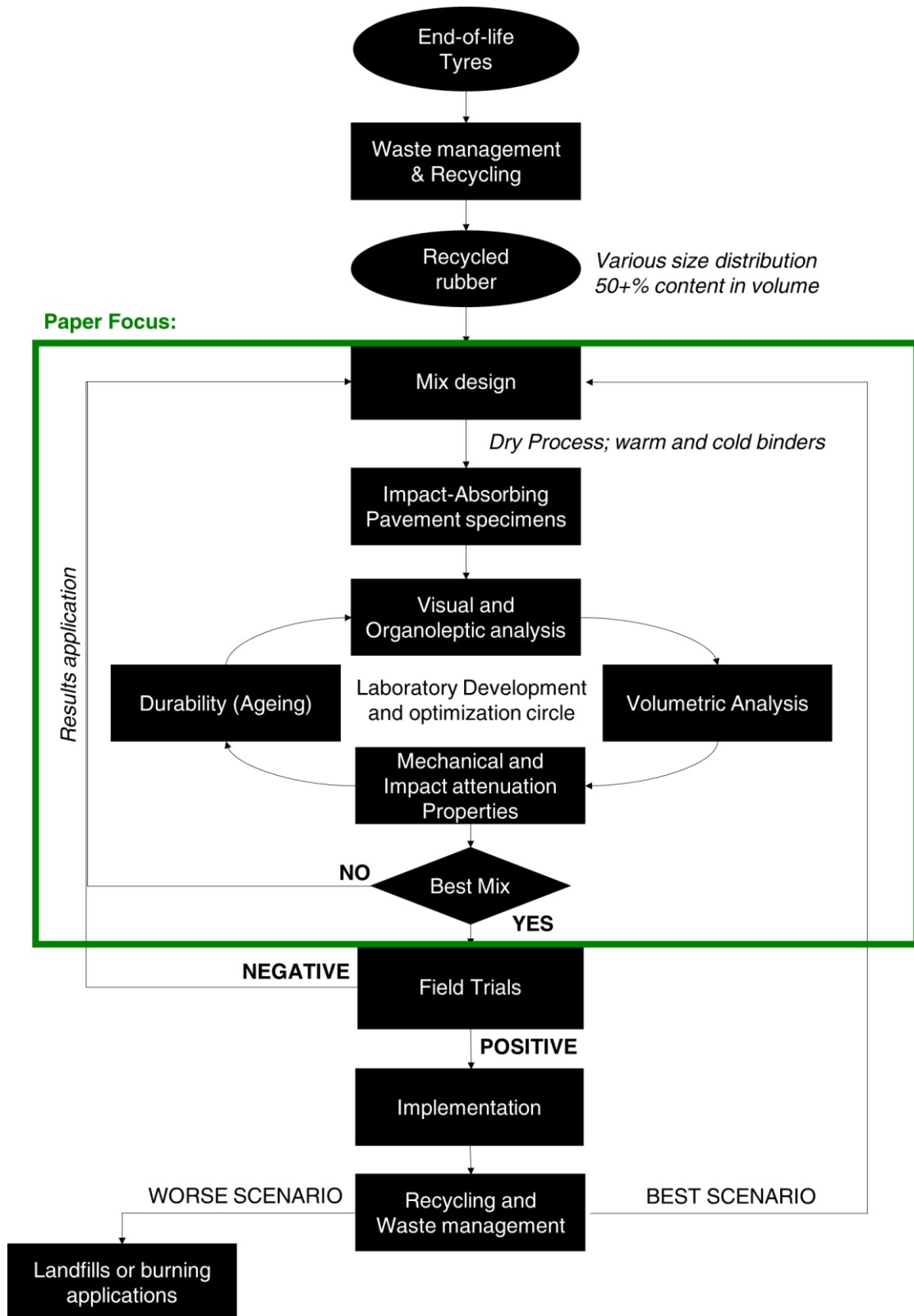


Figure 1.14: Article approach for impact-absorbing pavement design.

### 3.5. Materials and Methods

#### 3.5.1. Crumb rubber

The main component of the mixture is the recycled rubber. Crumb rubbers (CR) from End-of-life tyres (ELTs) coming from the European market were used. The CR was made using the ambient shredding process and classified into seven different granulate size distributions (from 0.8 to 7 mm). Only two fractions (Fine/mix 0.8-3.0 mm and Coarse 2.0-4.4 mm) were used for this trial to comply with the partial substitution of the mineral aggregates and fit the granulometric reference curve.

Before using the CR in the asphalt mixture, several tests have been generated to have typical information compiled in **Table 1.11**. Also, the parameter linked to the chemical characteristics and exposure risk of the worker and daily users of products containing rubber granules (Playgrounds, roads, artificial turfs ...) was included. One of the significant values is the Polycyclic aromatic hydrocarbons (PAHs) 8, strictly limited to 20 mg/kg (0.002 % by weight) [42]. The typical value for those rubber is below 15 mg/kg.

The rubber was not pre-treated to fully evaluate its behaviour in this novel mixture during the durability evaluation.

Table 1.11: CR typical values

Recycled Crumb Rubber granulates (CR)	Particle size [mm] ISO 13322-2	Bulk Density [kg.m <sup>3</sup> ] EN 1097-3	Specific Density [kg.m <sup>3</sup> ] ASTM D1817-05	PAHs 8 REACH [mg/kg] (specification ≤20)
Fine (Fm)	0.8-3	0.420	1.160	<15
Coarse (C)	2.0-4.0	0.455	1.160	<15

*Typical properties are given by the manufacturer*

#### 3.5.2. Aggregates

Limestones aggregates (4-14 mm) and limestone filler were used. The aggregates came from different Italian suppliers, and the typical values are shown in **Table 1.12**.

Table 1.12: Aggregates typical values

Virgin aggregates (VA)	Particle size [mm] EN 933-1	Specific Gravity EN 1097-6
Limestone 1	8-14	2.661
Limestone 2	4-8	2.669
Limestone filler	≤ 0.063	2.667

#### 3.5.3. Binders

Five different binders have been used in this study. The objective was to evaluate the effect of the binder type (cold or warm), its additives or base (bitumen or not) and the material properties for our purpose/application. Two warm binders (140-160°C),

including a Styrene-Butadiene- Styrene (SBS) modified bitumen designed to facilitate the work with a rubber using the dry method (1), and a 50/70 neat bitumen (2) were used. In addition, three cold emulsions (containing the same binder content), including two bitumen-based emulsions, one is Latex modified (3) while the other is SBS modified (4) and finally synthetic-based “yellow” emulsion (5), were also used. All the typical values of the binders are shown in the **Table 1.13** and **Table 1.14**

Table 1.13: bitumen’s typical values

Code	Bitumen	Type	Penetration at 25°C	Softening point	Resistance to hardening RTFOT (EN 12607-1)			Flash point COC	Dynamic viscosity
					change in mass (absolute value)	retained penetration at 25°C	increase in softening point (Severity 1)		
	Standards		UNI EN 1426	UNI EN 1427	-	UNI EN 1426	UNI EN 1427	EN ISO 2592	EN 13702
			dmm	°C	%	%	°C	°C	mPa.s
1	Bitumen	SBS	25-55	≥70	≤0.5	≥65	≤8	≥250	295 (135°C)
2	Bitumen	Neat	50-70	46-54	≤0.5	≥50	≤8	≥250	400-700 (160°C)

Table 1.14: Emulsions typical values

Code	Emulsions	Type	Binder Content	Breaking index	Viscosity at 40 ° C (cup discharge time 4 mm)	Adhesiveness	Penetration at 25°C	Softening point
					UNI EN			
	Standards		UNI EN 1428	UNI EN 13075-1	UNI EN 12846	UNI EN 13614	UNI EN 1426	UNI EN 1427
			%	-	sec	%	dmm	°C
3	Emulsion	Latex	63-67	110-195	5-70	≥ 90	≤ 100	≥ 55
4	Emulsion	SBS	63-67	70-155	5-70	≥ 90	45-80	≥ 60
5	Emulsion	Synthetic	63-67	>170	15-70	≥ 90	≤ 150	≥ 50

Given the highly innovative nature of this material, especially by using a cold protocol approach, the feasibility of the production needs to be assessed. The description of the procedures used from the design to the production is illustrated in **Figure 1.15** and given in the following paragraphs.

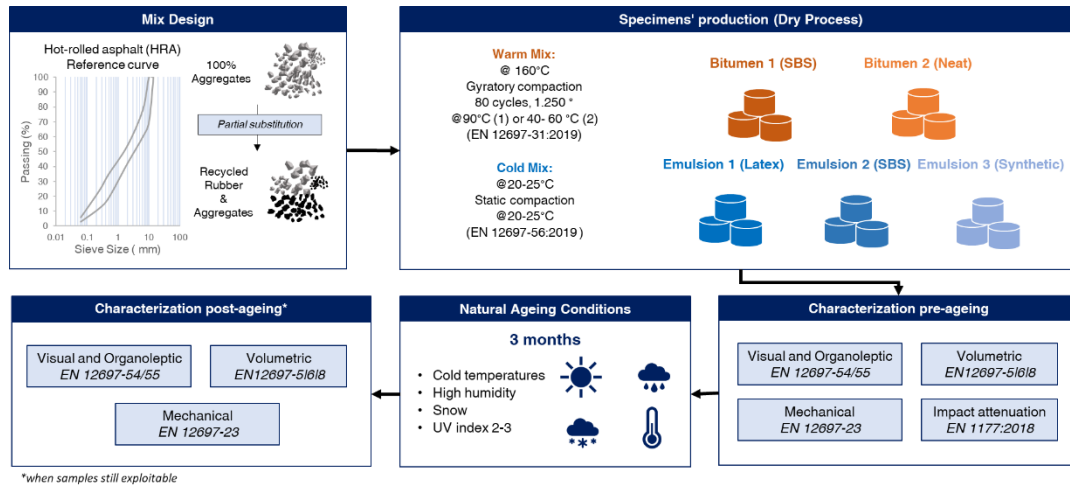


Figure 1.15 Experimental programme

### 3.5.4. Reference mix and size distribution

The known Hot Rolled Asphalt (HRA) type of mixture was defined as a reference for this study. The HRA is a very dense material containing a substantial amount of sand and fines. The whole work of mixture design and formulation was made using the HRA gradation curve, both applying the weight and the volume approach to obtain accurate values regarding the addition of a significant amount of rubber in the mixtures, a material less dense than mineral aggregates. Firstly, the rubber bulk density was used for the recipe proportions to have an estimated volume fraction based on this density [29]. Considered as aggregates, the crumb rubber partially replaces the 0-4 mm portion of the mineral limestone aggregate. The mixture gradation includes granulate from 0 to 14 mm.

### 3.5.5. Mixture's design

The dry process consisting of mixing the aggregates and binder before adding the rubber was used. In this method, the rubber is part of the aggregate portion. Two mixtures have been designed. Mix A contains 10% more rubber than mix B, as shown in **Figure 1.16**. The latter contains 10% added bigger aggregates to reduce binder consumption and increase the material's mechanical properties. Different binders have been used to decrease mixing and production issues due to the usage of a significant amount of rubber in the asphalt mixture. It is known that the use of rubber can cause workability, cohesion and fume and smell issues. The use of warm and cold

binders (modified or not) helps to identify when and how the issues occur and to address some of them.

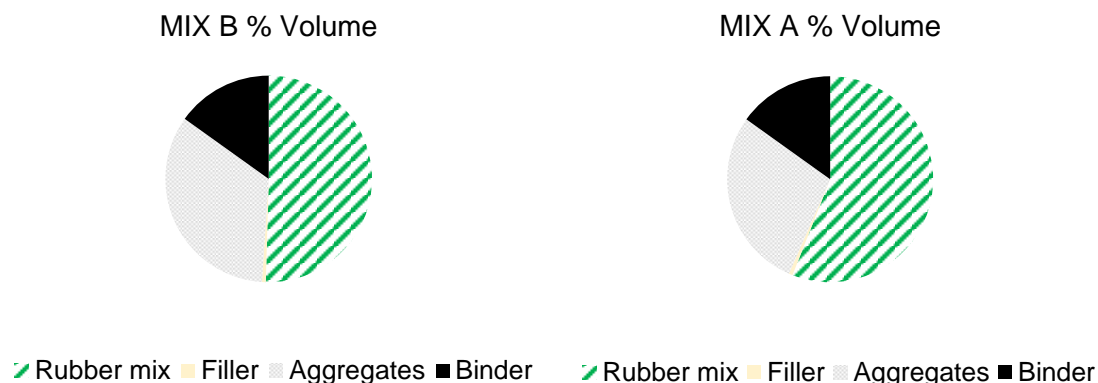


Figure 1.16: Graphical representation of the mixtures' proportions

### 3.5.6. Production of samples

Several samples of 150 mm diameter were produced following two main compaction methods: the gyratory compaction (EN 12697-31:2019) and the static compaction (EN 12697-56:2019). The mixture using the bitumen was mixed for 20-30 min @ 160°C, and Gyratory compacted using 80 cycles and 1.250 ° and 600.00KPa at 80 ±5°C (Bitumen 1) or 50 ±5°C °C (Bitumen 2). However, the cold formulations were mixed for 5 min at 23 ±2°C and Static compacted at 23 ±2°C (room temperature). The specimens were subjected to curing after being extracted from the mould and cured at room temperature. The tests were conducted on 40 mm thickness samples. However, the variation of height has interesting use in measuring the impact attenuation properties. In fact, the thicker samples, the more the impact could be reduced. Therefore, 70 mm thickness samples were also successfully produced.

### 3.5.7. Characterisations

All samples were characterised following a visual and organoleptic, volumetric, and mechanical analysis to evaluate and assess the different asphalt mixtures' behaviour. The description of the methods is explained in the following paragraphs.

#### 3.5.7.1. Organoleptic mixture descriptions.

The coating degree of the aggregates and rubber, the mix's consistency and cohesion, and the hydric or fluidity aspect assessment of the mixture were determined before and after compaction using the organoleptic methods described by the EN 12697-55 standard. This standard is meant to mainly assess the mixtures done with emulsion binder but was also used as a help to assess the mixtures done with warm bitumen. The classification given by the standard is explained in **Table 1.15**.

Table 1.15: Organoleptic assessment characterization

Class of Coating	Binder coverage [%]	Class of Consistency	Assessment	Class of Hydric aspect	Assessment
------------------	---------------------	----------------------	------------	------------------------	------------

C0	< 75	CS0	Low	HA0	Dry
C1	75 to 90	CS1	Normal	HA1	Normal
C2	90 to 97	CS2	High	HA2	Soup effect
C3	> 97				

#### 3.5.7.2. Expansions and swelling phenomenon

To assess the evolution of the cohesion of the compacted samples, the vertical and horizontal expansion was measured. In fact, the considerable amount of CR led to the swelling phenomenon between the rubber and the binders. Besides, rubber is a porous yet elastic material. Its compaction can lead to the formation of more void and expansion after the realised of the compaction load. The diameter and height of each sample were measured right several times to evaluate this phenomenon on the aspect of the samples.

#### 3.5.7.3. Volumetric analysis

The bulk and the maximum densities of the samples were calculated following the EN 12697-5 and EN12697-6. After obtaining the densities values, the air void content was calculated as specified in the EN 12697-8 standard as the ratio between the bulk and the maximum densities experimentally obtained before.

#### 3.5.7.4. Stiffness measurements

The Indirect Tensile Stiffness Modulus (ITSM) method described in the EN 12697-26 standards was used to assess the mechanical properties of the compacted samples. The method IT-CY giving information on the stiffness of the sample was performed. The standard suggests a test temperature of a minimum of 10°C. However, due to the presence of a considerable amount of rubber, making the sample highly soft in the apparatus, the test was performed at  $5 \pm 2^\circ\text{C}$  to be able to have exploitable values. This temperature also allows the assessment of stiffness in a cold environment when the samples are the stiffest.

#### 3.5.7.5. Head Injury Criterion (HIC) and Abbreviated Injury Scale (AIS)

According to the EN 1177:2018 standard, a drop test was used to evaluate the impact attenuation properties of each material. The test consists of the drop, from different heights, of approx. 5 kg hemispheric and concentric impactor (**Figure 1.5**). Thus, the impact speed and acceleration of the impactor were recorded and permitted the calculation of the Head Injury Criterion (HIC) and the Critical Fall Height (CFH) for a HIC equal to 1000. The standard suggests a sample size of at least 250×250 mm. However, cylindrical samples of smaller dimensions (150 mm diameter) were used due to the compaction parameters. A laser was used before the drop to impact the centre of the specimen. The test was assumed to be done by putting the rubberised samples on a rigid and constant ground and fixed with tape. Besides, the obtained HIC at 0.20 m for each material were compared using the Abbreviated Injury Scale (AIS) to assess the severity of the injury for each asphalt rubber and a neat HRA reference.

### 3.5.8. Natural ageing procedure (NAP) conditions

In parallel with the other characterisations, some samples were aged to evaluate the effect of the weather conditions on the overall properties of the asphalt rubber material. A Natural Ageing Procedure (NAP) of 3 months under light-exposed, cold, and humid weather conditions was made. The temperatures ranged between 15 and -7 °C, with 82% of humidity on average, including several rain and snow events. An estimated Ultra-Violet (UV) index of 2-3 corresponding to a low to moderate exposure level was registered during this period. The weather conditions are recorded in **Table 1.16**. After the ageing, the organoleptic, volumetric, and mechanical tests were newly conducted. For certain of the samples, only the characterisation before ageing was done because they were not exploitable after the ageing.

Table 1.16: Natural Ageing Procedure (NAP) weather conditions

	Units	Month 1			Month 2			Month 3		
		Max	Ave	Min	Max	Ave	Min	Max	Ave	Min
<b>Temperature</b>	°C	10	4	-2	11	2	-7	15	5	-6
<b>Rain</b>	mm	251.4			89.1			17.9		
<b>Snow</b>	cm	0			5.5			8.5		
<b>Humidity</b>	%	86			82			77		
<b>UV index</b>	/	2			2			3		
<b>Sun hours</b>	hours	155			163			232		

References: WorldWeatherOnline.com & Accuweather.com

## 3.6. Results and Discussion

### 3.6.1. Visual and Organoleptic properties of the mixtures and samples.

The analysis of loose mixture properties could give information on the future compatibility of mixtures. Given the novel aspect of this mix design, the organoleptic and visual assessments were highly used to define the overall aspect of the mix before compaction and after compaction. Both with the cold and the warm mix procedure, a dry or too wet aspect of the mix gave trouble during compaction. The mixing time had a substantial effect on the different organoleptic observations (*EN 12697-55*). **Figure 1.17** shows different aspects of the mixtures.



Figure 1.17: Visual and organoleptic assessment mixtures made with cold process.  
a. dry (too long mixing time); b. normal; c. soup effect (too short mixing time) (EN 12697-55)

After all the adjustments of mixing time, the mixtures, regardless of the binder type, were possibly compacted even if the rubber amount was above 50% (volume).

The mixtures made with the warm process resulted in a high coverage percentage of the aggregates. The mixtures done with the emulsion permitted a lower coverage percentage. In general, the lack of coverage was mainly observed on the samples' side in contact with the mould.

Besides, the workability is considerably increased using the emulsion, especially because of the presence of water during the mix, which decreases the mixture's stickiness. Furthermore, the emulsion curing time was slightly longer than the warm-made samples. However, this time is similar for the three types of emulsion. It was also seen that the slower curing, the better aggregate coverage.

Besides, the passage from the mix design A to B allowed the skeleton structure to be stronger and the mechanical properties to improve.

The passage from the warm process to the cold process allowed the decrease of energy consumption due to the heat of the binder, absence of fumes and smell occurring will heating the bitumen and rubber contained inside of the mixture and finally increased the workability while mixing.

After the NAP, two main phenomena were observed. Firstly, the loss of the shining aspect of the binder on the surface was making the surface more subject to particle loss **Figure 1.18 a and b**. This phenomenon can be explained by the presence of dust in the air sticking to the surface and oxidation of the surface-initiated by the UV and the light.

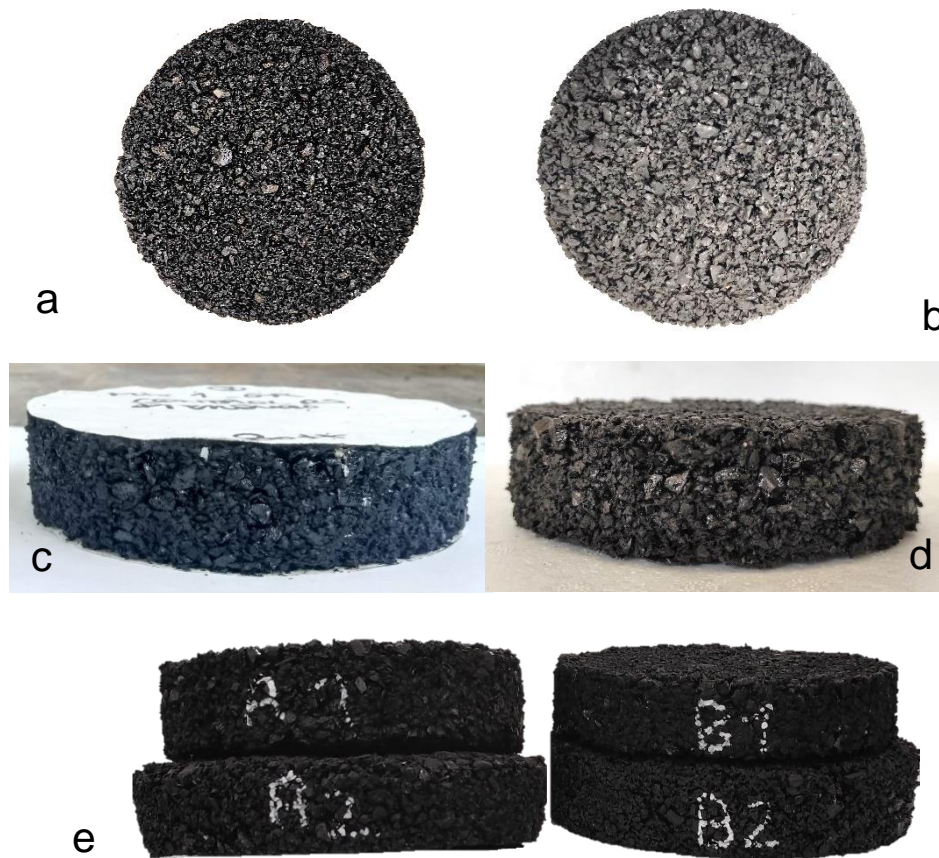


Figure 1.18: Visual aspect of the samples before and after the Natural Ageing Procedure (NAP). (a) A4 before NAP, shining; (b) A4 after NAP, dimness. (c) A1 shining and with low particle loss; (d) dimness with more particle loss. (e) samples made with binder 1 and samples made with binder 2 after the NAP.

In addition to this deterioration of properties due to the ageing, the expansion of the samples, especially those made with binder 2, was observed. Even if this phenomenon was also registered before the NAP, it was highly enhanced by the exposition to the real weather conditions. The calculated expansions are shown in *Figure 1.19*. The illustration of the considerable expansion of the samples made with binder 2 is shown in *Figure 1.18e*.

In general, the use of more than 50% of rubber in the mix made the assessment of the mixture's consistency different from traditional asphalt mixtures. The use of organoleptic tools enabled the repeatability of the obtained results and must be considered indispensable in the production process.

The visual assessment was used to evaluate the behaviour of the samples before and after the NAP and foster the classification of binder 2 as the less effective with this specific mixture. In fact, the cohesive properties were deficient and made samples A2 and B2 not reusable for testing after the NAP.

### 3.6.2. Volumetric properties of the different asphalt mixtures

As summarised in *Figure 1.18* and *Figure 1.19*, the type of binder influences the volumetric properties of the asphalt mixture.

The expansion of the sample is not the synonym for the increase of the air void. In fact, A2 or A1 has a low air void content and a very high vertical and horizontal expansion behaviour.

This behaviour can be explained by the swelling process that permits the CR to expand and partially fill the voids [32,58]. However, this swelling is also causing macroscopic changes. In fact, Binder 2 allows significant expansion and causes fewer particles cohesion. The phenomenon is notably illustrated in *Figure 1.18e*.

However, with the B2 mixture, the use of bigger aggregates combined with the lack of cohesion given by binder 2 can be responsible for the increase of void but less expansion than A2. This can be explained by the decrease of the rubber amount and thus the swelling of the rubber, which helps with the filling of the voids and causes this release of particles after their compaction.

The same explanation can also be given for A1 and B1, considering the use of SBS as a modifying agent in the binder that enhances the control of the swelling reaction and limits the overexpansion of samples. By reducing the rubber amount, the swelling phenomenon is less occurring and thus, the expansion of the sample too.

The expansion is naturally kept very low in the emulsion-based samples, but the air void content is high. A3 has a similar air void content to A1. However, A4 and A5 air void content is higher. These results find their answer in the different binder compositions. A3 seems to allow the rubber swelling that partially covers the voids, while binder 4 (similar to binder 1) and 5 allow less swelling.

This can be explained by the production method. The mix is not heated, and the swelling seems less developed in this case. Besides, the static compaction and the nature of the binder (including water that will evaporate during the curing) can promote the creation of voids after curing caused by the evaporation of water.

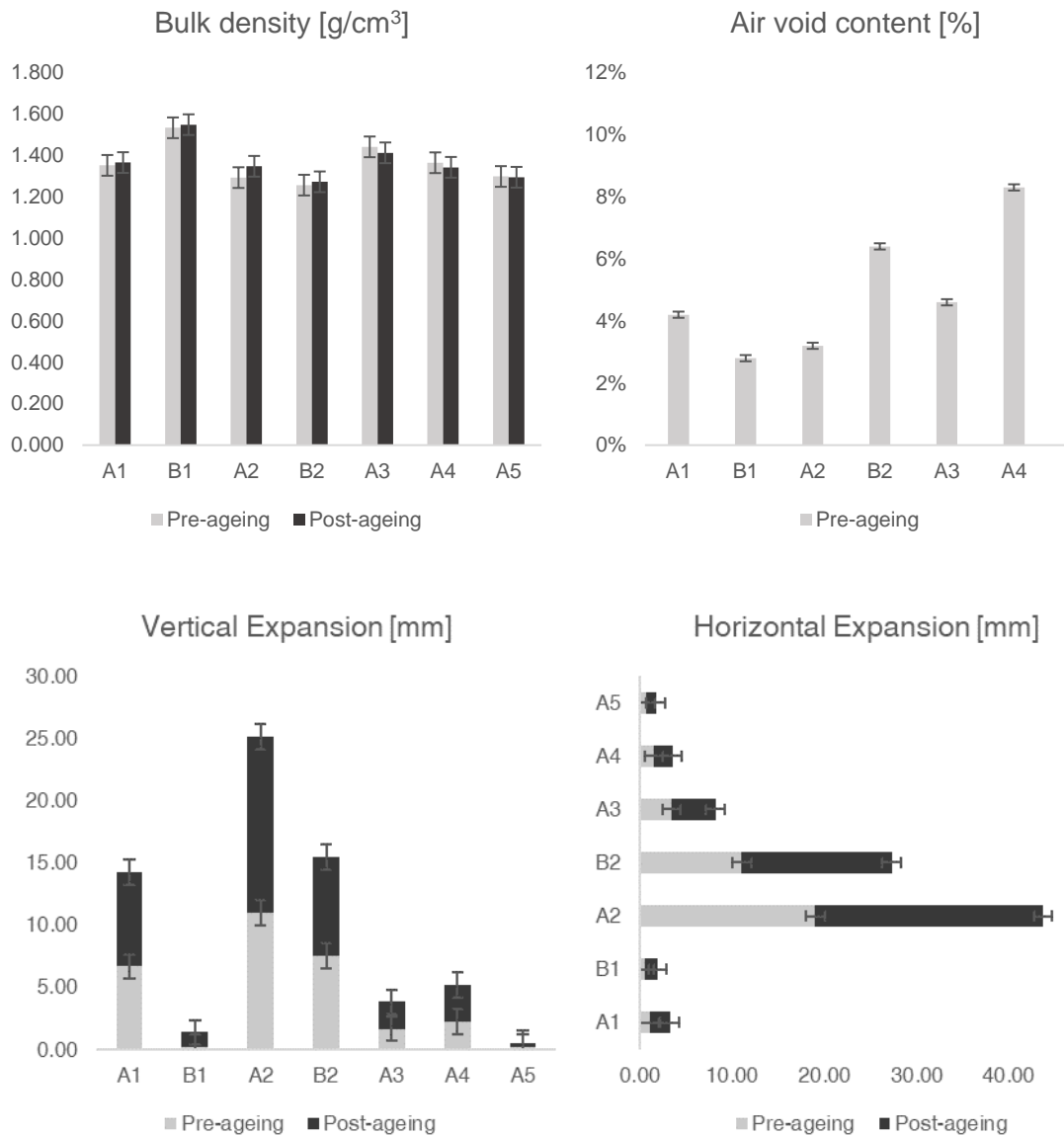


Figure 1.19: Volumetric properties and expansion values of the different asphalt mixtures

Generally, mixture B allows less expansion than mixture A and reduces the amount of rubber and the swelling phenomenon. In addition, the type of binder influences the volumetric behaviour of the mixture before and after compaction and before and after ageing.

The statically compacted samples have a different bulk density behaviour towards ageing.

The results show that the mixtures done with the binders 1, 3,4 and 5 have better ageing behaviour while focusing on the overall cohesion assessed thanks to the expansion of the samples.

### 3.6.3. Mechanical tests

#### 3.6.3.1. Stiffness and mechanical properties assessment pre- and post-natural ageing procedure.

The weather influence on the mechanical properties of the IAP samples is shown in **Figure 1.20**.

The first indirect tensile modulus was obtained in the original state of the mixtures. The ageing promotes the oxidation of the binder, which tends to make the sample stiffer. In fact, the ITSM increased after the NAP.

Besides, the samples made with the emulsion have lower ITSM values. This can be explained by the high air void content or by and higher resistance to the oxidation caused by the temperature or UV exposure during the NAP. The volumetric behaviour also influences the testability of the sample. Indeed, due to the significant expansion of A2 and B2 samples, primarily due to the use of binder 2, they couldn't be tested under the same conditions as provided before the NAP. This result is shown in **Figure 1.20**.

Previous studies have shown that to have acceptable mechanical performance together with good impact attenuation properties, the value of the stiffness modulus is between 200 and 300 MPa at 5°C [57]. As shown in **Figure 1.20**, apart from B1 values, the other ITSM values are contained inside this range both before and after the ageing period.

Generally, mixtures A 1, 3, 4 and 5 have good stiffness values to be used as an IAP. The mixture B1 has better mechanical performance with respect to the bearing of heavy loads but does not comply with the impact attenuation needs. Finally, mixtures A2 and B2 registered an expansion too high to be tested after the ageing. This can be interpreted as an unusable material if applied in natural conditions.

Table 1.17: Classification of the injuries type by HIC of the designed mixtures at 0.2 m of drop.

Mix	Rubber amount	Head injury Criterion	AIS code
HRA	0	1000	3
A1	66	96	0
B1	56	128	0-1
A2	66	59	0
B2	56	69	0
A3	66	89	0
A4	66	83	0
A5	66	91	0

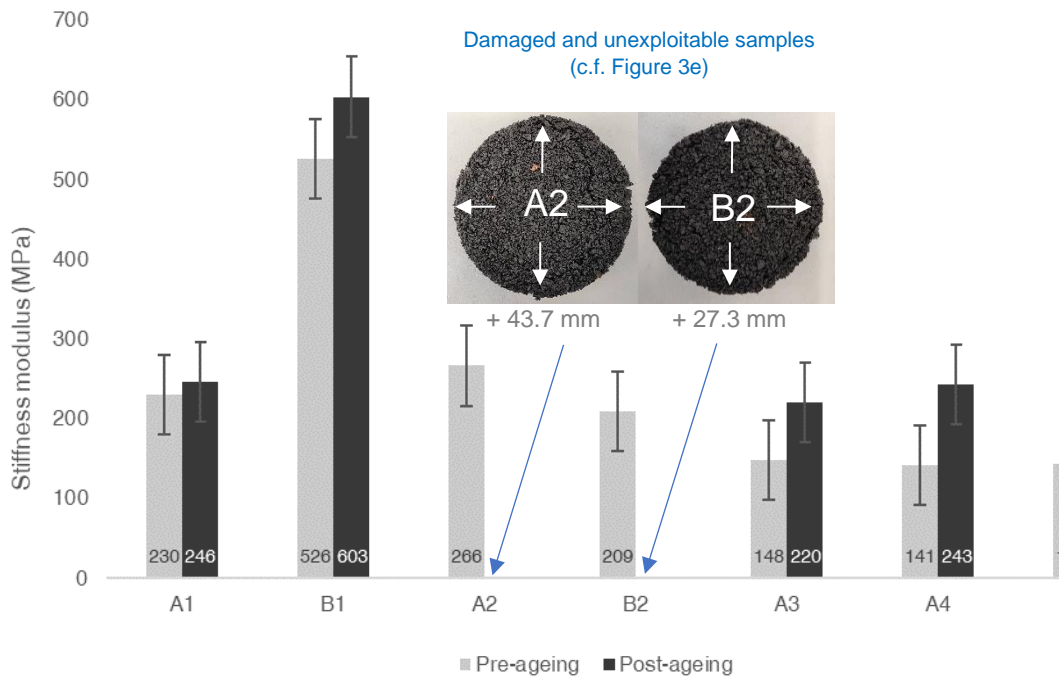


Figure 1.20: Stiffness and mechanical properties assessment pre and post NAP. ITSM [MPa] 5°C

### 3.6.3.2. Impact attenuation and injury prevention

The experimental results of the Critical Fall Height are reported in **Figure 1.21** with a standard deviation of  $\pm 0.5$  m. These results were obtained in the original state of the mixtures before the NAP. The values of the HIC and CFH are comprised in the acceptable range from 1 meter and above regarding the ability of the materials to reduce the injuries.

Apart from B1, all the mixes comply with the identified needs, such as enough impact attenuating property. In fact, the stiffness modulus of B1 is much higher than all the other mixtures.

Despite their good results regarding the impact attenuation performance, A2 and B2 do not represent suitable formulations for extended use under real weather conditions. The mix A1 is within the range but does not have very notable results.

The samples made with emulsions 3, 4 and 5 have the best results for the impact attenuation.

Generally, the mixtures A3, 4 and 5 have shown the best impact attenuation performance compared with the other mixtures.

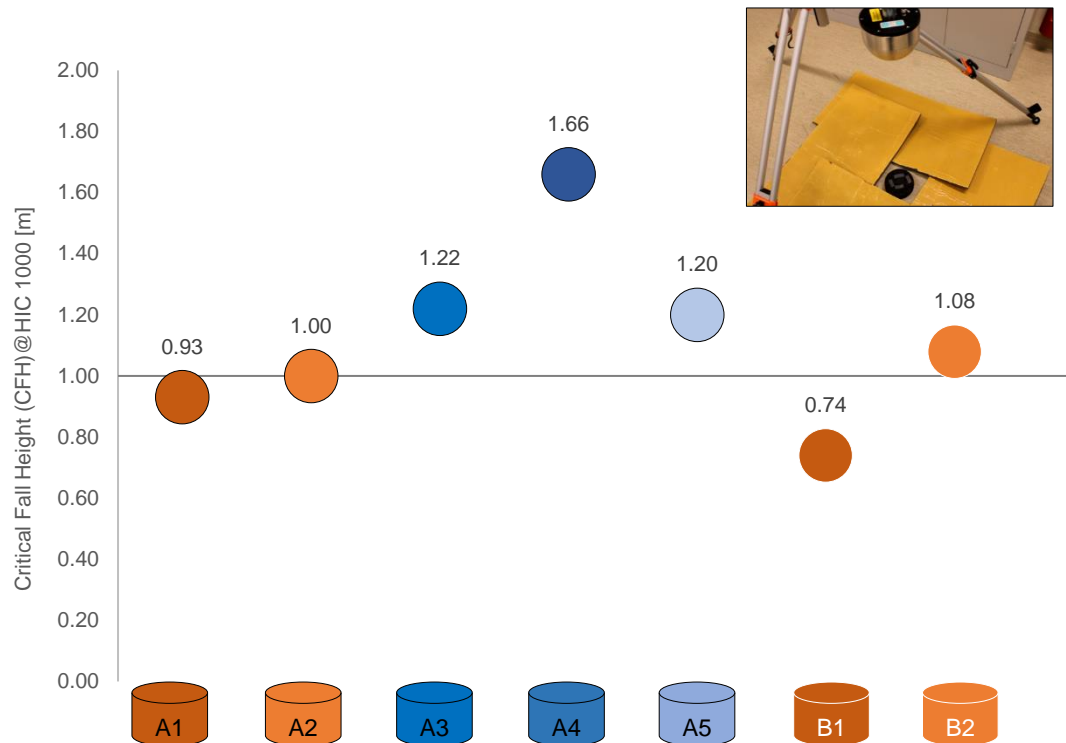


Figure 1.21: HIC meter installation and Impact attenuation and injury prevention performances Critical Fall Height (CFH) @ HIC 1000 [m]

### 3.7. Conclusions

The focus of this paper was the proof of feasibility and the assessment of Impact-Absorbing Pavements made with cold especially and warm mix asphalt binders and recycled rubber. The characterisation has given several results that allowed identification of the best mixture according to the defined criteria such as workability, the cohesion of the mixture, fume and smell release, impact attenuation and durability. This research may conduct to the organization of field trials to optimise and scale up the process with the development of a lower number of possible mixtures and formulations.

- The proof of the feasibility of 50%+ rubberised bituminous mixture has been made with cold mixing procedures and confirmed with the warm. The samples were produced and tested before and after a natural ageing period. Adapted standardised methods have been used to test all the samples.
- The samples produced with the cold binders made possible the absence of fumes and smell release. In parallel, the workability is considerably enhanced using the cold procedure. Altogether, the IAP A4 obtained the best.
- The binder highly influences the cohesive properties. The SBS modified binder (warm or cold) increases the mixture's cohesion and diminishes the expansion. The decrease of rubber amount gives better cohesive properties but

limits the impact attenuation performances. The synthetic binder gives high cohesive and low expansion results to the compacted samples.

- The obtained impact attenuation properties are similar to the previous studies' results. Additionally, the samples made with the cold binders have better impact-absorbing properties, and the A4 samples have the best results.
- The 3 months durability of the mixture made with binders 1, 3, 4 and 5 was observed. They are the only remaining intact samples after the natural ageing procedure. Indeed, the IAP A2 and B2 were already not exploitable after 3 months. A4 and A5 mixtures have shown the best overall results. However, durability assessment must be further investigated and evaluated through complete laboratory cycle procedures followed by field trials.

#### **4. Outcomes**

The section aimed to describe the approach used in the laboratory, prove the feasibility of the material, propose a production process, and choose the best mixtures to keep a limited number of formulations for further detailed analysis.

Thanks to the first study described, it was possible to propose a partial substitution of the aggregates using rubber. The substitutions ranged between 30% and 56% of the total mix volume. It was shown that the more rubber was added to the mix, the better were the impact-attenuation performances. Moreover, the first study proved that the mix with the highest amount of rubber was workable.

Thus, the variation of the binder was examined thanks to the second study. It was possible to produce the mixture containing 56% rubber with five different binders, two bitumen-based and one artificial emulsion poured at room temperatures (cold mixture), and two bitumens added at 160 °C. This phase was also an indicator of the viability of the substitution method developed in the first study. In all cases, the binder was poured at the end, and the rubber was considered an aggregate in the mixture; this complies with the dry process. The five mixtures were chosen as the ones to be deeply characterized. However, the cold mixture gave better outcomes regarding its possibility to be used without externalities such as the release of smell and fumes and the stickiness observed when using the 160°C mixing temperature instead.

Chapter 2 will describe the types of characterisation used, their outcomes and their usefulness for defining the best mixture among the five shortlisted.

## Chapter 2. Mechanical, Chemical and Freeze-thaw cycles analysis

The work proposed in this chapter is extracted from the following manuscripts:

- **Makoundou, C.**; Fathollahi, A.; Kleiven, S.; Sangiorgi, C; Coupe, S.; Mechanical and leaching characterisation of impact-absorbing rubberised asphalts for urban pavements. *Under review in Materials and Structures, Springer, Switzerland.*

*CM, AL: Conceptualisation; CM, AL: Data curation; CM, AL: Formal analysis; SK, CS, VW, KJ, SC: Funding acquisition; CM, AL: Investigation; CM, AL: Methodology; CS, VW, KJ, SC: Supervision; CM, AL: Writing - original draft; CM, CS, VW, KJ, AL, SC, SK: Writing - review & editing. All authors have read and agreed to the submitted version of the manuscript.*

- **Makoundou, C.**; Sangiorgi, C. Influence of Freeze–Thaw Cycles on the Mechanical Properties of Highly Rubberised Asphalt Mixtures Made with Warm and Cold Asphalt Binders. *Materials* 2022, 15, 2701.  
DOI: <https://doi.org/10.3390/ma15072701>

*Conceptualisation, C.M.; methodology, C.M.; software, C.M.; validation, C.M.; formal analysis, C.M.; investigation, C.M.; resources, C.M., C.S.; data curation, C.M.; writing—original draft preparation, C.M.; writing—review and editing, C.M., C.S.; visualisation, C.M.; supervision, C.S.; project administration, C.S.; funding acquisition, C.S. All authors have read and agreed to the published version of the manuscript.*

## **1. Overview**

Together with the mechanical and environmental performances, the material's durability has a crucial role in its functionality and technical success for a defined application. The second section focuses on the wide analysis of the formulated materials. The objective is to assess the technical performance of the material (strength, durability, rheology). Then it was also verified that these performances comply with the climatic need to reduce emissions and waste and propose non-hazardous materials. Finally, some analysis of the durability of the two best formulations (mechanically and environmentally) was assessed thanks to weather stress cycles in the laboratory.

This section is composed of two papers. The first one describes both the mechanical performances of the materials and the heavy metal leaching evaluation. Two major test procedures were adopted to assess these points: uniaxial compressive tests and dynamic leaching procedure. Finally, the second paper describes the role of freeze-thaw cycles on the potential degradations observed and measured on the materials.

The first paper describes the test made on four of the five previously shortlisted mixes, while the second focuses on only two shortlisted mixtures corresponding to the more durable and mechanically stable.

The problem and methods are introduced for each paper in this section. Then the procedure plan is explained, and the results are discussed. Finally, they are all concluded with the main results. The papers of the previous Chapter and the first paper of this Chapter helped with the reduction of the mixture list from five to two, thanks to their main results. These two mixes were used and described in the second paper of the Chapter.

## **2. Mechanical and leaching characterization of impact-absorbing rubberised asphalts for urban pavements**

### **2.1. Introduction**

The injuries and trauma caused by falls occurring on the pavement in urban areas are responsible for physical and mental consequences for road users worldwide [10]. Vulnerable road users (VRUs), as the most exposed users, are strongly impacted by this issue that is deemed to rise as the number of pedestrians and two-wheeled users is increasing [11,24].

Nowadays, rubberised (recycled or not) surface layers and pavements are successfully used in playgrounds, sports fields and other civil engineering applications for their lower stiffness if compared to standard paving solutions [30,59–61]. In particular, to prevent injuries for the VRUs, protective surfacing to be used at a larger scale in urban and peri-urban areas (e.g. in the pavements of sidewalk and bike lanes), are being developed to bring-in impact-attenuation properties that are essential to reduce severe head, hips or shoulders injuries, including fractures, concussions, or internal bleeding [52] and their connected costs for the society at large. In line with this perspective, the proposed rubberised asphalt impact-absorbing material has been conceived and studied to meet this goal. Its full development will possibly enable a wide implementation in cities and wherever users' falls are more likely to occur while preserving the standard asphalt traditional production and construction methods. Moreover, the use of recycled rubber from end-of-life tyres as the main layer constituent fosters a circular economy approach instead of a linear one, allowing the recycling of high quantities of End-of-Life tyre rubber [30,62].

Preliminary studies have confirmed the feasibility and potential effectiveness of the impact-absorbing pavements starting from various mix designs, using both warm [27,29,52,57] and cold bituminous binders; during their development process, a complete mechanical analysis of the material was required in order to assess their attenuation properties. The uniaxial compression test in different setups has usually been adopted to investigate the basic loading and relaxation behaviour of these materials [60,61] because the methods commonly used for traditional asphalt, like the ITSM test (EN 12697-26), are not able to describe the relevant soft behaviour of the samples.

Furthermore, along with the mechanical and durability performance of the material, the environmental impact of the innovative paving solutions must be considered in designing and building greener infrastructures [63,64]. A recent study by Fathollahi and Coupe (2021) showed that the extraction, transportation and end of life stages of using virgin aggregates for pavement construction purposes have the largest contributions toward life cycle environmental and cost impacts. This is the reason

behind the objectives of many studies conducted worldwide aiming to replace virgin aggregates and binders with recycled materials, thus reducing the pressure on the environment. Crumb rubber from end-of-life tyres goes in this direction, and it is one of the most popular recycled materials to replace natural aggregates and improve bituminous materials characteristics in pavements.

Up to now, limited scientific studies have investigated the behaviour of crumb rubber in contact with water and its potential to release heavy metals and trace elements [66], or reported the concentrations of leached As, Ag, Ba, Cd, Cr, Hg, Pb, and Se from tyre rubber used in artificial turfs [67], or examined the zinc leaching from tyre crumb rubber through column tests for a duration of 96 hours. The latter study reported an initial pulse of elevated zinc leaching of 3 mg/L before settling down to a steady-state value of 0.2 mg/L. Another study on crumb rubber samples from artificial turf playgrounds showed that the granulates contained up to 500 mg/kg of aluminium [68]; while, concentrations of cobalt, cadmium, copper, sodium, magnesium and iron in crumb rubber granulates from artificial playgrounds have been reported by other literature [69–73]. Nonetheless, the systematic assessment of the release of heavy metals and trace elements from asphalt specimens containing crumb rubber granulates in contact with urban runoff is not common. For this reason, the present study aims to evaluate the leaching performance of the rubberised asphalt according to the Regulations recognised by the European Commission (EC). In fact, more than one standard procedures have been identified by the EC for the investigation of the leaching behaviour of construction materials including the CEN/TS 16637-2:2014 and the CEN/TS 14405. In particular, the Dynamic Surface Leaching Test (DSL) CEN/TS 16637-2:2014 standard aims to determine the release of "Regulated Dangerous Substances" from construction products into soil, surface water and groundwater and it has been utilised by a number of studies to evaluate the leaching behaviour of construction materials [74–78]. The results from the leaching tests should be compared with the thresholds set by the EC or other regulatory bodies including the Water Framework Directive (WFD) [79] to ensure the safety of materials under investigation to be used in the urban environment.

In the light of the above, this paper wants to provide a complete uniaxial compression and leaching data analysis from the proposed innovative impact-absorbing material, thus contributing to the developing research steps of a promising paving solution.

Six mixes were designed using two different percentages of crumb rubber granulates content and four different binder types. Axial relaxation and recovery abilities and compressive strength values were obtained and compared to known playgrounds or rubber composites with sufficient shock-absorbing performances. In the leaching experiments section of the present study, the release of heavy metals and trace elements from the six rubberised asphalt concretes were evaluated according to the mentioned CEN/TS 16637-2:2014 standard.

## 2.2. Methodology

### 2.2.1. Experimental Plan

After the production of the specimens, the study was divided into two main characterisations: mechanical and chemical. The experimental plan is schematized in *Figure 2.1*

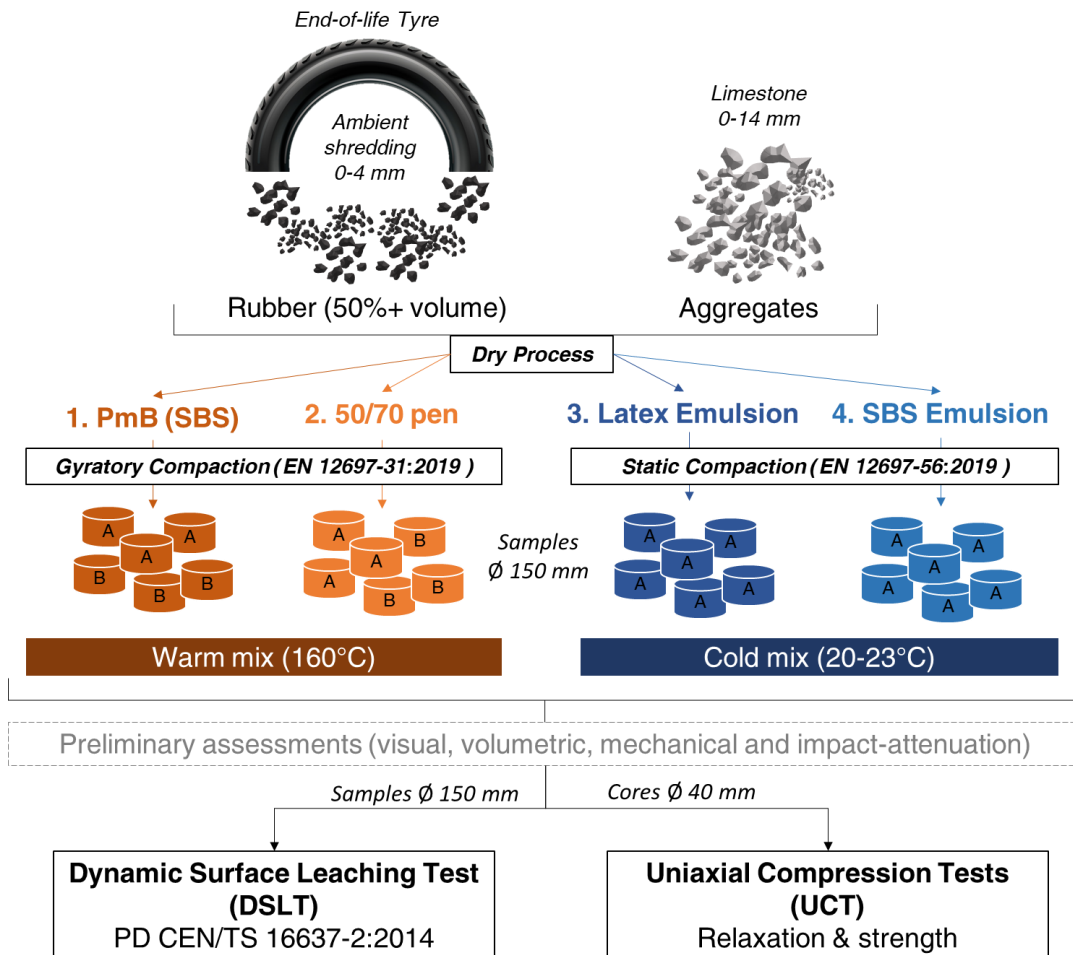


Figure 2.1: Experimental plan of the study. The scheme describes the raw materials used, including the rubber, the aggregates, and the different binders. The dry process was used to produce different specimens compacted by means of gyratory and static compaction. These were tested with the DSLTL and UCT tests.

### 2.2.2. Rubberised impact-absorbing asphalt mixture

Six types of rubberised IAP mixtures were produced. The dry process, consisting in mixing the aggregates and binder before adding the crumb rubber, was used. All the mixtures contain, as the main constituent, the crumb rubber from ELTs. The rubber was obtained from a company treating waste tyres utilising the common ambient shredding process. In all the proposed mixtures, the size distribution of rubber is 0-4 mm and 2-4 mm, as shown in *Figure 2.2*.

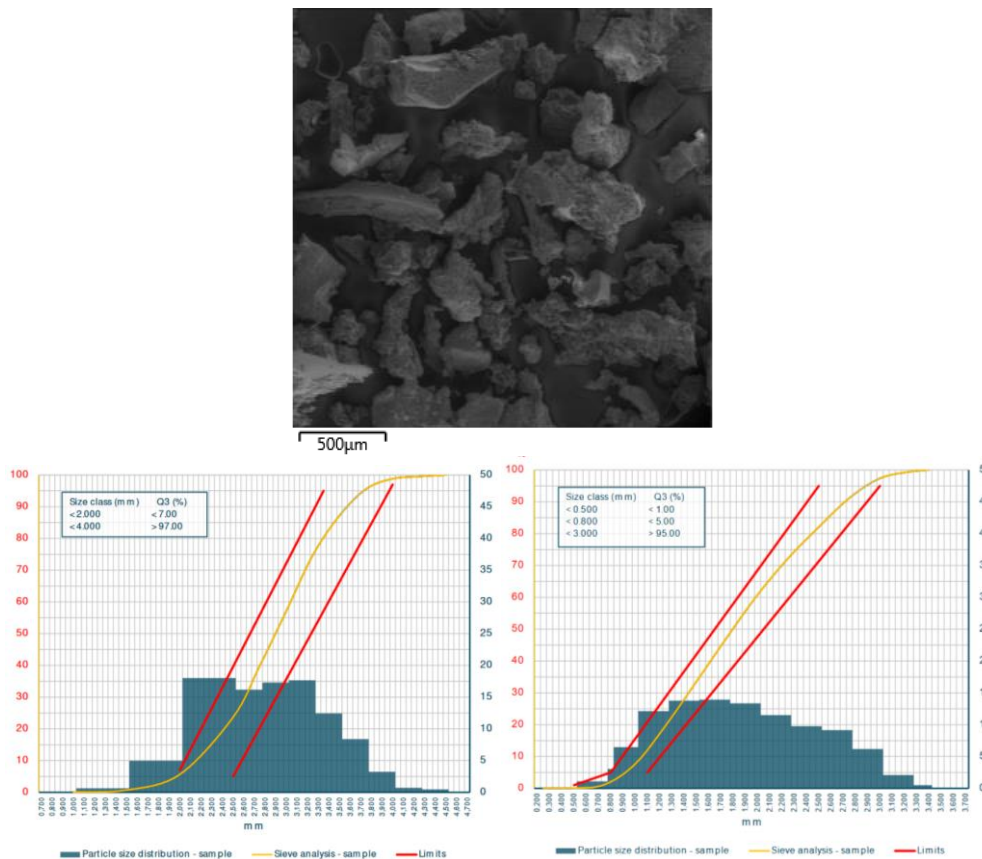


Figure 2.2: Neat rubber SEM and granulometry curves from [80]. The figure contains a SEM picture of the rubber mix and the granulometric data of the two adopted rubbers, allowing a rubber size distribution of 0-4 mm [80]

Two main mixes containing different recycled rubber amounts were assessed: the A-mixes with 56% rubber (by volume of the total mix) and the B-mixes with less rubber (50%). The natural aggregates mix constituent were 0-14 mm limestone aggregates, which were partially replaced by the rubber particles (in volume). In the A-mixes, the aggregates are partially substituted by the same size of rubber granulates, while in the B-mixes, a lower percentage of the largest size aggregates (10-14 mm) is adopted. Finally, four different bituminous binders were used: two commercial asphalt binders, including a Styrene-Butadiene-Styrene (SBS) modified bitumen purposely designed to incorporate rubber using the dry method (1), and a standard 50/70 penetration grade neat bitumen (2); and two cold bitumen-based emulsions (with the same residual binder content), a Latex modified one (3), and an SBS modified one (4).

### 2.2.3. Production of samples

The bituminous samples of 150 mm in diameter and 40 mm in thickness were produced following two main compaction methods: the gyratory compaction (EN 12697-31:2019) and the static compaction (EN 12697-56:2019), adopting the last one for cold bituminous mixes. The mixing times were defined using the organoleptic

assessment of mixtures (EN-12697-55:2019) to produce well coated and homogenous mixtures. The hot/warm mixes were gyratory compacted with 80 cycles at approximately 80°C (A1 and B1) or 50°C (A2 and B2), permitting a correct adhesion of all the components. Instead, the cold materials were statically compacted at approximately 20°C (room temperature). These cold samples were subjected to curing after being extracted from the mould and cured at room temperature. The leaching tests were conducted on the full original samples, while the stress-relaxation and compression tests required coring the samples to a smaller diameter to allow testing. Therefore, the original samples were cored using a 40 mm coring rig, as shown in **Figure 2.3**.

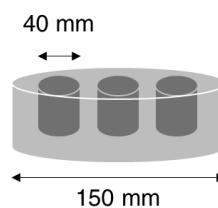


Figure 2.3: Scheme illustrating the 40 mm cores obtained from 150 mm samples for the uniaxial tests.

#### 2.2.4. Testing criteria

This study is part of a research project aimed at developing new materials for users' protection purposes, and that allow the recycling of ELT in large quantities. A preliminary laboratory study was recently conducted by the authors in which a set of initial physical and mechanical characteristics were determined on the impact-absorbing materials. In parallel, a Head Injury Criterion (HIC) testing investigation [50,81] was conducted on the same materials. All recorded data are listed in **Table 2.1**, and the same nomenclature has been used for the mixtures on which stress-relaxation and compression tests have been performed to allow a more specific mechanical analysis that could also be used for FEM modelling purposes. In addition, the chemical analysis outcomes and their potential influence on the environment (in specific on water) are very important for the comprehensive assessment and validation of the proposed material.

This paper aims both to investigate the mechanical uniaxial-compressive characteristics and to analyse the leachates in water, estimating the potential environmental impact of the six rubberised mixtures under assessment. These data will be used to optimize the material constituents in order to maximize the impact-absorbing properties, maximize the amount of recycled rubber, and minimize the contamination of waters while keeping the production and laying processes feasible at an industrial scale. The latter will have to be assessed with an ad hoc experimental site investigation already foreseen for the material development.

Table 2.1: Impact-Absorbing Pavements made with cold and hot/warm asphalt binders and recycled rubber: summary of the preliminary characteristics of the mixtures (Chapter 1, part 2).

Mixture	A1	A2	A3	A4	B1	B2
Rubber volume (total mix) [%]	56	56	56	56	50	50
Bitumen type	PmB-SBS	50/70 pen	E-Lat	E-SBS	PmB-SBS	50/70 pen
Bitumen volume (total mix) [%]	15	15	15	15	15	15
Bulk Density <i>EN 12697-6</i>	1.351	1.292	1.441	1.364	1.533	1.256
Voids content [%] <i>EN 12697-8</i>	4	3	5	8	3	6
Indirect Tensile Stiffness Modulus [MPa] (5°C) <i>EN 12697-26</i>	230	266	148	144	526	209
CFH* at HIC** 1000 [m] <i>EN 1177</i>	0.93	1.00	1.22	1.66	0.74	1.08

\* Critical Fall Height \*\* Head Injury Criterion

### 2.2.5. Mechanical tests

The UCT (relaxation and destructive) were performed at room temperature (20°C) on the 40 mm diameter cylindrical specimens using an Instron Electropuls E3000 testing machine (*Figure 2.4a*) at the KTH Neuronic Laboratory, Sweden. Trial tests have been performed to optimise the initial deformation allowing to record the complete relaxation of samples and the required displacements to reach failure without overcoming the compressive load limit of 3kN.

Various material parameters such as the elastic modulus, the elastic recovery and the mechanical behaviour are determined and shown as stress-strain curves illustrating the hysteresis during the testing phase (*Figure 2.4 b*).

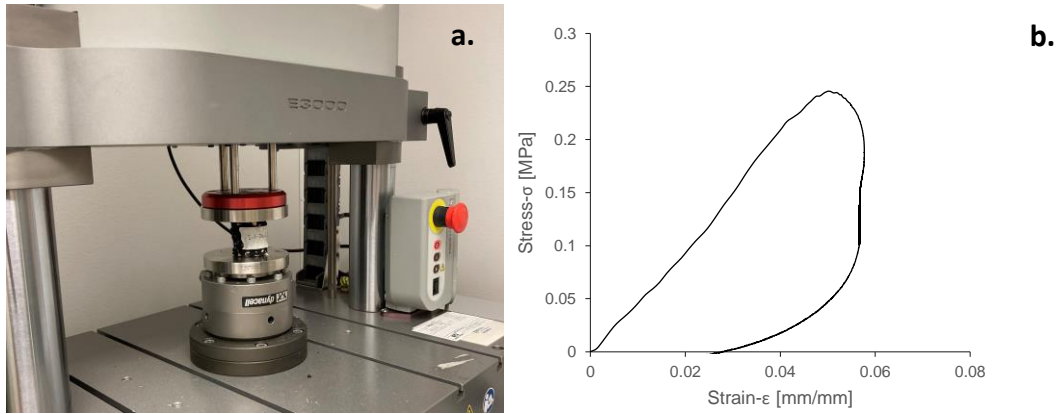


Figure 2.4: a. Compressive tests setup; b. Stress-strain graph of a stress-relaxation test illustrating the hysteresis during the relaxation phase.

### 2.2.5.1. Uniaxial Unconfined Stress-Relaxation test and calculations

After the initial calibration phase, some relaxation tests were carried out. Samples were compressed at approximately 5% (2.5mm) strain with a load application speed of 20mm/s. When reaching the target strain, the load was held for 60 seconds, after which the unloading phase was carried out at 0.6mm/s. Additionally, an elastic recovery test was carried out to verify the applied strain and assess the sample's relaxation in time from 1 to 30 minutes after the release of the initially applied stress. The machine-recorded parameters allow the calculation of the Relaxing Stress and Strain (Engineering) and of the Relaxation Modulus.

$$\text{Relaxing Stress [MPa]} = \frac{\text{Load [N]}}{\text{Original cross sectional area [mm}^2\text{]}} \quad (1)$$

$$\text{Strain} = \frac{\text{Displacement [mm]}}{\text{Sample Initial Height [mm]}} \quad (2)$$

$$\text{Relaxation Modulus [MPa]} = \frac{\text{Relaxing Stress [MPa]}}{\text{Strain}} \quad (3)$$

Then the Relaxation Modulus  $G(t)$  for a linear viscoelastic model (Standard linear solid) was fitted through a MATLAB script using the following equation:

$$G(t) = G_{\infty} + (G_0 - G_{\infty})e^{-\beta t} \quad (4)$$

where:

$G(t)$  = Relaxation Modulus Curve Approximation using 1 term

$G_0$  = Initial Relaxation Modulus

$G_{\infty}$  = Final Relaxation Modulus

$\beta$  = Time relaxation constant ( $s^{-1}$ )

### 2.2.5.2. Axial Unconfined Destructive Compression Procedure

The compression strength test was conducted at two different application speeds, corresponding to different strain rates, a quasi-static and a dynamic one. To calculate the speed of application, starting from the strain rate, the following relation has been considered:

$$\dot{\epsilon} [1/s] = \frac{v [mm/s]}{h [mm]} \Rightarrow v = \dot{\epsilon} \times h \quad (5)$$

with the strain rate  $\dot{\epsilon}$  being equal to:

- 0.01 [1/s] ( $v = 0.01.AVG H_0 = 0.43mm/s$ ) – Quasi-Static (D)
- 1 [1/s] ( $v = 1.AVG H_0 = 43mm/s$ ) – Dynamic (D)

The destructive uniaxial compressive test was carried out, and samples were compressed at approximately 50% (25mm) strain with an application speed of 0.43 (QS) and 43 (D) mm/s. When reaching the maximum displacement of 25 mm, the load was not held, and the unloading phase was carried at a speed of 0.43 (QS) and 43 (D) mm/s. Compressive Engineering stress, Engineering strain and Elastic modulus are calculated as follows.

$$Compressive\ Stress\ [MPa] = \frac{Load\ [N]}{Sample\ area\ [mm^2]} \quad (6)$$

$$Strain = \frac{Displacement\ [mm]}{Sample\ Initial\ Height\ [mm]} \quad (7)$$

$$Elastic\ Modulus\ [Mpa] = \frac{Compressive\ Stress\ [MPa]}{Strain} \quad (8)$$

### 2.2.6. Dynamic Surface Leaching Test

The leaching behaviour of rubberised asphalt specimens in the present study was evaluated based on CEN/TS 16637-2 standard for construction and building materials. Rubberised samples for DSLT were of 150 mm diameter and 40 mm thickness and compacted according to EN 12697-31:2019 and EN 12697-56:2019 standards. The leachant in DSLT, was deionised water with a conductivity less than 0.5 mS/m according to BS EN ISO 3696. A 0.1 mol/L nitric acid was used for rinsing purposes. A set of glass vessels with lids, were used as leaching tanks to avoid prolonged contact with the air and CO<sub>2</sub> uptake. Rubberised asphalt samples were placed in glass vessels with a minimum of 20 mm distance between specimens and glass vessels in all directions as shown in **Figure 2.5**.



Figure 2.5: Glass vessel containing the rubberised asphalt in direct contact with the water.

Small glass pieces were placed under the specimens to avoid direct contact of asphalt surfaces and leaching vessels and provide a direct contact between bottom side of specimens and leachant. A representative leachant sampling procedure was performed according to CEN/TS 16637-1 standard. The temperature of the lab was kept constant between 20-25°C. A L/A ratio of 80 was selected the leaching tests and volume of leachant was calculated according to the surface of specimens. The DSLT leaching tests were carried out in triplicates for all mix designs of rubberised asphalt specimens. Three glass vessels filled with deionised water and no asphalt specimens were assigned as controls to detect and eliminate the contamination from lab equipment and the surrounding environment. Samples from control replicates had to have less than 0.2 mS/m and elemental concentrations below the detection limit to fulfil the minimum requirements, otherwise, DSLT experiments had to be repeated. Leachants from control and asphalt specimens were sampled and renewed after 0.25, 1, 2.25, 4, 9, 16, 36, and 64 days from the experimental setup. Therefore, the leaching tests comprised of 8 stages with durations of 0.25, 0.75, 1.25, 1.75, 5, 7, 20 and 28 days.

Electric Conductivity and pH of the leachants were measured at the end of all stages of leaching tests according to the BS EN 16192:2011 standard, using an EC and pH meter. Leachant samples were then filtered off-line using 0.45 µm membrane filters. Samples were then centrifuged at 2000 g for 5 hours prior to storage at 5°C and elemental analysis. The concentration of heavy metals and trace elements in filtered samples from DSLT was evaluated using a Perkin-Elmer optima 5300 DV ICP-OES instrument. The elements under investigation in the present study included Al, As, B, Ba, Ca, Cd, Co, Cr, Cu, Fe, K, Mg, Mn, Mo, Na, Ni, Pb, Sb, Se, Si, Tl, V and Zn. Analytical methods for quantification of mentioned elements were developed and commissioned for ICP-OES instrument. After quantification of concentrations of described elements in leachants from different stages of DSLT, cumulative leached concentration for each element was calculated according to CEN/TS-16637-2 2014 as follows:

$$R_n = \sum_{i=0}^n r_i \quad (9)$$

where  $R_n$  (mg/m<sup>2</sup>) is the cumulative area release of the substance for period  $n$  including fraction  $i = 1$  to  $n$  of DSLT test,  $r_i$  is the area release of the substance in fraction  $i$ , and  $i$  is the DSLT stage. SPSS 21.0 software [82] was used to perform statistical analysis of data from DSLT.

## 2.3. Results and Discussions

### 2.3.1. Relaxation of the samples

#### 2.3.1.1. Elastic recovery of the materials

The materials' recoverability after applying a stress was tested and recorded at different times. **Figure 2.6** demonstrates the recovering abilities of the different mixtures after a compression applied to deform of approximately 2.5 mm.

When using the same binder but different rubber amounts (A1-B1 and A2-B2), the more rubber is contained in the mix, the faster are the material's recovery abilities. After 1 minute, A1 recovers at 98% while B1 at 94%, but after 30 minutes, they reach 99% of the recovery. In the case of binder 2, this difference is even more visible as, after 30 minutes, B2 is still not recovered at 95%.

The B2 mix shows a very low recovery capacity, and this represents an issue concerning future applicability in real conditions considering that daily stress will be applied to the material.

For the A-mixes, binder 2 shows better recovery values; however, concerning the B-mixes, binder 1 displays better recovery values. It can be seen that both the rubber and the binder affect the elastic recovery of the samples.

At an equal rubber amount (A1, A2, A3 and A4), the hot-made samples recover faster and better than the cold-made samples. This can be explained by the samples' structure, which has fewer air voids than A3 and A4 (**Table 2.1**). Additionally, for the same reason, the compaction method can impact this result (**Figure 2.1**).

A3 shows the lowest recovery possibilities. In fact, after 1 minute of a compressive load applied, the samples A1, A2 and A4 are already recovered at more than 95% of the initial height, while for A3, the 95% recovery is obtained just after 30 minutes. A3, like B2, doesn't have enough recovery potential and can lead to a fast deterioration of the material if applied on a sidewalk/bike lane portion. These were also observed in preliminary ageing results as reported in **Table 2.1**, in which A2, B2 and A3 were the least resistant materials and A1, B1 and A4 the more resistant ones. This observation is not verified by A2 elastic recovery. Additionally, the elastic recovery possibilities seem not to affect the HIC results because A3 has a high CFH and a poor recovery performance, A1 has a low CFH, but good recovery and A2 has a high CFH and a high recovery. As a matter of fact, it is difficult, through this test,

to anticipate the contribution of the recovery to the injury reduction measured with an HICmeter.

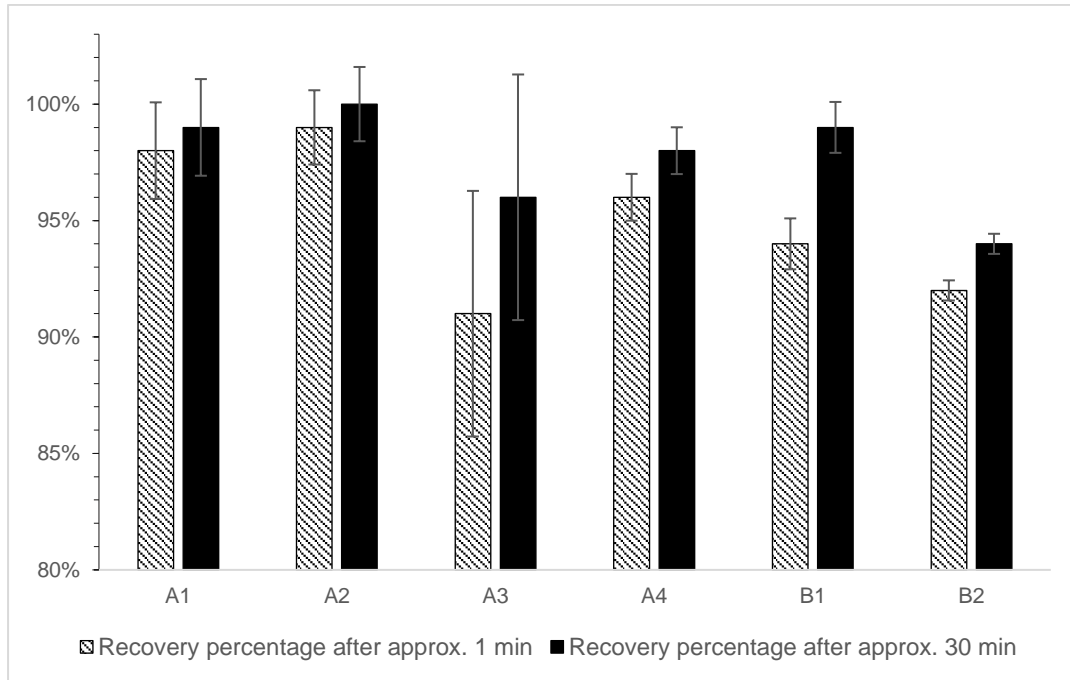


Figure 2.6: Average Elastic recovery values for the maximum applied strain

### 2.3.1.2. Stress-Strain analysis and calculation of the relaxation modulus

MATLAB was used to calculate the relaxation moduli of the six asphalt mixtures according to equation (4). **Figure 2.7** shows the test results used for the relaxation moduli for the six asphalt mixtures. The stress-strain curves have a similar shape apart from the A2 mixture one. B1 and B2 have larger hysteretic areas than A1 and A2, respectively; the lower rubber content can explain this in the B-mixes. The hysteretic loss is similar for A1 and B1 but very different for A2 and B2, with A2 recording more hysteretic loss. As for the A-mixes, the hysteretic areas from the higher to the lower can be listed as follows:  $A4 > A1 > A3 > A2$ . A1 and A2 record the lower hysteretic loss and A3 the higher. This confirms the elastic recovery observed in **Figure 2.6**.

B1 relaxation stress is much higher than all the other mixes. **Figure 2.7** also described a high possible deformation but with and high capability to recover.

In general, the mixture made with SBS modified binder (A1, A4 and B1) allows the specimen to have a noticeable deformation and maximum recovery after compression. However, this is not observable with the mixture made with the other binders.

Additionally, the non-modified binder and emulsion (numbers 2 and 3) lead to lower moduli. At the same rubber amount, mixture A1 provides the highest modulus and A3 the lowest. The type of binder used has a greater influence on the material behaviour

than the rubber amount. In fact, B2, even if containing less rubber, is more deformable than A1 or A4, and it is less likely to spring back to its original shape faster after loading. This data validates the results observed in previous investigations, including the outcomes of the elastic recovery. B2, A3 and A2 are less likely to resist daily stress than A1, A4 and B1.

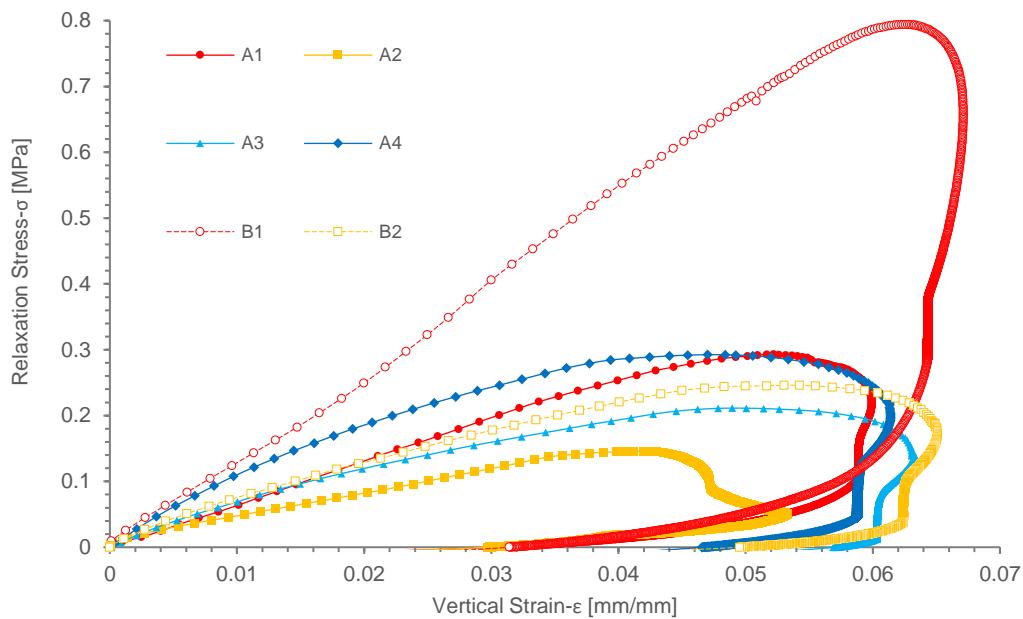


Figure 2.7: Relaxation Stress- $\sigma$  and Vertical Strain- $\epsilon$  curve

### 2.3.2. Failure behaviour during the compressive test

#### 2.3.2.1. Failure analysis

Two main sample failure behaviours have been registered during the compression strength study. These are shown in **Figure 2.8**. During the destructive UCT process, it was found that samples easily fail along with the interface between the rubber-binder matrix and mineral aggregate, no matter the binder type.

The samples made with the SBS-modified binders had still links after the compression (**Figure 2.8a**), while the samples made with the other binders scrambled without a valuable link in between the different components (**Figure 2.8b**). These observations confirmed the preliminary visual assessment of the cohesive aspect of the samples and the results of the relaxation tests. It was already seen that the samples made with binders 2 and 3 had the worst resistance to weather conditions, and they are less likely to be used as impact-absorbing pavements in real conditions due to their weak durability in time.

Also, this analysis confirmed the recovery and relaxation test results in which A3, B2 and A2 mixtures were less likely to be selected as valid IAP materials than A1, B1 and A4 mixtures.

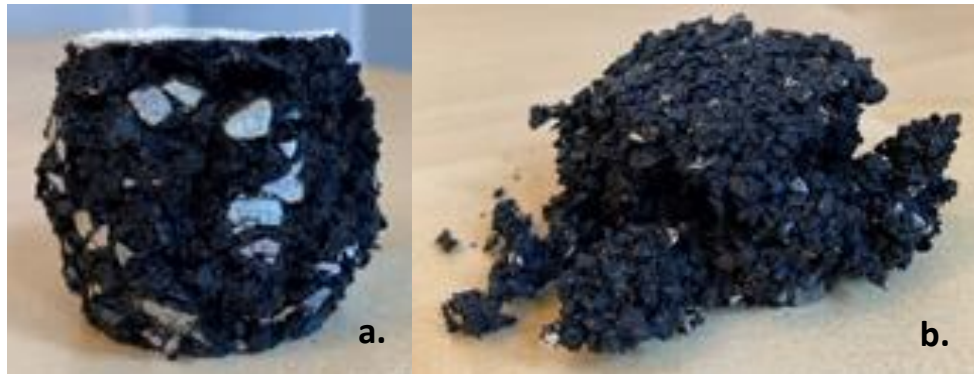


Figure 2.8: Typical failures after destructive testing. a. sample fails with no loss of cohesion (A1, A4 and B1); b. sample fails with loss of cohesion (A2, A3 and B2).

#### 2.3.2.2. Stress-strain curve analysis and calculation of the elastic modulus

The Elastic moduli of the six asphalt mixtures were calculated with MATLAB and according to equation (8) for the quasi-static and dynamic test. Values are shown in **Figure 2.9**.

According to **Figure 2.9**, the stress-strain behaviour of the samples is similar to the one observed on playgrounds [60,83]. The stress similarly ranges from 0 to 3 MPa. B1, A1, A2 and B2 samples could be reproducing a usual playground behaviour, while samples A4 and A3 are considered softer and, by extension, safer.

For various rubber amounts, the 1-mixes and 2-mixes have totally different stress-strain curves trends, but A1 and B1 curves have similar behaviour corresponding to harder materials and A2 and B2 corresponding to softer materials. These values confirm the CHF values collected with the HICmeter and are described in **Table 2.1**. B1 registers higher stress than A1; however, A2 has a higher stress value than B2. This can be explained by the crack and destruction configuration in which the asphalt composite is left without bonds, and rapidly, the calculated stress is attributed to aggregates interaction instead of the full material.

The strength rank as  $A2 > A1 > A4 > A3$  for the same amount of rubber. The A1 and A2 curves are different, while A3 and A4 are similar. A3 and A4 curves correspond to very soft materials. It also confirms the CFH values as A3 and A4 have the higher CFH, thus seem safer against injury reduction, especially fractures caused by the hard surfaces.

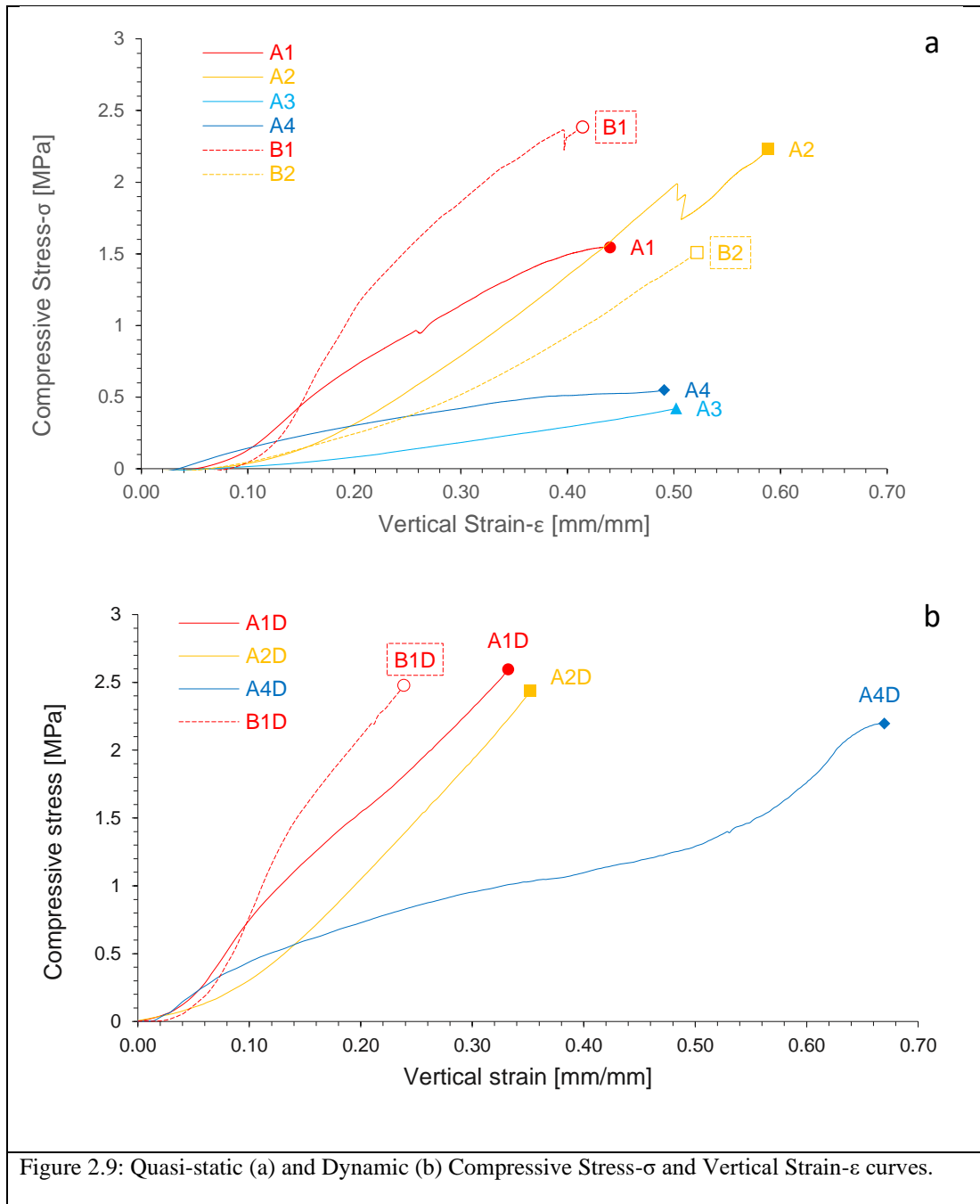


Figure 2.9: Quasi-static (a) and Dynamic (b) Compressive Stress- $\sigma$  and Vertical Strain- $\epsilon$  curves.

The dynamic study of the failure behaviour of the sample gives a more evident result regarding the characteristics of the mixtures. Due to a lack of cohesion of the samples during the coring, the A3 and B2 samples could not be tested. This observation also confirms the results discussed in the previous sections. This limits the study to A1, A2, A4 and B1 mixtures, which can be considered good alternatives to be applied in an in-situ trial.

At equal binder but different rubber amounts, the difference in the stress to failure is low. A4 has a higher rubbery behaviour than A2 and A1, and its deformation is higher at equivalent stress. This shows better energy-absorbing behaviour toward stress.

Thanks to these results, A4 seems to be the best compromise between the resistance and the softness with regard to injury reduction. In fact, B1 and A1 are considered too hard and stiff, while A2, B2 and A3 are not resistant and do not recover enough for such an application.

### 3.3 Dynamic Surface Leaching Test

#### 3.3.1 Electric Conductivity and pH

The pH and electric conductivity of leachants in contact with different rubberised asphalt mix designs during DSLT experiments were measured on day 0.25 to 64 according to the CEN/TS 16637-2 standard and are presented in **Figure 2.10**. The highest mean electric conductivities for mix design A1, A2, A3, A4, B1 and B2 were 986 (Day 16), 1071 (Day 9), 920 (Day 16), 962 (Day 4), 823 (Day 64) and 826 (Day 36) (uS/cm), respectively. As results suggest, B-mix designs showed lower electric conductivity in comparison with A-mix designs. Moreover, the maximum electric conductivity occurred at earlier stages of DSLT (Day 4-16) for A-mix designs compared to those of B-mix design (Day 36-64). This observation revealed that A-mix designs with a higher content of crumb rubber particulates released higher total ions in shorter time into the leachants during the DSLT. The electric conductivity of control replicates was lower than 0.2 mS/m which satisfied the first quality check of the DSLT experiments.

The pH evolution of leachants from DSLT experiment 6 types of rubberised asphalt are presented in **Figure 2.10b**. According to the results, the pH of leachants from all specimens showed a constant increase as the duration of contact increased. On days 0.25 and 1, the pH for all specimens stayed below 7.5. pH of all specimens increased from less than 7.5 to above 8 between day 1 and 36. However, the maximum pH (>8.5) was observed at the last stage of DSLT experiment were samples that stayed in contact with leachants for 28 days. The observed pH was associated to B1 mix design with a value of 9.35 on day 64 of DSLT. A deeper look at the data in **Figure 2.10b** reveals that leachants from B1 and B2 mix designs had lower pH than others at all stages of DSLT except day 36, where they showed the highest pH. This observation may be due to the slower release of ions from B1 and B2 mix designs, which reached their maximum on day 64 and 36, respectively. This phenomenon was observed in **Figure 2.10a** where maximum electric conductivity of leachants from B1 and B2 mix designs occurred on day 64 and 36. Maximum pH values for A-mix designs occurring at earlier stages of DSLT were also in line with their maximum electric conductivity occurrence at earlier stages (**Figure 2.10a**).

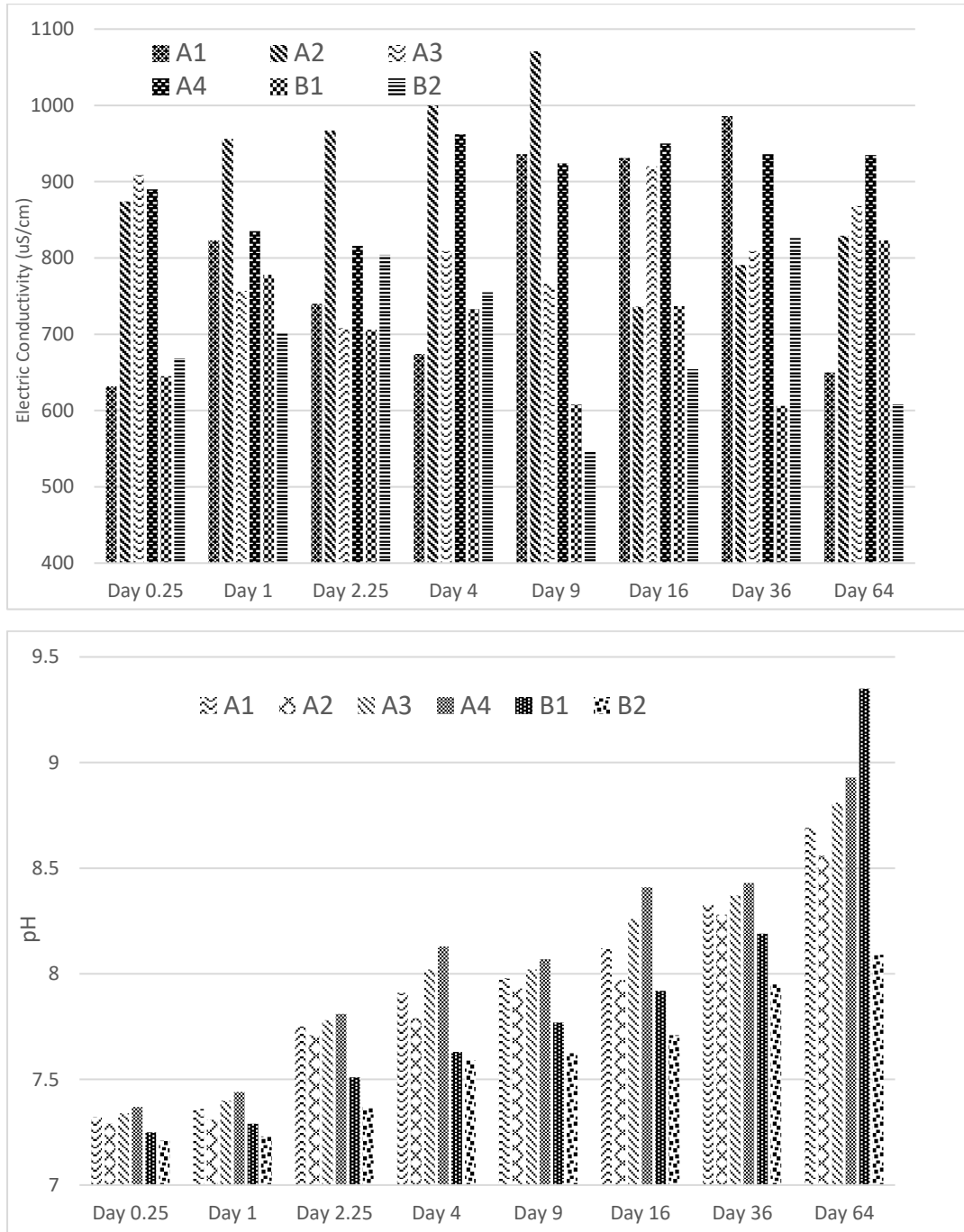
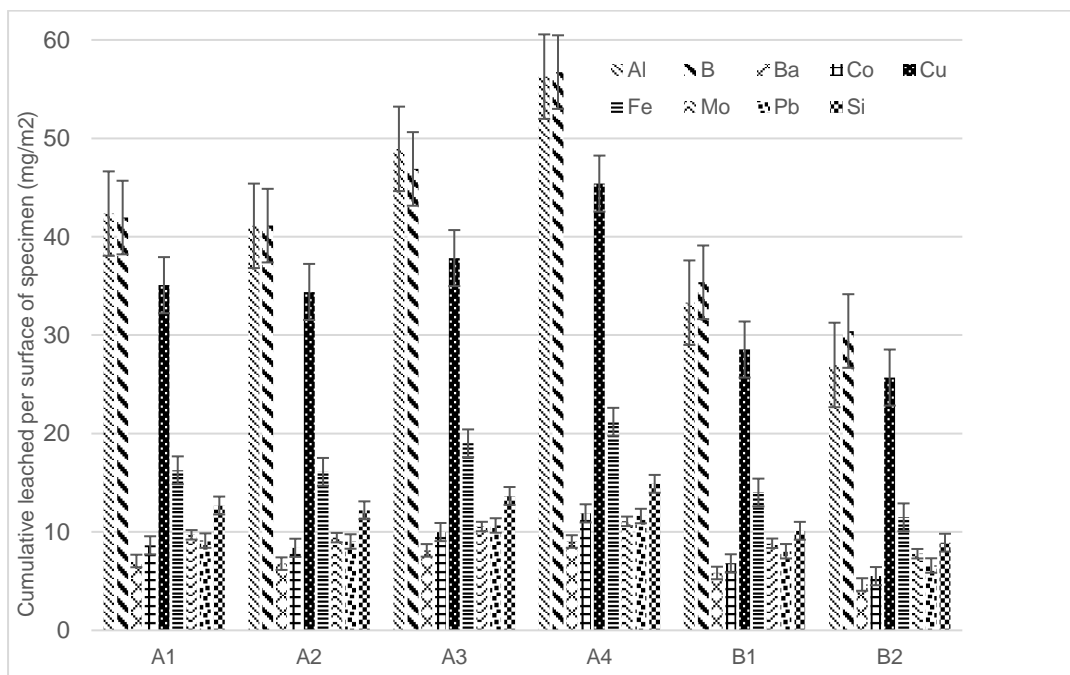
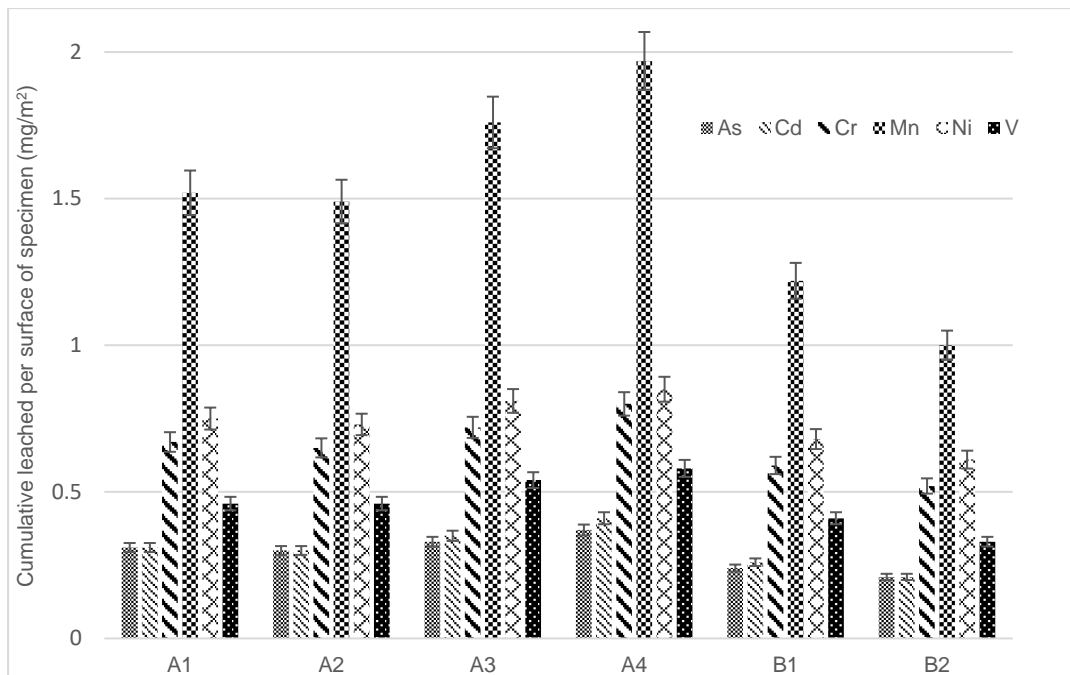


Figure 2.10: Changes in a) Electric conductivity and b) pH of leachants at different stages of DSLT for rubberised asphalt specimens.

### 3.3.2 Release of Heavy Metals and Trace Elements

Samples from different stages of DSLT for different rubberised asphalt mix designs in this study were analysed using ICP-OES. The mean concentrations of heavy metals and trace elements including Al, As, B, Ba, Ca, Cd, Co, Cr, Cu, Fe, K, Mg, Mn, Mo, Na, Ni, Pb, Sb, Se, Si, Tl, V and Zn, were quantified. The cumulative release of elements per unit surface of samples during DSLT (from start to day 64) are presented in **Figure 2.11**. **Figure 2.11a** is showing the release of elements with concentrations less than 6 mg/m<sup>2</sup>. Elements with released concentrations between 6 and 60 mg/m<sup>2</sup> are in **Figure 2.11b**. **Figure 2.11c** presents the leached elements with highest concentrations during DSLT of different rubberised asphalts. As illustrated in **Figure 2.11a**, the A4 mix design released the highest As (0.37 mg/m<sup>2</sup>), Cd (0.41 mg/m<sup>2</sup>), Cr (0.8 mg/m<sup>2</sup>), Mn (1.97 mg/m<sup>2</sup>), Ni (0.84 mg/m<sup>2</sup>) and V (0.58 mg/m<sup>2</sup>). The B2 mix design showed the lowest release of elements into the leachant, followed by B1, A2, A1 and A3 mix designs. The same trend was observed for elements with releases per unit surface area between 6 and 60 mg/m<sup>2</sup>. The overall release per surface area of mix designs for Al, B, Ba, Co, Cu, Fe, Mo, Pb and Si elements were as follows: A4 > A3 > A1 > A2 > B1 > B2. As the data shows, the release of elements from B-mix designs were generally lower than A-mix designs. This observation may be due to a lower content of crumb rubber in B1 and B2 mix designs, which reduces the potential of elemental leaching into the leachant. As **Figure 2.11c** illustrates, the minimum mean released Ca (118.71 mg/m<sup>2</sup>), K (167.64 mg/m<sup>2</sup>), Mg (171.14 mg/m<sup>2</sup>), Na (127.39 mg/m<sup>2</sup>) and Zn (327.86 mg/m<sup>2</sup>) elements during DSLT were associated with the B2 mix design. For all mix designs, the highest released element per unit surface area of samples were Zn, K, Mg, Na and Ca with concentrations higher than 100 mg/m<sup>2</sup>. The observed results were in line with previous studies which reported Zn as the highest leached elements from crumb rubber granulates used in artificial turfs [84] (MCPA, 1990; Downs et al, 1996; Edeskär, 2006; ETRMA, 2011). The concentrations of all elements under investigation in this study were lower than detection limit of the ICP-OES instrument which satisfied the second stage of quality check of the experiments and guaranteed no contamination of experimental setup. There is a lack of limitations set by the regulatory bodies on maximum released heavy metals and trace elements, per unit surface area of samples, from DSLT tests in mg/m<sup>2</sup> unit. Therefore, Dutch Soil Quality Decree (SQD) values were selected to compare the cumulative released elements from rubberised asphalt with the thresholds. The SQD has set 260, 1500, 3.8, 120, 60, 98, 1.4, 400, 144, 81, 4.8, 50, 320, 800 mg/m<sup>2</sup> for As, Ba, Cd, Cr, Co, Cu, Hg, Pb, Mo, Ni, Se, Sn, V and Zn, respectively. As **Figure 2.11** shows, the cumulative release of elements under investigation in this study from unit surface of all rubberise asphalts were lower than the thresholds set by the Dutch SQD.



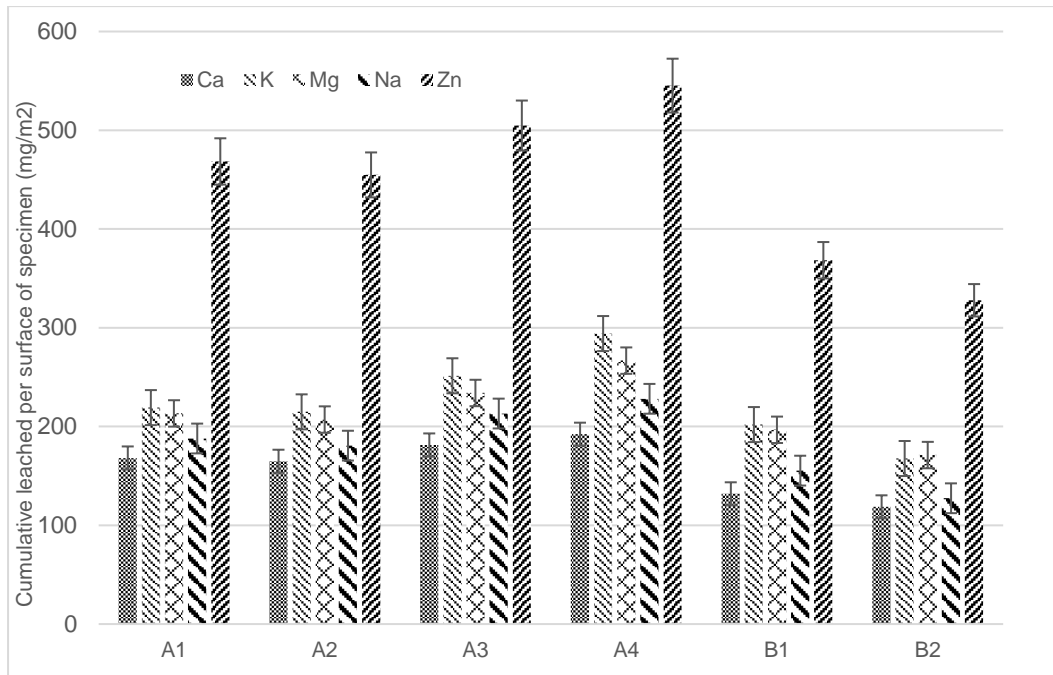


Figure 2.11: Cumulative release of elements from unit surface of rubberized asphalt specimens. a) Elements with release concentration <6 mg/m<sup>2</sup>, b) Elements with release concentration between 6 and 60 mg/m<sup>2</sup>, c) Elements with release concentration > 60 mg/m<sup>2</sup>.

## 2.4. Conclusions

This paper investigated the mechanical performance of a newly developed material and analyses the leaching and potential hazardousness, and environmental impact of six rubberised mixtures.

The compressive tests revealed the similarity in the loading behaviour of the mixtures to playgrounds or rubber composite materials, able to considerably reduce the injuries. Also, the change of binder can strongly affect the material's behaviour under stress, even when a constant amount of rubber is used.

The A-mixes have higher elasticity and provide the necessary impact attenuation properties. The A3, A2 and B2 mixes are less resistant, while the SBS-binder mix shows the best durability and cohesive properties while the mix B1 records a better strength but does not comply with the injury reduction performances. The results from the compressive test showed that the A-mixes have the best elastic and absorbing behaviour, especially the one made with an SBS-modified emulsion. Altogether, mix A4 has a low strength but high elasticity, essential for the impact attenuating behaviour. The use of A4 also brings in some energy-saving and decreased externalities during the production procedure.

The results of DSLT revealed that the B-mix asphalt specimens released lower concentrations of heavy metal and trace elements into the leachants, and A-mix specimens released the heavy metals and trace element ions at earlier stages of the DSLT compared to B-mix design specimens. During DSLT, the cumulative release of all elements under investigation in the present study were lower than the maximum thresholds set by Dutch Soil Quality Decree (SQD).

The A4 mix is the most promising mixture regarding the injury reduction performances and the environmental impact as it uses a cold binder; thus, the production process is considerably limiting the externalities. B2 has low leaching values but does not comply with the durability and resistance needs. B1 mechanical and leaching performances are acceptable; however, the injury reduction one is not appropriate for the aim application. At valuable mechanical and leaching performance, A1 seems an interesting alternative but barely complies with the injury reduction requirements.

Therefore, the early release of leachant observed for the A-mix, especially A4, suggests the possibility of handling the leaching with several solutions, including rubber coating treatment or water washing before their incorporation into the mix to prevent their leaching while enabling very high injury reduction performances.

### **3. Influence of Freeze-Thaw Cycles on Mechanical Properties of Highly Rubberised Asphalt Mixtures Made with Warm and Cold Asphalt Binders**

#### **3.1. Introduction**

Asphalt pavements are common materials for constructing transportation infrastructures, and they have been developed and optimised for many years [85]. While designing or improving the recipe of bituminous paving material, the mechanical loads applied by traffic and the climate actions, resulting in stresses and strains, moisture damage, temperature changes, and ageing, have an important role. These two main elements are always responsible for most pavement deterioration. Nevertheless, temperature variations and freeze-thaw cycles are known to be the main factors responsible for thermal fatigue and potholes because of the induction of water-caused distresses, which are the main causes of pavement failures in rigid climate regions [86,87].

In the past years, the evaluation of the weather's influence on asphalt materials, especially with cold temperatures, has been investigated in many studies [88–94]. The development of a correlation between the pavement temperature conditions and the mix design of the bituminous material in the targeted cold region was proven to be an important aspect of the mixture optimisation.

The research topic is more developed in regions with a relatively wide temperature range characterising climate, and where the pavement is usually subject to freeze-thaw (F–T) cycles. For instance, a study from El-Hakim et al. [86] presented a statistical assessment of the impact of F–T cycles on the deterioration of the mechanical properties of asphalt mixes in Canada. Other groups studied the effects of F–T cycles on the performances of asphalt mixtures in the cold regions of China and Iran [95–98], while in Sweden Lövqvist et al. implemented a model to show the effects of different parameters on the materials (the number of F–T cycles, the gradation of the microstructure, and the freezing time) thanks to computer-assisted F–T simulations [99]. The work done on F–T cycles can be easily applied to other cold regions as a conditioning procedure reproducing the climate evolution and the related F–T scenarios.

As far as rubberised pavements are concerned, a limited number of studies can be found on the F–T of paving materials containing rubber, even less on highly rubberised materials, despite the environmental advantages connected with the use of recycled ELT rubber [100]. A study conducted by Guo et al. demonstrates the correlation between the use of crumb rubber in a bituminous mixture and the reduction of the anti-fatigue performances and life of the specimen after F–T cycles [101]. However, some major limitations of using rubber in asphalt concretes are the swelling

and expansion that has a role in the degradation of the material [102]. The number of voids can turn the material more prone to deterioration caused by water infiltration. Moreover, the rubber tends to absorb the binder, allowing the adhesion and cohesion between the aggregates, partly allowing water ingress at interfaces and consequent damages [103]. However, in the parallel field of cementitious materials, a study conducted by Richardson et al. stated that crumb rubber particles smaller than 0.5 mm are optimal for providing freezing protection in rubberised concrete [104].

A similar observation has also been made with reference to the use of cold emulsified asphalt binder mixtures for chip-sealing purposes. You et al. focused on the durability characteristics of asphalt emulsion-based chip-seals and the effect of the asphalt aggregate combination at cold temperatures when exposed to multiple F–T cycles [105]. In the light of the above, this paper presents the results of geometrical, volumetric, and mechanical characterisation, carried out on highly-rubberised samples made with crumb rubber, warm and cold asphalt binders after freeze and thaw (F–T) cycles applied following the ASTM C666/C666M standard (Procedure B) [106].

The main research objective is to evaluate the resistance of the developed rubberised asphalt mixture—intended to be used as an impact-absorbing pavement (IAP) [57] to repeated cycles of F–T. No comparisons with ordinary and traditional asphalt are presented because of the vast disparity in performance and application intentions, especially regarding the strength and stiffness of the developed rubberised asphalt.

## 3.2. Materials and Methods

### 3.2.1. Raw Materials

The tested mixtures are made with two types of recycled rubber (with different size distributions from 0 to 4 mm) and a Polymer-modified Binder (PmB) or a Polymer-modified bituminous Emulsion (PmE). The adopted mixture design resulted from previous studies developed to define a viable and consistent formulation [57].

Ambient shredded rubber from two different Northern European suppliers, through the collaboration of the Swedish Tyre Recycling Association, was used to produce the rubberised samples. The rubber size distribution ranged between 0 and 4 mm, but the various products have different sieving curves. The rubber from both sources alternatively substitutes a portion of the mineral aggregates in the designed mixtures according to different specific volumetric recipes. Rubber characteristics are shown in *Table 2.2*, and the sieving analysis in *Table 2.3*

Table 2.2: Crumb rubber typical values

Rubber	Granulates	Particle size [mm] ISO 13322-2	Bulk Density [kg/m <sup>3</sup> ] EN 1097-3	Specific Density [kg/m <sup>3</sup> ]	PAHs 8 REACH [mg/kg] (specification ≤20)
Rubber 1	Fine	0-1.2	0.440	1.028 (EN 1097-6)*	6.5
	Medium	1.0-2.8	0.440	1.028 (EN 1097-6)*	6.5
	Coarse	2.5-4.0	0.440	1.028 (EN 1097-6)*	6.5
Rubber 2	Powder	0.2-0.8	0.345	1.160 (ASTM D1817-05)	<15
	Fine	0.8-3.0	0.420	1.160 (ASTM D1817-05)	<15
	Coarse	2.0-4.0	0.455	1.160 (ASTM D1817-05)	<15

Table 2.3: Crumb rubber sieve analysis

Sieve (mm)	Percent Retained per sieve [%]					
	Fine	Rubber 1		Powder	Rubber 2	
		Medium	Large		Fine mix	Coarse
4	0.00	0.00	0.15	0.00	0.00	0.00
2	0.00	34.18	97.90	0.00	22.00	95.79
1	0.09	58.68	1.88	0.00	73.88	4.18
0.5	65.96	6.94	0.00	85.30	4.01	0.04
0.25	23.91	0.02	0.01	14.50	0.03	0.00
0.125	8.22	0.05	0.03	0.20	0.01	0.00
0.063	1.71	0.10	0.03	0.00	0.05	0.00
< 0,063	0.11	0.03	0.00	0.00	0.02	0.00
Total	100.00	100.00	100.00	100.00	100.00	100.00

Limestone aggregates ranging from 4 to 14 mm and limestone filler (below 0.063 mm) were used to create the bituminous mastic and the lithic structure of the designed pavement. Intermediate-size aggregates (0–4 mm) were partially substituted with rubber of the same size to provide the material with the required elastic and impact-absorbing properties. The mineral aggregates' characteristics are listed in **Table 1.12**.

Two types of binders from the same supplier were used in this study. The first one is a warm styrene-butadiene-styrene (SBS) Polymer-modified Bitumen (PmB) that was purposely designed to be used with rubber powders, and the second one is an SBS Polymer-modified Emulsion (PmE) containing 67–69% of residual bitumen. The binders' properties are given in **Table 1.13** and **Table 1.14**.

### 3.2.2. Highly-rubberised asphalt concrete samples' production

As illustrated in **Figure 2.12**, two different mixing and compaction procedures corresponding to the variation of the binder type and the mixing and compaction temperatures were adopted. In both cases, the dry process was used to incorporate the rubber into the mixes.

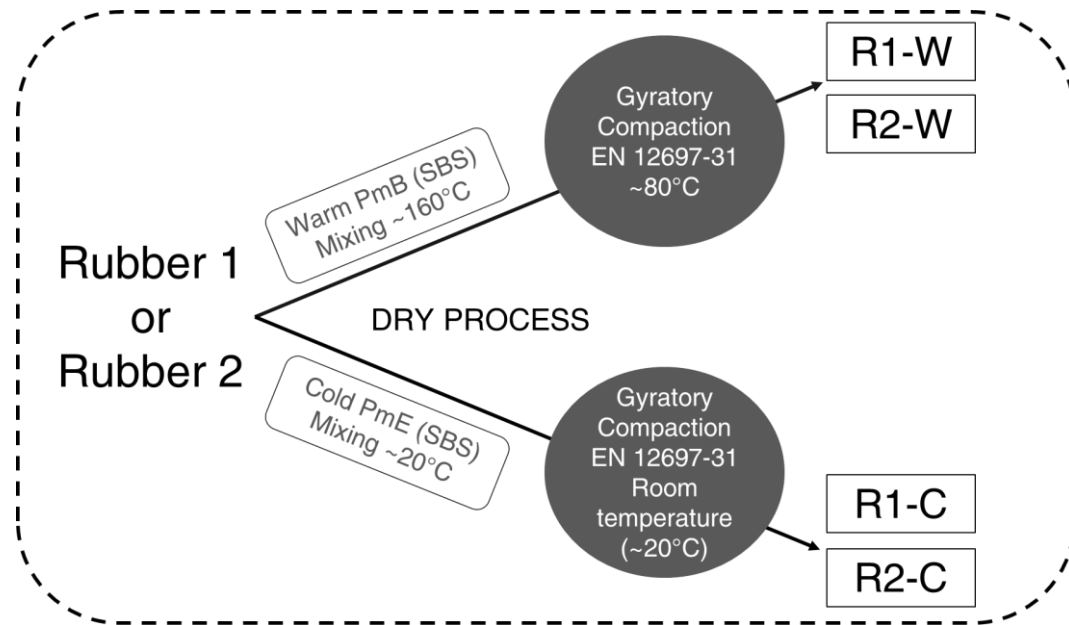


Figure 2.12: Rubberised asphalt production procedure.

In the case of the warm mix asphalt, the aggregates and the bitumen were heated at 160 °C in the oven before starting the procedure. At the beginning of the mixing process, the aggregates were added and homogenised for a few minutes in the mixer. Secondly, the bitumen and the filler were incorporated. The bituminous mixture was then mixed for five minutes. Finally, the crumb rubber mix was added, and the final mixture was mixed until homogenisation. After this process, the obtained mixture was divided into portions required to obtain a 100 mm diameter and approximately 40 mm thickness sample (approx. 600 g). The trays with the mixture were kept for a short period at a constant temperature corresponding to the adopted compaction one, i.e., 80 °C.

As for the production of the cold mix asphalt concrete, the aggregates, filler, and rubber particles are mixed and well homogenised before the addition of the emulsion. Using the mixture's organoleptic assessment preconised for the mixtures made with emulsions (EN 12697-55) [107], the mixing time was identified in less than five minutes. At the end of the mixing time, the mixture had a wet light-brown colour corresponding to that of an unbroken emulsion. This mixture was then weighted and divided into portions before the compaction at room temperature (approx. 20 °C).

The gyratory compactor (EN 1269-31) [108] was used for warm and cold mixtures. Each sample was compacted for 80 cycles. Twelve samples have been produced for each mix, and, independently of the production procedure, all samples incorporated the same amount of rubber, aggregates, and bitumen as listed in **Table 2.4**.

Table 2.4: Mixture composition in the percentage of the volume of the total mixture

(Volume of the total mix)	Warm PmB (SBS)		Cold PmE (SBS)	
	R1-W	R2-W	R1-C	R2-C
Rubber amount [%]	56		56	
Binder amount [%]	15		18	
Aggregates and filler [%]	29		26	

Additionally, the specimens' expansion from the original dimensions was measured right before and after one week from their compaction. The final expansion percentage is given in **Figure 2.13**. The cold-made samples expanded more than the warm-made samples, and the Rubber 1 samples expanded less than the Rubber 2 samples.

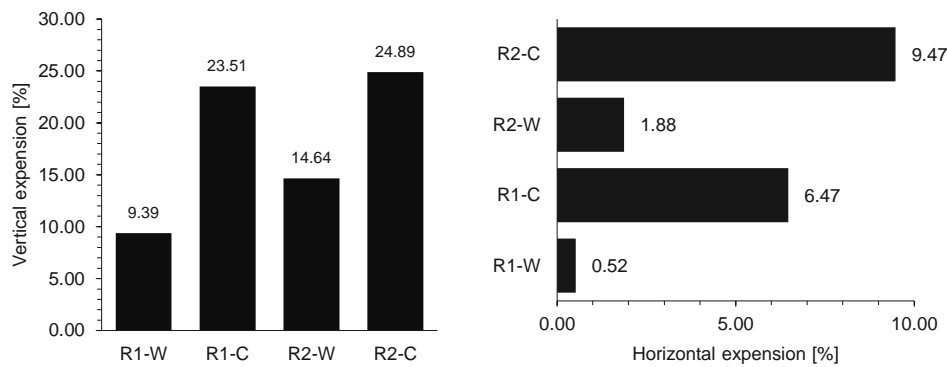


Figure 2.13: Vertical and horizontal expansion of the samples.

### 3.2.3. Freeze and thaw procedure

In addition to the effect of traffic loads, pavement deterioration can also be caused by cyclic climate actions. In recent years, thermal cracks and low temperature distresses have become a key concern for asphalt pavements in cold regions. In the laboratory, as in the real case, during the F–T cycles, the air temperature recurrently changes from positive to negative, and the layer is subject to repeated thermal stresses and related moisture effects. The compressive strength and the resilient modulus of the asphalt mix usually decrease when standard asphalt concrete is subjected to F–T cycles. Therefore, in this study, F–T cycles were also applied to the developed rubberised asphalt concrete to characterise and evaluate its behaviour in harsh conditions.

The samples were produced to carry out an F–T ageing procedure to analyse the cyclic temperatures, ice, and moisture effect on the degradation of rubberised samples. A sufficient amount of time of approximately 5 days was allowed before applying the cycles to provide complete curing for all samples. After a defined number of cycles

(0, 1, 5, and 10), volumetric, mechanical, and durability tests were conducted as schematised in **Figure 2.14**.

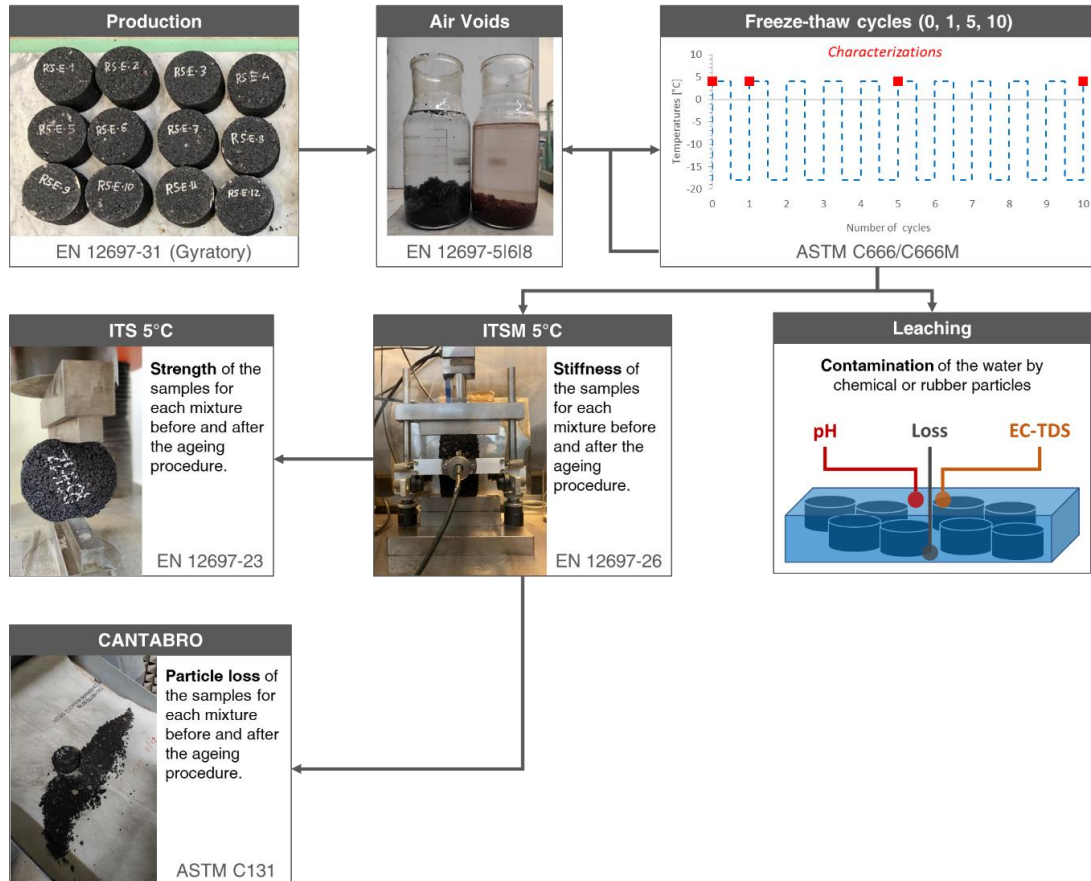


Figure 2.14: Summary of the experimental programme for each F-T cycle.

Following ASTM C666/C666-M [106], after the curing period and before starting the F–T cycles, each sample was conditioned for 48 h in water at  $23 \pm 2$  °C (room temperature). After the conditioning phase, the actual F–T cycles were started with a freezing phase set to reach  $-18 \pm 2$  °C and maintained for three hours (180 min), followed by the thawing phase carried out in cold water to reach  $+4 \pm 2$  °C and maintained for one hour and a half (90 min).

All samples of the control group (0 cycles) were tested following the ITSM procedure (EN 12697-26) [43]. Successively, some samples were destructively tested by means of the ITS (EN 12697-23) [44], while others underwent the Cantabro test (ASTM C131) [45], both destructive. This characterisation procedure was repeated on twin samples at 1 cycle, 5 cycles and 10 cycles of F-T, as shown in **Figure 2.14**. Finally, to obtain an outcome of the leaching potential of the samples when in contact with water, the pH and EC-TDS values of the thaw waters were analysed at the end of the cycles. The protocol of each method is detailed in the following sections, and the complete experimental programme is schematised in **Figure 2.14**.

### 3.2.4. Characterisation

After being produced and conditioned, the samples were characterised prior to the F–T procedure and during the treatment protocol at 1, 5, and 10 F–T cycles. Consequently, the air voids' content and densities [21-23], the Indirect Tensile Stiffness Modulus (ISTM) [43], the Indirect Tensile Strength (ITS) [44] and the Cantabro loss (CL) [45] results were recorded after each set of cycles. In addition, the pH and electric conductivity were also measured for each thaw water to investigate the potential leaching of the rubberised samples after prolonged contact with water in cold conditions.

#### 3.2.4.1. Densities and Air voids

The samples' bulk and maximum densities were calculated following the EN 12697-5 [110] and EN12697-6 [109] standards. After obtaining the densities values, the air voids' content was calculated as specified in the EN 12697-8 standard [111] by means of the previous parameters.

#### 3.2.4.2. Indirect Tensile Stiffness Modulus

The stiffness of the asphalt mixture has always been considered one of the main indicators of the material's mechanical properties at various temperatures, especially the extreme ones. In the case of highly rubberised mixtures, stiffness reveals how the rubber content influences the overall mix behaviour under dynamic loading. Thus, the ITSM was used to investigate the stiffness modulus of the rubberised mix asphalt at low temperatures, i.e., when surface layers are usually stiffer and prone to thermal cracking. The analysis was carried out following the EN 12697-26 [43] standards. It was chosen to adopt a 5 °C test temperature as an average low temperature enabling consistent testing and as an assessment of the stiffness in cold weather for a material conceived to be working at those temperatures. All samples have undergone 4-hour conditioning at 5 °C before being tested in the pre-cooled ITSM chamber.

#### 3.2.4.3. Indirect Tensile Strength

Like ITSM, the ITS is an indicator of the mechanical properties of the material, in particular of the maximum load to be applied before indirect tensile failure. The EN 12697-23 standard [22] has been used for its assessment. The cylindrical specimen is loaded diametrically with a constant displacement rate until failure. The indirect tensile strength is calculated according to the following equation:

$$ITS [MPa] = \frac{2 \times P}{\pi \times D \times H} \quad (1)$$

*ITS* is the Indirect Tensile Strength, expressed in MPa; *P* is the peak load, expressed in N; *D* is the diameter of the specimen, expressed in mm, and *H* is the height of the specimen, expressed in mm.

#### 3.2.4.4. Cantabro loss

The Cantabro test procedure measures the cohesive properties of compacted specimens using the Los Angeles Abrasion Machine. The percentage of weight loss (Cantabro loss) indicates the material durability and relates to the quantity and quality of the asphalt binder and mixture compaction. The Los Angeles machine is set to 30–33 revolutions per minute for 300 revolutions. After 300 revolutions, the loose mix (if applicable) is discarded, as shown in **Figure 2.14**, and the test specimen is weighted. ASTM C131 standard [45] was followed to carry out this test.

$$CL [\%] = \frac{W_{ini} \times W_{fin}}{W_{ini}} \times 100 \quad (2)$$

$CL$  is the Cantabro Loss [%];  $W_{ini}$  is the initial weight of the test specimen [g], and  $W_{fin}$  is the weight of the test specimen after the test completion [g]

#### 3.2.4.5. Measures of Particle loss, pH, and Electric Conductivity-Total Dissolved Solid

The leaching behaviour of the specimens was evaluated by analysing the thaw waters with a pH and EC-TDS meter. It was conducted to record the changes over time due to potentially released chemicals coming from the leaching of the asphalt specimen immersed in water. This tracking can show how leaching evolves.

The water was poured into the thawing tray, and the two parameters were measured at  $t = 0$ . Thus, samples (approximately 12 in each thaw tray) were immersed in water. Ten minutes later, the measurement was repeated. Additional pH and EC-TDS values were collected: one after the conditioning period of 48 h at room temperature before the start of the F–T process and others at the end of the F–T cycles number 1, 5, and 10.

In parallel with the leaching evaluation, the particles lost in the thawing water were collected, dried, and weighted to obtain a cumulative percentage of loss compared to the total weight of samples initially submerged in the tray. This measurement was made to control the potential particle loss to minimise micro-particle release in the environment.

These two protocols were conducted to have a quantitative view of the leaching and potential release of the rubberised asphalt developed during the F–T cycles procedure. The complete procedure is illustrated in **Figure 2.15**.

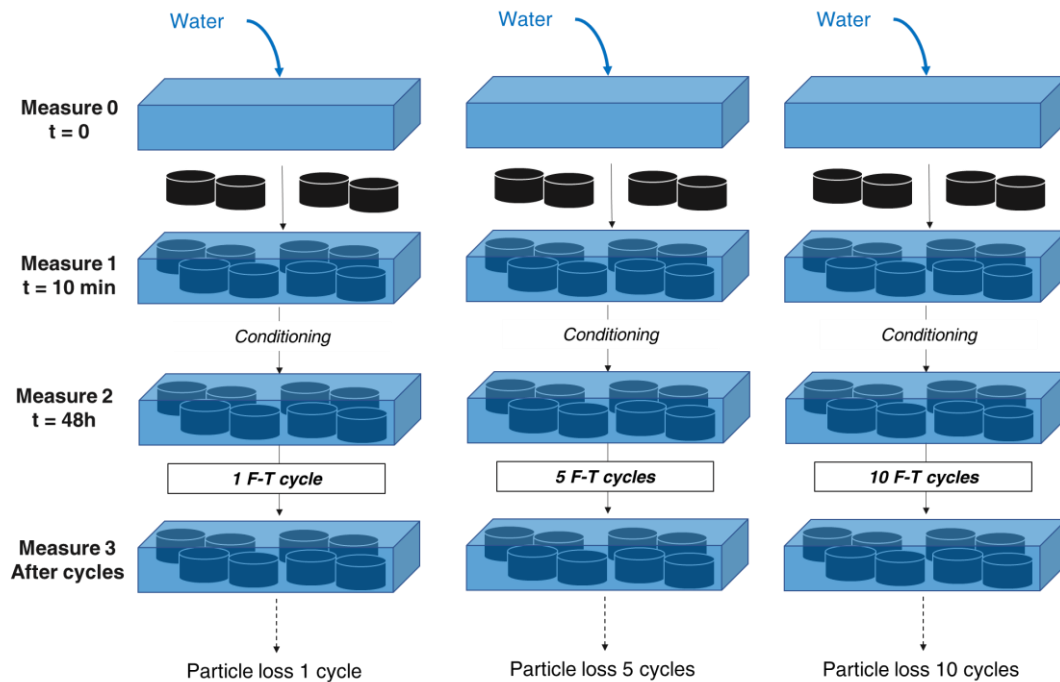


Figure 2.15: EC-TDS, pH and Particle loss measurement procedure

### 3.3. Results and Discussion

#### 3.3.1. Volumetric, geometrical properties of the mixtures and observations

The sample visual aspect is variable because of the type of binder used. The specimens made with the PmE have a softer consistency and a smoother surface texture than those made with PmB, and the specimens made with the PmE are generally softer than the others. Regarding the air voids' content, as shown in **Table 2.5**, the mixes are ranked as follows  $R1-C > R2-C > R1-W > R2-W$ . The samples made with PmE expand more and contain more voids than those made with PmB. In the case of the cold binder-based specimens, the expelled water can partially contribute to creating voids. Furthermore, the absence of heat also makes the rubber less malleable and less prone to digestion, i.e., swelling.

Table 2.5: Densities and voids values of the specimens produced

Mixes	EN12697-6 D Density	EN12697-5 B Maximum Density	EN12697-8 VA (%)	EN12697-8 VMA (%)
R1-W	1.467 ± 0.058	1.396	4.7 ± 3.7	34.0 ± 4.8
R2-W	1.406 ± 0.030	1.458	3.5 ± 2.0	31.7 ± 1.4
R1-C	1.300 ± 0.036	1.544	16.6 ± 2.3	42.4 ± 1.3
R2-C	1.430 ± 0.026	1.605	11.1 ± 1.6	39.7 ± 1.1

Any noticeable degradation was not observed on the samples during the F–T procedure. This observation was also made by Richardson et al., acknowledging the potential of the rubber to protect the concrete from F–T [104]. However, ice formation has been observed on the samples made with Rubber 2 and PmE binder (R2-C), but not on the samples made with the other mixes, as shown in *Figure 2.16*.



Figure 2.16: R2-C aspect after the 5<sup>th</sup> freezing cycle of the F-T cycles

### 3.3.2. Mechanical performances

#### 3.3.2.1. ITSM at 5°C

The ITSMs of the rubberised asphalt specimen were measured at 5 °C for control at  $t = 0$  and after 1, 5, and 10 F–T cycles and are shown in *Figure 2.17*.

At  $t = 0$ , the R1-C mixture exhibits the lowest stiffness values, while the R2-W has the highest. The mixture R2-W has a higher ITSM than R1-W, and R2-C records a higher stiffness than R1-C.

The R2-W mixture showed a higher stiffness than R1.W during the F–T cycles. In parallel, the overall tendency for R1-W and R2-W specimens is to increase their stiffness in the middle of the freeze and thaw procedure (precisely between cycles 1 and 5) before considerably decreasing at cycle 10 and reaching lower values than the other those of the control group (**Figure 2.17**).

The ageing of the binder can explain the initial increase in stiffness, and this phenomenon occurs in the first part of the procedure. The water diffusion inside of the samples may cause the decrease in the stiffness observed at the end, causing air voids to increase in the matrix, an expansion of the porosity, and confirming a lower ITSM value.

**Figure 2.17** shows that all samples could be tested at the control time (0 F–T), although sometimes it was challenging. On the contrary, the measurement of ITSM values at 1, 5, and 10 cycles was often impossible, mainly because of the low values and testing device limits.

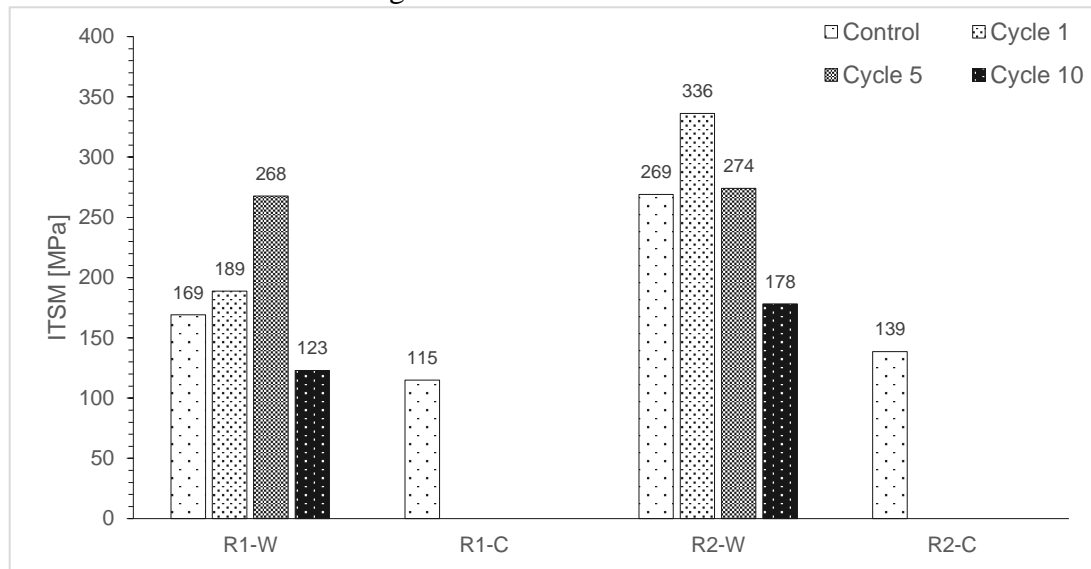


Figure 2.17: ITSM (@5°C) values for each mixture vs. cycles.

### 3.3.2.2. ITS at 5°C

The ITS tests of the rubberised asphalt specimens were performed at 5 °C for control at t = 0 and after 1, 5, and 10 F–T cycles. The visual and graphical results are presented in



Figure 2.18 and **Figure 2.19.**

In general, due to the high amount of rubber in the mixture, the cracks developed during testing are hard to see. However, the elastic behaviour of the materials was evident. At failure, samples are still cohesive and tend to spring back to their original shape. These observations are illustrated in



Figure 2.18.

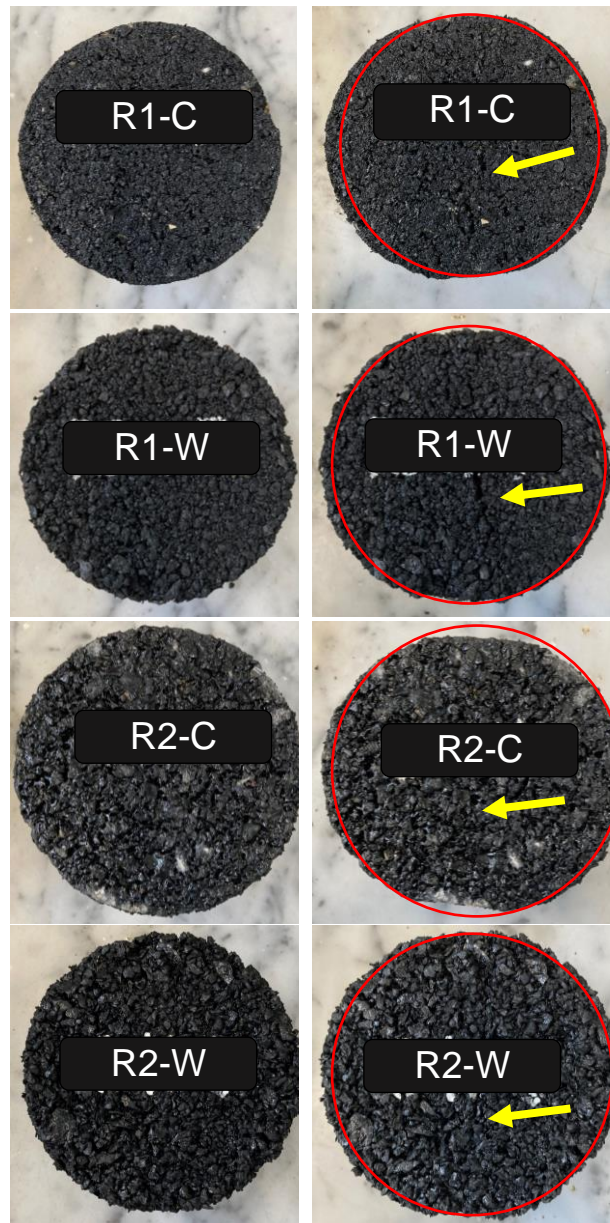


Figure 2.18: Comparison of the samples after 10 F-T cycles. In the left column, the samples before ITS test; in the right column, samples after testing. The red circle represents the deformation of the sample. The arrow highlights the crack initiated by the ITS on the samples.

Graphically, **Figure 2.19** shows that at  $t = 0$ , mixture R1-W had higher strength than R2-W, and R1-C had higher strength than R2-C. R1-W gave the highest value at 0.44 MPa, and R2-C the lowest at 0.06 MPa. Samples made with the warm bitumen had higher ITS than those made with cold emulsion. In the warm method, the temperature can contribute to the Physico-chemical interactions between the constituents, in particular, bitumen and rubber. In the cold mix, rubber is not heated, which allows the drop in fumes and odour emissions, but lacks in creating a strong, cohesive matrix

and the air voids' content remains higher, thus reducing the tensile strength of the -C samples.

With the increase in cycles, the ITS of samples made with PmB tends to decrease, while the ITS of the samples made with PmE does not vary. R1-W registered the highest reduction in strength along with the cycles. The decrease in the ITS registered for the PmB based samples can be explained by the same mechanism observed for the ITSM values.

Generally, the specimens made with PmE have a lower ITS than those made with PmB. The samples made with Rubber 1 have slightly higher ITS than those made with Rubber 2. Regarding the PmE based samples, a change in the visible mechanical structure is not evident. Indeed, the values of the ITS at 0 F-T cycles are low, and the same tendency is observed after all cycles. No increase or decrease in the ITS values is easily observed.

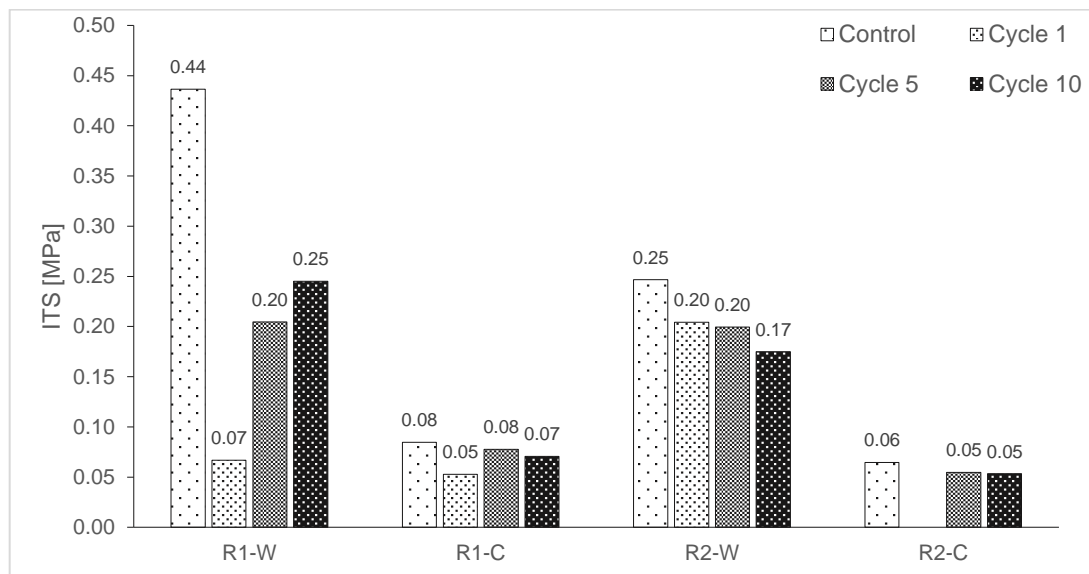


Figure 2.19: ITS values for tests carried out at 5°C and different cycles.

### 3.3.3. Particle loss

#### 3.3.3.1. Cantabro loss

The Cantabro loss of the rubberised asphalt specimens was measured at  $t=0$  (control) and after 1, 5 and 10 F-T cycles. Results are shown in **Figure 2.20** and **Figure 2.21**

For R1-W samples, the registered loss is stable, varying from 0% to 3% maximum. This range is the same observed in a previous study for a reference mix without rubber and made with SBS-PmB [23]. The Cantabro loss measured was around 1% without any F-T cycles, and a higher loss was observed after cycle 1. Concerning R2-W, the Cantabro loss is doubled comparing the control to cycle 10, with losses from 4% to

8%. Using the same warm binder, the mixture produced with R1 is stronger than with R2.

R1-C behaviour is hard to explain; the loss at  $t = 0$  is 60%; this value increases to approximately 90% in cycles 1 and 5, and it goes back to 61% after 10 cycles. However, with respect to R2-C, with the same binder, an increase in the amount of loss with cycles is evident. The loss values of R2-C samples at  $t = 0$ , 5, and 10 cycles are higher than those of R1-C ones.

As shown in **Figure 2.20** and **Figure 2.21**, in the case of R1-W, the F-T cycles seem not to strongly influence the loss. The durability of the mix is very high with reference to the applied F-T procedure. Effects of F-T cycles are visible on R2-W samples. R1-C and R2-C, both made with cold emulsion, are prone to consistent degradation due to the F-T. Nevertheless, the R1-C specimens appear to be somehow stronger. **Figure 2.21** also visually corroborates how the rubberised asphalt concretes made with Rubber 1 showed lower values in terms of the Cantabro loss test.

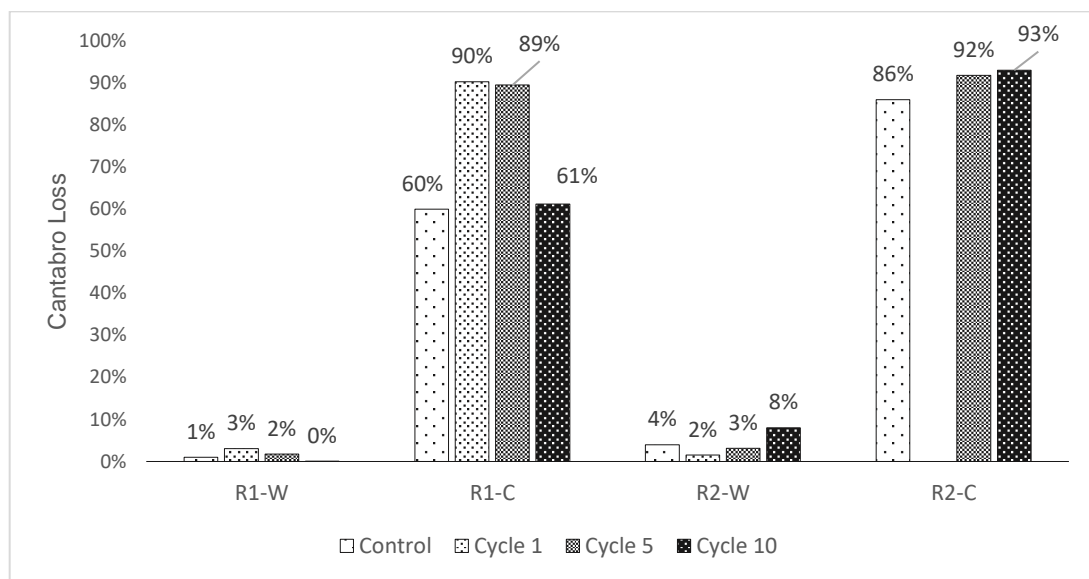


Figure 2.20: Cantabro loss percentage of the rubberised asphalt specimens at different stages of the F-T procedure

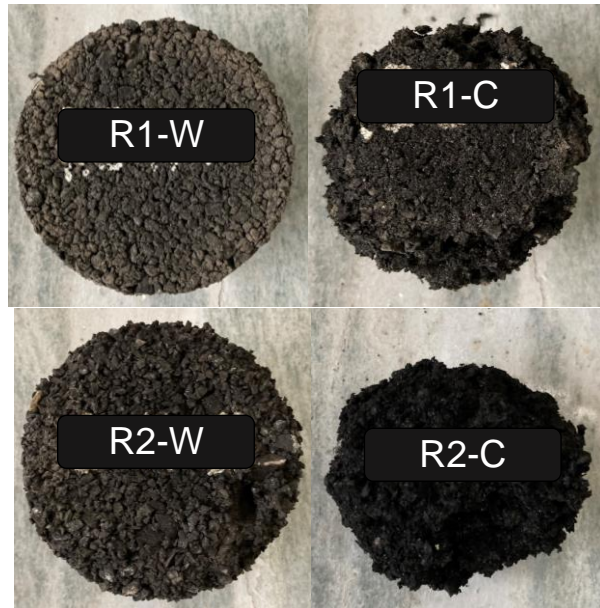


Figure 2.21: Aspect of the samples after the Cantabro test at the control time (no F-T).

### 3.3.3.2. Particle loss in the thaw waters

The particles lost in the thawing water were collected after 1, 5, and 10 cycles of F-T **Figure 2.22** shows that the alteration caused by the F-T procedure induces the release of particles in the water. In cycle 1, the loss is 0.04%, in cycle 5, it is 0.12%, and in cycle 10, the collected material corresponds to 0.19% of the total weight of the samples. This kind of loss in particles is often observed in standard asphalt concretes, where the iterative variation of temperatures can cause premature degradation of the material [86]. The results show that, in parallel to the Cantabro test results, the loss is higher for the mix made with the cold binder, which appeared more degradable. However, the measured loss is not a critical factor, and optimisation of the mix, such as a change in the gradation curve or improved control of the mixing process, could tackle the problem.

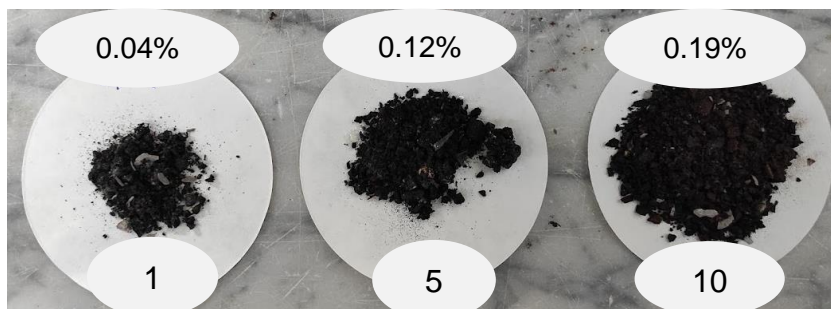


Figure 2.22: Loss of asphalt concrete samples material in the thaw waters after 1, 5 and 10 F-T cycles.

### 3.3.4. Leaching analysis

The leaching behaviour of materials is often studied because of its necessity in ensuring the safety of the materials used, in this case, the construction materials' safety and verifying their non-hazardousness to the environment. The leaching values collection was done by measuring the pH and electric conductivity of the water in contact with the rubberised asphalt samples during the F–T conditioning cycles. Data were collected before starting the F–T cycles at  $t = 0$ ,  $t = 10$  min,  $t = 48$  h, and during the F–T procedure at the end of the 1st, 5th, and 10th F–T cycles. Results are presented in **Figure 2.22**. The highest average electric conductivities were observed before starting the cycles after the 48 h of conditioning. Values decrease at the end of each cycle group (1, 5, or 10). The ECs after 1 cycle or 5 cycles are relatively similar, while after 10 cycles, the measured EC value increases. This observation revealed that the mixtures released some ions, and a higher number of ions is released in a short time into the water (after only 48 h). The EC also increases in relation to the time of contact of the samples with water.

The pH evolution of water was also tracked for the three thawing water and is shown in **Figure 2.23**. According to the results, the water pH from the F–T cycles increased as the duration of contact increased. At  $t = 10$  min, the pH of the water was verified, and it was relatively stable compared to the original water pH (7.2). After the 48 h conditioning period, the pH for all waters increased to 8.1–8.2. The pH of the three thaw water increased from 7.2 to above 8 between day 0 and day 2 and stabilised around 8.1 and 8.4 already after 1 cycle of F–T. However, the maximum pH (8.4) was observed at the last stage when samples were in contact with the water for longer (5 or 10 cycles). This observation confirms the EC results where the higher release of ions was observed after 5 or 10 cycles, regardless of the thaw waters. The maximum pH values for the rubberised materials occurring at earlier stages (after the conditioning period) were also in line with their maximum electric conductivity records at earlier stages (**Figure 2.23**).

The obtained values of EC and pH are comparable to those observed in a parallel study on highly rubberised asphalt leaching. In the study, the EC value increased at an early stage before decreasing, while the pH values were initially found below 7.5 and subsequently increased to 8–8.5 after 4–9 days, corresponding to the approximate time required for the present F–T procedure. It was also demonstrated that for a mix containing 56% rubber made with a cold or warm SBS modified bitumen, the recorded values were comprised in the thresholds set by the Dutch Soil Quality Decree [112]

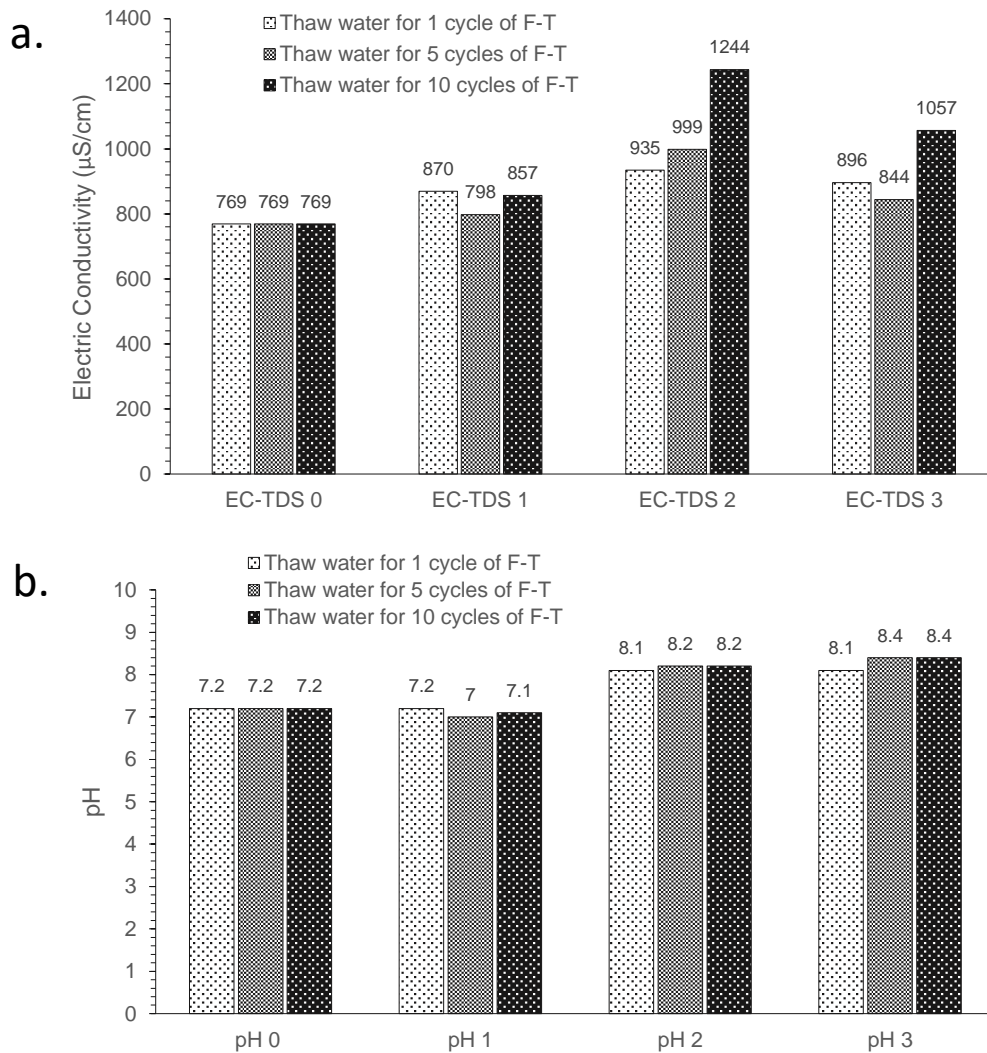


Figure 2.23: Changes in a. Electric conductivity and b. pH of thaw waters at different stages of F-T procedure for rubberised asphalt specimens.

### 3.4. Conclusions

This paper is part of a wider project aiming to develop a highly rubberised paving material that can offer important impact-absorbing performances and allow, in parallel, the recycling of end-of-life tyres in large quantities. Only a few studies have assessed similar materials in cold climate conditions and their potential degradation after several freeze and thaw cycles. The research investigated the stiffness, strength, and cohesive properties of the newly developed material, and it also measured the leaching of mixtures made with two different rubbers (1 and 2), bound with a warm (W) and a cold asphalt binder (C).

- The visual, geometrical, and volumetric assessments have shown that the specimens made with the cold binder are softer, expand more and contain more air voids than other samples.
- The ITSM test outcomes show that R2-W is stiffer than R1-W, and that specimens made with PmE are softer than those made with PmB. The cold mixtures were too soft even at 5 °C and could not be tested with the ITSM procedure. In this case, a uniaxial compressive analysis should be preferred.
- The ITS of specimens made with PmE are lower than those made with PmB. The samples made with Rubber 1 have slightly higher ITS than those made with Rubber 2. Regarding the PmE samples, a modification in the mechanical structure is less evident, certainly because the control values start low and no main fluctuation is observed, while the PmB-made samples show a clear decrease in the ITS value with the F–T cycles.
- Concerning the Cantabro loss method, the variation of particles lost along with the F–T cycles is very low for the cold specimens. The mixtures made with Rubber 1 record lower loss values after the Cantabro test, and R1-W have similar Cantabro loss than a standard asphalt concrete (without rubber) at 0 cycles.
- The values of EC and pH are comparable to those observed in a parallel study on highly rubberised asphalt leaching. The leaching is mainly observed in the first hours. The early leaching observed could be handled with several solutions such as rubber pre-treatment or water washing before their incorporation into the mix to limit and prevent their leaching into the pavement and consequently into the environment.

The cold mix should be preferred because of its important advantage regarding the workability and production methods by reducing externalities. However, improvements must be made to propose a viable and durable solution under freeze-thaw conditions, especially regarding the loss of particles.

Future studies should analyse the F–T effect of specimens made with the same formulation but incorporating rubber from a single source and treated with various surface modification methods.

#### **4. Outcomes**

The objective of this part was to assess the technical performance of the material (strength, durability, elasticity and stiffness). Then it was also verified that these performances comply with the climatic need to reduce emissions and waste and propose non-hazardous materials. Finally, some analysis of the durability to freeze-

thaw cycles of the two best formulations (mechanically and environmentally) was assessed thanks to F-T cycles in the laboratory.

The first part investigated the mechanical properties and analyzed the leaching of heavy in the water of the samples. It was possible to demonstrate that the 56% rubber-based material has a mechanical behaviour similar to the playgrounds. Further mechanical interpretations are foreseen.

While mentioning the leaching, part 1 showed that the release of heavy metals and ions was observed at an early stage and that the maximum threshold fixed by the used standard was not surpassed. Also, the leaching of PAHs was also analyzed to evaluate their leaching mode and amount also in water. The outcomes of this study are the objective of another publication not included in this thesis.

Finally, the F-T test conducted on the two best mixtures showed that no maximal degradation of the performances of the samples was observed and that the cold made specimens appeared to have a higher resistance to the variation of the temperatures.

In general, the mechanical and environmental status of the mixtures, especially the one made with the SBS binder, is not optimum. However, it is passing the standard regarding impact attenuation and leaching. This means that this material can be functional in its actual form. In addition, the performances and the problems found can be handled thanks to several outcomes and methods, such as tiny changes in the formulation or the use of additives and pretreatment control that will be proposed in the following sections of this dissertation.

## Chapter 3. Material modelling and accident cases simulations

The work proposed in this chapter is extracted from the following manuscript:

- Sahandifar, P.; **Makoundou, C.**; Fahlstedt, M.; Sangiorgi, C.; Johansson, K.; Wallqvist, V.; Kleiven, S.; A rubberised impact-absorbing pavement reduces the head injury risk for vulnerable road users: a bicycle and a pedestrian accident case study. *Accepted in Traffic Injury Prevention, Taylor & Francis, United Kingdom.*

*CM and CS developed the soft asphalt samples. PS, SK, CM, and CS designed the study. CM, KJ, and VW performed the standard HIC drop test. PS and CM performed mechanical testing. PS assessed test results, prepared the finite element models, and analysed the finite element simulations. MF provided the bicycle accident reconstruction. PS and CM wrote the original draft. SK, MF, CS, KJ, VW performed supervision, writing review, and editing. All authors critically reviewed and revised the manuscript.*

## **1. Overview**

An international and multidisciplinary research collaboration with the Neuronic Group in KTH, Sweden, allowed the development of an impact-absorbing paving material modelling and the simulation of pedestrians and cyclists accidents scenario.

This chapter aims to obtain more accurate results on the impact-attenuation and shock-absorbing properties of the developed material. Moreover, it is useful to quantify the reduction of the injuries registered thanks to the properties of the material designed in the laboratory. The study was based on the samples formulated and described in Chapter 1, especially the IAP 3 (made with a SBS modified bitumen containing 56% of rubber in the total mixture volume). This study aimed to obtain results on the actual injury reduction effect of the paving material on a full human body model when a fall occurs. The modelling of the material, based on the mechanical properties collected thanks to the same methods described in the previous chapter, allowed the simulation of two accident cases: one involving a pedestrian and another a cyclist. Indeed, the impact-absorbing material developed is meant to protect the VRUs. The test simulating real conditions is the best manner to optimize the formulations.

The paper is divided into a background part, a method, results and discussion, and the conclusions of the study's main results.

## **2. A rubberized impact-absorbing pavement can reduce the head injury risk in vulnerable road users: a bicycle and a pedestrian accident case study**

### **2.1. Background**

Between 20 to 40 percent of the road users in European cities are cyclists or pedestrians. Among all global traffic accident deaths and injuries, VRUs (pedestrians-cyclists-motorcyclists) share half of the victims [113]. Another published study comprising 31 cities' traffic fatalities from 2011 to 2015, of which 18 were European, suggests that the median urban traffic casualties are close to 80% for VRUs, where pedestrians and cyclists make up to 50% of those fatalities. It also states that the rate of fatality reduction is slower in cities compared to the corresponding national level. Although a possible reason for this difference is not clear, it can be speculated that VRUs do not similarly benefit from the safety and injury prevention advances in recent decades [114], such as 2+1 roads, anti-lock braking system, collision avoidance system, electronic stability control.

Despite the burden of the vulnerability of pedestrians and cyclists even in the absence of any vehicle, the pavements used by VRUs usually follow the same design and construction criteria as the light and heavy vehicle trafficked roads. In most pavements, stiff asphalt concrete is applied as a surface layer, where the pedestrians are not protected by any means, and cyclists can be protected only against head injury if wearing a helmet. The helmet use varies largely between countries and within countries [114]. Helmets have shown a protective effect [12]; however, more can be done in addition to personal protection, such as external/collective preventive measures, like improvement of the pavement layers, which have the potential to protect more road users independent of personal protection choices.

Many studies show that using recycled waste tires, also known as End-of-Life Tire (ELT) crumb rubber, can potentially improve the performance and the environmental friendliness of asphalt mixtures for pavement layers [33,34,115]. It is indicated that those rubberized mixtures have better durability, performance, and recoverability compared to traditional mixtures produced without rubber [115]. Although the capability of rubber in improving the characteristics of the asphalt concretes is tested extensively, only a few studies conducted tests to evaluate the injury prevention capability of rubberized asphalt mixtures [28]. A previous study [28] has shown that adding rubber in the asphalt mixtures could potentially reduce the head injury risk for VRUs. However, the effect of changing rubber content in the asphalt mixtures on reducing head injury has not been studied yet. Adding high quantities of rubber to the paving mixture could abate the pavement stiffness, thus

reducing the risks of injuries on footpaths or foot/bike lanes [57]. Previous studies limited the rubber content in the asphalt mixtures to prevent possible deterioration of asphalt characteristics, whereas this decision can limit the extent of the potential protective capacity of the asphalt.

The aim of the current study is to evaluate the potential effects of varying the rubber content in the rubberized asphalt concrete on reducing the risk of head injuries. Three different rubber contents of 14, 28, and 33 weight percent (%wt.), in addition to a reference asphalt mixture (0% rubber) and a playground material (100% rubber), were modelled in LS-Dyna. The developed material model for each mixture was validated using the standard Head Injury Criterion (HIC) drop test. Finally, the validated material model for each mixture was implemented in two low-speed accident reconstructions, a bicycle [116] and a pedestrian fall [117], to evaluate the preventive effect of varying the rubber content on the head injuries.

## **2.2. Methods**

Three asphalt mixtures, in addition to a reference non-rubberized mixture, were developed. A compressive test without permanent deformation and one with failure was performed on each of the mixtures. These tests were used to implement the mechanical behaviour of samples in LS-Dyna using the MAT\_SIMPLIFIED\_RUBBER material model. The developed material model for each sample was validated using the standard Head Injury Criterion (HIC) drop test. Finally, the validated material models were used to simulate both a bicycle and a pedestrian accident case. In addition to the asphalt mixtures, the two cases were also modelled using a typical playground rubber composite material.

### ***2.2.1. Samples Production Method***

The rubberized asphalt samples were produced following the same approach as detailed previously [57]. The mixture was designed and produced following methods similar to those already used in the asphalt industry. This is the main difference between the proposed paving solution and common playgrounds surfacing. Initially, the virgin aggregates and bitumen were heated up to 160 °C and mixed until homogenization. Later, the rubber was added to the mixture to obtain each of the samples containing respectively 14, 28, and 33 %wt. of rubber on the weight of the mixture. The mixing process lasted enough to have a fully coated and homogenous mixture. Finally, each group of specimens was compacted using a standard shear gyratory compactor (EN 12697-31[108]). A reference sample was also produced with no added rubber. The standard diameters of the cylindrical samples were 100 or 150 mm (**Table 3.1**). The samples were colour-coded for identification: the 0, 14, 28, and 33 percent rubberized samples' surfaces were coloured in orange, red, white, and

green, respectively (**Figure 3.1**).

Table 3.1: Summary of rubberized asphalt samples material properties and dimensions

	<i>Green</i>	<i>White</i>	<i>Red</i>	<i>Orange</i>
Rubber content (% wt.)	33	28	14	0
Bitumen content (% wt.)	18	18	18	8
Density (kg/m <sup>3</sup> )	1400	1450	1580	2222
D <sub>1</sub> * (mm)	38.5	38.7	38.3	38.2
D <sub>2</sub> * (mm)	150	100	150	150
H <sub>1</sub> * (mm)	44.3	37.2	47.1	40.8
H <sub>2</sub> * (mm)	39.8	37.1	42.6	34.9
Calculated Young's modulus (MPa)	0.93	2.03	2.73	260.6
Impact speed range in the Drop tests (m/s)**	[1.98–4.44]	[1.97–4.44]	[1.99–2.82]	N/A
Impact speed in the Drop tests (m/s)	1.98, 2.8, 2.82, 3.96, 3.97, 4.07, 4.19, 4.43, 4.44	1.97, 1.98, 2.8, 3.43, 3.71, 3.72, 3.95, 3.97, 4.19, 4.2, 4.42, 4.44	1.99, 2.41, 2.42, 2.46, 2.47, 2.52, 2.62, 2.65, 2.82	N/A
Stress-Strain destructive test results				N/A

\*D<sub>1</sub>/H<sub>1</sub>, D<sub>2</sub>/H<sub>2</sub> correspond to the diameter/Height of the samples for mechanical testing and Standard HIC drop test, respectively.

\*\*detailed impact speeds are presented in the Appendix II

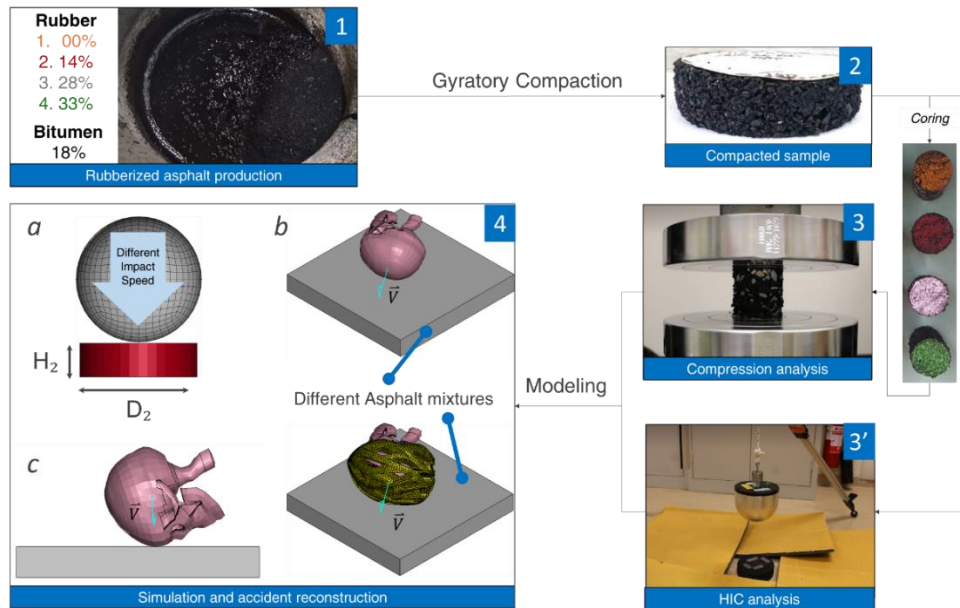


Figure 3.1: Study scheme of the experiments and simulations. (1,2) production of rubberized asphalt, (3) Compression test and HIC drop test on the samples, (4. a) HIC drop test simulations for different impact speeds, (4. b) An isometric view of the bicycle accident reconstruction case study on different asphalt mixtures, (4. c) The sagittal view of the pedestrian accident case on different asphalt mixture and the velocity vectors defined according to the local coordinate system on the center of gravity of the head. The blue arrow refers to the direction of the linear velocity.

### 2.2.2. Mechanical Testing and Material Modeling

The compacted asphalt samples were required to be smaller in diameter size to keep the forces below the limits of the available mechanical testing machines. Consequently, the sample was cored with a 40 mm coring rig (**Figure 3.1**). Two types of tests were performed on each of the mixtures: compressive test without permanent deformation and compressive test with failure (destructive test). A compressive elastic test on each sample was performed in which a 1% strain with a vertical displacement rate of 0.5 mm/min was applied. In the destructive test, samples were compressed with a vertical displacement rate of 5 mm/min until the failure point of either visible cracks in the samples or maximum absolute stress in the stress-strain curve. Both tests were performed using the Instron Universal Testing Machine model 5567 was equipped with a 30 kN load cell. Before the destructive tests, a relaxation test was performed on the green samples (33 % rubber) to measure their viscoelastic parameters. The Two types of tests were performed on each of the mixtures: compressive test without permanent deformation and compressive test with failure (destructive test). A compressive elastic test on each sample was performed in which a 1% strain with a vertical displacement rate of 0.5 mm/min was applied. In the destructive test, samples were compressed with a vertical displacement rate of 5 mm/min until the failure point of either visible cracks in the samples or maximum absolute stress in the stress-strain

curve. Both tests were performed using the Instron Universal Testing Machine Model 5567 was equipped with a 30 kN load cell. The viscoelastic parameters were neglected based on the evaluation of the 33% mixture **Figure 3.2**. Thanks to the linear regression analysis based on the evaluation of the IAP 3 sample (33% weight / 56% volume) (**Figure 1.13**), the viscoelastic parameters were neglected. All tests were performed at room temperature (21 °C).

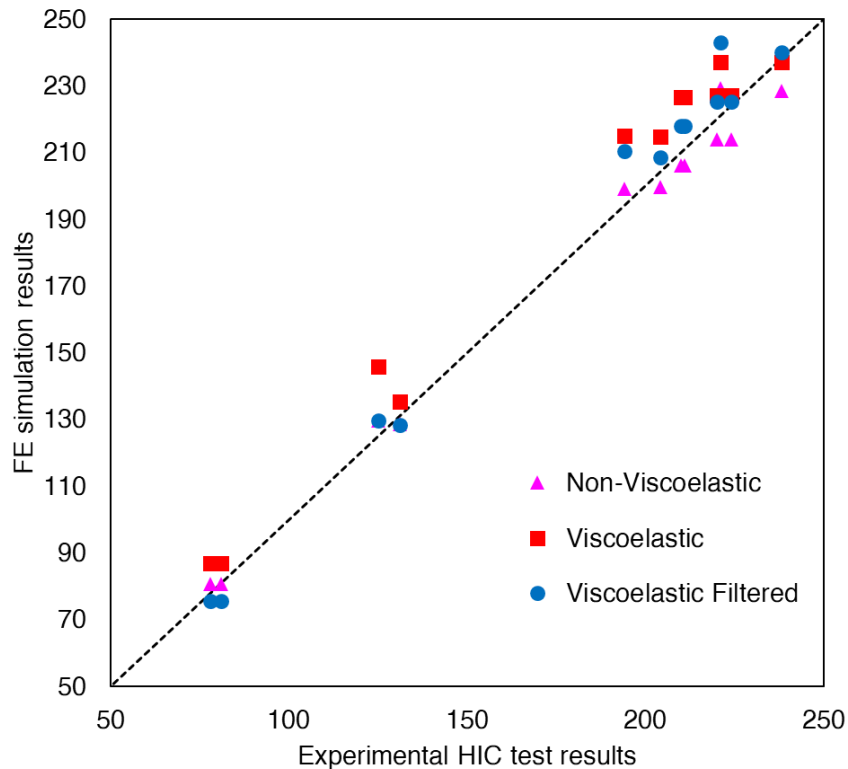


Figure 3.2: Linear regression analysis of the 33% sample material modeling with and without viscoelastic material parameters.

The constitutive behaviour of the samples was modelled using a material model \*MAT\_SIMPLIFIED\_RUBBER in LS-Dyna (LSTC 2020), and the samples were assumed to be isotropic. The destructive compression test results were directly implemented in the material card (**Table 3.1**).

The energy dissipation in the model during unloading was governed using a hysteresis unloading (HU) and shape factor of 0.1 and 5, respectively, for all samples. A summary of material properties can be found in **Table 3.1**. The stiffness of the reference sample (0% rubber) was significantly higher than the other samples. It was consequently modelled as rigid.

### 2.2.3. Validation Of Material Model Using Standard HIC Drop Test

A standard HIC drop test, according to EN 1177:2018+AC:2019 standard [41], was used to validate the material modelling of each sample that is implemented in LS-Dyna. A hemispheric 4.6 kg impactor with a diameter of 160 mm was released from different heights, and the impact speed and acceleration of the impactor were recorded (**Figure 3.1**). The standard suggests a sample size of at least 250×250 mm. Despite the recommended smallest dimensions for the asphalt samples, a cylindrical sample with 150 mm diameter for the 14% and 33% rubber content samples and 100 mm diameter for the 28% rubber content samples were used. However, impacts close to the edges were avoided to minimize the influence of edge effects. A summary of the impactor's impact speeds is reported in **Table 3.1** and used for the validation of the material model.

A steel spherical rigid impactor with the same diameter, weight, and impact velocity was simulated to impact the centre of the cylindrical asphalt samples. The samples were assumed to be on a rigid shell representing the ground (**Figure 3.1**). The acceleration of the rigid impactor was evaluated and compared to the measured acceleration at each impact speed of the same sample. All simulations were performed using version 971 revision 10.1.0 of LS-Dyna (shared memory parallel processing (SMP)-double precision).

### 2.2.4. Bicycle Accident Case

The asphalt material models were implemented into a single bicycle accident reconstruction where the bicyclist had lost control and fell on the ground [116] (Case 4) to evaluate the effectiveness of different rubber content of the asphalt mixture on preventing head injuries (**Figure 3.1**). A detailed finite element head model previously developed and validated against several cadaveric experiments [118] was used. The initial angular and linear velocities presented by [116] were applied to the head model. The head impacted each sample with 5.3 m/s ((3.42, 0.75, -4.00) in a global coordinate where Z is normal to the surface) and 4.7 rad/s resultant linear and angular velocities, respectively. The friction coefficient of 0.5 were applied to the head-ground contact according to [116]. It was assumed that the friction coefficient was not changed for different mixtures since the production method was the same as the regular asphalt. In addition to the head-only impact, a validated helmet model was implemented [12] to assess the combined effect of wearing a helmet and having the rubberized asphalt on head injury prevention. More details of the models can be found in previous publications [12,116,118]. In addition to the asphalt samples, a typical playground rubber-composite material was simulated as a reference to illustrate the effect of a rubber-only material [60,83].

The maximum von Mises stresses of the cortical and trabecular bone were compared to evaluate the ability of the asphalt mixtures to prevent skull fractures. The skull bone

was originally modelled with a plastic material model, where plasticity levels were set to 80 MPa for the cortical bone and 32.7 MPa for the trabecular bone [116]. The risk of skull fracture corresponding with linear acceleration and the risk of brain concussion corresponding with principal Green-Lagrange strain were evaluated using the risk functions presented by [119] and [118], respectively. The linear accelerations were filtered using SAE 300 filter.

### 2.2.5. Pedestrian Accident Case

The asphalt material models and the playground material were also implemented in a pedestrian accident case [117,120]. An elderly person tripped and fell forward onto a concrete pavement (case 3 in the [117] study). The initial impact occurred to the head, and the fall could not be stopped with any body parts. The initial resultant linear and rotational velocities (**Figure 3.1**) of 5.35 m/s ((1.53, 0, -5.1) in a global coordinate where Z is normal to the surface) and 1.36 rad/s were implemented according to the pre-impact velocities of the center of gravity of the head [117]. Same outputs and risks were presented for this case as for the bicycle case.

## 2.3. Results

The peak linear acceleration of the respective impact speeds in the HIC standard tests was compared between the simulations and experiments using the linear regression analysis (**Figure 3.3**). Accordingly, the 33% and 28% mixtures were in good agreement (slope  $\approx 1$ ;  $r^2 > 0.99$ ) with the experimental results, whereas the peak linear acceleration of the 14% mixture was underestimated (slope = 0.79;  $r^2 > 0.99$ ). The acceleration-time curves for different impact speeds on each were conducted.

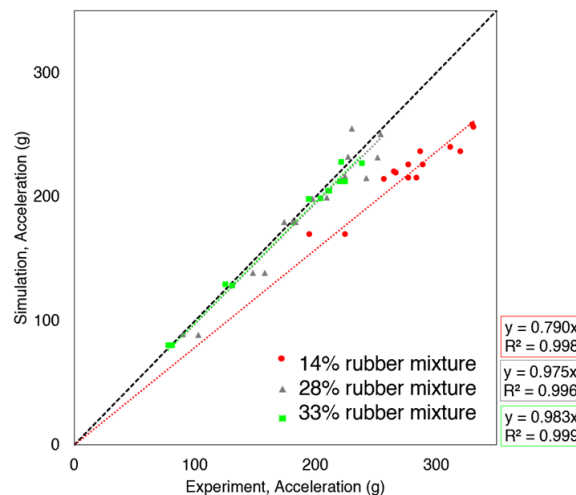


Figure 3.3: Linear regression analysis of maximum acceleration from the HIC drop test results and the simulation results for each asphalt sample.

The 14% mixture does not effectively reduce the peak von Mises stresses **Table 3.2**, and both bicycle and pedestrian cases reach the plastic stress level of 80.0 MPa defined in the material card. The 28% mixture reduces the stresses by approximately 11 percent in the cortical bone compared to the reference (0% rubber content) sample in both cases. The 33% mixture reduces the stresses on the cortical bone by 70 and 50 percent compared with the reference model for bicycle and pedestrian cases, respectively **Figure 3.4**. Moreover, wearing a helmet on the 33% mixture could further reduce the stresses on the cortical bone by 25 percent compared with the helmets on the reference (0% rubber content) asphalt mixture.

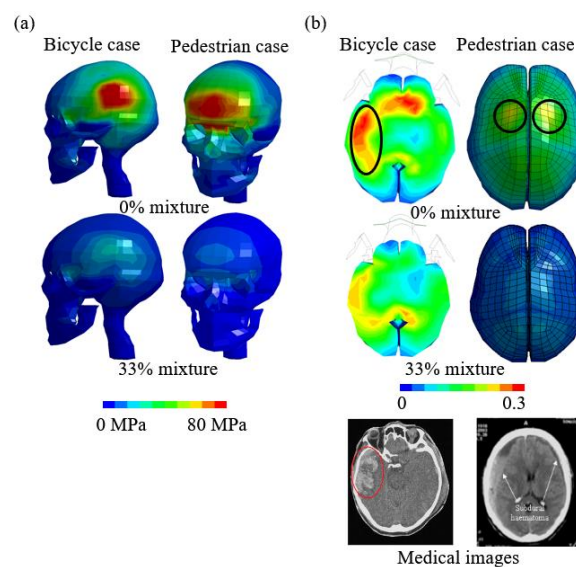


Figure 3.4: a) Comparison of peak von Mises stresses (MPa) on the cortical bone between the 0% and 33% rubber contents. The level of plasticity for cortical bone was set to 80.0 MPa. The highest stresses on the skull bone occurred at the impact position for the individual case; (b) Comparison of the peak 1st principal Green-Lagrange strain on the brain tissue between 0% and 33% rubber contents. The black circles correspond to the reported medical records of head injury in the bicycle and pedestrian case. Medical image for the bicycle case is from *The Accident Analysis & Prevention*, Vol. 91, Madelen Fahlstedt, Peter Halldin, Svein Kleiven, *The protective effect of a helmet in three bicycle accidents—A finite element study*, 135-143, Copyright (2021, Licence number: 5218740986803), with permission from Elsevier; the injury region is marked with a red circle. Medical image for the pedestrian case is from “An in-depth analysis of real world fall accidents involving brain trauma.” (2009), Michael D. Gilchrist and Mary C. Doorly, Copyright (CC BY-NC-ND 3.0 IE), the injury region is marked with arrows.

The 1st principal strain is evaluated on the brain tissue in each sample for both bicycle and pedestrian cases **Table 3.2**. In the bicycle case, the strain was not reduced in the 14% mixture and slightly increased (1.1 percent), whereas it only reduced about 13 percent in the 28% mixture. The 33% mixture has the most notable reduction among the asphalt samples, compared with the no-helmet case, with 27 and 75 percent in the bicycle and pedestrian cases, respectively **Figure 3.4**. Although wearing a helmet

when falling on the 33% mixture further reduced the stress and acceleration results, the principal strain slightly increased (6.6 percent).

In the bicycle case, the risk of skull fracture significantly drops up to 70 percent for the 33% mixture, whereas playground material can reduce it up to 90 percent **Table 3.2**. The risk of concussion was only reduced by 16 percent, which is still high compared to the helmet on the reference asphalt mixture case. In the pedestrian case, the risk of skull fracture for the 33% mixture is about three times the playground material (0.63 compared to 0.23), whereas their risk of brain concussion is similar (0.07).

Table 3.2: simulation results of the pedestrian accident on different rubberized asphalt samples

	<i>Bicycle case</i>				<i>Pedestrian case</i>			
	Peak von Mises stress for cortical bone (MPa)	Peak 1 <sup>st</sup> principal Green-Lagrange strain	Risk of skull fracture based on risk curve from [121]	Risk of concussion based on the risk curve from [122]	Peak von Mises stress for cortical bone (MPa)	Peak 1 <sup>st</sup> principal Green-Lagrange strain	Risk of skull fracture based on risk curve from [121]	Risk of concussion based on the risk curve from [122]
0% mixture-without helmet	80	0.52	0.99	0.97	80	0.31	1.00	0.64
14% mixture	80	0.52	0.98	0.97	80	0.26	1.00	0.48
28% mixture	70.7	0.45	0.77	0.92	69.6	0.13	0.96	0.14
33% mixture	24.1	0.38	0.29	0.81	39.2	0.08	0.63	0.07
Playground	17.6	0.38	0.07	0.83	29.3	0.08	0.23	0.07
0% mixture-with helmet	21.4	0.27	0.06	0.51	–	–	–	–
33% mixture-with helmet	15.9	0.29	0.04	0.57	–	–	–	–

## 2.4. Discussion

It was indicated that increasing the rubber content and indirectly reducing the stiffness of the material improves the capacity of the asphalt mixtures to reduce the risk of injury. Although the softest asphalt mixture, with the highest rubber content, was not as effective as wearing a helmet, it greatly reduced the risk of skull fracture for the bicycle accident case study. Similarly, the same mixture reduced the brain strain up to 75 percent and reduced the von Mises stresses on the skull up to 50 percent for the pedestrian case.

For the bicycle accident case, the peak linear acceleration decreases as the rubber content increases in the different rubberized asphalts. Although the peak linear acceleration is reduced in all rubberized samples, the 14% mixture was not soft enough to prevent the skull fracture (*Figure 3.5*).

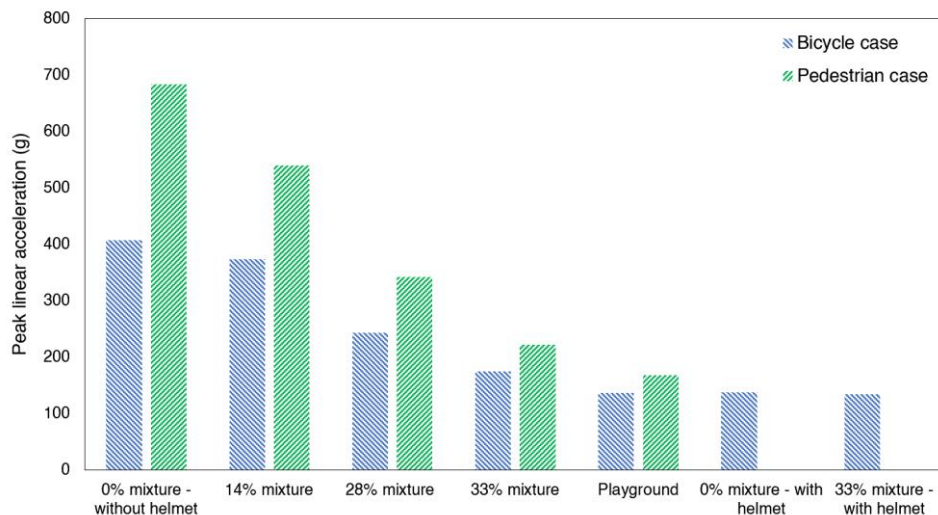


Figure 3.5: Comparison of the peak linear acceleration (g) between different rubber contents in the bicycle and pedestrian case. The risk of skull fracture was calculated for each of the simulations using the acceleration-time nodal history of a node on the center of gravity of the head.

The peak stress of the cortical and trabecular bone was reduced in the 28% and 33% mixtures alongside the peak linear acceleration, which could potentially indicate that increasing the rubber content above a specific threshold can reduce the skull fracture risk. It was indicated that reducing the linear acceleration can mainly reduce the risk of skull fracture, which is supported by previous findings [119,123].

It is shown that a helmet is still the best preventive tool with a 48 percent reduction of peak principal strain and around 50 percent risk of brain concussion. The helmet model used in the current study is similar to the traditional helmet designs currently available on the market. Wearing those types of helmets on the asphalt mixture with 33% rubber further reduces the risk of skull fracture. However, the peak principal

strain in the brain tissue increased to 0.29 (from 0.27) compared to wearing the helmet on the regular asphalt (0%). A possible explanation might be due to the increased contact area and contact time. The rubberized asphalt deforms after the impact, which increases the contact area between the helmet and the asphalt layer. Moreover, the time of contact increases due to the reduced stiffness of the material. Those two factors can change the dynamic of the head and the rotational acceleration, which indirectly correlates with the increased brain tissue strains.

In the pedestrian accident case, the peak linear acceleration of the 0% mixture was 683.2 g, which is comparable to the HIII headform experiment result (686.9 g) of a similar pedestrian accident reconstruction [120]. The peak linear acceleration dropped down to 67 percent for the 33% mixture. Despite the medical reports of no skull fracture for the pedestrian case, the peak stresses in a small number of elements have reached the limit of the cortical bone for the 14% and 0% mixtures. Even the risk of skull fracture for the 33% mixture was above 50 percent, which was higher than for the playground material (100% rubber).

The brain injury risk was developed using the logistic regression method. Therefore, small differences in the risk would be expected for deviations in the strain when it is closer to each end of the risk curve. The brain injury risk in the bicycle case when falling on the 0% asphalt sample was approximately 1, whereas the risk for the pedestrian case was 0.64. It means that the same relative reduction of maximum strain can cause a greater reduction in the risk of injury for the pedestrian case. The 28% asphalt mixture could merely reduce the peak principal strain up to 13 percent, while the 33% asphalt mixture reduced the strain up to 27 percent for the bicycle case. The peak principal strain and the risk of brain concussion were reduced considerably for the 33% and 28% mixtures for the pedestrian case. In addition to the nature of logistic regression curves, the initial conditions for the pedestrian case led to lower rotational velocity and linear accelerations during impact compared to the bicycle accident. It was shown [118] that lower rotational kinematics leads to lower strains in the brain tissue, which contributes to the better performance of the asphalt mixtures in the pedestrian case. It suggests a potential preventive effect of the rubberized asphalt samples for pedestrian accidents.

There are some limitations in the current study. The number of different rubber contents was limited to three (14, 28, and 33 %wt.), which did not allow for any practical conclusions about recommended thresholds for the minimum and maximum amount of rubber needed to ensure the preventive effects of the rubberized asphalt. Furthermore, the simulations are run without the inclusion of the neck and the rest of the body, which could influence the results. [124] showed that the influence of neck and body was affected by the impact situations on the concrete surface in a bicycle accident. In pedestrian-car accidents where the simulation duration or the impact

velocities are higher compared to pedestrian or bicycle accidents, the influence of the neck muscles was shown to be more noticeable [125]. Other studies have suggested that the compliance of the impact surface influences the importance of including the neck and the rest of the body. For instance, [126] concluded that the impact to the turf in jockey accidents had a long contact duration between the head and turf which motivates the inclusion of the neck. The experiments were limited to two samples for each rubber content for the compression tests. This limitation can increase the influence of inhomogeneity or production defects in the modelling of mixtures. The 28% and 33% mixtures had good agreement with the experimental result, which could alleviate the concerns for this limitation; however, the 14% mixture underestimated the experimental results (*Figure 3.3*), which could indicate that a simpler model like the elastic model could be a better material model for this mixture. Another limitation is that the drop tests were performed on smaller sample diameters than the suggested dimensions according to the standard. This size could potentially affect the resultant impact responses of the sample due to edge effects. The drop tests were not used as an indicator of the injury prevention capability of the rubberized asphalt mixtures, and it was only used for validation of the material models. Furthermore, the friction coefficient of the samples was assumed to be the same for head-to-ground contacts. [127] performed a sensitivity analysis for the friction coefficient ( $\pm 0.2$ ) and demonstrated that the peak strain responses change approximately  $\pm 0.07$  in head-to-ground contacts. Moreover, the asphalt mixtures were produced similar to non-rubberized mixtures, and the surface was not specifically treated to affect the friction. This supports the similar friction coefficient assumption for the asphalt mixtures. Ultimately, the samples were assumed to be isotropic and nearly incompressible due to the presence of rubber. The bulk modulus of the samples was indirectly calculated using Young's modulus and Poisson's ratio. Despite the above limitations, it was indicated that the rubberized asphalt mixtures could potentially reduce the head injury risk when the rubber content increases.

Among the three rubber contents tested, the softest asphalt mixture containing 33 %wt. rubber reduced the risk of skull injury and brain tissue injury in the bicycle accident by 70 and 16 percent. The risk of brain concussion reduced most in the pedestrian case, where it was lowered to 7 percent with the 33 % rubberized asphalt mixture. Given that only one pedestrian and one cyclist head impact cases were studied, and these types of impacts can vary greatly in real-world accidents, it is still necessary to further investigate the minimum rubber content that is required to minimize the risk of any head injuries. Ongoing research is addressing the improvement of material workability and durability by means of alternative binders and rubber surface treatment. In parallel, reduced severity in case of human impact

and mitigation of the environmental footprint are considered in the development of the impact-absorbing pavements.

### **2.5. Conclusions**

In the current study, the potential effects of varying the rubber content to reduce the risk of head injuries were evaluated in a set of rubberized asphalt mixtures. Three different rubber contents were tested; among them, the softest asphalt mixture containing 33 percent rubber on the material weight reduced the risk of skull injury and brain tissue injury in the bicycle accident by 70 and 16 percent. The risk of brain concussion reduced most in the pedestrian case, where it was lowered to 7 percent with the 33 % rubberized asphalt mixture. It is still necessary to further investigate the minimum rubber content that is required to minimize the risk of any brain injuries. Ongoing research is addressing the improvement of the material workability and durability by means of alternative binders and rubber surface treatment. In parallel, reduced severity in case of human impact and mitigation of the environmental footprint are considered in the development of the impact-absorbing pavements.

### **3. Outcomes**

The objective of this section was to obtain results on the impact-attenuation and shock-absorbing properties of the developed material on a real human body if a pedestrian and cyclist fall on the IAP. It permitted to quantify the reduction of the injuries registered thanks to the properties of the material designed in the laboratory.

The IAP 1, 2 and 3 were able to be modelled and studied in bicycle and pedestrian accident simulations. The content of rubber of the IAP 1 was proved to be not effective enough for skull fracture prevention. The IAP 3 (33% weight/56% rubber volume) can diminish the risk of brain injuries and concussions. The use of such a pavement can approach the protective abilities of a helmet.

The study also confirmed that the IAP 3 is the best one of the three studied.

More studies on the material injury reduction properties are foreseen. Indeed, some comparisons between the IAP materials and the known values with helmets collected through helmet ranking studies are to be conducted.

## Chapter 4. Field trial

The work proposed in this chapter is extracted from the following manuscript:

**Makoundou, C.;** Sangiorgi, C.; Johansson, K.; Wallqvist, V.; Kleiven, S.;  
Laboratory and in-situ characterisation of a dry recycled-based Impact-absorbing  
pavement cold produced and laid. *In preparation for submission to Scientific  
reports, Nature, United Kingdom.*

*C.M. conceived the study, and developed impact-absorbing material produced with the cold method thanks to the concept initiated by V.W. and K.J. C.M. performed the laboratory characterisation. C.S. and V.W. performed the HIC test in situ. C.M and C.S performed the tests and verifications after 6 months of exploitation. C.M. analysed the data and wrote the original draft of the manuscript. C.S, V.W and K.J. reviewed and edited the manuscript. All authors have read and agreed to the submitted version of the manuscript.*

## 1. Overview

The focus of this Chapter is the possibility of reproducing the laboratory tests and the issues arising from the upscaling of the production process. Indeed, the developed material is meant to be used under outdoor conditions on road infrastructures.

The three previous chapters allowed to identify the best mixture regarding the feasibility (chapter 1), mechanical or environmental impact and ageing resistance in cold weather (chapter 2), and the injury reduction (chapter 3).

Furthermore, after achieving the optimal combinations, it was decided to test the cold one in situ. The cold process was preferred because it facilitated the workability and made the mixing in situ possible. Besides, it avoided the release of smell and smoke, and reduced the workability typical of the use of rubber in high quantities.

Three rounds of adjustments and optimisations were made before the final trial site in Imola, Italy. This permitted to vary the rubber gradation and the emulsion characteristics thanks to a collaboration with the suppliers. The mixture used was an optimized version of “IAP A4 or Rubber-Cold” (33% wt / 56% vol of rubber and the SBS modified bitumen-based emulsion). The optimization consisted of changing the rubber size for the same percentage of rubber (less fine). Moreover, cement was added to the aggregates mix and additive agents were added to the emulsion.

The chapter is an essential part of the doctoral research because it describes upscaling the production and testing methods from the laboratory to the field. The specimens were tested for mechanical, friction, and impact-attenuation properties in the lab. The pavement laid on the trial hybrid (both bike and pedestrian path) lane in Imola was tested for walkability, cyclability, friction and impact-absorbing performance. Furthermore, the experimental pavement was trafficked by pedestrians and cyclists for six months, from June 2021 to November 2021. After this period, how the weather affected the newly developed material was controlled. Also, it was possible to verify the bonding conditions of the IAP layer on the binder course underneath and simulate possible maintenance that may occur on a used pavement by patching the core holes with the same mixture.

## **2. Laboratory and in-situ characterisation of a recycled-based Impact-absorbing pavement made with a dry and cold production and construction procedure**

### **2.1. Introduction**

The growing population and traffic in the urban areas have led to remarkable changes in the development of road infrastructures. As the demand for new paving solutions increases, various studies on traditional and innovative road materials are pursued.

Road pavements are crucial materials of outdoor transportation infrastructures and occupy an important part of the human mobility ecosystem. Nowadays, they have evolved from constructions that were simply designed and built to support the vehicles passing daily to materials made with a circular use of resources and recycling with significant environmental potential and economic importance [63,128]. In addition, pavement functions such as energy harvesting[129], hydronic performance[130], permeability [131], urban heat island mitigation [132], noise reduction [133] and vulnerable users' friendly impact-absorption[52] are also expected.

Crumb rubber is a raw material used to successfully reach the two latter functions mentioned above. In addition to its recycling impact[30,32,35], recycled rubber is known for its effectiveness in designing low-noise pavements or impact-attenuation applications, thanks to its residual elastic properties [60,134,135].

Several studies on crumb rubber as a partial replacement of the mineral aggregates by using the dry process[55,136,137] exist. Nevertheless, the volume percentage of the replaced aggregates is limited[100]. This is because the goal and the final application are very different. In fact, when the rubber amount is limited, the objective is to enhance the flexibility of the pavement for wheeled and heavyweight vehicles [40,138]. However, in the case of shock-absorbing pavements, the aim is to propose the impact-absorbing surfaces for sidewalks, bike lanes and hybrid portions for safety and security purposes. Concerning the last cited, some work has already been done on the development of IAPs with more than 50 vol-% of crumb rubber of the aggregates. Their ability to reduce fall-related injuries have already been studied. However, in these cases, only hot or warm mixing methods were tested, and the data collection on the durability of the material over time is limited. Additionally, in these studies, the rubber was mixed with concrete or hot and warm asphalt binders [27,29,52,57].

The current project aims to (develop, test and) evaluate the mechanical, impact-attenuation and friction performances of an Impact-absorbing pavement material able to reduce the injuries caused by falls, mainly intended for sidewalks and bike lanes in urban areas. A portion of the mineral aggregates (0-4 mm) was replaced by the same volume and particle size distribution of crumb rubber recycled from end-of-life tyres to produce this material. The use of rubber is motivated by the willingness to obtain

an elastic material fostering the circular economy of the tyres in the transportation ecosystem. Also, an SBS-modified emulsion was used, and it made possible a cold production and a dry process. It facilitates the mixture's workability and makes it possible to avoid the release of smell, smoke, and stickiness problems. Firstly, several samples of the IAP material of different sizes (A -150 mm and B-40 mm diameter), with different compaction levels (10, 20, 30 and 80 cycles) and with different surface configurations (non-treated, simple treatment, and aggregates treatment) were produced in the laboratory to conduct mechanical, HIC and Slip analysis. Then, an upscaling of the process was made to produce and construct a trial field to verify the production's repeatability and feasibility. On this trial site, the HIC measurements were repeated. After 6 months of usage and weather tracking, the friction was assessed, and some measures and observations were made on the evolution of the surface and its durability over time. It is expected to verify the impact-attenuation performances and the material's durability when laid in outdoor conditions. Also, the collection of mechanical and friction results will make possible the definition of acceptance criteria to ameliorate and optimise the IAP material for further use in cities. Its implementation would reduce the injury and cost related to the fall of vulnerable road users (VRU) on the surface.

## 2.2. Methods

An overview of the study plan, including the usage of different components, the laboratory and field preparations and productions, and the corresponding characterisations carried out, is shown in **Figure 4.1**. Further details are explained in the following section.

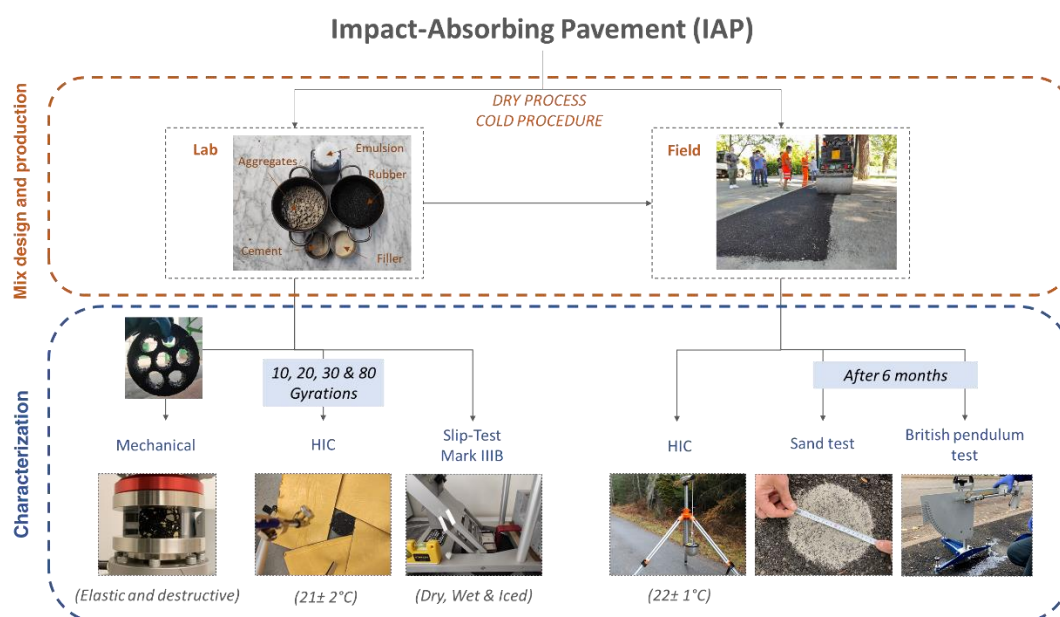


Figure 4.1: Scheme of the research plan conducted in this study.

### 2.2.1. Preparation and production of the samples in the laboratory

Two types of samples were needed. The type A samples were used for the laboratory HIC and Slip tests, while the type B samples were used for the mechanical tests (**Figure 4.1**).

The impact-absorbing asphalt (IAA) mixture is made of 56% by volume of aggregates of crumb rubber (0-4 mm) recycled from end-of-life tyres (**Figure 4.2**).



Figure 4.2: Image of the rubber mix used in the IAP formulation: Coarse, Medium, and fine.

This mixture was produced by partially substituting the mineral aggregates portion (0-16 mm) with the same volume of rubber using a hot-rolled asphalt sieving curve as reference (**Figure 4.3**). The final mixture weight contains 46% wt (22% vol) of aggregates (larger than 4 mm), 34% wt (56% vol) rubber (smaller than 4 mm). All production was made at room temperature using the dry process coupled to a bitumen-based SBS-modified emulsion (PmE) with a dosage of 21-22% by total mixture mass. 1 % wt of cement was used as an additive to the mixture and breaking facilitator for the emulsion. The mixing process lasted 1-2 minutes to have a fully coated and homogenous mixture. This assessment was made using the organoleptic procedure described in the standard EN 12697-55 [107]

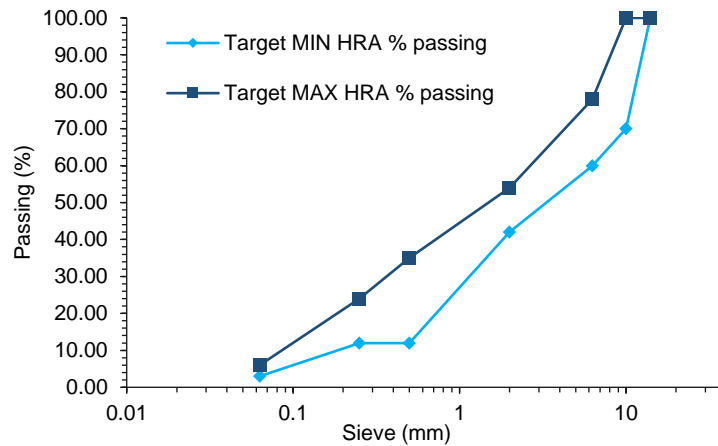


Figure 4.3: Gradation curve of the HRA used as a reference for the design of the IAP

The specimens (150 mm diameter and approx. 40-45 mm thick) were compacted using the gyratory compactor. Samples were produced for each number of gyratory cycles: 10, 20, 30 and 80 to compare the laboratory compaction to the field one. Finally, some samples were produced by modifying the surface characteristics to simulate the after treatment intended to be used in the field site. These samples underwent some after treatment consisting of coating the surface with a thin layer of:

- Transparent artificial emulsion (Simple treatment (ST)) **Figure 4.4** (centre)
- 3-4 mm aggregates and transparent artificial emulsion (Aggregate treatment (AT)) **Figure 4.4** (right)



Figure 4.4: Sample with different surface characteristics: Non-treated (NT); Simple treatment (ST); Aggregate treatment (AT).

For the mechanical tests, the compacted IAP samples were required to be smaller to maintain the forces below the limits of the available testing device. Therefore, the specimens were cored to reach 40 mm diameter with a coring tool, as shown in **Figure 4.1**.

### 2.2.2. Production of the IAP and construction in-situ.

For a material intended to be used as a protective layer in urban road areas, an *in-situ* study is indispensable to validate the laboratory results, proving the repeatability and reproducibility and identifying problems due to the upscaling of the process.

The same mixture used in the lab was used to build a trial site in Imola, Italy. The mixing, laying and compaction were done in the field. As mentioned previously, the cold mixing procedure was preferred over the warm one used in the previous studies[52,57] because it facilitates the mixture's workability and makes it possible to avoid the release of smell and smoke, as well as stickiness problems.

The pavement was tested for HIC and friction (British pendulum value and sand test). Thus, after six months of exploitation, observations, coring and patching of the holes were also conducted to simulate short maintenance of the portion.

### **2.3. Characterisation methods**

#### ***2.3.1. Mechanical characterisation of the IAP***

Two types of tests were performed on the mixture: a compression-relaxation test by applying a small strain at time=0 and holding it constant for 60 s (elastic test without permanent deformation (elastic test) and a compressive test until failure, both with quasi-static and dynamics vertical displacement rates (destructive test).

The compressive stress-relaxation test on the cored samples was performed in which a 5% strain with a vertical displacement rate of 20 mm/smin was applied. In the destructive test, samples were compressed with a vertical displacement rate of 0.43 mm/s (QS), 43 mm/s (D1) and 430 mm/s (D2) to reach approx. 60% of deformation corresponding to the failure point of either visible cracks in the samples or maximum absolute stress in the stress-strain curve. The tests were performed using an Instron Electropuls E3000 testing machine equipped with a 3 kN load cell.

#### ***2.3.2. Shock-attenuation performance of the IAP.***

The HIC drop test was conducted according to EN 1177 standard [41]. It was used to determine the sample's material impact-attenuation performance at different compaction levels. The criteria of general protection standards are fixed by a peak acceleration of 200G and a value of 1000 for the HIC. A hemispheric and concentric 4.6 kg impactor simulating the weight of a human head was released from different heights, and the impact speed and acceleration of the impactor were recorded. The same method was used in the lab and in-situ.

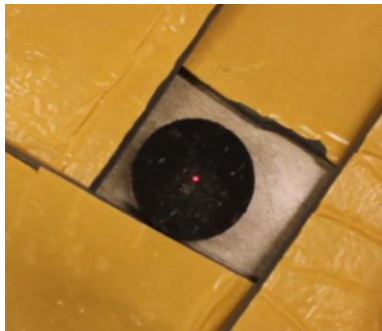


Figure 4.5: Delimitation of the impact zone with a laser.

Regarding the laboratory testing, the standard suggests a sample size of at least 250×250 mm. However, 150 mm diameter cylindrical samples were used due to the laboratory production configuration. A laser was used to restrict the impact zone, as shown in **Figure 4.5**. The samples were assumed to be on a rigid support and tested in the same laboratory.

### ***2.3.3. Surface analysis and friction behaviour of the material***

#### ***2.3.3.1. Skidding analysis in the laboratory using a Slip Tester***

Measurement of the coefficient of friction (COF) between the shoe/sole and the floor is essential in understanding the risk of slipping accidents. Therefore, the COF of the same material with three different surface configurations were measured under three surface conditions: dry, water-wetted, and iced. The COF measurements were conducted using a Brungraber Mark IIIB slip tester, a Portable Inclinable Articulated Strut Slip Tester (PIAST) [139] (**Figure 4.6 left**). It simultaneously applies parallel and normal forces to a surface by impacting a footwear sample on the material. The angle of the strut is increased until a slip occurs. The starting angle should be smaller than the angle at which a slip is anticipated, and the angle is slowly increased until the slip occurs. The tangent of the angle is the COF marked on the tester. The test was repeated at one location and averaged to better represent surface conditions.

This test was performed with four footwear materials: Flat rubber (FR), Textured Rubber (TR), Grooved neolite (GN), and Grooved Rubber (GR), as illustrated in **Figure 4.6 (right)**. All materials simulate shoe (or bike) material that may be used on-site.

Under amelioration and optimization and regulated by an ASTM standard, it gives a preliminary outcome on the behaviour of the surfaces under different footwear and climatic conditions, both in the laboratory and in the field. It also allows the evaluation of the surface by using footwear available on the current market.

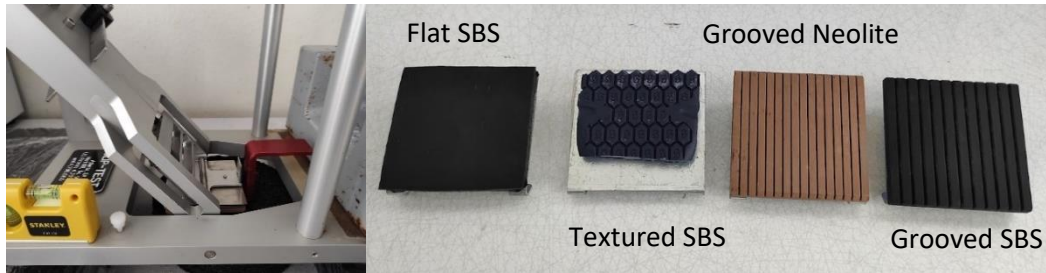


Figure 4.6: Illustration of the Brungraber Mark IIIB slip tester and feet tests used.

### 2.3.3.2. Skidding in-situ analysis using a British pendulum

The slip and skidding risk was assessed in-situ by using the British pendulum (**Figure 4.7**) as described in the EN 13036-4 [140]. This test was useful to estimate the risk and probability of skidding on a surface.



Figure 4.7: British Pendulum test in-situ

### 2.3.3.3. Sand test

The method described in the EN ISO 13473-1[141] standard and illustrated in **Figure 4.8** was used to determine the mean profile depth as well as the macro roughness and texture of the surface. This test is useful for estimating the skid resistance and surface characteristics of the material or finishing technics. In this case, it was intended to characterise the surface of the newly developed material in the field.



Figure 4.8: Determination of the macrotexture depth according to the volume sand patch method

### 2.3.4. Tracking of the Natural Ageing of the trial field.

The pavement was laid outdoors, and its evolution was visually tracked over time have been assessed at  $t = 0, 1$  and 6 months for six months. **Figure 4.9** shows the variations in temperature, rainfall, humidity, and UV index in the city of Imola, measured from June 2021 to November 2021 [142].



Figure 4.9: Weather measured from June 2021 to December 2021 in Imola, Italy [142].

## 2.4. Results and Discussion

### 2.4.1. Mechanical properties

The Compressive tests were conducted on the type B specimens produced in the laboratory due to the apparatus's maximum load limit to assess the mechanical behaviour of the IAP. Both viscoelastic (relaxation) and destructive (strength) tests were carried out on the samples as described in the Methods section.

**Figure 4.10** shows the graphical results of the carried tests. **Figure 4.10.a** and **b** respectively show the relaxation modulus over time and the compressive stress over the strain of the samples. These results demonstrate that the samples have a

viscoelastic relaxation response to an applied constant strain the stress. Indeed, the value of the stress decreases progressively over time. Moreover, the sample did not relax instantly after unloading and tended to find the original shape after a certain amount of time (some minutes). These results reveal that the material can be compressed, and this property is mainly needed for impact-attenuation performance.

Concerning the compressive strength of the material, three different behaviours have been observed depending on the rate of load application. When applying a quasi-static load, the material elastic behaviour is more present. However, the viscoelastic behaviour is dominant when a dynamic rate is applied, showing a typical increased stiffness with an increased deformation rate **Figure 4.10 a**. This observation is useful to show the absorbing and cushion effect of the material under compression. Finally, after their destruction, the relaxation of the samples was still observed, and the specimens tended to stay bounded, especially at the rubber-binder interface.

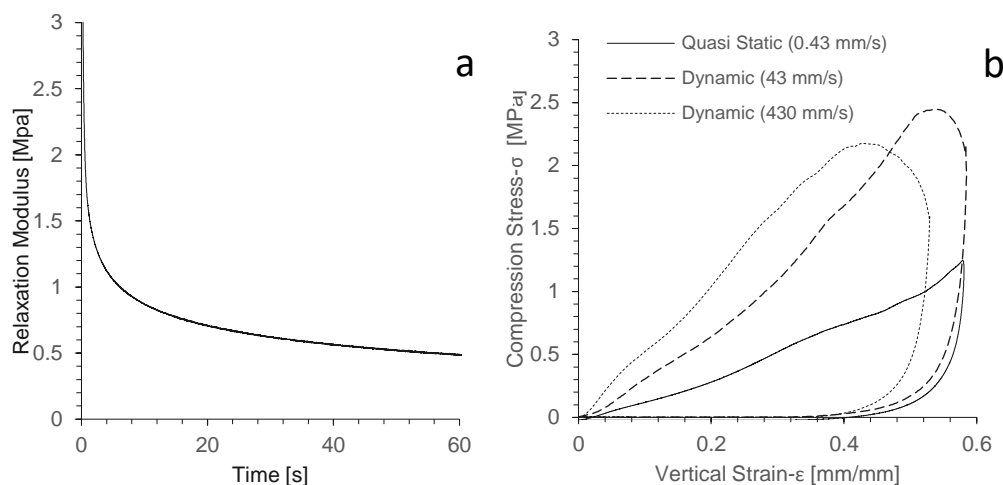


Figure 4.10: Mechanical properties of the IAP material. a. Relaxation stress - time; b. Compression Stress - vertical strain;

#### 2.4.2. Impact-attenuation properties

To analyse the impact-absorbing performances of the IAP, the standardised impact attenuation test, described in the Methods section, is used both in the laboratory and in situ, as illustrated in **Figure 4.1**.

After drops in different pavement regions, the results show that the final CFH calculated in the lab is similar to the one on-site. The IAP is six times more impact-absorbing than the traditional asphalt. The CFH value increased from 0.2 m to an average value of 1.2m in the field. Besides, the field and laboratory tests show that all the values of CFH are above the standard-recommended limit of CFH=1, regardless of the number of compaction cycles. As illustrated in **Figure 4.11 (left)**, the CFH *in-*

*situ* (roller compaction) is closer to the CFH measured on the samples compacted with 30 cycles.

Even if this method is simplified, it is possible to show that a fall will be less life-threatening if a cyclist or pedestrian falls from the critical fall height of 1.2 m. Even if the forces measured by the HIC meter are not fully the ones happening in the case of a real accident case, it was shown in Chapter 3 that similar CFH and HIC values were sufficient to considerably reduce the skull fractures, for instance, **Figure 4.11 (right)** gives a visual approximation of the height for the HIC. This scheme also compares the HIC obtained with the Abbreviated Injury Score (AIS) score from 0 to 6 points[50]. This figure explains that if a person falls from 0.2 m (approximately the level of the shin/tibia) on a traditional asphalt, the injury is classified as serious. Instead, if the fall occurs at the same height on the IAP, no injury will occur. This comparison shows the protective capability of the material for its users if a fall occurs. Also, previous studies conducted to compare the HIC measures showed that a similar material, made with the same quantity of rubber, permitted a protective performance to prevent injuries, especially on the skull. This is thanks to the modelling of the material and the simulation of pedestrian and cyclist accidents (Chapter 3).

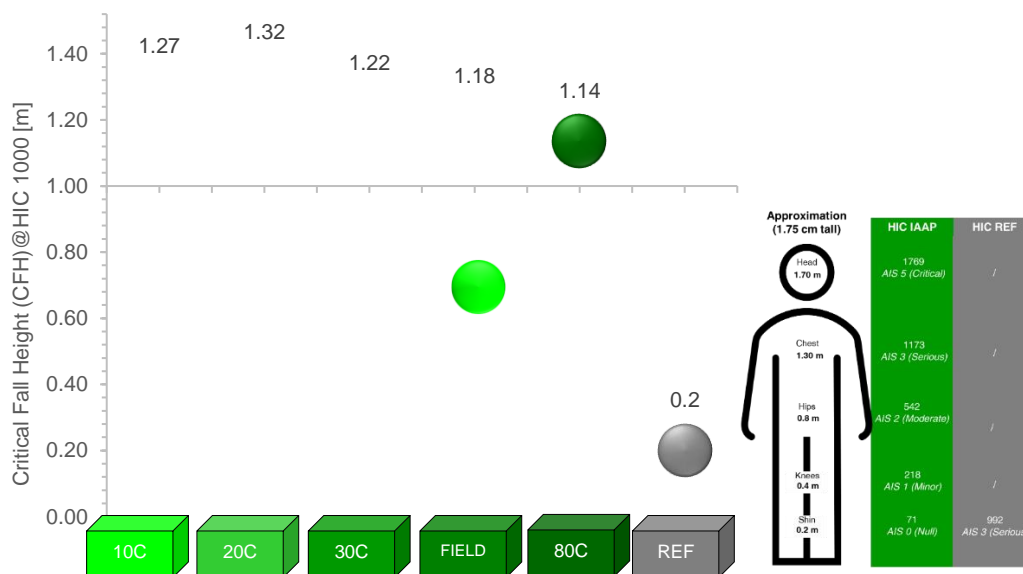


Figure 4.11: IAP Impact-attenuating performances of the IAP material.

### 2.4.3. Friction values

#### 2.4.3.1. Macrotexture and roughness

To obtain information on the surface macrotexture, the sand test described by the standard EN ISO 13473-1[141] was used. The average diameter of the circle is 180 mm with an HS of 1 mm, as shown in **Figure 4.12**. The laid IAP has a macro-

roughness categorised as Coarse, and it can be associated with a sufficient texture, giving this surface a good skid resistance property.



Figure 4.12: Visual macrotexture of the pavement and results of the sand test after six months of exploitation.

#### 2.4.3.2. Slip risk and coefficient of friction.

To confirm the results observed in the visual and macrotexture test, slip tests were conducted in the laboratory and *in-situ*. Furthermore, it helped to assess different surface configurations and surface behaviour under several conditions. Therefore, the laboratory slip test was conducted on three types of samples made with the same mixture but with different surface configurations: Non-treated (NT), Simple Treatment (ST) and Aggregate treatment (AT). Also, the samples were tested under three different temperature conditions as described in the Methods section. Additionally, four different footwear soles simulating different kinds of materials used by pedestrians or cyclists. The test procedure is described in the Methods section. **Figure 4.13** illustrates all the Coefficients of friction (COF) obtained.

On a dry surface, the COF is higher when the footwear sole is made with rubber. The ST does not affect the surface considerably; however, for the AT sample, no matter the footwear, the slip possibility was lower. With the textured rubber (TR) footwear, the slip risk is the lowest, while the highest occurs with the grooved neolite (GN) material. All the surfaces succeed in the 0.5 COF common safety standard [139].

The same observation was made regarding the foot material test on wet surfaces. The COF is higher with the SBR or SBS -based ones. Nevertheless, with this condition, the ST affect the surface by slightly decreasing the COF. This observation is almost not seen with the TR material. Also, on a wet surface, the COF observed on the AT samples is similar to or higher than that on NT ones.

On the iced samples, it was observed an important reduction of the COF, especially when the samples were tested with the rubber-based test sole. In the case of the GN material, this decrease is less significant.

The NT samples register the best COF values. The ST samples obtained very low values and all under the 0.5 COF safety limit; this shows that when the surface is frozen, it can be dangerous. Thus, two distinct behaviours were observed. For the flat

rubber (FR) and TR, the surfaces were more slippery with the AT than the ST. However, the same surfaces (AT and ST) were less slippery for the two grooved feet soles. In this case, the grooving may have played a role in reducing the slippery effect of the aggregate-treated surface.

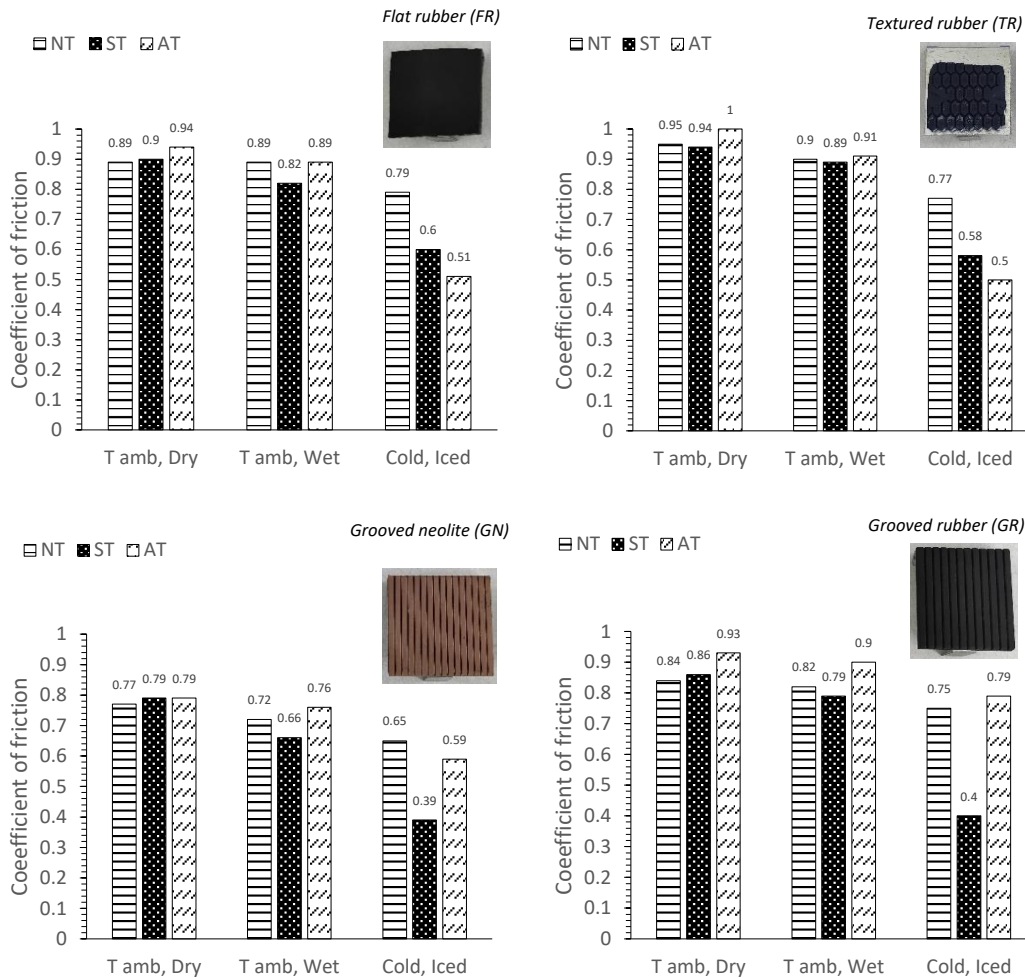


Figure 4.13: COF of the different samples (non-treated (NT), simple treatment (ST) and aggregate treatment (AT)), tested with different footwear pads (FR, TR, GN and GR), at 3 different surface configurations (dry, water-wetted and iced).

#### 2.4.3.3. BPN value and skidding risk in-situ

Skidding has a role in the cyclists' or pedestrians' potential falls that lead to injuries. Thus, the skidding risk was also evaluated *in-situ* by means of the pendulum test described in Methods. The average value of BPN of the IAP is very high (81) and corresponds to a very low risk and probability of skidding with an SBR or SBS rubber-made footwear on a wet surface. This value is in line with the ones registered with the

slip test in the laboratory. It is also confirmed by the sand test that categorised the material's surface as a coarse one.

#### **2.4.4. Observations on the trial site**

After constructing the test line, visual observations and walking and biking trails were made. It was verified that the laid pavement was fully walkable and bikeable, as shown in **Figure 4.14**.



Figure 4.14: Walking and biking trails on the IAP after its construction.

After 6 months, corresponding to the summer and autumn of 2021 (June to November), a visual inspection of the surface was made. The weather conditions of the location during the test period are shown in **Figure 4.15**. **Figure 4.15 a** represents the pavement conditions the day after the laying, while **Figure 4.15 b** shows it after six months.

The general property of the material is conserved, and the IAP is still exploitable, walkable and bikeable after 6 months. However, the comparison easily shows a slight degradation of the surface. During the production phase, a lack of coating by the binder of the mineral aggregates has been detected, which can be one of the causes of the degradation on the surface. Yet, this degradation may also be caused by several factors, including the weather condition and the traffic. Indeed, the pavement underwent intense UV exposure, high temperatures and rain episodes (**Figure 4.15**). Also, the paved portion is hybrid (for pedestrians' and cyclists' usage) and situated in an intersection between a foot-bike lane and a crossing lane. The observation gives an outcome on the necessary reinforcements and the improvements of the formulation to be made to optimize this newly developed material.



Figure 4.15: Visual assessment of the degradation of the surface after and before six months of exploitation.

Besides, maintenance of the pavement was simulated. Several samples were cored, and the holes were patched with the same mixture. **Figure 4.16** shows that the IAP top layer is clearly bound to the existing base layer. Furthermore, the compaction made with the roller during the *in-situ* construction gives similar results to the specimen produced in the laboratory.



Figure 4.16: Profile picture of a core and picture of the top and base layer of the field trial

## 2.5. Conclusions

The development of an impact-absorbing pavement is a promising approach to make road infrastructures and urban areas more accessible and safer for the users, especially the vulnerable road users. The current study investigated the preliminary performance of a rubber-based IAP produced following a cold procedure both from a laboratory and field test perspective. The mechanical, impact-attenuation and friction properties, as well as the durability under outdoor conditions, were measured and evaluated.

The study confirmed the possibility of producing and laying a highly rubberised IAP (56% vol, 34% wt) using the dry method coupled with an emulsified binder and cold method. This material has an elastic behaviour and can be compressed and relaxed fully after a stress of  $\leq 5$  % of vertical deformation. These mechanical properties are needed for the pavement to handle a load of users together, maintaining the impact-attenuation expectations.

In general, the macrotexture of the pavement is categorised as coarse, and the risk and the probability of skidding on the surface of the IAP is very low, as shown by the slip and skidding results. More specifically, a post-treatment made with a thin emulsion layer does not affect considerably the surface and roughness of the IAP but can foster the skidding effect if the surface is frozen. However, an after-treatment made with chipped aggregated before adding the emulsion layer can increase the slipping of the IAP when the surface is iced.

After the field construction, it was verified that the pavement was walkable and bikeable after approximately 24 hours. Regarding its ageing, a slight degradation is observed after six months. This degradation is mainly due to the formulation of the mixture that creates mineral aggregates coating issues. This problem can be solved using pre-coated aggregates such as RAP material. Nevertheless, the pavement's overall performance appears to be conserved and still valuable. In fact, after six months, the BPN and Sand tests are correct and encouraging. Besides, the coring of the material on-site permitted to conclude that the IAP is well bound to the base layer, and the patching of the holes with the same rubberised and cold mixture is possible. This is an important outcome concerning the future and maintenance of the newly developed material.

### 3. Outcomes

The role of this section was to describe the upscaling of the process from the laboratory to the field by using several testing methods to assess the pavement performance. The main objective was to verify the repeatability and reproducibility of the methods and characterize the material in real outdoor conditions.

This trial field validated the reproducibility of the mixture tested in the laboratory on site. Moreover, a portion of an experimental lane was built using the same mixture and methods proposed in the laboratory. The impact-attenuation performances were verified, and they were similar to those measured in the laboratory (Chapters 1-2) or using the material modelling (Chapter 3). In addition, the friction and the skidding and slip risks were assessed. The slip and skidding risks are very low in the laboratory and on-site. This adds to the impact-absorbing pavement a valuable point and reduces the possibility of slip related fall injuries.

Furthermore, after six months of use, pavement degradation was observed. The use of additives could partially solve the problem linked to the coating of the mineral aggregates, but this aspect must be further investigated. Furthermore, it is probably one of the main causes of the degradation of the surface. Therefore, the use of RAP instead of virgin aggregates could help in the compatibility of the residual bitumen from the emulsion and the recycled aggregates. Finally, it was possible to core and patch the holes with the same mixture. This step anticipated the possible maintenance that may occur on an aged pavement during its life cycle.

The field trial outcomes are promising for the future implementation of protective material on the bicycle lanes and sidewalks. They also confirm the possibility of this material being laid cold and having impact-attenuation performances. However, it also demonstrates the need to investigate more deeply and, at a chemical level, the possibility of modifying the mix or the rubber surface to solve some of the problems linked to the cohesiveness of the mixture (aggregate-rubber-binder). The study of these properties is a valuable method to handle the leaching and surface degradation of the material.

In the last chapter, the perspectives for this material will be analysed from a technical, especially focusing on the surface chemistry, environmental and a circular economy implementation point of view.

## **Chapter 5. Optimization to extend the industrial perspective of the IAP**

The work proposed in this chapter is extracted from the following publication:

- **Makoundou, C.; Johansson, K.; Wallqvist, V.; Sangiorgi, C.** Functionalization of Crumb Rubber Surface for the Incorporation into Asphalt Layers of Reduced Stiffness: An Overview of Existing Treatment Approaches. *Recycling* 2021, 6, 19.  
DOI: <https://doi.org/10.3390/recycling6010019>

*All authors have read and agreed to the published version of the manuscript.*

## **1. Overview**

This chapter focuses on the improvements and optimisations that can enhance the overall performance of the IAP material.

It was shown in the first chapter that the quantity of rubber could be a limiting factor. Indeed, its incorporation may cause an overuse of binder or stickiness problems while using the warm method. The use of the emulsion solved some of the problems as described in the findings of this chapter; however, the evaluation of the leaching and of the ageing resistance in Chapter 2 shows that prior treatment or functionalization of the rubber can potentially decrease the leaching and increase the resistance of the material thanks to better cohesion and coating and adhesion properties.

This chapter contains a review of the possible treatments of the rubber that can be applied before the incorporation into the mixture. These treatments mainly focus on the physical modification of the surface of the rubber. These treatments do not alter rubber elastic properties because they modify only the very surface of the material and not its bulk. This aspect is essential in the described IAP, which needs the residual elastic properties of the rubber to be functional and effective.

The paper's objective was to place the context of the need for potential rubber pre-treatment and mention the background of the use of rubber in paving solutions. Then several types of functionalization were described. Finally, a comparison and a definition of the best utilisation were made to select methods suitable for the rubber and the desired application.

## **2. Functionalization of Crumb Rubber Surface for the Incorporation into Asphalt Layers of Reduced Stiffness: An Overview of Existing Treatment Approaches**

### **2.1. Introduction**

The environmental issues related to the quantities of waste rubber and plastics on the planet are perpetually increasing. One of the most common wastes arising from the transportation industry is ELTs. Undeniably, large quantities of rubber can be found in household appliances. However, the described evolution is mainly due to the increase in the world population, thus increasing the production of the vehicle: the transportation market represents 63% of rubber use. Every year, nearly 3 million tons of waste tyres are generated in Europe, of which approximately 2 million tonnes are either recycled or recovered, as reported by the European Tyre & Rubber Manufacturers' Association. Composed in the majority of highly engineered rubber, the non-biodegradable stage of the final tire product is involved in several waste management problems [143,144]. ELTs usually enter a waste management system based on recycling the constituent materials and the recovery of energy by controlled combustion, and still, in some countries, on the landfilling on vast land surfaces.

In terms of recycling, many industries in the field of construction materials and other engineering fields use CR from ELTs in various forms for applications such as rubberized asphalt concretes [53,145,146], non-structural materials, especially for thermal and acoustical insulation [134,147], as well as playgrounds and artificial turf surfaces [59,148]. Indeed, the ELT rubber benefits are well known in civil engineering, particularly in the road pavement sector, since the first rubberized asphalt was produced in the last century. The elasticity of rubber has been proven to positively influence the mechanical performance, i.e., the pavement layers' durability, while its low stiffness can contribute to abating the noise generation [144]. As a matter of fact, in the latest years, the CR obtained from ELTs following different possible processes has been proven to be an efficient solution to reduce the accumulation of waste tyres while contributing to the sustainability and carbon footprint reduction of road transport [31,145,149].

However, ELTs' rubber is not the only component involved in the mix-design of rubberized asphalt mixtures. Generally, when the rubber addition or substitution query occurs, the level of interaction between the rubber particles and asphalt binder during the production (either wet or dry) and laying processes can bring issues in terms of workability and emissions. These issues are particularly experienced when the ratio between the rubber and aggregate quantities is high. Depending on the time and temperature of the mentioned interaction, the rubber particles are known to swell in asphalt by adsorbing the bitumen's lightweight components [150]. The small molecular size of maltenes diffuses inside the rubber particles, and rubber volume

expands [145]. The described phenomenon is not happening just because of each component's chemical properties; the size distribution of rubber and, mostly, the time and temperatures of interaction have a considerable effect on rubber swelling within the asphalt binder. The swelling of rubber particles can change the volumetric proportions of the components in the mixture and modify the structure of their close bonds and, hence, alter the properties of the final asphalt layer. To counteract this phenomenon, several methods aiming to control the swelling behaviour of rubber exist. The addition of chemicals to the mixture [151,152], the possible devulcanization [153–156] or, last but not least, the surface treatment of the CR employing physical or chemical procedures [143,157–161] are some of the most frequent solutions. The rubber's surface treatment represents an evolving method, preferably used when the dry incorporation method is adopted.

This review aims to describe the contribution of possible physical surface modifications of rubber on the enhancement of its properties for the use in road engineering materials, including modified binders and asphalts pavements.

## **2.2. Rubber tyres and their use in asphalt pavements**

### ***2.2.1. 2.1 History and waste management of tyres***

Originating from Charles Goodyear's discovery of the vulcanization of rubber in 1839 - the process of transforming the rubber with sulphur and heat to reinforce the rubber - and from John Boyd Dunlop's invention of the pneumatic tyre in 1888 [38], tyres became a fundamental piece of the economy of every nation that relies on the transportation of goods and people on rubber.

The development continued when in 1891, the Michelin brothers made it removable from the rim. As a result of these discoveries, tyres can be recycled, and nowadays, used tyres are regularly retreated, potentially reused, or recycled to promote the circular economy of the product and its constituents, save costs for the domestic economies, and preserve the environment.

Undeniably, tyres' composition and design differ by category (i.e., passenger vehicle, utility vehicle, truck, etc.) or manufacturers. However, it always includes four primary material groups: rubber, carbon blacks/silicas, material reinforcement, and facilitators. *Figure 5.1* shows the common tyre constituents and the generic weight composition for the passenger car and truck vehicle [162]. Tyres contain a mixed composition of both natural and synthetic rubber compounds, which are the primary materials used in tyres' production as they are crucial to meet the safety performance and environmental requirements. Unfortunately, rubber usage also has effects on land space consumption that can cause degradation and loss of natural habitats due to the required Hevea tree exploitation [38].

Altogether, the wastage and recycling of polymer-made products have attracted considerable public attention thanks to a broad concern about climate change, and the percentage of rubber recycled in the European Union (EU28) was found to be 91% in 2018 [162]. Therefore, it is clear that in the EU, there is still excellent room for exploitation as far as tyres and rubber recycling are concerned [163].

Nowadays, while being recycled, the materials from waste tyres can be recovered or sorted and reused by employing different processes: ambient or cryogenic shredding and thermal pyrolysis (**Figure 5.1**). The ELTs are regularly reprocessed in other material design applications and should be considered like newly engineered products for roads or building construction, sports equipment or clothes and fuel [163]. Fabrics, steel, and especially the rubber contained in the tyres can be recycled in a different form to replace the raw constituent materials, hence reducing the extraction of resources, land use, Greenhouse gas (GHG) emissions, pollution, and water consumption. Additionally, the whole ELT structure can have an essential role in other fields of applications, as shown in **Figure 5.1**.

One of the most central materials recycled from ELTs is the rubber. It can be shredded and marketed in small particles (chips, coarse, powder), which are used in artificial grass, playgrounds, surfaces for horseback riding, asphalt pavements and safety or acoustic barriers, among many other uses [162,164].

Using the ELT material reduces the need to extract and produce new raw rubber for other applications and fosters the circular use of resources. The final objective of ELT recycling, as illustrated in **Figure 5.1**, is to be able to use the newly produced material through different applications depending on the shape [38].

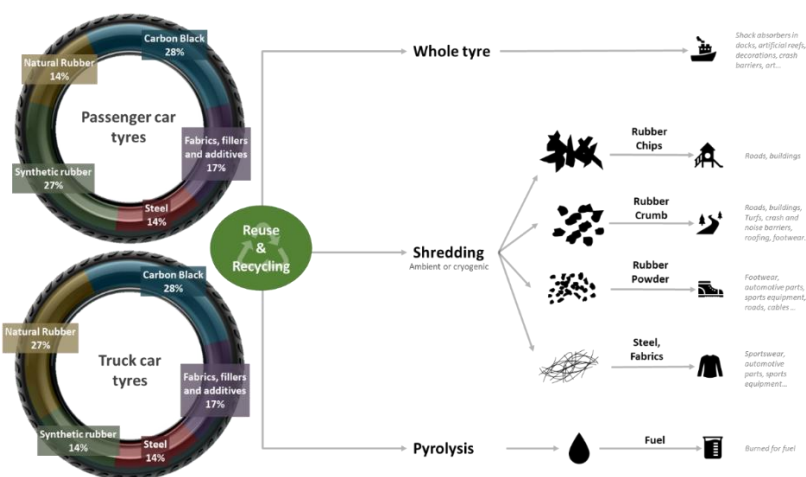


Figure 5.1: Different rubber recycling processes and potential applications (adapted from European Tyre Recycling Association, Rubber Manufacturers' association, Swedish Tyre Recycling Association).

### **2.2.2. Properties of the recycled rubbers**

The physical properties of ELT rubber depend on the adopted recovering process (**Figure 5.1**) and have an essential role as far as the subsequent use of those materials is concerned [40,145,165,166]. Despite the sorting process, the various sources of tyres and the vulcanization reaction can generate utterly different rubber granulates from a chemical and physical point of view. Also, the reprocessing can itself create variation, particularly concerning the rubber particles' surface characteristics [59,145,148].

Starting from their manufacture, tyres are made of highly engineered material. If recycled as constituent material in other applications, they will require an evaluation of several properties to be conducted to cope with its new use and assess the non-hazardousness for new goods production. Thus, typical properties, including geometrical and structural properties, elemental characterization, and dust or chemical leaching assessments, among others, are evaluated to meet the health and safety specifications and produce sustainable products with RR. The rubber's chemical composition can also be diagnosed through a representative sample and can be used to study the rubber's compatibility with other components while reusing it for new applications. Crucial data are related to the measurement of Polycyclic Aromatic Hydrocarbons (PAHs) to protect the environment, the workers, and the users from possible noxious emissions, during and after the manufacturing processes. Leaching of the rubber should remain at a very low value as for food or water production values. A possibility to decrease this value using a treatment will assess a significant improvement.

### **2.2.3. The use of recycled rubber in the road construction sector**

#### *2.2.3.1. Wet and dry processes in asphalt pavements applications*

Rubber chips, powders, or crumb particles have been used for many years worldwide on road pavements. They are known for their effectiveness in designing low-noise pavements or in fatigue-resistant asphalt applications, thanks to their residual elastic properties [134]. In addition to the improvement regarding the circular use of materials, the aim of using ELTs rubber in the asphalt pavement was to improve the performance of the already existing pavements or reach comparable values but also develop innovative materials. [30] In Fact, the incorporation of CR in substantial amounts can decrease the layers' stiffness and increase the pavement's overall performance while improving the ELTs waste management impact [40,145,165].

To produce a rubberized asphalt, aggregates, rubber (chip, crumb, powder), and bitumen must be mixed. Two well-known processes were and are generally used: the wet and the dry process. During the wet process, the rubber is firstly mixed and blended with the bitumen at high temperatures, as described in Zanetti et al. studies [40]. This process provides several technical and rheological advantages to the bitumen, including improvement regarding fatigue and rutting resistance [167].

However, it needs high temperatures (not less than 170-175°C), continuous agitation, and prolonged contact time between rubber and bitumen to produce a rubberized bitumen before adding the aggregates [40,145]. The second process is known as the dry one. The rubber substitutes a portion of the aggregate mix gradation. CR is added to aggregates and heated in the mixer before adding the binder. Mixing temperatures are generally lowered (160°C), but a short contact time between the rubber and the binder is preferable for better control of the rubber's binder absorption. Compared to the wet process aiming to enhance the binder's elastic properties, rubber particles' leading role in the dry process is to fill spaces between aggregates and provide an elastic buffer between the mineral aggregates' skeleton. Improvement of skid resistance was also recorded by using the last-mentioned process. Furthermore, even if the moisture resistance can be decreased [167], the dry method is appreciated for its positive environmental issues improvement as it can use lower temperatures, and it permits the addition of larger shapes and quantities of rubber in the mixture thus recycling more tyres. [40,145].

Each process has advantages and disadvantages and can be used for different applications. In principle, the primary condition of rubberized mixture design is evaluating the rubber and the binder properties separately, but it is also crucial to assess how they interact within the mixture.

#### 2.2.3.2. Rubber-Binder interaction

For many years, rubber-bitumen interactions have been the central aspect of rubberized-asphalt investigations. Indeed, rubber and bitumen's chemical and surface properties present specific interactions that can modify their structure, as explained in Hassan et al., Zanetti et al., and Li et al. [40,145,166]. The role of bitumen in these interactions is predominant as the exchange of oils depends on its chemical nature, bearing in mind that the binder must coat the aggregates for adhesion first.

As it can be found in the studies mentioned above, the diffusion of bitumen fraction into the rubber, the swelling reaction, happening either with the wet or the dry process, seems to be the significant reaction occurring during mixing. This reaction occurs depending on the CR (chemistry, shape) and bitumen properties.

In fact, a diffusion phenomenon happens when a rubber particle is in contact with the liquid bitumen. When this contact starts, the rubber absorbs some of the bitumen fractions, namely the lighter ones. The small molecular size of maltenes permits their diffusion in the rubber particles; consequently, rubber volume expansion happens [145]. The chemical properties of the bitumen are one of the causes of this phenomenon. The higher the penetration grade is, the higher amounts of maltenes are available, and the swelling tends to increase. However, the described phenomenon is not happening just because of the chemical properties of each part. The size

distribution of rubber, rubber surface characteristics, time, and interaction temperature significantly affect rubber swelling within the bituminous mix.

For instance, more bitumen fractions can be incorporated inside the rubber particles via their porosities with a long time of contact. Finally, the surface texture has a substantial effect on the swelling phenomenon.

Undeniably, the RR's surface type and the specific area have a vital role in the final mixture behaviour. Therefore, any modification to the surface properties could affect the rubber's swelling behaviour and, consequently, the final mixture's rheological properties. In light of the above, rubber pre-treatments should be able to modify the surface properties to control the swelling phenomenon connected to the migration of light fractions from bitumen to rubber without compromising the elasticity of the rubber or the adhesion between the rubber, the bitumen, and the aggregates.

### **2.3. Surface treatments and their effect on rubber-bitumen interactions**

#### ***2.3.1. Surface modification of polymers***

Polymers such as rubber are generally inherently hydrophobic, low surface energy materials and thus less prone to adhere to other substances. Adhesion improvement is the most common use, but other surface characteristics, such as wettability, porosity, water- and chemical resistance, and moisture transmission, are also addressed [168,169].

Two distinct types of modification exist as two main categories: physical and chemical modification. The first can also be divided into two groups, the first involved with chemical alteration of the surface layer, while the second with external layer deposition on the polymer material. The chemical modification consists of modifying the chemical composition of polymer surfaces either by direct chemical reaction or by the creation of covalent bonds with the chemicals [170].

Many types of polymers, like rubber, are commonly treated before subsequent processing. A wide range of methods, from treatment made using a vacuum to atmospheric pressure, wet to dry, simple to sophisticated, and inexpensive to very costly to obtain the required functional characteristics of polymers exist [169,170].

This review aims to discuss a set of developed methods for the pre-treatment of rubber polymer to overcome surface reaction issues and improve the adhesion ability between rubber, binder, and aggregates in a rubber concrete asphalt mixture. The environmental impact and the uncomplicated nature of the adopted methods are crucial parameters (*Figure 5.2*).

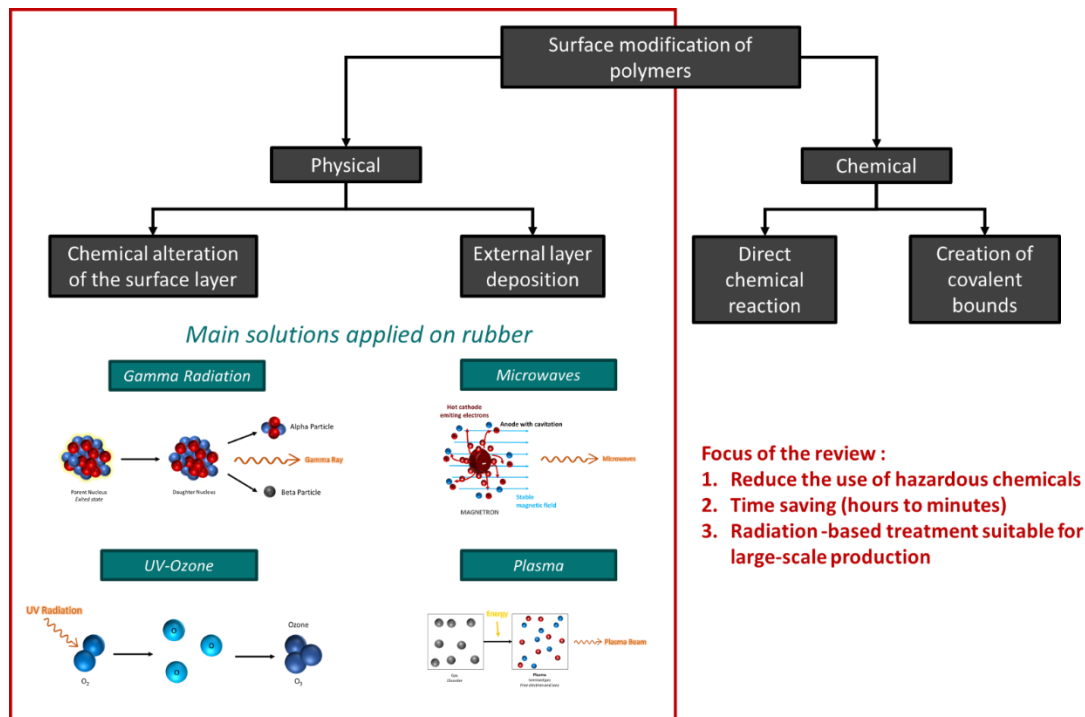


Figure 5.2: Scheme of the different possible treatment methods and the main solutions described in this review (adapted from [160,171–181])

### 2.3.1.1. Gamma radiation

Gamma-ray is an electromagnetic radiation that results in the disintegration of radioactive atomic nuclei and the decay of certain subatomic particles (alpha and beta), as shown in **Figure 5.3a**. Gamma-ray is a highly penetrating electromagnetic radiation with very short wavelengths (a few tenths of an Angstrom) and very energetic (greater than tens of thousands of electron Volts) [182]. This reaction is generally initiated in nuclear reactors. This reaction can be made at Lab-scale (**Figure 5.3b**) or industrial scale (**Figure 5.3c**) to treat large quantities of materials [173,183].

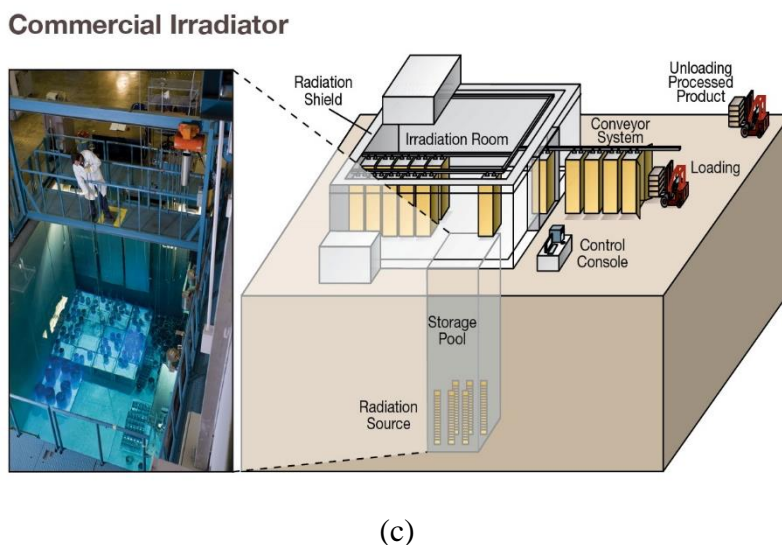
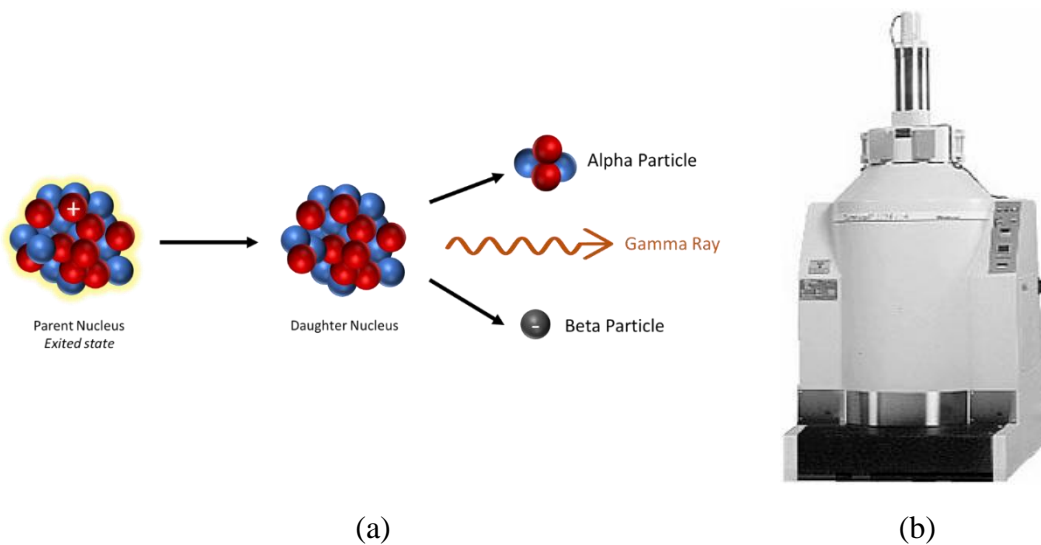


Figure 5.3: (a) Simplified scheme of the gamma ray initiation; (b) Picture of a GammaCell 220 instrument designed for lab work *Nordion*<sup>TM</sup>; (c) Scheme of a commercial irradiator designed for industrial scale work *Nordion*<sup>TM</sup>.

The gamma radiation has been used successfully for several years to improve the properties of recycled polymer-based materials, including the rubber [183] and can cause changes in polymers' chemical structure and mechanical behaviour. These modifications occur due to the reorganization of bonds, which allows an increase in the degree of cross-link or reticulation (**Figure 5.4**). Several polymers (recycled or not) have been modified to optimize properties and increase their overall compatibility [184]. Such technology is feasible from both an ecological and economic point of view as it can be applied in large quantities of materials at lower costs.

Its main effect is the creation of possible cross-link improving the recovery of polymers; scission producing low molecular masses able to be used as raw materials or inducers, or chain branching including advanced polymerization to design more environmentally friendly materials that can increase, decrease or consolidate the original polymer's structure [161,169,184–187].

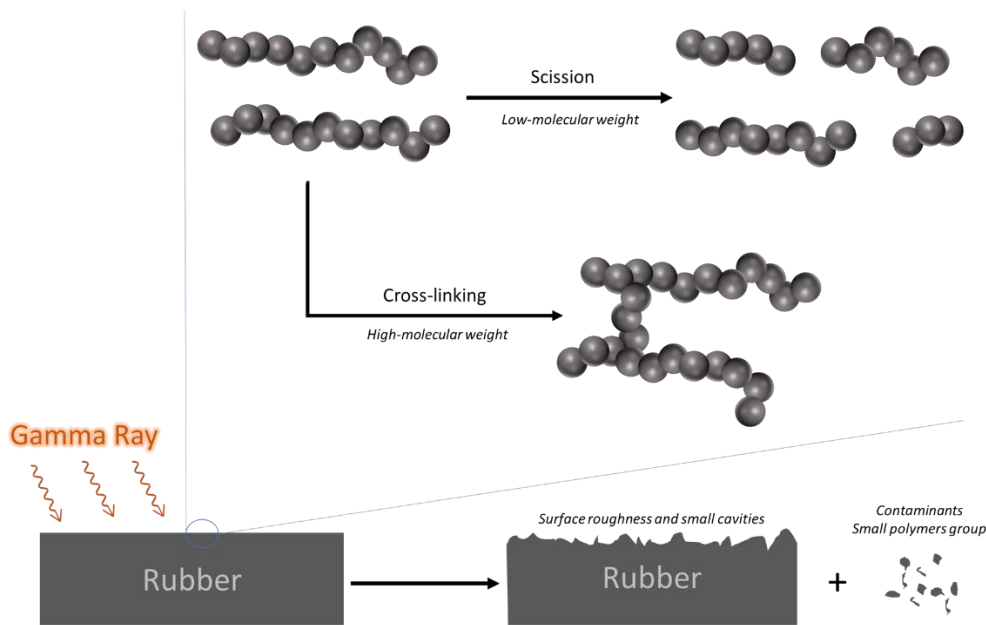


Figure 5.4: Simplified scheme of the gamma ray reaction initiation and effect on rubber surface.

In a specific study, Faldini et al. [188] examined the irradiation of crumb rubber samples at several levels of absorbed radiation doses (100-1000 kGy). The samples were characterized by thermal analysis, including Differential Scanning Calorimetry (DSC) and Thermogravimetric analysis (TGA), infrared (IR) and UV-visible spectroscopy (UV-Visible) and scanning electron microscopy (SEM). Through the analysis, the same tendency was observed in several various case studies [161,183,188,189]. The SEM evaluation has shown an increase in the roughness, small cavities and cracks on the surface when the irradiation increase. The higher the gamma radiation absorption, the higher the roughness. However, the spectroscopy analysis confirms the non-alteration of rubber's chemical structure.

The research from Chen et al. [190] discussed the effect of gamma-ray on recycled and vulcanized butyl-rubber-based damping materials irradiated at doses from 10 to 350 kGy. When the absorbed dose increases, the chain scission reactions are stronger and conducted to decrease molecular weight and small decomposition [187]. These degraded low-molecular-weight compounds made the rubber softer with increasing absorbed dose. A reduction of surface porosity is also observed without impacting the roughness.

In the studies of Martínez-Barrera et al. [53], the CR were irradiated the gamma rays at 200, 25 and 300 kGy. Two significant improvements are observed when mixing the irradiated particles with concrete. Apart from the size of particles showing the effectiveness in increasing the softness of the concrete, the rubber particles' irradiation could permit the use of more tyres particles and reduce the use of raw materials. Thus, high irradiation doses produce physicochemical changes in the CR particles, mainly cross-linking polymer chains, allowing high physical interactions with the concrete components. The irradiation of particles at 300 kGy, by initiating surface roughness and cracks due to cross-linking reactions, improves the elastic modulus and the deformation of the concrete-based sample; the material is more flexible. Gamma rays generate cross-linking of polymer chains on the rubber, which restricts the movement of their molecules. Then, weak interfacial interactions are produced between cement in this case.

In the work of Ibrahim et al. [23], the irradiated rubber was mixed with an asphalt binder. The anti-ageing performance was evaluated through the Rolling Thin Film Oven Test (RTFOT) in terms of subsequent penetration, softening point, ductility, weight loss, viscosity, etc. The results showed that the bitumen samples using 10% of CR irradiated at 300 kGy had high-temperature stability, low-temperature ductility, and anti-ageing performance improved. The rheological studies also illustrated that the modified bitumen with CR irradiated at 300 kGy has the most considerable properties, and the rubber is better dispersed into the binder. [161]

Previous investigations [187] have shown that a low dose (from 0-70 KGy) leads to cross-linking after a long time of exposition and less scission, while higher doses (more than 70 and from 300kGy in Ibrahim et al. study) lead to both reactions with a stronger scission. The result of those reactions is the formation of softer and more viscous rubber with a rough surface that eases adsorption, among other components in the mix. A gain in the stability of the asphalt mixes is shown with the use of gamma rays. The irradiation increases the compatibility of the components.

These studies have shown a substantial impact of the gamma radiation on crumb rubber properties and, by extension, on the modified bitumen or asphalt concrete rheological aspect. The modification of the crumb rubber's surface due to cross-linking and scission reaction positively impacts the material's mechanical properties. Viscosity and ageing, also altered, prove the treatment's effectiveness while adding a considerable amount of irradiated rubber into the asphalt. The reduced need to control expositions' distance makes this method suitable for powder materials as for more oversized shape materials (*Table 5.1*).

Table 5.1: Summary of studies on the procedures and results using Gamma ray treatment.

Reference	Method/Procedures	Analysis	Results
Faldini et al. [188]	<u>Rubber type:</u> ELTs Rubber	SEM	<ul style="list-style-type: none"> <li>• Increase of roughness with irradiation.</li> </ul>
	<u>Rubber size:</u> (0.044 – 4.75 mm)		<ul style="list-style-type: none"> <li>• Less porosity with 1000 kGy</li> </ul>
	<u>Dose rate:</u> 11.6 kGy/h	FTIR	<ul style="list-style-type: none"> <li>• Absence of bulk degradation and composition modification</li> </ul>
	<u>Doses:</u> 500 & 1000 kGy	TGA DSC	<ul style="list-style-type: none"> <li>• Insignificant change in thermal decomposition</li> </ul>
		Soxhlet extraction	<ul style="list-style-type: none"> <li>• Small extractive increase with absorbed does</li> </ul>
Chen et al. [190]	<u>Rubber type:</u> Butyl rubber-based damping material (vulcanized)	FTIR	<ul style="list-style-type: none"> <li>• Increase of organic compounds due to the radiolysis and scission</li> </ul>
	<u>Rubber size:</u> Several	SEM	<ul style="list-style-type: none"> <li>• Holes decrease and smoother surface with the increase of doses</li> </ul>
	<u>Dose rate:</u> 6.6 kGy/h	Dynamic mechanical properties	<ul style="list-style-type: none"> <li>• Elongation breaks increase with irradiated dose</li> </ul>
	<u>Doses:</u> 10; 100; 200; 350 kGy	Tensile properties	<ul style="list-style-type: none"> <li>• Tensile strength decreases with dose increase</li> </ul>
Martínez-Barrera et al. [189]		SEM	<ul style="list-style-type: none"> <li>• Increase in texturization with the radiation dose</li> </ul>
		XRD	<ul style="list-style-type: none"> <li>• Crystallinity maintained but decreased with increasing dose.</li> </ul>
	<u>Rubber type:</u> ELTs Rubber		<ul style="list-style-type: none"> <li>• Maximum cross-link at 250kGy</li> </ul>
	<u>Rubber size:</u> 0.85 – 2.8 mm	FTIR	<ul style="list-style-type: none"> <li>• Increase of organic fractions due to scission reactions.</li> </ul>
	<u>Dose rate:</u> 2.5 kGy/h	Raman	<ul style="list-style-type: none"> <li>• Chemical structure not changed</li> </ul>
	<u>Doses:</u> 200; 250; 300 kGy	UV-Visible	<ul style="list-style-type: none"> <li>• Increase in reflectance with the dose</li> </ul>
	<u>Institutional Reactor</u> <sup>60</sup> Co	TGA DSC	<ul style="list-style-type: none"> <li>• The hardness of rubber increases with the dose.</li> <li>• Polymer more amorphous due to cross-link reactions</li> </ul>

Reference	Method/Procedures	Analysis	Results
	<i>Inside of concrete</i> 1, 2 and 5% by weight	Compressive strength and elasticity modulus (ASTM C39/C39M-14)	<ul style="list-style-type: none"> <li>• Increase in elasticity with higher dose of irradiation</li> </ul>
Ibrahim et al. [161]	<u>Rubber type:</u> ELTs Rubber	SEM	<ul style="list-style-type: none"> <li>• Irregular domain size, small roughness and decrease of holes</li> </ul>
	<u>Rubber size:</u> 2 mm		
	<u>Dose rate:</u> 2.8 kGy/h	FTIR	<ul style="list-style-type: none"> <li>• Observation of carbon-oxygen based groups due to scission</li> </ul>
	<u>Doses:</u> 100; 200; 300 kGy Institutional Reactor	Rheological	<ul style="list-style-type: none"> <li>• Plastic viscosity decreases with the increase in dose</li> </ul>
	<i>Inside of asphalt</i> 5 and 10% weight	RTFOT Anti-ageing	<ul style="list-style-type: none"> <li>• Low mass-loss and phase separation with the increase of dose</li> <li>• Improvement in stability with the increase of dose</li> </ul>

### 2.3.1.2. UV-Ozone treatment

Results of UV radiation's action on dioxygen molecules (O<sub>2</sub>), the Ozone, even atmospheric, is a well-known component to be in charge of surface sanitation of materials using like rubber-based products UV-Ozone generator (**Figure 5.5 ab**). Indeed, the ozone has a huge effect on the modification of carbon bonds by oxidation of the rubber [191] and is also used for large-scale water purification (**Figure 5.5c**). An ozone-oxidation or ozonation reaction permits the creation of ozone-based layer formation that initiates surface ablation yet an increase in the texture of the material's layer.[192]

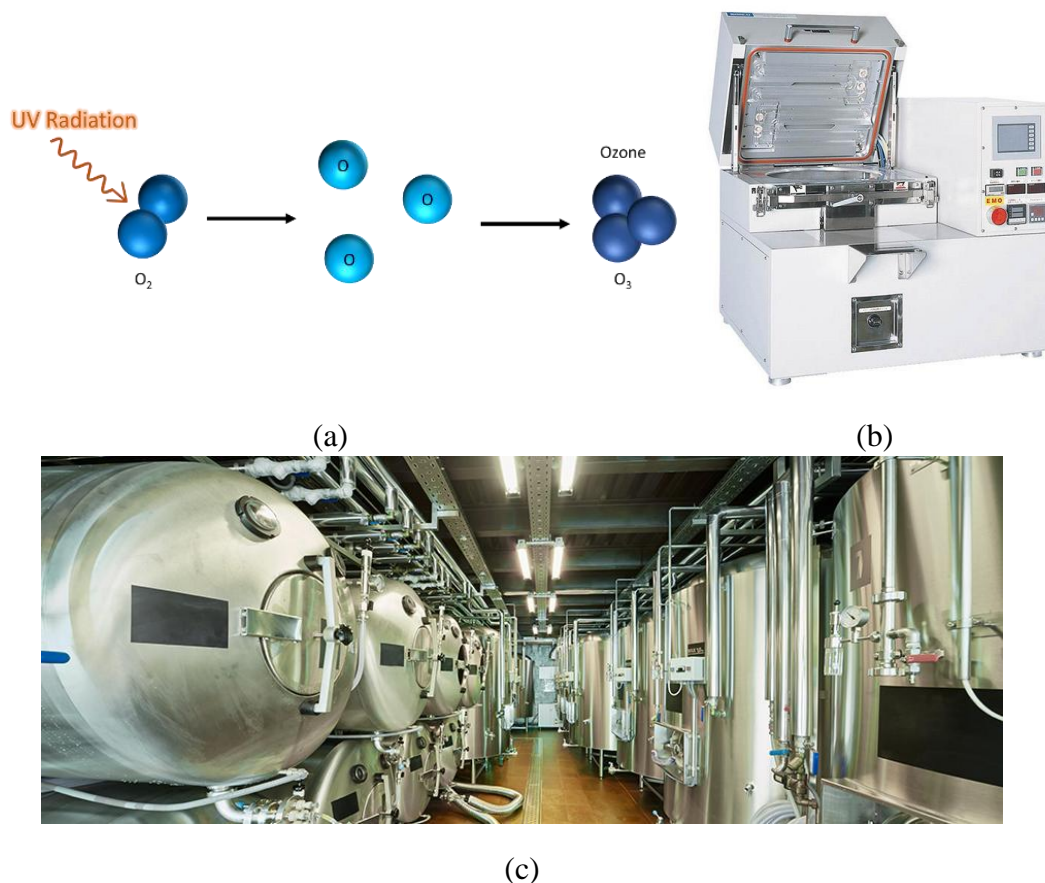


Figure 5.5: (a) Simplified scheme of the UV-Ozone initiation; (b) Picture of a UV-Ozone instrument designed for lab work *Samco*<sup>™</sup>; (c) Picture of a brewing industry using UV-Ozone treatment *Mellifig*<sup>™</sup>.

Therefore, as for Gamma radiation, UV radiation is a possible ionizing electromagnetic ray candidate for replacing polymers' chemical surface reaction and modification using solvent-based chlorination. Indeed, despite its proven effectiveness, chlorination of rubber requires long times of reaction and organic solvents. Furthermore, chlorine production is environmentally dangerous and can cause potential health problems. A combination of UV radiation and Ozone at different concentrations has been proven to enhance the rubber surface's bonding performance, thus improving the vulcanized rubber's surface energy (**Figure 5.6**). The use of this physical treatment is considered to be cleaner and faster than others [160,169,193]. However, it has to be made in the very controlled condition in order to avoid the full degradation of the rubber. The exposition distance [21,58,59] or the humidity [56] are inevitably responsible for the degree of ozone-oxidation.

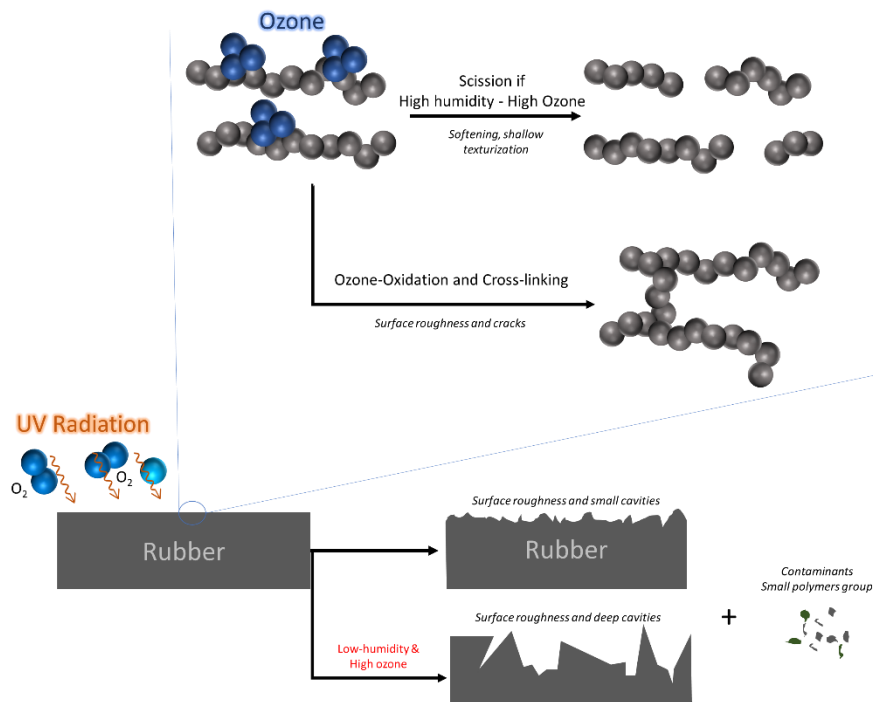


Figure 5.6: Simplified scheme of the Ozone reaction initiation and effect on rubber surface.

In the study of Moyano et al. [22], the treatment with UV-Ozone increased the rubber's adhesion to polyurethane adhesive. The highest adhesion was obtained for the tests made with UV-ozone treated rubber for 3 min at a UV radiation source-surface distance of 5 cm with a limited concentration of Ozone [160]. The reaction of ozone-oxidation allows having cross-linking reaction causing an increase in the texture. The reaction is responsible (as for the gamma irradiation) for improving the CR's mechanical properties. However, more variables are concerned and must be controlled. Indeed, the distance of treatment along with time are important factors. For instance, the effectiveness observed at 1 cm for 3 min treatment was less than the one observed at 5 cm. A too-close UV radiation or too long a time can negatively affect the rubber.

Iwase et al. [56] assessed the humidity's effect on the degradation of Carbon black vulcanized rubber (very similar to tyres rubber). The presence of constant Ozone concentration has higher oxidative capabilities and is more aggressive without humidity. Under low humidity, the ozone leads to an aggressive cross-linking reaction allowing deeper cracks, while under high humidity, chain scission can also be observed. It leads to more shallow cracking of the layer and regular texturization, as observed in *Figure 5.7*.



Figure 5.7: Simplified scheme of the Ozone action under different humidity conditions [192].

Regardless of the application, UV-Ozone treatment influences the surface behaviour of rubber and other polymers. Adhesion between the binder is the most wanted property, and this should have a potential effect even for the final rubberized asphalt or other binder applications. However, it has to be controlled to avoid deep degradation of the rubber and lead to a decrease in the elastic properties. The concentration of ozone, the distance of the UV radiation and the humidity during the treatment must be controlled and can make this treatment less advantageous for treating large quantities of materials (*Table 5.2*).

Table 5.2: Summary of the studies on the procedures and results using UV-Ozone treatment.

Reference	Method/Procedures	Analysis	Results
Moyano et al. [160]	<u>Rubber type:</u> Vulcanized SBS rubber <u>UV lamp:</u> 254 nm (90%) and 185nm (10%) <u>Radiation intensity:</u> 10mW/cm <sup>2</sup> <u>Distance from lamp:</u> 1-5cm <u>Ozone concentration:</u> Low <u>Humidity:</u> Uncontrolled	ATR-IR	<ul style="list-style-type: none"> <li>Hydroxyl groups formation</li> </ul>
		XPS	<ul style="list-style-type: none"> <li>Proof of oxidation group</li> </ul>
		Contact angle	<ul style="list-style-type: none"> <li>Best at 5cm for a shorter time (3min)</li> <li>Less at 1cm</li> </ul>
		SEM	<ul style="list-style-type: none"> <li>Bad when but too long (9min) at 5 cm</li> <li>Production of ablation for the short length of treatment, and roughness and cracks are created for the long length of treatment</li> </ul>
		T-peel test	<ul style="list-style-type: none"> <li>Increase in adhesion with polyurethane after treatment.</li> </ul>
Iwase et al. [192]	<u>Rubber type:</u> Vulcanized carbon black-filled Rubber. <u>Ozone concentration:</u> High <u>Humidity and temperature:</u> 40°C 80%RH or 80°C 20%RH	SEM	<ul style="list-style-type: none"> <li>Shallow cracks at high humidity, deep cracks at low humidity</li> <li>Hydroxyl group are formed due to the oxidation</li> </ul>

### 2.3.1.3. Microwaves irradiation

Similarly to Gamma and UV, microwave radiation is electromagnetic and generally produced by a magnetron (**Figure 5.8a**). However, the microwave frequency range is lower than Gamma and UV (0.3 - 300 GHz), making the microwave non-ionizing, less hazardous to humans, and widely used for telecommunications, small or large microwave devices (**Figure 5.8bc**). The wavelength conducts to an energy photon unable to divide molecular bond and so induce chemical reactions by direct absorption of electromagnetic energy instead of ultraviolet. The microwave's role is to accelerate and enhance the rate of a variety of chemical reactions happening slowly without microwave excitation. Indeed, the length of treatment can be lowered from hours to minutes [179,194,195].

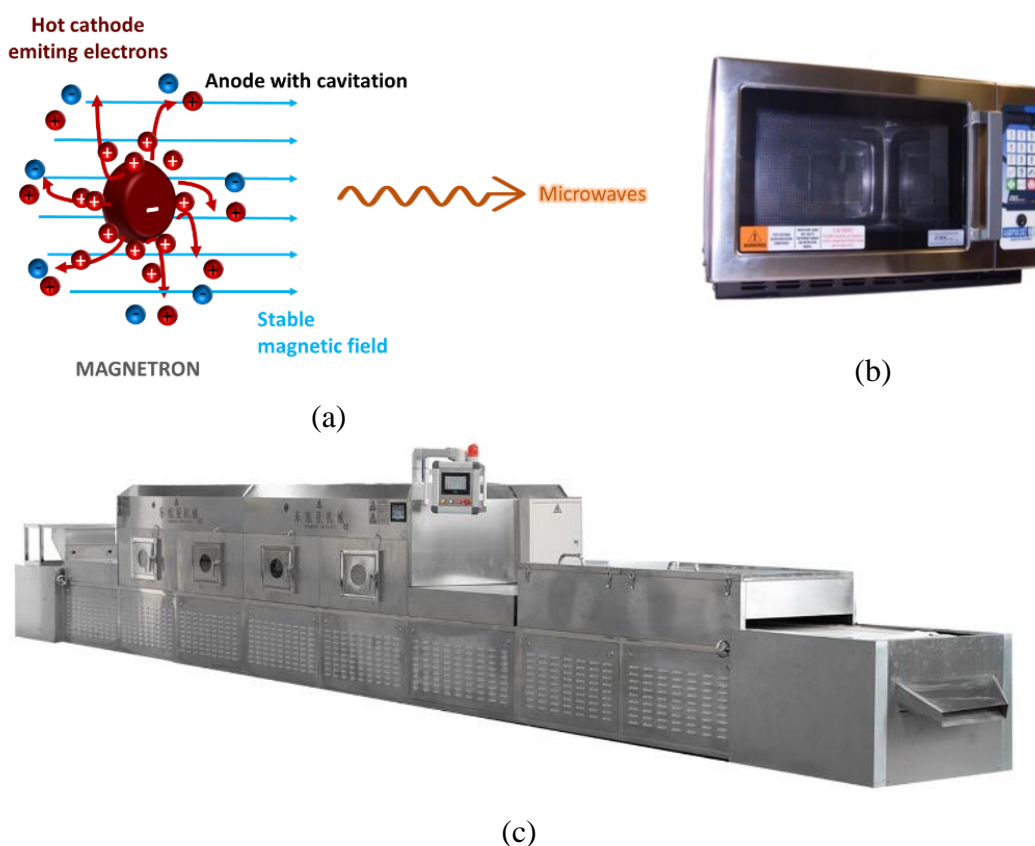


Figure 5.8: (a) Simplified scheme of the microwaves formation by magnetron; (b) Picture of a microwave instrument designed for lab work *Labpulse*®; (c) Picture of Large-scale microwave chain *Xujia*™.

It is known that microwaves increase molecular vibrations and lower the energy needed for radical initiation or surface activation. Therefore, nowadays, microwaves irradiation is generally used to enhance polymerization in the presence of radicals [196] that can create small fragmentation and reticulations or permit to devulcanize of the network created by the bonding (**Figure 5.9**) due to the addition and reaction

with sulphur and, subsequently, improve rubber's viscoelastic nature [153,154,194,197].

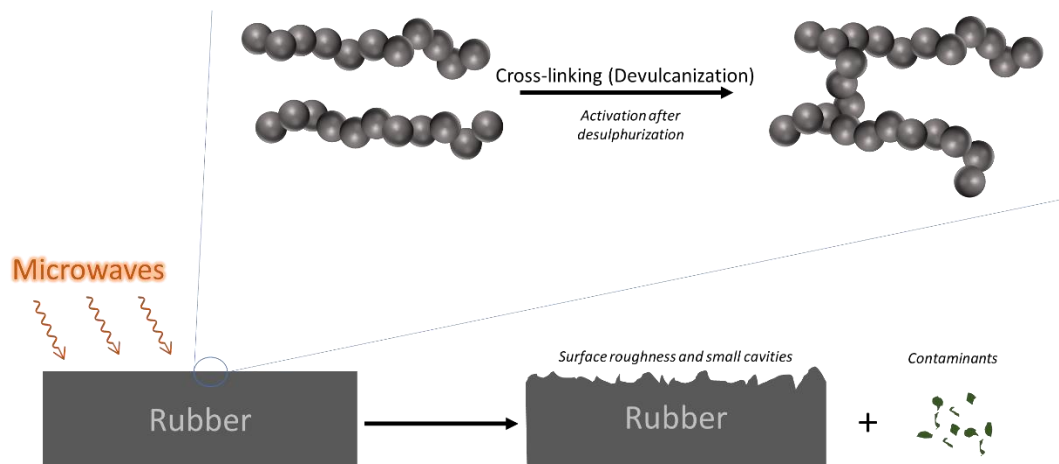


Figure 5.9: Simplified scheme of the microwaves effect on rubber surface.

This method effectively makes the vulcanized rubber more viscoelastic and easier to recover, but it can damage the material's whole structure by breaking surface sulphur links or creating other uncontrolled bonds if using aggressive power, for instance. Thus, the process needs to be correctly monitored to avoid the degradation of the leading chains. The exposure to the microwave radiation and the rubber's temperature at the end of the reaction needs to be defined not to degrade the rubber structurally. Indeed, the higher the exposition to the microwaves, the higher the temperature at the end of the reaction; hence the higher will be the devulcanization. When the aim is to modify the surface, the exposure should not last longer (1 to 5 minutes) and be too aggressive (up to 800 Watts) [152,156]. The radiation can also be combined with activators to enhance the rubber materials' irradiation's desired effect [154]. The combination of both microwave (400 watts) and soft biochemical modification improves the modification level.

Yang et al. [62] have proposed a reaction mechanism happening while CR is treated or not with microwave for 90 seconds at 800 W. The cross-linking reaction causing cracks on the surface to enhance the stability of the rubber inside of the mix and reduce the phase segregation created by the usual swelling of untreated particles as illustrated in **Figure 5.10**. The microwaves also show positive behaviour regarding the high-temperature performances and the release of volatile gases after DSR and FT-IR analysis.

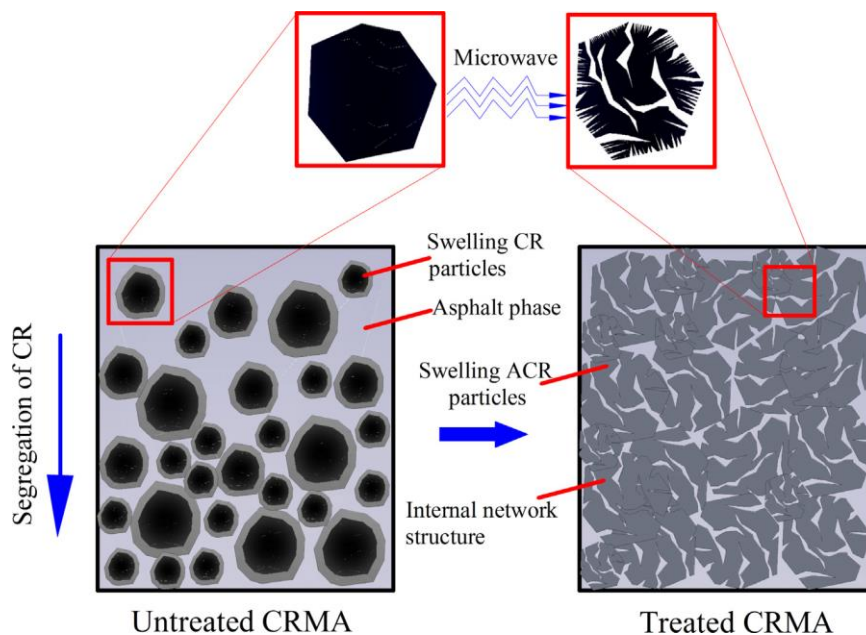


Figure 5.10: Proposed mechanism while incorporating microwaves-treated or untreated rubber [198].

On the other hand, the study made by Liang et al. [63] proved the effectiveness of microwave treatment in enhancing surface modification and permit to the rubber to resist to thermal cracking due to high-temperature drop [199]. However, the defined procedure could give negative results regarding the stability of the mix with asphalt if the reactions enhanced by the microwaves are too aggressive. The microwave has to be severely controlled to not undergo a negative behaviour regarding the asphalt binder because it can increase the surface porosity.

The microwave action is already well-known for rubber devulcanization but also shows the specific action on the rubber when mixing with the asphalt binder. Indeed, the treatment can minimize the swelling, improve the mix's stability and reduce the release of volatile gas when mixing it into the binder [198]. As the microwave process needs little time and, because the aim is not to modify the rubber's whole structure, the use of this method can be successfully transposed to the mass-treatment approach and thus applied while mixing asphalt binder and CR (**Table 5.3**).

Table 5.3: Summary of studies on the procedures and results using microwaves treatment.

Reference	Method/Procedures	Analysis	Results
	<u>Rubber type</u> : ELTs crumb rubber	ATR-FTIR	• Long exposure new liaison Sulphur
De Sousa et al. [154]	<u>Rubber size</u> : 0.177 mm <u>Power</u> : 800 watts <u>Treatment length</u> : 1, 5 and 5.5 min	Sol-Gel content	• Increase of devulcanization during the time decrease of gel fraction with time

Reference	Method/Procedures	Analysis	Results
Yang et al. [198]	<u>Rubber type:</u> ELTs crumb rubber	SEM	<ul style="list-style-type: none"> <li>• Increase of surface texture</li> </ul>
	<u>Rubber size:</u> 0.35 mm	DSR	<ul style="list-style-type: none"> <li>• Microwaves improve high temperature performance.</li> </ul>
	<u>Power:</u> 800 watts	GPC	<ul style="list-style-type: none"> <li>• More swelling reaction of the without microwave pre-treatment</li> </ul>
	<u>Treatment length:</u> 1.5 min	AFM	<ul style="list-style-type: none"> <li>• More uniform structure with pre-treated rubber</li> </ul>
	<i>Inside of asphalt binder</i>	TGA	<ul style="list-style-type: none"> <li>• Decomposition temperature decreased with microwaves</li> </ul>
	10, 15, 20% rubber weight	FT-IR	<ul style="list-style-type: none"> <li>• Cross-linking reaction happening</li> </ul>
Liang et al. [199]	<u>Rubber type:</u> Cryogenic ELTs crumb rubber	SEM	<ul style="list-style-type: none"> <li>• Increase of texture</li> </ul>
	<u>Rubber size:</u> 0.420 mm	Low temperature creep behaviour	<ul style="list-style-type: none"> <li>• Better with microwave treatment</li> </ul>
	<u>Power:</u> 500 watts	Viscoelastic performance intermediate temperatures	<ul style="list-style-type: none"> <li>• Degraded with microwave treatment</li> </ul>
	<u>Treatment length:</u> 5 min	Storage stability	<ul style="list-style-type: none"> <li>• better with microwave treatment</li> </ul>
	<i>Inside of asphalt binder</i>		
	4.5% rubber weight		

#### 2.3.1.4. Plasma treatment

Plasma is the fourth state of matter considered after solid, liquid, and gas, resulting in a gas's ionization (**Figure 5.11a**). It has been used in the laboratory (**Figure 5.11b**) and large-scale polymer materials coating and functionalization in diverse fields such as textiles, medicine, hazardous waste handling or electronics in the last 60 years, as shown in **Figure 5.11c** [193,200].

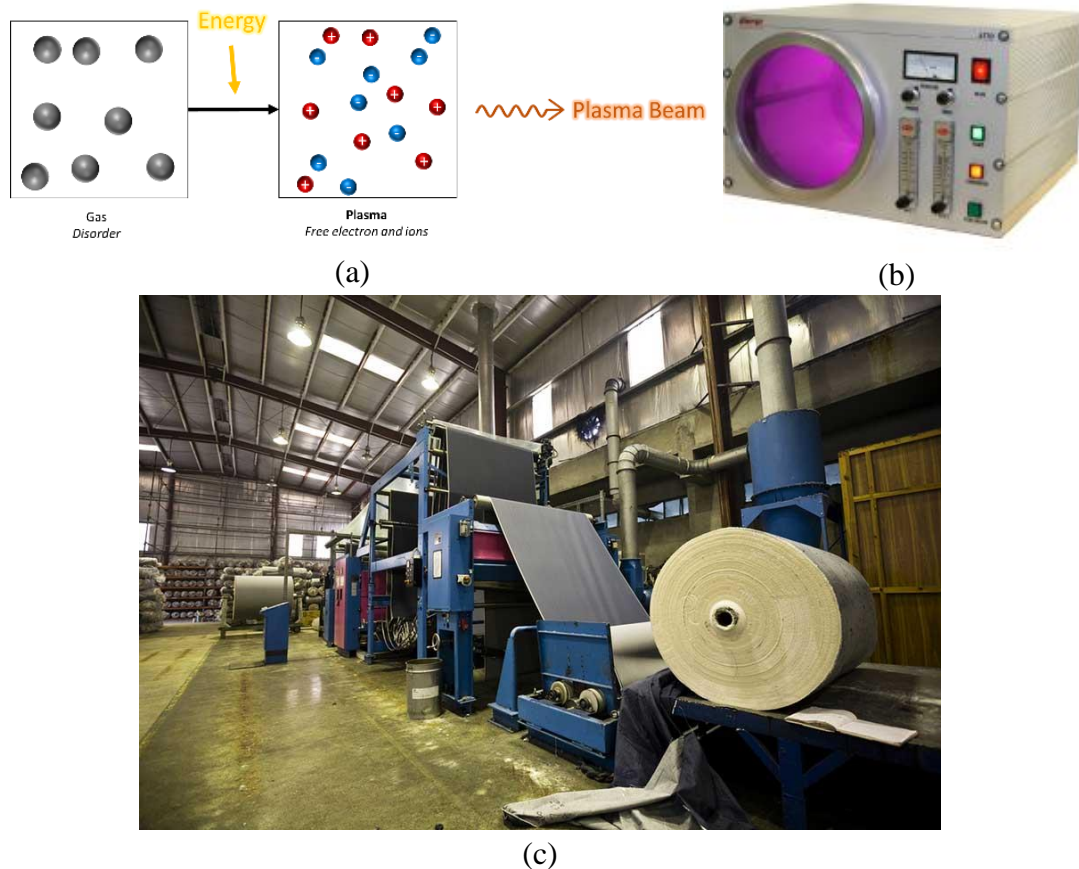


Figure 5.11:(a) Simplified scheme of the Plasma formation; (b) Picture of a plasma generator designed for lab work *Rotalab™*; (c) Picture of a Large-scale plasma treatment chain *Henniker™*.

Most of these applications involve the use of low pressure and low-temperature plasma. Its treatment has several significant benefits compared to traditional wet chemistry techniques. The plasma treatment modifies only the top 0.01 microns of the material layer and permits faster reaction on the surface thanks to the free ions and electrons and the beam's high energy (**Figure 5.12**). Thus, various materials' desired surface properties, including rubber-based, are achieved without altering their bulk material characteristics. Plasma has been found to improve rubbers' adhesion thanks to an increase in surface roughness caused by polar moieties' formation on the surface and ablation of low molecular weight compounds cleaning the surface. [169,201].

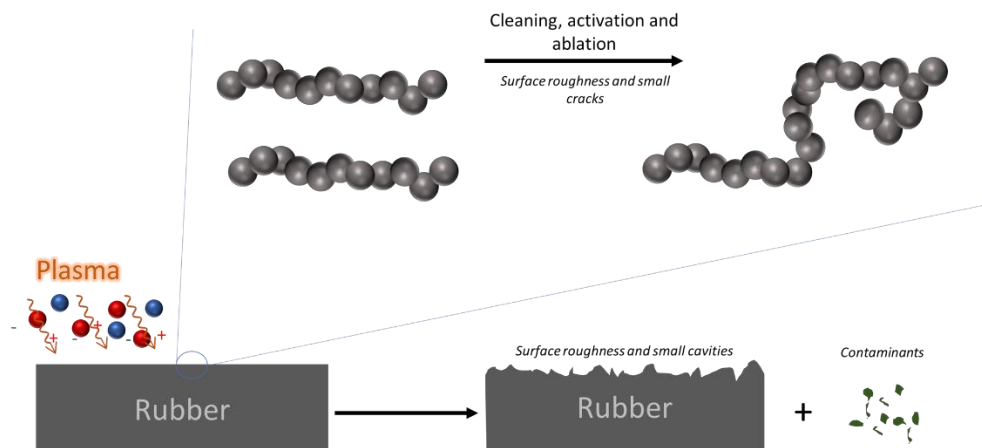


Figure 5.12: Simplified scheme of plasma effect on rubber surface.

In a research by Ortiz-Magan et al. [66], both nitrogen  $N_2$  and oxygen  $O_2$  plasma treatment were used to improve rubber adhesion to another polymer (polyurethane), generally used for playgrounds or in the shoe industry together with the crumb rubber. The reaction was conducted for 1-15 min using a 50 W power reactor. In general, the Zinc and oil on rubber, due to the vulcanization, create an anti-adherent layer on the surface, decreasing the interaction between the rubber and the studied adhesive. In this specific study, the more noticeable effect was the grafting of oxygen and enhancing rubber's surface texture thanks to  $O_2$  plasma [202]. The wettability was considerably improved thanks to removing the sulphur layer on the surface and creating  $C=O$  surface bonds. This sulphur layer reduction is also an actor in the enhancement of the viscosity of the rubber.

Similar results were observed in the study made by Xiaowei et al. [67] by using  $O_2$  plasma. Even if the final aim was to initiate another polymerization after pre-treatment of rubber by plasma, the rubber has precisely the same behaviour. The plasma cause ablation able to clean the surface and make it more reactive.

Li et al. [68] discussed the use of cold plasma (air)-treated powder rubber ((0.177 mm, 0.420, 0.595 mm) inside of a binder. After incorporating 15% weight of treated and untreated rubber, the plasma treatment has shown improvement in the high temperature performances, and the thermal storage stability of the asphalt binder by improving the rubber's contact reactivity.

The studies show that  $O_2$  and cold (air) plasma treatment can represent a solution for using crumb rubber inside of asphalt mixes regarding the stability and compatibility properties. Methods exist for the treatment of powders; however, it adds difficulty to the treatment for large scale processing. While treated with plasma, the rubber can directly be incorporated inside of the asphalt binder (wet), fostering the link possibilities between the binder and the rubber. This effect can be enhanced while

using an emulsion type of binder, thanks to the rubber surface's wettability (**Table 5.4**).

Table 5.4: Summary of studies on the procedures and results using plasma treatment.

References	Method/Procedures	Standard for assessment	Results
Ortiz-Magan et al [202]	<u>Rubber type</u> : Vulcanized SBS rubber	ATR-IR	<ul style="list-style-type: none"> <li>• Modification of the surface chemistry</li> <li>• Formation of Si-O group due to removal of Sulphur liaison</li> <li>• Hydrocarbon group due to oxidation. More polar group on the surface</li> </ul>
	<u>Type of plasma</u> : Low-Pressure N <sub>2</sub> and O <sub>2</sub>	XPS	<ul style="list-style-type: none"> <li>• Hydrocarbon-rich rubber surface. Oxidation of the surface</li> </ul>
	<u>Power</u> : 50 W	SFM	<ul style="list-style-type: none"> <li>• Texturization increase with time treatment</li> </ul>
	<u>Treatment length</u> : 1 to 15 min Lab plasma chamber	SEM	<ul style="list-style-type: none"> <li>• O<sub>2</sub> decrease of porosity increase of texturization</li> </ul>
		Contact angle	<ul style="list-style-type: none"> <li>• Decrease of contact angle with water and ethane diol after 1 minute treatment.</li> <li>• High wettability with ethane diol after N<sub>2</sub> plasma treatment</li> </ul>
		T-peel	<ul style="list-style-type: none"> <li>• Adhesion improved with O<sub>2</sub>. Need extended treatment with N<sub>2</sub></li> </ul>
Xiaowei et al [203]	<u>Rubber type</u> : Crumb rubber	ATR-IR	<ul style="list-style-type: none"> <li>• Modification of the surface chemistry</li> </ul>
	<u>Pressure</u> : 10 Pa		<ul style="list-style-type: none"> <li>• Formation of Si-O group due to removal of Sulphur liaison</li> </ul>
	<u>Plasma type</u> : O <sub>2</sub> plasma	Contact angle	<ul style="list-style-type: none"> <li>• More polar group on the surface</li> </ul>
	<u>Power</u> : 60, 80, 100, 120 W		<ul style="list-style-type: none"> <li>• Increase of texture</li> </ul>
	<u>Treatment length</u> : 1 to 5 min Lab plasma chamber	SEM	<ul style="list-style-type: none"> <li>• Increase of texture</li> </ul>
		XPS	<ul style="list-style-type: none"> <li>• Oxygen group content increase</li> </ul>

References	Method/Procedures	Standard for assessment	Results
	<p><u>Rubber type:</u> ELTs crumb rubber</p> <p><u>Size of particles:</u> (0.177 mm, 0.420, 0.595 mm)</p> <p><u>Plasma Type:</u> Air plasma</p> <p><u>Power:</u> 250W</p> <p><u>Treatment length:</u> 8 min</p> <p>Lab plasma chamber</p>	SEM	<ul style="list-style-type: none"> <li>• Surface roughness enhancement, surface contamination removal</li> </ul>
Li et al. [204]	<p><i>Inside of the binder</i></p> <p>2 Type of binder</p> <p>15% weight rubber</p>	<p>High-Temperature Properties (Rotational viscosity, failure temperature, rutting factor, phase angle, storage modulus, loss modulus)</p>	<ul style="list-style-type: none"> <li>• Enhancement of High-Temperature Properties</li> <li>• Better thermal storage of modified binder</li> </ul>

### 2.3.2. Advantages and disadvantages of the main solution for an application to highly rubberized road pavements.

Each treatment solutions presented have a crucial effect on the rubber surface modification. However, several limitations arise while mentioning the use of a considerable amount of rubber for the construction of road surface layers. **Table 5.5** compares the characteristics of the main proposed solutions.

Highly referenced, the gamma-ray enables the increase of the rubber surface's roughness without modifying its high elastic properties and the gain in mix stability while mixed with asphalt binder. However, this radiation remains radioactive and highly penetrating, thus requiring high surveillance while treating the materials, either during lab or industrial treatment. Also, to obtain the described results, the length of treatment is considered to last hours.

Despite its well-known cleaning effect on the surface of the treated materials improving adhesive properties, and its rapidity, the UV-Ozone treatment is

challenging to apply because of the considerable number of parameters to control (Ozone concentration, humidity, distance of exposition). Besides, the treatment of fine rubber powders can be troublesome.

The Microwave treatment proved its efficacy in controlling rubber's swelling reaction in contact with asphalt binder. Besides, thanks to its effect on the rubber causing specific surface parameters, the use of microwaved rubber can reduce the release of volatile and hazardous gases. However, the length and power of radiation must be short and controlled to avoid full devulcanization or parasite polymerizations.

The plasma has been presented as the fastest method permitting effective results after a few seconds of treatment. Furthermore, thanks to the decrease of surface contaminant and rubber texture, the treatment enhances the high-temperature and thermal storage while mixed with the asphalt binders.

For either the dry and wet processes, the microwaves and plasma treatments appear to correspond with the usual procedure, potential hazardousness, length treatment and results obtained while mixing with asphalt binder. The ease of acquiring a microwave generator compared to a plasma chamber makes microwaved treatment easier to replicate also in lab conditions.

Table 5.5: Comparison between main physical surface treatment solutions.

Methods	Major effect on the surface	Radiation type	Treatment length	Parameters Control	Applicability
Gamma	Softening Texturization	Radioactive Highly Penetrating and Ionizing	hours	Control of the absorbed dose and length of treatment	Applicable to several shapes of material  Difficult to acquire gamma-ray equipment.
UV-Ozone	Ablation Softening Texturization	Penetrating and ionizing	hours	Control of radiation distance, ozone concentration and humidity values.	Applicable to several shapes of materials but challenging with powders.  Several existing apparatuses
Microwaves	Reactions accelerations Desulfurization Softening	Non-penetrating	minutes	Control of the length of treatment and power	Applicable to several shapes of material  Easy to acquire microwave equipment.
Plasma	Activation Ablation Texturization	Non-penetrating	seconds	Control of the source of plasma and length of treatment	Applicable to several shapes of materials but challenging with powders.  Several existing apparatus

## 2.4. Conclusions

This review focuses on using physical surface treatment to modify the rubber surface characteristics for the use of abundant CR generated from ELTs in pavement engineering applications.

The standard trend in all the presented methods is the gain of time during the functionalization reaction. These methods need a limited amount of time to produce a positive effect in terms of rubber surface modification.

The presented methods have also in common the structural modification of the surface. Either a specific characteristic can be created on the surface, and others can be removed from the surface. Surface texturization can lead to better-mixing

properties and affinity with the constituent, in particular the bituminous-based ones. Creating a more textured surface on top of the rubber is essential when mixing it with an asphalt binder to improve their bonding. The surface texturization results allow for modifying the surface energy, and it is also likely to enhance the adhesion properties, thus reducing the phase separation.

For asphalt applications, especially when incorporating a subsequent rubber quantity, the priority should be given to fast treatments. A dry and chemicals-free process permits the non-alteration of the rubber's bulk structure and limits the hazardous possibilities of the rubber modification process.

For either the dry or wet processes, all the mentioned solution gives desirable properties to the rubber for mixing inside bituminous materials. Nevertheless, the microwaves and plasma treatments appear to give better results with regards to the application in usual procedures, potential hazardousness, and length of treatment mostly. For instance, these treatments allowed the collection of better ageing, high temperatures performances or the reduction of volatile gas when mixed in asphalt or bituminous mixtures. However, the time and power of exposure to the different treatments as key parameters to control should be mastered to avoid any reverse effects on the properties when mixing the rubber with the asphalt binder.

The highest percentage of CR is targeted to study the suitability of its use in soft surface applications such as sports pitches and advanced impact-absorbing pavements for urban surfaces. Finally, other methods using chemical additives also exist (use of rejuvenators, waxes, chemicals, etc.); however, when using recycled material, an eco-compatible treatment should be mainly addressed to expand the possible reclaiming lifetime of CR and rubberized asphalt.

### **3. Outcomes**

This chapter aimed to propose possible improvements that could enhance the performances of the IAP materials, focusing on the rubber.

A good impact-attenuating performance is reached; however, room is left to increase the influence in the injury reduction. It can be reached by adding more recycled rubber; however, it was described as the limit of utilising a high amount of rubber. Furthermore, one of the main objectives of the full research project is to study an innovative solution to meet the technical, environmental, and economic performance needs.

Thanks to the published paper described above, it was possible to overview several functionalization techniques that can possibly be used on rubber in paving applications. Plasma and microwaves appear to be the best methods for using large quantities of rubber. Also, their treatment is limited in time, and interesting properties can be obtained after just a few minutes of treatment.

## Conclusions

This doctoral research grew in a multidisciplinary context to propose the design of an innovative, functional, and durable solution for the development of the cities of the future. This research aimed to create a material able to make the road infrastructures less dangerous, emphasising the VRUs in the urban ecosystem and their safety.

The research focused on the possibility of making an IAP for bike lanes and sidewalks pavements. This thesis proposed the result and the methodology of this study. Each chapter investigated a special topic of the research; nevertheless, all the chapters are strongly linked, and they aim to help answer the main research questions presented in the introduction; moreover, the goal was to examine as many aspects as possible of the development of this material.

The laboratory mix design was the starting point of the study and permitted the formulation of the material.

- The dry process permitted considerable rubber quantities in the mixtures and was the only process used during the thesis.
- The preferred method of rubber incorporation was the partial substitution of the mineral aggregates (0-4mm). Thus, the use of raw resources was limited, and the recycling of the ELT rubber was fostered. This partial substitution was made on the volume.
- Using the HRA reference permitted the design of a dense mix that allowed this partial substitution.
- It was possible to incorporate up to 56% of rubber in the total mix volume (33% in weight) by substituting the 0-4 mm portion in the HRA gradation curve.
- The material produced with this amount of rubber showed sufficient impact-attenuation properties.
- The production of the specimen was repeated with several rubber and binders.
- The investigation of the variation of the binders with different properties, temperatures of production and laying was a key study to solve the issues linked to using a large amount of rubber.
- The workability problem, typical of using a warm binder with a consistent amount of rubber, was solved using a cold binder.
- The absence of heat decreased the stickiness observed in the hot/warm mix. Likewise, it made it possible to avoid fumes and smells in the production.
- The question of the binder consumption was investigated by modifying the size distribution of the rubber without decreasing its total amount of it. The decrease in fines helped in the diminution of binder usage.

- The material was designed as a top-layer surface, generally adapted to the sidewalks and bike lane configuration.
- Two methods of improving the IAP visibility were investigated: the colouration of the bulk material or the use of fluorescent stones on the surface.

Among the different combinations of rubber and binders, the mix containing 56% of rubber was shortlisted, and the material was characterised in several aspects to understand its overall properties. Therefore, the mechanical and chemical parameters under different conditions were preliminarily measured. Methods recognised in the research on asphalt, playgrounds and other impact-attenuation materials were combined to find the most accurate way to characterise this type of material, bituminous made and highly rubberised.

- Several challenges needed to be overcome to analyse these materials with the asphalt methods, often reserved for very stiff and rigid materials.
- The methods applied in the playground and impact attenuation material development were more adapted. However, some limitations were still noticeable, especially regarding the dimension of the samples needed to have a deep characterisation.
- These mechanical characterisations confirmed the results on the softness and elastic behaviour of the material.
- The chemical analysis evaluated the leaching of the material in the water after a period of immersion. All the leaching observed were not surpassing the threshold fixed by the standard used [112]. These values confirmed that the developed pavement would have a controlled effect on the environment.
- The characterisation of the material's resistance to cold temperature by the F-T analysis did not show important degradation due to the temperature change and the repetition of the cycles.

The studies presented in the Chapters 1 and 2 focused on materials science, while the one described in Chapter 3 focused on material modelling and accident simulations.

- The biomechanical investigations helped evaluate injury prevention, particularly head ones, during computer-simulated accident cases.
- It was possible to prove the effectiveness of the material containing 56% of rubber in reducing skull fractures considerably and limiting concussions.
- However, comparing these two, it could be observed that the percentage of concussion reduction was lower than the skull fracture one.

Chapters 1,2 and 3 permitted to choose a limited number of formulations with the best performances. The role of Chapter 4 was to investigate the reproducibility and upscale the laboratory procedures thanks to in-situ construction.

- The willingness to use the research conducted during the doctoral research to provide a version of IAP to be implemented was fulfilled.
- The trial site results confirmed some of the laboratory criteria and put light on other parameters such as the time needed between the mixing and the laying or the importance of the compaction level that can also enhance the impact attenuation properties of the material.
- In general, the performance observed in the laboratory regarding the impact attenuation was conserved.
- The bounding of the IAP material to an existing base layer was proved.
- This trial site was also the opportunity to assess the roughness of the material and the skidding risk, both positive. Also, it was proved the possibility to patch the holes with the same mixture.
- After six months, despite the after treatment used to prevent deterioration, some signs of degradation were observed on the pavement's surface, and this part must be more investigated. Indeed, particle loss can represent an environmental problem and must be handled.

Finally, Chapter 5 presented possible optimisation paths to a material already functional and performant against injuries. The main issues were observed at a microscopic and chemical level.

- Several possible optimisations have already been identified and will be the object of future research on the IAP.
- Functionalisation can have an important effect on the rubber. The rubber is the material's central resource, and it needs to be well prepared before the incorporation. This can prevent issues observed on the binder use or the coverage. The later mentioned problem can also be handled thanks to already covered aggregates such as reclaimed asphalt. Its use may enhance the recycling impact of the material while possibly enhancing the performance of the IAP.

In conclusion, several aspects can be further investigated to optimise the results obtained during this doctoral research. The orientation of the research in this direction may be a possibility for the road infrastructures to be greener and more sustainable. Some of the possible development will be stated in the next paragraphs.

Regarding the design of the material:

- The increase of the rubber size distribution from 0-4 mm to 0-7 mm, for instance, is possibly a solution to increase the amount of rubber in the mix
- The design of a several-layers pavement with different rubber amounts in each layer can be studied.

- The use of recycled aggregates (RAP, wasted concrete ...) could help the compatibility of the residual bitumen from the emulsion and the recycled aggregates and allow better coating of all the aggregates.
- The possibility of reducing the binder overuse by pre-treating or coating the aggregates can also be evaluated.
- More investigation on the binder compatibility with the rubber and aggregates can be foreseen.
- Extending the environmental influence of the research with the use of bio-based binders, such as lignin, has been discussed. The lignin is often not desired in paper-based materials and is abundant like the tyres. Other paving solutions development projects demonstrated the feasibility of lignin use in pavement technologies. Partial substitution of the petroleum-based bitumen with the lignin is studied [205–209].

About the overall characterisations:

- More testing methods, especially mechanically, may be used. Flexural, shear or direct tensile tests should be investigated to complement the one used so far and propose a complete mechanical testing procedure for the specific material.
- The surface of the pavement must be more characterised, especially regarding the effect of daily walking and biking on it (loss, shear)
- Chemically, several methods are discussed to minimise the leaching values of the pavement materials. The pre-treatment of the rubber already mentioned may positively affect the decrease of leaching. Also, methods such as prewashing the rubber aggregates can be studied.
- More ageing and durability tests such as UV and heat cycles tests can be done.

About the modelling and simulation of accidents:

- Only head injuries were investigated. The hips, shoulder, arms, or leg injuries can also be investigated as they represent the body part with VRUs are generally injured the most.
- Further comparison with the value collected with helmets and without helmeted on traditional or IAP can also be studied.

On the field:

- The material can be produced in higher quantities and laid on a larger portion to be able to adapt to the laboratory results.
- The material was tested in Italy; the test in Sweden can help to assess the behaviour in other climatic conditions.
- The durability test must continue.

- Also, to better understand the influence on the development of such material, the economic (studying the market and status of the waste management of tyres) and environmental potential (Life Cycle Analysis - LCA) of the IAP are foreseen.
- The recyclability at the end of the life of this material must be studied to assure the conclusion of the circle of use sustainably.

## References

1. Snieška, V.; Zykiene, I. The Role of Infrastructure in the Future City: Theoretical Perspective. *Procedia - Social and Behavioral Sciences* **2014**, *156*, 247–251, doi:10.1016/j.sbspro.2014.11.183.
2. Cities of the Future Available online: <https://citiesofthefuture.eu/> (accessed on 20 January 2022).
3. Nations, U. Building Cities of the Future Must Start Today Available online: <https://www.un.org/en/academic-impact/building-cities-future-must-start-today> (accessed on 20 January 2022).
4. Dunn, N.; Cureton, P. Future Cities: New Challenges Mean We Need to Reimagine the Look of Urban Landscapes Available online: <http://theconversation.com/future-cities-new-challenges-mean-we-need-to-reimagine-the-look-of-urban-landscapes-151709> (accessed on 20 January 2022).
5. Sustainable Smart Cities | UNECE Available online: <https://unece.org/housing/sustainable-smart-cities> (accessed on 20 January 2022).
6. Centre, E.C.-J.R. The Future of Cities Available online: <https://urban.jrc.ec.europa.eu/thefutureofcities/> (accessed on 18 January 2022).
7. LANGE, T. The Future of Cities - Opportunities, Challenges and the Way Forward Available online: <https://ec.europa.eu/jrc/en/facts4eu/future/future-of-cities> (accessed on 20 January 2022).
8. The Future of Cities | United Nations Development Programme Available online: <https://www.undp.org/speeches/future-cities> (accessed on 20 January 2022).
9. The Global Future Cities Programme | UN-Habitat Available online: <https://unhabitat.org/programme/the-global-future-cities-programme> (accessed on 20 January 2022).
10. World Health Organization Road Traffic Injuries 2021.
11. European Conference of Ministers of Transport *Safety in Road Traffic for Vulnerable Users*; OECD, 2000; ISBN 978-92-821-1255-7.
12. Fahlstedt, M.; Halldin, P.; Kleiven, S. The Protective Effect of a Helmet in Three Bicycle Accidents—A Finite Element Study. *Accident Analysis & Prevention* **2016**, *91*, 135–143, doi:10.1016/j.aap.2016.02.025.
13. Helmets: A Road Safety Manual for Decision-Makers and Practitioners Available online: <https://www.who.int/publications-detail-redirect/helmets-a-road-safety-manual-for-decision-makers-and-practitioners> (accessed on 22 January 2022).
14. King, M.B.; Tinetti, M.E. A Multifactorial Approach to Reducing Injurious Falls. *Clin Geriatr Med* **1996**, *12*, 745–759.
15. Schepers, P.; den Brinker, B.; Methorst, R.; Helbich, M. Pedestrian Falls: A Review of the Literature and Future Research Directions. *J Safety Res* **2017**, *62*, 227–234, doi:10.1016/j.jsr.2017.06.020.
16. Connell, B.R. Role of the Environment in Falls Prevention. *Clin Geriatr Med* **1996**, *12*, 859–880.
17. How Safe Is Walking and Cycling in Europe? (PIN Flash 38) | ETSC Available online: <https://etsc.eu/how-safe-is-walking-and-cycling-in-europe-pin-flash-38/> (accessed on 18 January 2022).
18. Urgent Action Needed to Tackle Deaths of Pedestrians and Cyclists | ETSC Available online: <https://etsc.eu/urgent-action-needed-to-tackle-deaths-of-pedestrians-and-cyclists/> (accessed on 18 January 2022).
19. Pedestrian Safety: A Road Safety Manual for Decision-Makers and Practitioners Available online: <https://www.who.int/publications-detail-redirect/pedestrian-safety-a-road-safety-manual-for-decision-makers-and-practitioners> (accessed on 20 January 2022).

20. Inside the New Plan to Make Paris ‘100% Cyclable.’ *Bloomberg.com* 2021.
21. London and Stockholm Boldly Reimagine Bicycle Commuting. *Mobility Lab* 2015.
22. Paris to Become “One of the Most Bike Friendly Cities in the World” By 2026 Available online: <https://www.archdaily.com/971436/paris-to-become-one-of-the-most-bike-friendly-city-in-the-world-by-2026> (accessed on 18 January 2022).
23. Bike lane, l’ultima evoluzione delle ciclabili. La risposta di Bologna alla bici mania Available online: [https://bologna.repubblica.it/cronaca/2021/10/06/news/bologna\\_piste\\_ciclabili\\_corsie\\_bike\\_lane\\_bicipan\\_ciclisti\\_urbani\\_tangenziale\\_delle\\_biciclette-320723105/](https://bologna.repubblica.it/cronaca/2021/10/06/news/bologna_piste_ciclabili_corsie_bike_lane_bicipan_ciclisti_urbani_tangenziale_delle_biciclette-320723105/) (accessed on 18 January 2022).
24. Kraus, S.; Koch, N. Provisional COVID-19 Infrastructure Induces Large, Rapid Increases in Cycling. *PNAS* **2021**, *118*, doi:10.1073/pnas.2024399118.
25. Park, J.Y.; Mistur, E.; Kim, D.; Mo, Y.; Hoefer, R. Toward Human-Centric Urban Infrastructure: Text Mining for Social Media Data to Identify the Public Perception of COVID-19 Policy in Transportation Hubs. *Sustainable Cities and Society* **2021**, 103524, doi:10.1016/j.scs.2021.103524.
26. COVID-19 – Rappports sur les tendances de mobilité Available online: <https://www.apple.com/covid19/mobility> (accessed on 23 August 2021).
27. Kraft, L.; Rogers, P.; Brandels, A.; Gram, A.; Trägårdh, J.; Wallqvist, V. Experimental Rubber Chip Concrete Mixes for Shock Absorbent Bike Lane Pavements.; 57° Congresso Brasileiro do Concreto -CBC2015: Bonito, Brasil, October 29 2015.
28. Wallqvist, V.; Kjell, G.; Cupina, E.; Kraft, L.; Deck, C.; Willinger, R. New Functional Pavements for Pedestrians and Cyclists. *Accident Analysis & Prevention* **2017**, *105*, 52–63, doi:10.1016/j.aap.2016.04.032.
29. Wallqvist, V.; Kraft, L. Prototype Bike Lanes -Placement Practices and Properties.; 57° Congresso Brasileiro do Concreto -CBC2015: Bonito, Brasil, October 29 2015.
30. Ardefors, F.; Roupé, J. *The Road to Sustainability. White Paper 2020-2030*; The Swedish Tyre Industry Association, 2020; ISBN 978-91-639-9111-0.
31. Pettinari, M.; Dondi, G.; Sangiorgi, C.; Hededal, O. The Effect of Cryogenic Crumb Rubber in Cold Recycled Mixes for Road Pavements. *Construction and Building Materials* **2014**, *63*, 249–256, doi:10.1016/j.conbuildmat.2014.04.060.
32. Lo Presti, D. Recycled Tyre Rubber Modified Bitumens for Road Asphalt Mixtures: A Literature Review. *Construction and Building Materials* **2013**, *49*, 863–881, doi:10.1016/j.conbuildmat.2013.09.007.
33. Dondi, G.; Tataranni, P.; Pettinari, M.; Sangiorgi, C.; Simone, A.; Vignali, V. Crumb Rubber in Cold Recycled Bituminous Mixes: Comparison between Traditional Crumb Rubber and Cryogenic Crumb Rubber. *Construction and Building Materials* **2014**, *68*, 370–375, doi:10.1016/j.conbuildmat.2014.06.093.
34. Eskandarsefat, S.; Sangiorgi, C.; Dondi, G.; Lamperti, R. Recycling Asphalt Pavement and Tire Rubber: A Full Laboratory and Field Scale Study. *Construction and Building Materials* **2018**, *176*, 283–294, doi:10.1016/j.conbuildmat.2018.05.031.
35. Al-Tayeb, M.M.; Abu Bakar, B.H.; Ismail, H.; Akil, H.M. Effect of Partial Replacement of Sand by Recycled Fine Crumb Rubber on the Performance of Hybrid Rubberized-Normal Concrete under Impact Load: Experiment and Simulation. *Journal of Cleaner Production* **2013**, *59*, 284–289, doi:10.1016/j.jclepro.2013.04.026.
36. Naeem, Z. Road Traffic Injuries – Changing Trend? *Int J Health Sci (Qassim)* **2010**, *4*, v–viii.
37. United Nations, Department of Economic and Social Affairs The 17 Goals Available online: <https://sdgs.un.org/goals> (accessed on 12 July 2020).
38. Ardefors, F.; Roupé, J. *The Road towards Sustainability in the Swedish Tyre Industry Association* 2019.
39. Dhir, R.K.; de Brito, J.; Silva, R.V.; Lye, C.Q. 12 - Use of Recycled Aggregates in Road Pavement Applications. In *Sustainable Construction Materials*; Dhir, R.K., de Brito, J., Silva,

- R.V., Lye, C.Q., Eds.; Woodhead Publishing Series in Civil and Structural Engineering; Woodhead Publishing, 2019; pp. 451–494 ISBN 978-0-08-100985-7.
40. Zanetti, M.C.; Fiore, S.; Ruffino, B.; Santagata, E.; Dalmazzo, D.; Lanotte, M. Characterization of Crumb Rubber from End-of-Life Tyres for Paving Applications. *Waste Management* **2015**, *45*, 161–170, doi:10.1016/j.wasman.2015.05.003.
  41. Standard - EN 1177:2018 Impact attenuating playground surfacing - Methods of test for determination of impact attenuation.
  42. European Chemicals Agency *European Chemicals Agency Scientific Committees Support Restricting PAHs in Granules and Mulches*; European Chemicals Agency: Helsinki, Finland, 2019;
  43. Standard - EN 12697-26:2018 Bituminous Mixtures - Test Methods - Part 26: Stiffness.
  44. Standard - EN 12697-23:2017 Bituminous Mixtures - Test Methods - Part 23: Determination of the Indirect Tensile Strength of Bituminous Specimens.
  45. Standard - ASTM C131/131M Test Method for Resistance to Degradation of Small-Size Coarse Aggregate by Abrasion and Impact in the Los Angeles Machine.
  46. Product Safety Commission *GS Specification: Testing and Assessment of Polycyclic Aromatic Hydrocarbons (PAHs) in the Awarding of GS Marks - Specification Pursuant to Article 21 (1) No. 3 of the Product Safety Act (ProdSG)*; Federal Institute for Occupational Safety and Health: Dortmund, Germany, 2020; p. 13;.
  47. European Chemicals Agency Standard - An Evaluation of the Possible Health Risks of Recycled Rubber Granules Used as Infill in Synthetic Turf Sports Fields 2017.
  48. Lerda, D. *Polycyclic Aromatic Hydrocarbons (PAHs) Factsheet*; European Commission Joint Research Centre: Geel, Belgium, 2011;
  49. Christensen, J.; Bastien, C. Vehicle Architectures, Structures, and Safety Requirements. In *Nonlinear Optimization of Vehicle Safety Structures*; Christensen, J., Bastien, C., Eds.; Butterworth-Heinemann: Oxford, 2016; pp. 1–49 ISBN 978-0-12-804424-7.
  50. Davies, J.; Wallace, W.A.; Colton, C.; Tomlin, O.; Payne, A.; Kaynar, Ö. The Head Injury Criteria and Future Accident Investigations. In Proceedings of the Proceedings of the International Society of Air Safety Investigators (ISASI) Annual Seminar; The Hague, September 3 2019.
  51. Jo, B.; Lee, Y.; Kim, J.; Jung, S.; Yang, D.; Lee, J.; Hong, J. Design of Wearable Airbag with Injury Reducing System: In Proceedings of the Proceedings of the 3rd International Conference on Information and Communication Technologies for Ageing Well and e-Health; Scitepress - Science and Technology Publications: Porto, Portugal, 2017; pp. 188–191.
  52. Wallqvist, V.; Kjell, G.; Cupina, E.; Kraft, L.; Deck, C.; Willinger, R. New Functional Pavements for Pedestrians and Cyclists. *Accident Analysis & Prevention* **2017**, *105*, 52–63, doi:10.1016/j.aap.2016.04.032.
  53. Sangiorgi, C.; Eskandarsefat, S.; Tataranni, P.; Simone, A.; Vignali, V.; Lantieri, C.; Dondi, G. A Complete Laboratory Assessment of Crumb Rubber Porous Asphalt. *Construction and Building Materials* **2017**, *132*, 500–507, doi:10.1016/j.conbuildmat.2016.12.016.
  54. Sangiorgi, C.; Lantieri, C.; Dondi, G. Construction and Demolition Waste Recycling: An Application for Road Construction. *International Journal of Pavement Engineering* **2015**, *16*, 530–537, doi:10.1080/10298436.2014.943134.
  55. Arabani, M.; Tahami, S.A.; Hamed, G.H. Performance Evaluation of Dry Process Crumb Rubber-Modified Asphalt Mixtures with Nanomaterial. *Road Materials and Pavement Design* **2018**, *19*, 1241–1258, doi:10.1080/14680629.2017.1302356.
  56. Buncher, M.S. Evaluating The Effects of the Wet and Dry Processes for Including Crumb Rubber Modifier in Hot Mix Asphalt, Auburn University: Auburn, Alabama, 1995.
  57. Makoundou, C.; Sangiorgi, C.; Johansson, K.; Wallqvist, V. Development of Functional Rubber-Based Impact-Absorbing Pavements for Cyclist and Pedestrian Injury Reduction. *Sustainability* **2021**, *13*, 11283, doi:10.3390/su132011283.

58. Read, J.; Whiteoak, D. *The Shell Bitumen Handbook*; Thomas Telford Publishing, 2003; ISBN 978-0-7277-3880-6.
59. Fédération Internationale de Football Association (FIFA) Fédération Internationale de Football Association (FIFA) Quality Programme for Football Turf Handbook of Test Methods. 2015.
60. Huang, T.J.; Chang, L.T. Design and Evaluation of Shock-Absorbing Rubber Tile for Playground Safety. *Materials & Design* **2009**, *30*, 3819–3823, doi:10.1016/j.matdes.2008.12.024.
61. Li, X.; Kleiven, S. Improved Safety Standards Are Needed to Better Protect Younger Children at Playgrounds. *Sci Rep* **2018**, *8*, doi:10.1038/s41598-018-33393-z.
62. Makoundou, C.; Johansson, K.; Wallqvist, V.; Sangiorgi, C. Functionalization of Crumb Rubber Surface for the Incorporation into Asphalt Layers of Reduced Stiffness: An Overview of Existing Treatment Approaches. *Recycling* **2021**, *6*, 19, doi:10.3390/recycling6010019.
63. Siverio Lima, M.S.; Hajibabaei, M.; Hesarkazzazi, S.; Sitzenfrei, R.; Buttgereit, A.; Queiroz, C.; Tautschnig, A.; Gschösser, F. Environmental Potentials of Asphalt Materials Applied to Urban Roads: Case Study of the City of Münster. *Sustainability* **2020**, *12*, 6113, doi:10.3390/su12156113.
64. Siverio Lima, M.S.; Hajibabaei, M.; Hesarkazzazi, S.; Sitzenfrei, R.; Buttgereit, A.; Queiroz, C.; Haritonovs, V.; Gschösser, F. Determining the Environmental Potentials of Urban Pavements by Applying the Cradle-to-Cradle LCA Approach for a Road Network of a Midscale German City. *Sustainability* **2021**, *13*, 12487, doi:10.3390/su132212487.
65. Fathollahi, A.; Coupe, S.J. Life Cycle Assessment (LCA) and Life Cycle Costing (LCC) of Road Drainage Systems for Sustainability Evaluation: Quantifying the Contribution of Different Life Cycle Phases. *Science of The Total Environment* **2021**, *776*, 145937, doi:10.1016/j.scitotenv.2021.145937.
66. Cheng, H.; Hu, Y.; Reinhard, M. Environmental and Health Impacts of Artificial Turf: A Review. *Environ. Sci. Technol.* **2014**, *48*, 2114–2129, doi:10.1021/es4044193.
67. Rhodes, E.P.; Ren, Z.; Mays, D.C. Zinc Leaching from Tire Crumb Rubber. *Environ. Sci. Technol.* **2012**, *46*, 12856–12863, doi:10.1021/es3024379.
68. Celeiro, M.; Dagnac, T.; Llompарт, M. Determination of Priority and Other Hazardous Substances in Football Fields of Synthetic Turf by Gas Chromatography-Mass Spectrometry: A Health and Environmental Concern. *Chemosphere* **2018**, *195*, 201–211, doi:10.1016/j.chemosphere.2017.12.063.
69. Llompарт, M.; Sanchez-Prado, L.; Pablo Lamas, J.; Garcia-Jares, C.; Roca, E.; Dagnac, T. Hazardous Organic Chemicals in Rubber Recycled Tire Playgrounds and Pavers. *Chemosphere* **2013**, *90*, 423–431, doi:10.1016/j.chemosphere.2012.07.053.
70. Menichini, E.; Abate, V.; Attias, L.; De Luca, S.; di Domenico, A.; Fochi, I.; Forte, G.; Iacovella, N.; Iamiceli, A.L.; Izzo, P.; et al. Artificial-Turf Playing Fields: Contents of Metals, PAHs, PCBs, PCDDs and PCDFs, Inhalation Exposure to PAHs and Related Preliminary Risk Assessment. *Science of The Total Environment* **2011**, *409*, 4950–4957, doi:10.1016/j.scitotenv.2011.07.042.
71. Ruffino, B.; Fiore, S.; Zanetti, M.C. Environmental–Sanitary Risk Analysis Procedure Applied to Artificial Turf Sports Fields. *Environ Sci Pollut Res* **2013**, *20*, 4980–4992, doi:10.1007/s11356-012-1390-2.
72. Schneider, K.; de Hoogd, M.; Madsen, M.P.; Haxaire, P.; Bierwisch, A.; Kaiser, E. ERASSTRI - European Risk Assessment Study on Synthetic Turf Rubber Infill – Part 1: Analysis of Infill Samples. *Science of The Total Environment* **2020**, *718*, 137174, doi:10.1016/j.scitotenv.2020.137174.
73. Tóth, G.; Hermann, T.; Da Silva, M.R.; Montanarella, L. Heavy Metals in Agricultural Soils of the European Union with Implications for Food Safety. *Environment International* **2016**, *88*, 299–309, doi:10.1016/j.envint.2015.12.017.

74. Bandow, N.; Gartiser, S.; Ilvonen, O.; Schoknecht, U. Evaluation of the Impact of Construction Products on the Environment by Leaching of Possibly Hazardous Substances. *Environmental Sciences Europe* **2018**, *30*, 14, doi:10.1186/s12302-018-0144-2.
75. Gupta, N.; Kluge, M.; Chadik, P.A.; Townsend, T.G. Recycled Concrete Aggregate as Road Base: Leaching Constituents and Neutralization by Soil Interactions and Dilution. *Waste Management* **2018**, *72*, 354–361, doi:10.1016/j.wasman.2017.11.018.
76. Maia, M.B.; De Brito, J.; Martins, I.M.; Silvestre, J.D. Toxicity of Recycled Concrete Aggregates: Review on Leaching Tests. *The Open Construction & Building Technology Journal* **2018**, *12*, doi:10.2174/1874836801812010187.
77. Solouki, A.; Fathollahi, A.; Viscomi, G.; Tataranni, P.; Valdrè, G.; Coupe, S.J.; Sangiorgi, C. Thermally Treated Waste Silt as Filler in Geopolymer Cement. *Materials* **2021**, *14*, 5102, doi:10.3390/ma14175102.
78. Spreadbury, C.J.; Clavier, K.A.; Lin, A.M.; Townsend, T.G. A Critical Analysis of Leaching and Environmental Risk Assessment for Reclaimed Asphalt Pavement Management. *Science of The Total Environment* **2021**, 775, 145741, doi:10.1016/j.scitotenv.2021.145741.
79. Introduction to the EU Water Framework Directive - Environment - European Commission Available online: [https://ec.europa.eu/environment/water/water-framework/info/intro\\_en.htm](https://ec.europa.eu/environment/water/water-framework/info/intro_en.htm) (accessed on 29 January 2022).
80. Genan Rubber Granulate - Choose between 6 Different Standard Fractions. *Genan*.
81. Hutchinson, J.; Kaiser, M.J.; Lankarani, H.M. The Head Injury Criterion (HIC) Functional. *Applied Mathematics and Computation* **1998**, *96*, 1–16, doi:10.1016/S0096-3003(97)10106-0.
82. SPSS Statistics 21.0 Available for Download Available online: <https://www.ibm.com/support/pages/spss-statistics-210-available-download> (accessed on 29 January 2022).
83. Li, X.; Kleiven, S. Improved Safety Standards Are Needed to Better Protect Younger Children at Playgrounds. *Scientific Reports* **2018**, *8*, 15061, doi:10.1038/s41598-018-33393-z.
84. Edeskär, T. Use of Tyre Shreds in Civil Engineering Applications: Technical and Environmental Properties. *undefined* **2006**.
85. Jiang, W.; Huang, Y.; Sha, A. A Review of Eco-Friendly Functional Road Materials. *Construction and Building Materials* **2018**, *191*, 1082–1092, doi:10.1016/j.conbuildmat.2018.10.082.
86. El-Hakim, M.; Tighe, S. Impact of Freeze-Thaw Cycles on Mechanical Properties of Asphalt Mixes. *Transportation Research Record: Journal of the Transportation Research Board* **2014**, *2444*, 20–27, doi:10.3141/2444-03.
87. ud Din, I.M.; Mir, M.S.; Farooq, M.A. Effect of Freeze-Thaw Cycles on the Properties of Asphalt Pavements in Cold Regions: A Review. *Transportation Research Procedia* **2020**, *48*, 3634–3641, doi:10.1016/j.trpro.2020.08.087.
88. Xu, H.; Shi, H.; Zhang, H.; Li, H.; Leng, Z.; Tan, Y. Evolution of Dynamic Flow Behavior in Asphalt Mixtures Exposed to Freeze-Thaw Cycles. *Construction and Building Materials* **2020**, *255*, 119320, doi:10.1016/j.conbuildmat.2020.119320.
89. Fan, Z.; Xu, H.; Xiao, J.; Tan, Y. Effects of Freeze-Thaw Cycles on Fatigue Performance of Asphalt Mixture and Development of Fatigue-Freeze-Thaw (FFT) Uniform Equation. *Construction and Building Materials* **2020**, *242*, 118043, doi:10.1016/j.conbuildmat.2020.118043.
90. Fakhri, M.; Ali Siyadati, S.; Aliha, M.R.M. Impact of Freeze–Thaw Cycles on Low Temperature Mixed Mode I/II Cracking Properties of Water Saturated Hot Mix Asphalt: An Experimental Study. *Construction and Building Materials* **2020**, *261*, 119939, doi:10.1016/j.conbuildmat.2020.119939.
91. Meng, A.; Xu, H.; Feng, X.; Tan, Y. Feasibility of Freeze-Thaw Damage Analysis for Asphalt Mixtures through Dynamic Nondestructive Testing. *Construction and Building Materials* **2020**, *233*, 117220, doi:10.1016/j.conbuildmat.2019.117220.

92. Kavussi, A.; Karimi, M.M.; Ahmadi Dehaghi, E. Effect of Moisture and Freeze-Thaw Damage on Microwave Healing of Asphalt Mixes. *Construction and Building Materials* **2020**, *254*, 119268, doi:10.1016/j.conbuildmat.2020.119268.
93. Ishaq, M.A.; Giustozzi, F. Rejuvenator Effectiveness in Reducing Moisture and Freeze/Thaw Damage on Long-Term Performance of 20% RAP Asphalt Mixes: An Australian Case Study. *Case Studies in Construction Materials* **2020**, *13*, e00454, doi:10.1016/j.cscm.2020.e00454.
94. Teltayev, B.B.; O. Rossi, C.; Izmailova, G.G.; Amirbayev, E.D. Effect of Freeze-Thaw Cycles on Mechanical Characteristics of Bitumens and Stone Mastic Asphalts. *Applied Sciences* **2019**, *9*, 458, doi:10.3390/app9030458.
95. Gao, J.; Fan, T.; Ping, K. Influence of Freeze–Thaw Cycles on Thermal Conductivity, Water Permeability and Mechanical Properties of Asphalt Mixtures. *Iran J Sci Technol Trans Civ Eng* **2020**, doi:10.1007/s40996-020-00491-w.
96. Feng, D.; Yi, J.; Wang, D.; Chen, L. Impact of Salt and Freeze–Thaw Cycles on Performance of Asphalt Mixtures in Coastal Frozen Region of China. *Cold Regions Science and Technology* **2010**, *62*, 34–41, doi:10.1016/j.coldregions.2010.02.002.
97. Guo, Q.; Li, G.; Gao, Y.; Wang, K.; Dong, Z.; Liu, F.; Zhu, H. Experimental Investigation on Bonding Property of Asphalt-Aggregate Interface under the Actions of Salt Immersion and Freeze-Thaw Cycles. *Construction and Building Materials* **2019**, *206*, 590–599, doi:10.1016/j.conbuildmat.2019.02.094.
98. Karimi, M.M.; Dehaghi, E.A.; Behnood, A. A Fracture-Based Approach to Characterize Long-Term Performance of Asphalt Mixes under Moisture and Freeze-Thaw Conditions. *Engineering Fracture Mechanics* **2021**, *241*, 107418, doi:10.1016/j.engfracmech.2020.107418.
99. Löqvist, L.; Balieu, R.; Kringos, N. A Micromechanical Model of Freeze-Thaw Damage in Asphalt Mixtures. *International Journal of Pavement Engineering* **2019**, *0*, 1–13, doi:10.1080/10298436.2019.1656808.
100. Tahami, S.A.; Mirhosseini, A.F.; Dessouky, S.; Mork, H.; Kavussi, A. The Use of High Content of Fine Crumb Rubber in Asphalt Mixes Using Dry Process. *Construction and Building Materials* **2019**, *222*, 643–653, doi:10.1016/j.conbuildmat.2019.06.180.
101. Guo, Z.; Wang, L.; Feng, L.; Guo, Y. Research on Fatigue Performance of Composite Crumb Rubber Modified Asphalt Mixture under Freeze Thaw Cycles. *Construction and Building Materials* **2022**, *323*, 126603, doi:10.1016/j.conbuildmat.2022.126603.
102. Li, D.; Leng, Z.; Wang, H.; Chen, R.; Wellner, F. Structural and Mechanical Evolution of the Multiphase Asphalt Rubber during Aging Based on Micromechanical Back-Calculation and Experimental Methods. *Materials & Design* **2022**, *215*, 110421, doi:10.1016/j.matdes.2022.110421.
103. Xiao, R.; Polaczyk, P.; Huang, B. Measuring Moisture Damage of Asphalt Mixtures: The Development of a New Modified Boiling Test Based on Color Image Processing. *Measurement* **2022**, *190*, 110699, doi:10.1016/j.measurement.2022.110699.
104. Richardson, A.; Coventry, K.; Edmondson, V.; Dias, E. Crumb Rubber Used in Concrete to Provide Freeze–Thaw Protection (Optimal Particle Size). *Journal of Cleaner Production* **2016**, *112*, 599–606, doi:10.1016/j.jclepro.2015.08.028.
105. You, L.; You, Z.; Dai, Q.; Xie, X.; Washko, S.; Gao, J. Investigation of Adhesion and Interface Bond Strength for Pavements Underlying Chip-Seal: Effect of Asphalt-Aggregate Combinations and Freeze-Thaw Cycles on Chip-Seal. *Construction and Building Materials* **2019**, *203*, 322–330, doi:10.1016/j.conbuildmat.2019.01.058.
106. Standard - ASTM C666/C666M Test Method for Resistance of Concrete to Rapid Freezing and Thawing.
107. Standard - EN 12697-55:2019 Bituminous Mixtures - Test Methods - Part 55: Organoleptic Assessment of Mixtures with Bitumen Emulsion.
108. Standard - EN 12697-31:2019 Bituminous Mixtures. Test Methods. Specimen Preparation by Gyrotory Compactor.

109. Standard - EN 12697-6:2020 Bituminous Mixtures. Test Methods. Determination of Bulk Density of Bituminous Specimens.
110. Standard - EN 12697-5:2018 Bituminous Mixtures. Test Methods. Determination of the Maximum Density.
111. Standard - EN 12697-8:2018 Bituminous Mixtures. Test Methods. Determination of Void Characteristics of Bituminous Specimens.
112. Building Materials, Soil and Dredging Spoil Available online: <https://business.gov.nl/regulation/building-materials-soil-dredging-spoil/> (accessed on 27 January 2022).
113. World Health Organization *Global Status Report on Road Safety 2018*; World Health Organization: Geneva, 2018; ISBN 978-92-4-156568-4.
114. OECD *Safer City Streets: Global Benchmarking for Urban Road Safety*; Organisation for Economic Co-operation and Development: Paris, 2018;
115. Zhang, B.; Chen, H.; Zhang, H.; Kuang, D.; Wu, J.; Zhang, X. A Study on Physical and Rheological Properties of Rubberized Bitumen Modified by Different Methods. *Materials* **2019**, *12*, 3538, doi:10.3390/ma12213538.
116. Fahlstedt, M.; Depreitere, B.; Halldin, P.; Vander Sloten, J.; Kleiven, S. Correlation between Injury Pattern and Finite Element Analysis in Biomechanical Reconstructions of Traumatic Brain Injuries. *Journal of Biomechanics* **2015**, *48*, 1331–1335, doi:10.1016/j.jbiomech.2015.02.057.
117. Gilchrist, M.; Doorly, M.C. An In-Depth Analysis of Real World Fall Accidents Involving Brain Trauma. *undefined* **2009**.
118. Kleiven, S. Predictors for Traumatic Brain Injuries Evaluated through Accident Reconstructions. *Stapp Car Crash J* **2007**, *51*, 81–114.
119. Chan, P.; Lu, Z.; Rigby, P.; Takhounts, E.; Zhang, J.; Yoganandan, N.; Pintar, F. DEVELOPMENT OF A GENERALIZED LINEAR SKULL FRACTURE CRITERION. 11.
120. Post, A.; Hoshizaki, T.B.; Gilchrist, M.D. Comparison of MADYMO and Physical Models for Brain Injury Reconstruction. *International Journal of Crashworthiness* **2014**, *19*, 301–310, doi:10.1080/13588265.2014.897413.
121. Chan, P.; Diego, S.; Rigby, P.; Takhounts, E.; Zhang, J. Development of a Generalized Linear Skull Fracture Criterion. **2007**.
122. Kleiven, S. Predictors for Traumatic Brain Injuries Evaluated through Accident Reconstructions. In Proceedings of the SAE Technical Papers; SAE International, October 29 2007; Vol. 2007-October.
123. Kleiven, S. Why Most Traumatic Brain Injuries Are Not Caused by Linear Acceleration but Skull Fractures Are. *Frontiers in Bioengineering and Biotechnology* **2013**, *1*.
124. Fahlstedt, M.; Halldin, P.; Alvarez, V.S.; Kleiven, S. Influence of the Body and Neck on Head Kinematics and Brain Injury Risk in Bicycle Accident Situations. In Proceedings of the IRCOBI Conference 2016; Malaga (Spain), 2016; pp. 459–478.
125. Yu, C.; Wang, F.; Wang, B.; Li, G.; Li, F. A Computational Biomechanics Human Body Model Coupling Finite Element and Multibody Segments for Assessment of Head/Brain Injuries in Car-To-Pedestrian Collisions. *International Journal of Environmental Research and Public Health* **2020**, *17*, 492, doi:10.3390/ijerph17020492.
126. Rueda, M.A.F.; Gilchrist, M.D. Equestrian Helmet Design: A Computational and Head Impact Biomechanics Simulation Approach. In Proceedings of the 6th World Congress of Biomechanics (WCB 2010). August 1-6, 2010 Singapore; Lim, C.T., Goh, J.C.H., Eds.; Springer: Berlin, Heidelberg, 2010; pp. 205–208.
127. Fahlstedt, M.; Halldin, P.; Kleiven, S. The Protective Effect of a Helmet in Three Bicycle Accidents - A Finite Element Study. *Accident Analysis and Prevention* **2016**, *91*, 135–143, doi:10.1016/j.aap.2016.02.025.
128. Solouki, A.; Tataranni, P.; Sangiorgi, C. Mixture Optimization of Concrete Paving Blocks Containing Waste Silt. *Sustainability* **2022**, *14*, 451, doi:10.3390/su14010451.

129. Zabihi, N.; Saafi, M. Recent Developments in the Energy Harvesting Systems from Road Infrastructures. *Sustainability* **2020**, *12*, 6738, doi:10.3390/su12176738.
130. Inestroza Mercado, A.I.; Hess, R. *Contribution of Pavements to Decreasing the Urban Heat Island Effect*; 2020;
131. Gupta, A.; Slebi-Acevedo, C.J.; Lizasoain-Arteaga, E.; Rodriguez-Hernandez, J.; Castro-Fresno, D. Multi-Criteria Selection of Additives in Porous Asphalt Mixtures Using Mechanical, Hydraulic, Economic, and Environmental Indicators. *Sustainability* **2021**, *13*, 2146, doi:10.3390/su13042146.
132. Kousis, I.; Fabiani, C.; Ercolaloni, L.; Pisello, A.L. Using Bio-Oils for Improving Environmental Performance of an Advanced Resinous Binder for Pavement Applications with Heat and Noise Island Mitigation Potential. *Sustainable Energy Technologies and Assessments* **2020**, doi:10.1016/j.seta.2020.100706.
133. Copetti Callai, S.; Sangiorgi, C. A Review on Acoustic and Skid Resistance Solutions for Road Pavements. *Infrastructures* **2021**, *6*, 41, doi:10.3390/infrastructures6030041.
134. Mikhailenko, P.; Piao, Z.; Kakar, M.R.; Bueno, M.; Athari, S.; Pieren, R.; Heutschi, K.; Poulikakos, L. Low-Noise Pavement Technologies and Evaluation Techniques: A Literature Review. *International Journal of Pavement Engineering* **2020**, *0*, 1–24, doi:10.1080/10298436.2020.1830091.
135. Fahlstedt, M.; Kleiven, S.; Li, X. Current Playground Surface Test Standards Underestimate Brain Injury Risk for Children. *Journal of Biomechanics* **2019**, *89*, 1–10, doi:10.1016/j.jbiomech.2019.03.038.
136. Chavez, F.; Marcobal, J.; Gallego, J. Laboratory Evaluation of the Mechanical Properties of Asphalt Mixtures with Rubber Incorporated by the Wet, Dry, and Semi-Wet Process. *Construction and Building Materials* **2019**, *205*, 164–174, doi:10.1016/j.conbuildmat.2019.01.159.
137. Moreno, F.; Rubio, M.C.; Martinez-Echevarria, M.J. The Mechanical Performance of Dry-Process Crumb Rubber Modified Hot Bituminous Mixes: The Influence of Digestion Time and Crumb Rubber Percentage. *Construction and Building Materials* **2012**, *26*, 466–474, doi:10.1016/j.conbuildmat.2011.06.046.
138. Chiu, C.-T. Use of Ground Tire Rubber in Asphalt Pavements: Field Trial and Evaluation in Taiwan. *Resources, Conservation and Recycling* **2008**, *52*, 522–532, doi:10.1016/j.resconrec.2007.06.006.
139. Chang, W.-R.; Brunette, C.; Chang, C.-C. Development of an Objective Determination of a Slip with a Portable Inclineable Articulated Strut Slip Tester (PIAST). *Safety Science* **2010**, *48*, 100–109, doi:10.1016/j.ssci.2009.07.001.
140. Standard - EN 13036-4 – Road and Airfield Surface Characteristics – Test Methods – Part 4: Method for Measurement of Slip-Skid Resistance of a Surface – the Pendulum Test.
141. Standard - EN ISO 13473-1:2019 Characterization of Pavement Texture by Use of Surface Profiles — Part 1: Determination of Mean Profile Depth.
142. Imola Climate Weather Averages Available online: <https://www.worldweatheronline.com/imola-weather-averages/emilia-romagna/it.aspx#June> (accessed on 9 January 2022).
143. Ateeq, M.; Al-Shamma'a, A. Experimental Study on the Optimisation of Chemical Treatment to Reduce Waste Rubber Aggregates Absorption Properties. *Construction and Building Materials* **2016**, *126*, 274–285, doi:10.1016/j.conbuildmat.2016.09.021.
144. Kashani, A.; Ngo, T.D.; Hemachandra, P.; Hajimohammadi, A. Effects of Surface Treatments of Recycled Tyre Crumb on Cement-Rubber Bonding in Concrete Composite Foam. *Construction and Building Materials* **2018**, *171*, 467–473, doi:10.1016/j.conbuildmat.2018.03.163.
145. Abdul Hassan, N.; Airey, G.D.; Putra Jaya, R.; Mashros, N.; A. Aziz, Md.M. A Review of Crumb Rubber Modification in Dry Mixed Rubberised Asphalt Mixtures. *Jurnal Teknologi* **2014**, *70*, doi:10.11113/jt.v70.3501.

146. Eskandarsefat, S.; Sangiorgi, C.; Dondi, G.; Lamperti, R. Recycling Asphalt Pavement and Tire Rubber: A Full Laboratory and Field Scale Study. *Construction and Building Materials* **2018**, *176*, 283–294, doi:10.1016/j.conbuildmat.2018.05.031.
147. Aliabdo, A.A.; Abd Elmoaty, A.E.M.; AbdElbaset, M.M. Utilization of Waste Rubber in Non-Structural Applications. *Construction and Building Materials* **2015**, *91*, 195–207, doi:10.1016/j.conbuildmat.2015.05.080.
148. Rubber Granulate 2017.
149. Dondi, G.; Tataranni, P.; Pettinari, M.; Sangiorgi, C.; Simone, A.; Vignali, V. Crumb Rubber in Cold Recycled Bituminous Mixes: Comparison between Traditional Crumb Rubber and Cryogenic Crumb Rubber. *Construction and Building Materials* **2014**, *68*, 370–375, doi:10.1016/j.conbuildmat.2014.06.093.
150. Dong, D.; Huang, X.; Li, X.; Zhang, L. Swelling Process of Rubber in Asphalt and Its Effect on the Structure and Properties of Rubber and Asphalt. *Construction and Building Materials* **2012**, *29*, 316–322, doi:10.1016/j.conbuildmat.2011.10.021.
151. Daly, W.H.; Balamurugan, S.S.; Negulescu, I.; Akentuna, M.; Mohammad, L.; Cooper, S.B.; Cooper, S.B.; Baumgardner, G.L. Characterization of Crumb Rubber Modifiers after Dispersion in Asphalt Binders. *Energy Fuels* **2019**, *33*, 2665–2679, doi:10.1021/acs.energyfuels.8b03559.
152. Lamperti, R.; Grenfell, J.; Sangiorgi, C.; Lantieri, C.; Airey, G.D. Influence of Waxes on Adhesion Properties of Bituminous Binders. *Construction and Building Materials* **2015**, *76*, 404–412, doi:10.1016/j.conbuildmat.2014.11.058.
153. Bockstal, L.; Berchem, T.; Schmetz, Q.; Richel, A. Devulcanisation and Reclaiming of Tires and Rubber by Physical and Chemical Processes: A Review. *Journal of Cleaner Production* **2019**, *236*, 117574, doi:10.1016/j.jclepro.2019.07.049.
154. de Sousa, F.D.B.; Scuracchio, C.H.; Hu, G.-H.; Hoppe, S. Devulcanization of Waste Tire Rubber by Microwaves. *Polymer Degradation and Stability* **2017**, *138*, 169–181, doi:10.1016/j.polyimdegradstab.2017.03.008.
155. Asaro, L.; Gratton, M.; Seghar, S.; Aït Hocine, N. Recycling of Rubber Wastes by Devulcanization. *Resources, Conservation and Recycling* **2018**, *133*, 250–262, doi:10.1016/j.resconrec.2018.02.016.
156. Seghar, S.; Asaro, L.; Rolland-Monnet, M.; Aït Hocine, N. Thermo-Mechanical Devulcanization and Recycling of Rubber Industry Waste. *Resources, Conservation and Recycling* **2019**, *144*, 180–186, doi:10.1016/j.resconrec.2019.01.047.
157. Hosseinnzhad, S.; Kabir, S.F.; Oldham, D.; Mousavi, M.; Fini, E.H. Surface Functionalization of Rubber Particles to Reduce Phase Separation in Rubberized Asphalt for Sustainable Construction. *Journal of Cleaner Production* **2019**, *225*, 82–89, doi:10.1016/j.jclepro.2019.03.219.
158. Mousavi, M.; Hosseinnzhad, S.; Kabir, S.F.; Burnett, D.J.; Fini, E.H. Reaction Pathways for Surface Activated Rubber Particles. *Resources, Conservation and Recycling* **2019**, *149*, 292–300, doi:10.1016/j.resconrec.2019.05.041.
159. Han, L.; Zheng, M.; Li, J.; Li, Y.; Zhu, Y.; Ma, Q. Effect of Nano Silica and Pretreated Rubber on the Properties of Terminal Blend Crumb Rubber Modified Asphalt. *Construction and Building Materials* **2017**, *157*, 277–291, doi:10.1016/j.conbuildmat.2017.08.187.
160. Moyano, M.A.; Martín-Martínez, J.M. Surface Treatment with UV-Ozone to Improve Adhesion of Vulcanized Rubber Formulated with an Excess of Processing Oil. *International Journal of Adhesion and Adhesives* **2014**, *55*, 106–113, doi:10.1016/j.ijadhadh.2014.07.018.
161. Ibrahim, I.M.; Fathy, E.S.; El-Shafie, M.; Elnaggar, M.Y. Impact of Incorporated Gamma Irradiated Crumb Rubber on the Short-Term Aging Resistance and Rheological Properties of Asphalt Binder. *Construction and Building Materials* **2015**, *81*, 42–46, doi:10.1016/j.conbuildmat.2015.01.015.
162. Circular Economy Available online: <https://www.etma.org/key-topics/circular-economy/> (accessed on 30 December 2020).

163. Bontoux, L., Leone, F., Nicolai, M., Papameletiou, D. *The Recycling Industry in the European Union: Impediments and Prospects*; Institute for Prospective Technological Studies; European Commission - Joint Research Centre Institute for Prospective Technological Studies: Sevilla, Spain, 1996; p. 59;.
164. European Tyres Rubber Manufactures Association *European Tyre Rubber Manufactures Association, 2014. European Tyre and Rubber Industry – Statistics.*; 2019; p. 52;.
165. Re Depaolini, A.; Bianchi, G.; Fornai, D.; Cardelli, A.; Badalassi, M.; Cardelli, C.; Davoli, E. Physical and Chemical Characterization of Representative Samples of Recycled Rubber from End-of-Life Tires. *Chemosphere* **2017**, *184*, 1320–1326, doi:10.1016/j.chemosphere.2017.06.093.
166. Li, P.; Ding, Z.; Zou, P.; Sun, A. Analysis of Physico-Chemical Properties for Crumb Rubber in Process of Asphalt Modification. *Construction and Building Materials* **2017**, *138*, 418–426, doi:10.1016/j.conbuildmat.2017.01.107.
167. Piao, Z.; Mikhailenko, P.; Kakar, M.R.; Bueno, M.; Hellweg, S.; Poulikakos, L.D. Urban Mining for Asphalt Pavements: A Review. *Journal of Cleaner Production* **2021**, *280*, 124916, doi:10.1016/j.jclepro.2020.124916.
168. Park, J.; Ju, W.; Paek, K.; Kim, Y.; Choi, Y.; Kim, J.; Hwang, Y. Pre-Treatments of Polymers by Atmospheric Pressure Ejected Plasma for Adhesion Improvement. *Surface and Coatings Technology* **2003**, *174–175*, 547–552, doi:10.1016/S0257-8972(03)00689-3.
169. Johansson, K.S. 20 - Surface Modification of Plastics. In *Applied Plastics Engineering Handbook (Second Edition)*; Kutz, M., Ed.; Plastics Design Library; William Andrew Publishing, 2017; pp. 443–487 ISBN 978-0-323-39040-8.
170. Purbrick, M.D. *Polymer Surfaces: From Physics to Technology, Revised and Updated Edition / Wiley*; John Wiley and Sons Ltd: Chichester UK, 2000; ISBN 0-471-97100-6.
171. Types of Radioactivity: Alpha, Beta, and Gamma Decay Available online: [https://chem.libretexts.org/Courses/can/intro/17%3A\\_Radioactivity\\_and\\_Nuclear\\_Chemistry/17.03%3A\\_Types\\_of\\_Radioactivity%3A\\_Alpha%2C\\_Beta%2C\\_and\\_Gamma\\_Decay](https://chem.libretexts.org/Courses/can/intro/17%3A_Radioactivity_and_Nuclear_Chemistry/17.03%3A_Types_of_Radioactivity%3A_Alpha%2C_Beta%2C_and_Gamma_Decay) (accessed on 9 February 2021).
172. Gamma Rays Compared with X-Rays for Radiographic Inspection Available online: <https://www.twi-global.com/technical-knowledge/faqs/faq-what-are-the-advantages-and-disadvantages-of-gamma-rays-when-compared-with-x-rays-for-radiographic-inspection.aspx> (accessed on 9 February 2021).
173. Bikit, I. *Gamma Rays: Technology, Applications and Health Implications*; 2013; p. 413;.
174. McKeen, L.W. 10 - Elastomers and Rubbers. In *The Effect of UV Light and Weather on Plastics and Elastomers (Fourth Edition)*; McKeen, L.W., Ed.; Plastics Design Library; William Andrew Publishing: Oxford, United Kingdom, 2019; pp. 279–359 ISBN 978-0-12-816457-0.
175. Upadhy, K. A Review of: “Fundamentals Of Plasma Chemistry And Technology” By H.V. Boenig Technomic Publishing Co. Lancaster, PA 17604 417 Pages, Hard Cover, 1988. *Materials and Manufacturing Processes* **1991**, *6*, 557–559, doi:10.1080/10426919108934786.
176. Henniker Plasma Atmospheric Plasma Treatment Explained Available online: <https://plasmamatreatment.co.uk/pt/plasma-technology-overview/atmospheric-plasma-treatment> (accessed on 5 February 2021).
177. Sivaram, S. Fundamentals of Plasma Chemistry. In *Chemical Vapor Deposition: Thermal and Plasma Deposition of Electronic Materials*; Sivaram, S., Ed.; Springer US: Boston, MA, 1995; pp. 119–143 ISBN 978-1-4757-4751-5.
178. Plasma Technology. What Is Plasma? | Plasmamatreat Available online: <https://www.plasmamatreat.com/plasma-technology/what-is-plasma.html> (accessed on 9 February 2021).
179. ScienceDirect Topics Microwave Irradiation - an Overview Available online: <https://www.sciencedirect.com/topics/medicine-and-dentistry/microwave-irradiation> (accessed on 5 February 2021).

180. February 09, J.L.-L.S.C.; 2018 What Are Microwaves? Available online: <https://www.livescience.com/50259-microwaves.html> (accessed on 10 February 2021).
181. program, L.A.U.H.P.B. Plasma Deposition, Treatment, And Etching Of Polymers. *Materials and Manufacturing Processes* **1993**, *8*, 385–390, doi:10.1080/10426919308934842.
182. Bagher, A.M. Advantages of Gamma Radiation in Science and Industry. *Journal of Advanced Physics* **2014**, *3*, 97–103, doi:10.1166/jap.2014.1110.
183. Martínez-Barrera, G.; Ávila-Córdoba, L.I.; Martínez-López, M.; Herrera-Sosa, E.S.; Viguera-Santiago, E.; Barrera-Díaz, C.E.; González-Rivas, F.U.-N. and N. Gamma Radiation as a Recycling Tool for Waste Materials Used in Concrete. *Evolution of Ionizing Radiation Research* **2015**, doi:10.5772/60435.
184. Burillo, G.; Clough, R.L.; Czikovszky, T.; Guven, O.; Le Moel, A.; Liu, W.; Singh, A.; Yang, J.; Zaharescu, T. Polymer Recycling: Potential Application of Radiation Technology. *Radiation Physics and Chemistry* **2002**, *64*, 41–51, doi:10.1016/S0969-806X(01)00443-1.
185. ScienceDirect Topics Surface Activation - an Overview Available online: <https://www.sciencedirect.com/topics/engineering/surface-activation> (accessed on 11 December 2019).
186. Gupta, S.K.; Singh, P.; Singh, R.; Kumar, R. Impact of Swift Heavy Ions and Gamma Radiation upon Optical, Structural, and Chemical Properties of Polypropylene Polymer Films. *Advances in Polymer Technology* **2015**, *34*, doi:10.1002/adv.21518.
187. Albano, C.; Reyes, J.; Ichazo, M.; González, J.; Hernández, M.; Rodríguez, M. Mechanical, Thermal and Morphological Behaviour of the Polystyrene/Polypropylene (80/20) Blend, Irradiated with  $\gamma$ -Rays at Low Doses (0–70 KGy). *Polymer Degradation and Stability* **2003**, *80*, 251–261, doi:10.1016/S0141-3910(02)00405-6.
188. Faldini, S.B.; Terence, M.C.; Miranda, L.F.; Munhoz, A.H.; Domingues, L.S.; Coghetto, G. Characterization Of Crumb Rubber Modified By Gamma Radiation. **2013**, *11*.
189. Martínez-Barrera, G.; del Coz-Díaz, J.J.; Álvarez-Rabanal, F.P.; López Gayarre, F.; Martínez-López, M.; Cruz-Olivares, J. Waste Tire Rubber Particles Modified by Gamma Radiation and Their Use as Modifiers of Concrete. *Case Studies in Construction Materials* **2020**, *12*, e00321, doi:10.1016/j.cscm.2019.e00321.
190. Chen, H.-B.; Wang, P.-C.; Liu, B.; Zhang, F.-S.; Ao, Y.-Y. Gamma Irradiation Induced Effects of Butyl Rubber Based Damping Material. *Radiation Physics and Chemistry* **2018**, *145*, 202–206, doi:10.1016/j.radphyschem.2017.11.001.
191. Newton, R.G. Mechanism of Exposure-Cracking of Rubbers. With a Review of the Influence of Ozone. *Rubber Chemistry and Technology* **1945**, *18*, 504–556, doi:10.5254/1.3546750.
192. Iwase, Y.; Shindo, T.; Kondo, H.; Ohtake, Y.; Kawahara, S. Ozone Degradation of Vulcanized Isoprene Rubber as a Function of Humidity. *Polymer Degradation and Stability* **2017**, *142*, 209–216, doi:10.1016/j.polymdegradstab.2017.06.025.
193. Lippens, P. 3 - Low-Pressure Cold Plasma Processing Technology. In *Plasma Technologies for Textiles*; Shishoo, R., Ed.; Woodhead Publishing Series in Textiles; Woodhead Publishing, 2007; pp. 64–78 ISBN 978-1-84569-073-1.
194. Liu, J.; Liu, P.; Zhang, X.; Lu, P.; Zhang, X.; Zhang, M. Fabrication of Magnetic Rubber Composites by Recycling Waste Rubber Powders via a Microwave-Assisted in Situ Surface Modification and Semi-Devulcanization Process. *Chemical Engineering Journal* **2016**, *295*, 73–79, doi:10.1016/j.cej.2016.03.025.
195. Martin, D.; Ighigeanu, D.; Mateescu, E.; Craciun, G.; Ighigeanu, A. Vulcanization of Rubber Mixtures by Simultaneous Electron Beam and Microwave Irradiation. *Radiation Physics and Chemistry* **2002**, *65*, 63–65, doi:10.1016/S0969-806X(01)00680-6.
196. Phetarporn, V.; Loykulnant, S.; Kongkaew, C.; Seubsai, A.; Prapainainar, P. Composite Properties of Graphene-Based Materials/Natural Rubber Vulcanized Using Electron Beam Irradiation. *Materials Today Communications* **2019**, *19*, 413–424, doi:10.1016/j.mtcomm.2019.03.007.

197. Asaro, L.; Gratton, M.; Seghar, S.; Aït Hocine, N. Recycling of Rubber Wastes by Devulcanization. *Resources, Conservation and Recycling* **2018**, *133*, 250–262, doi:10.1016/j.resconrec.2018.02.016.
198. Yang, X.; Shen, A.; Li, B.; Wu, H.; Lyu, Z.; Wang, H.; Lyu, Z. Effect of Microwave-Activated Crumb Rubber on Reaction Mechanism, Rheological Properties, Thermal Stability, and Released Volatiles of Asphalt Binder. *Journal of Cleaner Production* **2020**, *248*, 119230, doi:10.1016/j.jclepro.2019.119230.
199. Liang, M.; Xin, X.; Fan, W.; Ren, S.; Shi, J.; Luo, H. Thermo-Stability and Aging Performance of Modified Asphalt with Crumb Rubber Activated by Microwave and TOR. *Materials & Design* **2017**, *127*, 84–96, doi:10.1016/j.matdes.2017.04.060.
200. Chtourou, H.; Riedl, B.; Kokta, B.V. Surface Modification of Polyethylene Pulp Fiber by Ozone Treatment. An Analytical and Thermal Characterization. *Polymer Degradation and Stability* **1994**, *43*, 149–156, doi:10.1016/0141-3910(94)90237-2.
201. Martín-Martínez, J.M.; Romero-Sánchez, M.D. Strategies to Improve the Adhesion of Rubbers to Adhesives by Means of Plasma Surface Modification. *European Physical Journal Applied Physics* **2006**, *34*, 125–138, doi:10.1051/epjap:2006038.
202. Ortiz-Magán, A.B.; Pastor-Blas, M.M.; Ferrándiz-Gómez, T.P.; Morant-Zacarés, C.; Martín-Martínez, J.M. Surface Modifications Produced by N<sub>2</sub> and O<sub>2</sub> RF Plasma Treatment on a Synthetic Vulcanized Styrene-Butadiene Rubber. *Plasmas and Polymers* **2001**, *6*, 81–105, doi:10.1023/A:1011352903775.
203. Xiaowei, C.; Sheng, H.; Xiaoyang, G.; Wenhui, D. Crumb Waste Tire Rubber Surface Modification by Plasma Polymerization of Ethanol and Its Application on Oil-Well Cement. *Applied Surface Science* **2017**, *409*, 325–342, doi:10.1016/j.apsusc.2017.03.072.
204. Li, J.; Xiao, F.; Amirkhanian, S.N. High Temperature Rheological Characteristics of Plasma-Treated Crumb Rubber Modified Binders. *Construction and Building Materials* **2020**, *236*, 117614, doi:10.1016/j.conbuildmat.2019.117614.
205. Verma, S.; Ray, D.S. Use of Modified Bitumen by Lignin and Waste Plastic in Bituminous Concrete. **2020**, *8*.
206. Tokede, O.O.; Whittaker, A.; Mankaa, R.; Traverso, M. Life Cycle Assessment of Asphalt Variants in Infrastructures: The Case of Lignin in Australian Road Pavements. *Structures* **2020**, *25*, 190–199, doi:10.1016/j.istruc.2020.02.026.
207. Hashmi, S.; Jabary, A. Case Study of Lignin-Based Asphalt for the Swedish Market. 67.
208. Pérez, I.P.; Rodríguez Pasandín, A.M.; Pais, J.C.; Alves Pereira, P.A. Use of Lignin Biopolymer from Industrial Waste as Bitumen Extender for Asphalt Mixtures. *Journal of Cleaner Production* **2019**, *220*, 87–98, doi:10.1016/j.jclepro.2019.02.082.
209. form, Q. about this project? A. dr ing Rjag.C. Huge Boost for Bio-Asphalt Based on Lignin Available online: <https://www.wur.nl/en/Research-Results/Research-Institutes/food-biobased-research/show-fbr/Huge-boost-for-bio-asphalt-based-on-lignin.htm> (accessed on 6 July 2020).

